

# **Role of hemidesmosomal linker proteins in neoplastic progression of squamous cell carcinomas**

**By**

**Pratik Rajeev Chaudhari**

**(LIFE09201204012)**

**Tata Memorial Centre, Mumbai**

*A thesis submitted to the  
Board of Studies in Life Sciences*

*In partial fulfillment of  
requirements for the Degree of*

**DOCTOR OF PHILOSOPHY**

**of**

**HOMI BHABHA NATIONAL INSTITUTE**



**February, 2018**

# Homi Bhabha National Institute

## Recommendations of the Viva Voce Committee

As members of the Viva Voce Committee, we certify that we have read the dissertation prepared by Mr. Pratik Rajeev Chaudhari entitled "Role of hemidesmosomal linker proteins in neoplastic progression of squamous cell carcinomas" and recommend that it may be accepted as fulfilling the thesis requirement for the award of Degree of Doctor of Philosophy.



Date: 26/2/18

Chairman – Dr. Sorab N. Dalal



Date: 26/02/18

Guide/Convener – Dr. Milind M. Vaidya



Date: 26/2/18

External Examiner – Prof. Subhash C. Lakhota



Date: 26/2/18

Member 1 – Dr. Prasanna Venkatraman



Date: 26/2/18

Member-2 – Dr. Sanjay Gupta

Final approval and acceptance of this thesis is contingent upon the candidate's submission of the final copies of the thesis to HBNI.

I hereby certify that I have read this thesis prepared under my/our direction and recommend that it may be accepted as fulfilling the thesis requirement.

Date: 26/02/18  
Place: Navi Mumbai

  
Dr. Milind M. Vaidya  
Guide

## **STATEMENT BY AUTHOR**

This dissertation has been submitted in partial fulfillment of requirements for an advanced degree at Homi Bhabha National Institute (HBNI) and is deposited in the library to be made available to borrowers under rules of the HBNI.

Brief quotations, from this dissertation, are allowable without special permission provided that accurate acknowledgement of source is made. Requests for permission for extended quotation from or reproduction of this manuscript in whole or in part may be granted by the Competent Authority of HBNI when in his or her judgment, the proposed use of the material is in the interests of scholarship. In all the other instances, however, permission must be obtained from the author.

Pratik Rajeev Chaudhari

## **DECLARATION**

I, hereby declare that the investigation presented in the thesis has been carried out by me. The work is original and has not been submitted earlier as a whole or in part for a degree/diploma at this or any other Institution or University.

Pratik Rajeev Chaudhari

## **List of Publications arising from the thesis**

### **Journals:**

1. **“Hemidesmosomal linker proteins regulate cell motility, invasion and tumorigenicity in oral squamous cell carcinoma derived cells”**, Pratik Rajeev Chaudhari, Silvania Emlit Charles, Zinia Charlotte D’Souza, Milind Murlidhar Vaidya, *Experimental Cell Research*, **2017**, 360(2), 125-137.
2. **“Role of BPAG1e in neoplastic progression of oral squamous cell carcinoma derived cells”**, Pratik Rajeev Chaudhari, Silvania Emlit Charles, Milind Murlidhar Vaidya, *International Journal of Pharma and Bio Sciences*, **2017**, 8(1), 519-527.
3. **“Versatile hemidesmosomal linker proteins: structure and function”**, Pratik Rajeev Chaudhari, Milind Murlidhar Vaidya, *Histology and Histopathology*, **2015**, 30(4), 425-434.

### **Conferences:**

1. **Platform presentation at XXXVIII All India Cell Biology Conference (AICBC)** on Cellular response to drugs held during 10-12 December, 2014 at Central Drug Research Institute (CDRI), Lucknow, India.  
(Received Prof. V. C. Shah memorial award for best platform presentation)
2. **Platform presentation at Gordon Research Seminar on Intermediate Filaments and Poster presentation at Gordon Research Conference on Intermediate Filaments** held during 11-17 June, 2016 at Stoweflake Conference Center, Stowe, VT, USA.  
(Received Nature travel grant to attend the conference)

3. **Platform presentation at 13<sup>th</sup> National Research Scholars Meet in Life Sciences** held during 14-15 December, 2017 at Advanced Centre for Treatment, Research and Education in Cancer (ACTREC), Kharghar, Navi Mumbai, India.  
(Received First prize for best platform presentation)

**Others:**

1. Received **Prof. V. C. Shah memorial award for best platform presentation at XXXVIII All India Cell Biology Conference (AICBC)** held during 10-12 December, 2014 at Central Drug Research Institute (CDRI), Lucknow, India.
2. **Part of organizing committee of 11<sup>th</sup> National Research Scholars Meet in Life Sciences** held during 17-18 December, 2015 at Advanced Centre for Treatment, Research and Education in Cancer (ACTREC), Kharghar, Navi Mumbai, India.
3. Attended **TMC Platinum Jubilee: A conference of new ideas in cancer: challenging dogmas** held during 26-28 February, 2016 at National Centre for the Performing Arts, Nariman Point, Mumbai.
4. Received **Nature travel grant** to attend the **Gordon Research Conference on Intermediate Filaments** held during 11-17 June, 2016 at Stoweflake Conference Center, Stowe, VT, USA.
5. Received **First prize for best platform presentation at 13<sup>th</sup> National Research Scholars Meet in Life Sciences** held during 14-15 December, 2017 at Advanced Centre for Treatment, Research and Education in Cancer (ACTREC), Kharghar, Navi Mumbai, India.

*This Thesis is dedicated to*

*My beloved family*

*and*

*All those who supported and inspired me  
throughout my educational journey*

## Acknowledgement

A Number of enzymes, coenzymes, catalysts etc. are required to complete any biochemical pathway. Likewise, during the entire duration of a Ph.D. course, several people acted as enzymes, coenzymes, catalysts; who helped, supported and inspired me to complete this project in time. I take this opportunity to acknowledge these enzymes, coenzymes and catalysts!!!

The list begins with my mentor! Dr. Milind Vaidya. He is not only a good researcher but also a great human being. His "Never give up" attitude has a huge impact on me. I thank him for giving me all the liberty to work in the lab. His immense support and care provided a positive environment to work in the lab. During this Ph.D. tenure, he always stood firmly by me as and when it was most needed. Indeed, I am very lucky to work under "Keratin Man's" guidance. He is really a great inspiration to all of us.

I would like to express special thanks to Dr. Shubhada Chiplunkar, Director, ACTREC for providing good research infrastructure. I am also thankful to her for providing academic and technical support. I thank Dr. Sudeep Gupta, Dy. Director, CRC, ACTREC and Dr. HKV Narayan, Dy. Director, ACTREC for their constant support and encouragement. I am also thankful to Dr. Rajiv Sarin (former Director) and Dr. Surekha Zingde (former Dy. Director).

I am extremely thankful to my Doctoral committee: Dr. Milind M. Vaidya, Dr. Sorab N. Dalal, Dr. V. Prasanna, Dr. Sanjay Gupta and former DC Chairman Dr. Girish Maru. Their scientific inputs and critical assessment helped in shaping up the project. I have really admired Sorab since course work days for his dedication and ways to teach us how to pursue quality research. I am thankful to him for generously sharing reagents. I thank Dr. Sanjay Gupta for his relentless support throughout the tenure. I thank Dr. Prasanna for motivating me throughout the project.

Vaidya laboratory! A lab which provides positive work environment. I am grateful to all my former and current lab members. I thank Mrs. Vinita Sawant for all the support, guidance and offering snacks during these years. I thank Mrs. Vaishali Dange for teaching me tissue culture work. I thank senior students, Deepak and Alam, whom I know by the reagents and methods they developed, since both completed their PhD before I joined. I am grateful to a very humble person, Sapna, for giving confidence and support during early days of my Ph.D. I thank Soni for his constant support and yummy food. I am thankful to Badi didi, Richa, for scientific inputs which helped me to perform scientifically sound experiments. I thank Choti didi, Crismita, for being a source of motivation for me during this tenure, for unconditional help and solving my stupid doubts. I learnt ethics in science from Richa and Crismita. I am thankful to a very calm personality in our lab, Saumya, for her valuable suggestions both at personal and professional front. I am immensely thankful to Mandar, Sylvania and Zinia for working with me with dedication on this project. I could finish the benchwork and thesis in time because Mandar, Sylvania and Zinia contributed immensely to the project work. Mandar (December 2014 - May 2015) is a hardworking and quick-witted person.

Silvania (August 2015 - September 2016) is meticulous, dependable, sincere and technically, a very sound person. I thank her for maintaining the western blot data systematically and performing some of the experiments single handedly. Zinia (September 2016 - April 2017) is very sharp minded, quick learner and professional person. I admire Silvania and Zinia for correcting thesis with dedication in time. Thanks three of you for bearing with me! I am thankful to Swapnil, who taught me western blotting. I would like to thank my so called brothers, Harsh and Pankaj, for creating the cheerful lab environment. I will always cherish the time spent and enjoyed while playing cricket, table tennis, Badminton, volleyball and (not to forget) many creative indoor games! I thank Ankur for making the lab environment joyful with his laughter. I would like to thank Sunita for keeping the lab environment lively, happening and for yummy food. I am also thankful to other lab members: Archana, Saie, Sonam, Sayli, Sai, Fatima, Vidhi, Pavan, Jashkaran, Aarti, Neha, Cyrus, Nandini, Manish, Nikhil, Sweta, Rashmi, Apurva, Shruti, Bhagyashree, Shweta, Krishna, Chetan, Yashvi, Meghna etc. I thank Rajesh for helping in washing, packing of glassware and ordering reagents. I thank Shridhar for his help in animal work and washing, packing of glassware. I would like to thank Ram and Naresh for doing daily work with dedication. I am also thankful to Prema Madam and Yashwant Kaka for their blessings and helping me throughout Ph.D. tenure. I will always cherish the moments we all had during lab picnics and parties.

Batch 012! I am lucky to have cheerful batchmates (Arunabha, Gopal, Bhawik, Bhushan, Jacinth, Sameer, Saujanya, Mukul, Prajish, Niraja, Shilpi and Pratibha) during this tenure. A special thanks to Gopal and Bhawik for being best buddies of mine and for making their room available to have fun and food. I am grateful to batchmate cum sister Arunabha for understanding and supporting me throughout the tenure. I would like to thank Bhushan for being a supporting roommate for last five years. I will always cherish the memories we all had during batch picnics, birthday celebrations, Friday dinner parties and organizing several events including NRSB 2015!

I would like to thank the entire ACTREC students' community for all their support and cooperation throughout the tenure. Very special thanks to Shalaka, my M.Sc. dissertation partner and close friend, for motivating me to do Ph.D. The situation would have been different if you would not have pushed me to pursue Ph.D. I am thankful to her for unconditional support and care in every situation. Thanks for the delicious food too! I also thank Akash, my friend since B.Sc. days, for his constant support and care. I am thankful to Crismita, Silvania and Arunabha for their wholehearted support during my Gordon conference visit in USA. I would like to thank "Sports team" from ACTREC: Rahul, Rushikesh, Gopal, Bhawik, Harsh, Pankaj, Asif, Ajay, Manish, Moquit, Manohar, Dilip, Rajan, Ram etc. for making life stress free. A special thanks to ACTREC colleagues: Kedar, Manohar, Rushikesh, Rahul, Roopa, Atul, Abira, Sonali, Prasanna, Rasika, Priyanka, Srikanta, Nikhil, Indrajit, Dilip, Prasad, Poonam, Madhura, Amir, Raikamal, Harish, Purna, Shweta, Anagha, Joel, Rahul, Mythreyi, Rajashree, Raghav, Ajay, Nilesh etc. I share a special bonding with members of Shirsat lab, Sorab lab, Waghmare lab, Bhattacharyya lab, Teni lab and Rukmini lab. Thank you all!

Very special thanks to Mr. Uday Dandekar for his dedication to keep equipments and machines functional. He is the person whom we can approach anytime. I am extremely thankful to Dr. Ingle, Dr. Thorat, Mahesh, Pawar and Shashi from Laboratory animal facility for helping me with animal work. I thank Vaishali, Tanuja and Jairaj for their immense help in microscopy and analysis of the images. I am also thankful to the Photography, Stores, Purchase, Library, Engineering, Security, Administration, Accounts, Housekeeping and Pharmacy department for their cooperation. I am also thankful to Tea/Coffee machine operators Anil and Vidya.

I am grateful to Prof. Harish Pant (NINDS, NIH, USA) for being huge inspiration to me to do research. I thank Dr. Jonathan Jones (Washington State University, USA) and all the PIs of ACTREC for sharing reagents and plasmid constructs. I am thankful to Dr. Narendra Joshi for his helpful suggestions and guidance. I thank Dr. Aparna Bagwe for always supporting me. I thank Dr. Mahesh Kulkarni, Dr. B. Santhakumari and Mr. Yugendra Patil (National Chemical Laboratory, Pune, India) for SWATH analysis. I thank ACTREC-DAE for the fellowship and Terry Fox foundation for funding the project. I also thank Nature Travel Grant program, Homi Bhabha National Institute, Kantiben Patel fellowship trust and Sam Mistry Fund for financially supporting me to attend the Gordon conference on Intermediate Filaments.

I would like to thank my M.Sc. dissertation guide, Dr. Suresh Kamble, for constantly motivating me to pursue career in research. I am also thankful to my ex-colleagues from FMR, Mumbai (Anirvan, Purva, Pooja and Sanjana) for pushing me to do Ph.D. from ACTREC. I would like to thank my school friends (Krunal, Akshay, Girish, Mahesh, Amol, Sanket, Prasad, Kaustubh etc.) for making my life joyful. I also thank Taloja train group (Lisa, Chitra, Nikhil, Kamlesh, Madhura, Hrushikesh, Rajni, Prashant, Ganesh etc.). I wish to thank my "Papdy" villagers for constantly supporting me throughout my entire educational journey.

And last but not the least, My family! I thank my parents, Vijaya Chaudhari and Rajeev Chaudhari for their endless love, support and being my source of strength. I fondly remember my late grandmother Sunanda Chaudhari who always motivated me to pursue good education. I thank my elder brother Viraj and sister-in-law Namita for equally supporting and understanding me everytime. I also thank my little niece Advika for making my life cheerful. Finally, I would like to thank the Almighty, without whose blessings life would not have been the way it is.

Pratik Rajeev Chaudhari

## INDEX

|  |           |
|--|-----------|
| <b>Synopsis</b> .....  | <b>5</b>  |
| <b>List of Figures</b> .....                                       | <b>23</b> |
| <b>List of Tables</b> .....  | <b>25</b> |
| <b>Abbreviations</b> .....   | <b>26</b> |
| <b>1. Introduction</b> .....                                       | <b>29</b> |
| 1.1 Aim: .....   | 32        |
| 1.2 Objectives: .....  | 32        |
| <b>2. Review of Literature</b> .....                               | <b>33</b> |
| 2.1 Hemidesmosomes (HDs): .....                                    | 34        |
| 2.2 $\alpha 6\beta 4$ integrin: .....                              | 35        |
| 2.3 CD151: .....   | 36        |
| 2.4 BPAG2 (BP180, COL17A): .....                                   | 36        |
| 2.5 Plakin family proteins: .....                                  | 37        |
| 2.6 Hemidesmosomal linker proteins: .....                          | 38        |
| 2.6.1 BPAG1e (BP230): .....  | 38        |
| 2.6.2 Plectin: .....   | 38        |
| 2.7 Interactions mediated by hemidesmosomal linker proteins: ..... | 39        |
| 2.8 Events involved in Type I HD assembly: .....                   | 40        |
| 2.9 Animal models: .....   | 41        |
| 2.9.1 BPAG1 null mouse: .....                                      | 41        |
| 2.9.2 Plectin null mouse: .....                                    | 42        |
| 2.10 Functions of HD linker proteins: .....                        | 42        |
| 2.10.1 BPAG1e and cell migration: .....                            | 42        |
| 2.10.2 BPAG1e and cancer: .....                                    | 43        |
| 2.10.3 Plectin and cytoskeletal stability: .....                   | 43        |
| 2.10.4 Plectin, cancer and cell signaling: .....                   | 44        |
| 2.11 Intermediate filaments: .....                                 | 45        |
| 2.12 IF Structure: .....   | 45        |
| 2.13 IF Classification: .....                                      | 46        |
| 2.14 Keratins: .....   | 47        |
| 2.15 Keratin 8/18: .....   | 48        |

|  |           |
|--|-----------|
| 2.16 Fascin: -----   | 48        |
| 2.17 NDRG1: -----  | 49        |
| <b>3. Materials and Methods -----</b>  | <b>51</b> |
| 3.1 Routine maintenance of cell lines: -----   | 52        |
| 3.2 Reagents:-----   | 52        |
| 3.3 Revival of cells:-----   | 55        |
| 3.4 Subculture/Trypsinization and transfer of cells:-----  | 56        |
| 3.5 Freezing and cryopreservation of cells:-----   | 56        |
| 3.6 Plasmids and cloning: -----  | 56        |
| 3.7 Preparation of ultra-competent <i>E. coli</i> DH5 $\alpha$ cells:-----                         | 59        |
| 3.8 Transformation: -----  | 60        |
| 3.9 Plasmid extraction using alkaline lysis method (Mini-Prep):-----                               | 60        |
| 3.10 Virus production: -----   | 61        |
| 3.11 Lentivirus mediated transduction of OSCC derived cell line: -----                             | 62        |
| 3.12 Protein estimation by modified Lowry's method:-----   | 62        |
| 3.13 Sodium dodecyl sulfate polyacrylamide gel electrophoresis (SDS-PAGE):-----                    | 63        |
| 3.14 Western blotting: -----   | 63        |
| 3.15 List of antibodies: -----   | 64        |
| 3.16 RNA extraction: -----   | 67        |
| 3.17 Reverse transcriptase - Polymerase chain reaction (RT-PCR): -----                             | 67        |
| 3.18 Real-Time Quantitative PCR: -----   | 68        |
| 3.19 Co-immunoprecipitation (Co-IP): -----   | 69        |
| 3.20 Immunofluorescence: -----   | 69        |
| 3.21 Actin organization:-----  | 70        |
| 3.22 MTT (3-(4, 5-Dimethylthiazol-2-yl)-2, 5-Diphenyltetrazolium Bromide) cell viability assay: -- | 71        |
| 3.23 Colony forming assay: -----   | 71        |
| 3.24 In vitro wound healing assay for migration: -----   | 71        |
| 3.25 Transwell migration assay and boyden chamber cell invasion assay:-----                        | 72        |
| 3.26 Soft agar assay: -----  | 72        |
| 3.27 In vivo Tumorigenicity assay: -----   | 73        |
| 3.28 Gelatin zymography: -----   | 73        |
| 3.29 Isolation of Cytoplasmic and nuclear fractions: -----   | 74        |
| 3.30 RhoA/Rac1/Cdc42 activation assay:-----  | 74        |

|  |            |
|--|------------|
| 3.31 Fractionation and Quantification of F-Actin: .....  | 75         |
| 3.32 SWATH (sequential window acquisition of all theoretical fragment ion spectra) analysis: ----  | 76         |
| 3.33 Histology and Immunohistochemistry: .....   | 77         |
| 3.34 Densitometry quantification and Statistical analysis: .....   | 78         |
| <b>4. Results</b> .....  | <b>79</b>  |
| 4.1 BPAG1e interacts with K8 in OSCC derived cells.....  | 80         |
| 4.2 Knockdown of hemidesmosomal linker proteins in AW13516 cells .....   | 81         |
| 4.3 Phenotypic assays for cell transformation .....  | 84         |
| 4.3.1 Loss of Hemidesmosomal linker proteins led to reduced cell migration, cell invasion and alterations in actin organization.....                             | 84         |
| 4.3.2 Downregulation of hemidesmosomal linker proteins led to reduction in the tumorigenic potential of AW13516 cells .....                                      | 90         |
| 4.4 Expression of associated proteins upon loss of hemidesmosomal linker proteins.....   | 94         |
| 4.5 SWATH analysis demonstrated differential expression of several proteins in linker proteins knockdown AW13516 cells as compared to vector control cells. .... | 95         |
| 4.6 NDRG1 upregulation in HD linker protein knockdown cells .....  | 96         |
| 4.7 Knockdown of NDRG1 in BPAG1e-Plectin downregulated AW13516 (NDRG1-BPAG1e-Plectin triple knockdown) and parental AW13516 cells (NDRG1 single knockdown) ..... | 98         |
| 4.8 NDRG1 downregulation rescues HD linker proteins knockdown phenotype.....   | 99         |
| 4.9 NDRG1 regulates cell motility through p21 .....  | 107        |
| 4.10 The phenotypic and molecular changes observed upon HD linker proteins are not cell line specific .....  | 108        |
| <b>5. Discussion</b> .....   | <b>113</b> |
| <b>6. Summary and Conclusion</b> .....   | <b>123</b> |
| 6.1 Summary:.....  | 124        |
| 6.2 Conclusion: .....  | 125        |
| <b>7. References</b> .....   | <b>127</b> |
| <b>Annexure 1</b> .....  | <b>155</b> |



# *Synopsis*



## Homi Bhabha National Institute

### Ph. D. PROGRAMME

- 1. Name of the Student:** Pratik Rajeev Chaudhari
- 2. Name of the Constituent Institution:** TMC-ACTREC
- 3. Enrolment No.:** LIFE09201204012
- 4. Title of the Thesis:** Role of hemidesmosomal linker proteins in neoplastic progression of squamous cell carcinomas
- 5. Board of Studies:** Life Sciences

### Synopsis

#### Introduction:

#### 1. Hemidesmosomal assembly:

Hemidesmosomes (HDs) are located at the basal side of epithelial cells where they link the extracellular matrix to the intermediate filament network in the cell. Thus, HDs provide stable adhesion of epithelia to the basement membrane and contribute to the resistance to mechanical stress of epithelial tissues. There are two types of HDs having different protein composition. The skin and other complex epithelia assemble type I HDs, which consist of the  $\alpha 6\beta 4$  integrin, plectin, CD151 and the bullous pemphigoid antigens BP230 (BPAG1e) and BP180 (BPAG2).  $\alpha 6\beta 4$

integrin, BP180 and CD151 are transmembrane proteins while plectin and BPAG1e are located in the cytoplasm. Among these proteins  $\alpha 6\beta 4$  integrin connects the cells to laminin-5 of the basement membrane whereas plectin and BPAG1e connect the keratin filaments to hemidesmosomal junction through  $\alpha 6\beta 4$  integrin. Type II HDs are found in simple epithelia such as intestine, and are composed of proteins  $\alpha 6\beta 4$  integrin and plectin <sup>1-4</sup>.

## **2. Hemidesmosomal linker proteins:**

Plectin and BPAG1e are two members of the plakin family of cytoskeletal linker proteins. The fibronectin domain of  $\beta 4$  integrin interacts with N-terminal Plakin domain of BPAG1e and Plectin <sup>5</sup>. Interaction of the BPAG1e and plectin with intermediate filaments is mediated by Plakin repeat domain (PRD) within their COOH terminus <sup>4</sup>. Loss of either BPAG1e expression in keratinocytes results in the formation of blisters, due to disruption of basal cell/dermal adhesion <sup>6</sup>. These data emphasize the importance of plakins in regulating adhesion in the skin. BPAG1e-null animals also display impaired wound healing *in vivo* <sup>6</sup>. This result indirectly implicates that BPAG1e as a potential regulator of keratinocyte migration. It has been reported that increased BPAG1e expression is found in invasive squamous cell carcinomas <sup>7</sup>. A recent report has shown that BPAG1e regulates keratinocyte migration by acting as a scaffold for  $\beta 4$  integrin mediated signaling to Rac1 <sup>8</sup>. The other linker protein, Plectin, promotes the migration and invasion of HNSCC cells through activation of Erk 1/2 kinase <sup>9</sup>. It has been also reported that plectin regulates invasiveness in colon carcinoma cells and is targeted to podosome-like adhesions in an isoform-specific manner <sup>10</sup>. Moreover, transient knockdown of plectin alters hepatocellular motility in association with higher Rac1 activity <sup>11</sup>.

## **3. Keratin Intermediate filaments:**

Keratins (K) are divided into type I acidic keratins (K9-K10, K12-K28, K31-K40) and type II basic keratins (K1-K8, K71-K86) on the basis of their biochemical properties. They are obligate noncovalent heteropolymers that include at least one type I and one type II keratins which pair together during filament formation<sup>12</sup>. Keratins are expressed in a tissue specific and differentiation dependent manner. e.g. K8/18 in simple epithelial cells like hepatocytes and K5/14 in stratified squamous epithelia like skin<sup>13-14</sup>.

#### **4. Keratin 8/18 and Cancer:**

Aberrant expression of K8/18 is seen in case of squamous cell carcinomas (SCC)<sup>15-17</sup>. Transgenic mice expressing human K8 in the epidermis have a dramatic increase in the progression of papillomas towards malignancy<sup>18</sup>. Previous work in our laboratory has shown that K8 overexpression leads to neoplastic transformation and increased metastatic potential in FBM cell line<sup>19</sup>. It has also been reported that K8/18 expression indicates a poor prognosis in SCC of the oral cavity<sup>17</sup>. It has been shown that loss of K8/18 leads to alterations in  $\alpha 6\beta 4$  integrin-mediated signaling and decreased neoplastic progression in an oral tumor derived cell line<sup>20</sup>.

#### **Rationale:**

In our previous study, we have shown that  $\beta 4$  Integrin mediated signaling is modulated in response to K8 down regulation in OSCC derived cells<sup>20</sup>. Linker proteins like Plectin and BPAG1e anchor keratin proteins to cell surface via  $\beta 4$  integrin<sup>3-4</sup>. The importance of plakins in maintaining tissue integrity is well understood. However the role of these linker proteins in cell motility is not yet well studied. BPAG1e null animals display impaired wound healing *in vivo*<sup>6</sup>. This observation indirectly implicates BPAG1e as a potential regulator of keratinocyte migration. Increased expression of BPAG1e in squamous cell carcinomas has also been shown<sup>7</sup>. Thus,

knockdown of BPAG1e in OSCC derived cell line will enable us to understand the role of linker proteins in keratin mediated regulation of  $\beta$ 4 integrin signaling in neoplastic progression of SCC.

**Key Questions:**

1. What is the role of linker proteins in keratin mediated regulation of  $\beta$ 4 integrin signaling in neoplastic progression of squamous cell carcinomas?
2. Do linker proteins regulate cell motility and invasion in SCC, if yes then how?

**Specific objectives:**

To-

1. knockdown BP230 gene in an oral SCC derived cell line AW13516 using shRNA technology.
2. study interactions between keratin 8 and  $\beta$ 4 integrin in parental and knockdown cells.
3. carry out phenotypic assays for cell transformation for parental and knockdown cells and compare them with K8 knockdown cells.
4. study effects of downregulation of BP230 on polymerization of cytoskeletal elements such as actin, keratins and their regulators.

**Materials and methods:**

**Ethics statement**

All protocols for animal studies were approved by the Institutional Animal Ethics Committee (IAEC) (approval ID: 04/2015). A Committee formed under the guidelines of Committee for the Purpose of Control & Supervision of Experiments on Animals (CPCSEA), Government of India.

**Cell lines and Plasmids**

The human tongue SCC derived cell lines AW13516 and AW8507 were previously established in Cancer Research Institute, Tata memorial Centre, Parel, Mumbai <sup>21</sup>. These cell lines were

cultured in IMDM supplemented with 10% fetal bovine serum and antibiotics under a 5% CO<sub>2</sub> atmosphere at 37°C.

The pLKO1.puro (plasmid #10878), pLKO1.neo (plasmid #13425) and pLKO1.hygro (plasmid #24150) plasmids were purchased from Addgene, USA. The pLKO1.puro plasmid containing shRNA sequence against BPAG1e was a kind gift from Dr. Jonathan Jones, Washington State University, USA. shRNA sequences against Plectin and NDRG1 were designed and cloned in pLKO1.neo and pLKO1.hygro plasmids respectively. BPAG1e-Plectin double knockdown was generated by transducing lentivirus encoding shRNA against BPAG1e in Plectin knockdown cells. The empty vector backbone was used to generate the respective vector control clones.

#### **qRT-PCR, western blotting, immunoprecipitation and immunofluorescence**

qRT-PCR were performed as described previously<sup>22</sup>. Cell lysates for western blotting were prepared in SDS lysis buffer. For immunoprecipitation, cell lysates were made by pooling both NP-40 (1%) and Empigen (2%) fractions as described previously<sup>23</sup>. Immunofluorescence assay was performed as described previously<sup>22</sup>.

#### **Phenotypic assays for cell transformation**

Scratch wound migration assay, soft agar assay, *in vivo* tumorigenicity assay and gelatin zymography were performed as described previously<sup>20, 24-25</sup>. Transwell migration assay was carried out in a manner similar to invasion assay, without coating the matrigel<sup>26</sup>. Cell proliferation and clonogenic assays were performed as described previously<sup>22</sup>.

#### **SWATH analysis**

SWATH analysis was performed at NCL, Pune as described previously<sup>27</sup>.

#### **Densitometric quantification and statistical analysis:**

Densitometric quantification of scanned images was performed by ImageJ software (NIH, USA). Band intensities were normalized to respective loading controls. All the statistical analyses were performed using GraphPad Prism software (version 6.01). Two groups of data were statistically analyzed by Student's t test. A *p* value less than 0.05 was considered statistically significant.

## **Results:**

### **BPAG1e interacts with K8 in OSCC derived cells**

BPAG1e is expressed in the basal layer of squamous cell epithelia, whereas K8 is normally expressed in simple epithelia<sup>3, 28</sup>. In case of OSCC and OSCC derived cell lines, K8/18 is aberrantly expressed<sup>15-16, 20</sup>. Therefore, to understand whether BPAG1e interacts with K8, immunoprecipitation (IP) assay was performed. Co-IP of K8 was observed when antibody for BPAG1e was used for IP. Similarly, pull down fraction of K8 IP showed presence of BPAG1e. These results indicated that K8 interacts with BPAG1e in OSCC derived cells.

### **Knockdown of hemidesmosomal linker proteins in AW13516 cells**

Both single and double knockdown of Plectin and/or BPAG1e was carried out using shRNA technology. Down regulation of HD linker proteins was confirmed at mRNA and protein level. BPAG1e knockdown clones C4 and C12 displayed ~79% decrease in BPAG1e protein. Plectin knockdown clones C1 and C2 showed about ~94% reduction in Plectin expression at protein level whereas Further, decrease in Plectin (~93%) and BPAG1e (~81%) protein levels were observed in double knockdown cells.

### **Loss of Hemidesmosomal linker proteins led to reduced cell migration, cell invasion and alterations in actin organization**

Scratch wound healing assay demonstrated decrease in cell migration in both single and double linker proteins knockdown clones as compared to respective vector control clones. The rate of cell migration was reduced by ~29%, ~33% and ~36% in BPAG1e, Plectin and BPAG1e-Plectin double knockdown cells respectively. It is well documented that cell migration is regulated by changes in the actin organization<sup>29</sup>. Therefore, actin organization was analyzed using phalloidin staining followed by confocal microscopy. filopodia in vector control cells were found to be uniformly present on cell membrane whereas in case of loss of hemidesmosomal linker proteins, filopodia were non-uniformly organized. Moreover, the length of membrane protrusions was reduced in linker proteins knockdown cells. A number of proteins are involved in the regulation of cell motility, out of which Rho GTPases play a crucial role in the reorganization of the actin cytoskeleton. One of the Rho GTPases family member, Cdc42, regulates cellular motility by controlling filopodia formation<sup>30</sup>. Cdc42 activation assay revealed that activity of Cdc42 was significantly reduced upon linker proteins knockdown. Further, actin polymerization assay revealed reduced levels of F-actin in BPAG1e, Plectin and BPAG1e-Plectin knockdown cells as compared to respective vector control cells. Actin related proteins (Arp) 2/3 complexes are one of the important actin regulators which participate in nucleation and branching of actin filaments<sup>31</sup>. In BPAG1e, Plectin and BPAG1e-Plectin knockdown cells, we observed reduction in Arp2 and Arp3 protein levels. Altogether, these results indicated that reduced Cdc42 activity in linker proteins knockdown cells led to decreased expression of Arp2 and Arp3 proteins, resulting in shorter and fewer filopodia. This explains the reduced cell migration observed in linker proteins knockdown cells.

Furthermore, linker proteins knockdown cells were less invasive as compared with respective vector control cells. The invasion was reduced by ~30-35%, ~32-35% and ~37- 40% in BPAG1e,

Plectin and BPAG1e-Plectin double knockdown cells respectively. It has been shown that increased activity of Matrix Metalloproteinases (MMPs) (MMP2 and MMP9) correlates with invasive potential of OSCC <sup>32</sup>. The MMP9, but not MMP2, activity was significantly reduced in double knockdown cells as compared to vector control cells.

### **Downregulation of hemidesmosomal linker proteins led to reduction in the tumorigenic potential of AW13516 cells**

In our previous study, we have demonstrated that loss of K8 in AW13516 cells leads to reduction in tumorigenic potential of OSCC derived cells <sup>20</sup>. BPAG1e, Plectin and BPAG1e-Plectin double knockdown clones showed a significant reduction in number of colonies by ~20-30% and colony size by ~60-65% as compared with respective vector control clones. Furthermore, the *in vivo* tumorigenicity of linker proteins knockdown and respective vector control clones was assessed by subcutaneous injection in NOD-SCID mice (n=5). At the end of 8 weeks, the mean tumor volume of the mice bearing BPAG1e, Plectin and BPAG1e-Plectin double knockdown tumors was significantly reduced as compared with the average volume of tumors formed by the respective vector control cells.

### **Expression of associated proteins upon loss of hemidesmosomal linker proteins**

Previous study from our lab had shown downregulation of  $\beta$ 4 integrin and actin bundling protein Fascin in response to K8 knockdown <sup>20</sup>. Surprisingly, no changes were observed in expression of  $\beta$ 4 integrin and Fascin at protein level upon knockdown of HD linker proteins. Further, immunofluorescence studies demonstrated sparse filament organization for K8 and K5 upon loss of both hemidesmosomal linker proteins, indicating that linker proteins are essential to anchor keratins to the cell surface at hemidesmosomal sites. This observation indicated that linker proteins may not have role in K8 mediated effects observed in OSCC cells.

**SWATH analysis demonstrated differential expression of proteins in linker protein knockdown AW13516 cells as compared to vector control cells.**

To understand global changes in protein profile of linker protein knockdown cells as compared to vector control cells, we performed SWATH analysis for BPAG1e-Plectin knockdown clone C4 and respective vector control clone. We shortlisted proteins with p-value less than 0.05. The cut off value for upregulated and downregulated proteins was 1.3 and 0.76 respectively. After filtering, total 45 proteins were found to be significantly altered (17 upregulated and 28 downregulated). Some of the differentially expressed proteins were Vimentin, LIMA1, NDRG1, Galectin, 14-3-3 protein epsilon, S100-A6 etc. Out of which, we selected NDRG1 (N-myc downstream regulated gene 1) for further analysis, as it is an anti-metastatic protein which plays role in actin organization, cell migration, cell invasion and tumorigenesis<sup>33-35</sup>.

**NDRG1 downregulation rescues HD linker protein knockdown phenotype**

To validate the results obtained from SWATH analysis, we performed western blot for NDRG1 in linker proteins knockdown cells. Indeed, NDRG1 protein expression was found to be upregulated in BPAG1e (~1.6 fold), Plectin (~1.75 fold) and BPAG1e-Plectin (~2.1 fold) knockdown clones as compared to respective vector control clone. To verify whether the phenotype associated with cell transformation in HD linker proteins knockdown cells was due to higher NDRG1 levels, it was stably down regulated in Plectin-BPAG1e double knockdown clone C4. In NDRG1-Plectin-BPAG1e triple knockdown cells, NDRG1 protein expression was reduced by ~80%. The triple knockdown clones (C1, C7) displayed only ~10% decrease in rate of cell migration, whereas double knockdown cells showed ~39% decrease in cell migration. The filopodia in triple knockdown cells were found to be uniformly present which was similar to respective vector control cells, whereas in case of loss of hemidesmosomal linker proteins, filopodia were found to

be non-uniformly organized. Additionally, filamentous actin and Arp2/3 levels were restored in NDRG1-BPAG1e-Plectin triple knockdown cells as compared to BPAG1e-Plectin double knockdown cells. Further, *In vitro* invasion was reduced by only ~10-15% in triple knockdown cells as compared to ~37% reduction in double knockdown cells. Furthermore, triple knockdown cells showed restoration of MMP9 activity as compared to double knockdown cells. Moreover, triple knockdown cells showed ~10% decrease in number of colonies on soft agar as compared to ~30% reduction in colony number in double knockdown cells. Further, *in vivo* experiments suggested that there was no significant difference in mean tumor volume of mice bearing triple knockdown cells and vector control cells. Furthermore, NDRG1 single knockdown in AW13516 cells resulted in increased cell motility, invasion and tumorigenicity. Altogether, these results indicated that NDRG1 knockdown displayed rescue in HD linker protein knockdown phenotype.

#### **NDRG1 upregulates p21 by targeting $\Delta$ Np63**

Previously, it has been reported that NDRG1 expression leads to down regulation of  $\Delta$ Np63 levels, which allows transactivation of the p21 gene by TAp63 leading to upregulated p21 levels. Further, increased p21 can inhibit cell migration and reduce the metastatic potential of cancer cells<sup>36</sup>. Upon loss of HD linker proteins, NDRG1 and p21 were up regulated whereas  $\Delta$ Np63 expression was reduced. Contrary to this, NDRG1 knockdown in parental AW13516 cells resulted in decreased p21 levels and increased  $\Delta$ Np63 levels. Moreover, triple knockdown cells exhibited similar results as that of NDRG1 knockdown cells. Likewise, NDRG1 single knockdown resulted in decreased p21 and increased  $\Delta$ Np63 protein levels. These results indicate that hemidesmosomal linker proteins can also regulate cell motility through NDRG1-  $\Delta$ Np63-p21 pathway in OSCC derived cells.

#### **Validation of results in another tongue SCC derived cell line AW8507**

To find out whether the effects observed in AW13516 cells were cell line specific, we carried out similar experiments in another tongue SCC derived cell line AW8507. AW 8507 cells were derived from poorly differentiated epidermoid carcinoma of the tongue <sup>21</sup>. Both single and double knockdown of BPAG1e and/or Plectin in AW8507 cells was carried out using shRNA technology. The linker protein knockdown AW8507 cells also showed increased NDRG1 levels. Further, to verify whether the phenotype associated with cell transformation in HD linker proteins knockdown AW8507 cells was due to higher NDRG1 levels, NDRG1 was stably downregulated in BPAG1e-Plectin knockdown clone GDC3. The results of phenotypic assays for cell transformation like Boyden chamber transwell assay, *in vitro* invasion assay, soft agar assay and *in vivo* tumorigenicity assay for AW8507 knockdown systems were similar to those found in AW13516 knockdown system indicating that molecular and phenotypic alterations observed upon loss of BPAG1e and Plectin are not cell line specific.

**Summary and significance of the study:**

1. BPAG1e interacts with K8 in OSCC derived AW13516 cells.
2. BPAG1e and/or Plectin knockdown in tongue SCC cell lines resulted in reduction in cell motility, cell invasion, tumorigenicity and altered actin organization.
3. SWATH analysis for linker proteins knockdown and vector control cells showed alterations in levels of several proteins, out of which, NDRG1 was upregulated in linker proteins knockdown cells.
4. Partial rescue of phenotype for cell transformation was observed upon knockdown of NDRG1 in BPAG1e-Plectin triple knockdown cells as compared to BPAG1e-Plectin double knockdown cells.

5. NDRG1 single knockdown in AW13516 cells showed increase in cell motility, cell invasion and tumorigenic potential.
6. BPAG1e-Plectin knockdown cells displayed non-uniformly organized filopodia, whereas NDRG1-BPAG1e-Plectin knockdown cells showed uniformly arranged filopodia. Consistent with altered actin organization, Cdc42 activity, filamentous actin levels and Arp2/3 levels were reduced in BPAG1e-Plectin double knockdown cells, whereas Cdc42 activity, filamentous actin levels and Arp2/3 expression was rescued in NDRG1-BPAG1e-Plectin triple knockdown cells. This could be one of the possible mechanism by which decreased cell migration was observed upon loss of linker proteins.
7. Upregulation of p21 by targeting  $\Delta$ Np63 in response to NDRG1 upregulation was observed in BPAG1e-Plectin knockdown cells, whereas NDRG1-BPAG1e-Plectin triple knockdown cells showed restoration of levels of p21 and  $\Delta$ Np63. This could be another possible mechanism by which reduced cell migration was observed upon loss of linker proteins.
8. MMP9 activity was substantially decreased in BPAG1e-Plectin double knockdown cells, whereas it was partially restored in NDRG1-BPAG1e-Plectin triple knockdown cells which correlated with results of *in vitro* invasion assay.
9. The results in another tongue SCC derived cell line (AW8507) revealed that the role of hemidesmosomal linker proteins is not cell line specific.

In conclusion, this study demonstrates that BPAG1e and/or Plectin play role in cell motility, actin organization, cell invasion and tumorigenicity in OSCC derived cells possibly through NDRG1. Thus, the current project is a step forward in our quest to understand functional significance of aberrant expression of intermediate filaments and their associated proteins and further their use as a battery of biomarkers for management of human oral cancer.

## References:

1. Fontao L., Favre B., Riou S., Geerts D., Jaunin F., Saurat J., Green K., Sonnenberg A., Borradori L. Interaction of the Bullous Pemphigoid Antigen 1 (BP230) and Desmoplakin with Intermediate Filaments Is Mediated by Distinct Sequences within Their COOH Terminus. *Mol Biol Cell* (2003). 14: 1978–92.
2. Litjens SH, de Pereda JM, Sonnenberg A. Current insights into the formation and breakdown of hemidesmosomes. *Trends Cell Biol* (2006). 16(7): 376-83.
3. Jones JCR, Hopkinson SB and Goldfinger LE. Structure and assembly of hemidesmosomes. *BioEssays*, (1998). 20: 488-494.
4. Chaudhari PR, Vaidya MM. Versatile hemidesmosomal linker proteins: structure and function. *Histol Histopathol* (2015). 30(4):425-34.
5. de Pereda JM, Ortega E, Alonso-Garcia N, Gomez-Hernandez M, Sonnenberg A. Advances and perspectives of the architecture of hemidesmosomes: lessons from structural biology. *Cell Adh Migr* (2009). 3(4): 361-4.
6. Guo L, Degenstein L, Dowling J, Yu QC, Wollmann R, Perman B, Fuchs E. Gene targeting of BPAG1, abnormalities in mechanical strength and cell migration in stratified epithelia and neurologic degeneration. *Cell* (1995). 81: 233–43.
7. Herold-Mende C, Kartenbeck J, Tomakidi P, Bosch FX. Metastatic growth of squamous cell carcinomas is correlated with upregulation and redistribution of hemidesmosomal components. *Cell Tissue Res* (2001). 306: 399-408.
8. Hamill KJ, Hopkinson SB, DeBiase P, Jones JCR. BPAG1e Maintains Keratinocyte Polarity through  $\beta$ 4 Integrin-mediated Modulation of Rac 1 and Cofilin Activities. *Mol Biol Cell* (2009). 20: 2954–62.
9. Katada K, Tomonaga T, Satoh M, Kazuyuki M, Tonoike Y, Kodera Y, Nomura F, Okamoto Y. Plectin promotes migration and invasion of cancer cells and is a novel prognostic marker for head and neck squamous cell carcinoma. *J Proteomics* (2012). 75: 1803–1815.
10. McInroy L, Maatta A. Plectin regulates invasiveness of SW480 colon carcinoma cells and is targeted to podosome-like adhesions in an isoform-specific manner. *Exp Cell Res* (2011). 317: 2468–78.
11. Cheng CC, Lai YC, Lai YS, Hsu YH, Chao WT, Sia KC, Tseng YH, Liu YH. Transient knockdown-mediated deficiency in plectin alters hepatocellular motility in association with activated FAK and Rac1-GTPase. *Cancer Cell Int* (2015). 15:29-35
12. Schweizer J, Bowden PE, Coulombe PA, Langbein L, Lane EB, Magin TM, Maltais L, Omary MB, Parry DA, Rogers MA, Wright MW. New consensus nomenclature for mammalian keratins. *J Cell Biol* (2006). 174(2): 169-74.
13. Coulombe PA, Omary MB. 'Hard' and 'soft' principles defining the structure, function and regulation of keratin intermediate filaments. *Curr Opin Cell Biol* (2002). 14(1): 110-22.

14. Fuchs E, Weber K. Intermediate filaments: structure, dynamics, function, and disease. *Annu Rev Biochem* (1994). 63: 345-82.
15. Vaidya MM, Borges AM, Pradhan SA, Bhisey AN. Cytokeratin expression in squamous cell carcinomas of the tongue and alveolar mucosa. *Eur J Cancer* (1996). 32B(5): 333-6.
16. Schaafsma HE, Van Der Velden LA, Manni JJ, Peters H, Link M, Rutter DJ, Ramaekers FC. Increased expression of cytokeratins 8, 18 and vimentin in the invasion front of mucosal squamous cell carcinoma. *J Pathol* (1993). 170(1): 77-86.
17. Fillies T, Werkmeister R, Packeisen J, Brandt B, Morin P, Weingart D, Joos U, Buerger H. Cytokeratin 8/18 expression indicates a poor prognosis in squamous cell carcinomas of the oral cavity. *BMC Cancer* (2006). 6: 10-17.
18. Casanova ML, Bravo A, Martinez-Palacio J, Fernandez-Acenero MJ, Villanueva C, Larcher F, Conti CJ, Jorcano JL. Epidermal abnormalities and increased malignancy of skin tumors in human epidermal keratin 8-expressing transgenic mice. *FASEB J* (2004). 18(13): 1556-8.
19. Raul U, Sawant S, Dange P, Kalraiya R, Ingale A, Vaidya M. Implications of cytokeratin 8/18 filament formation in stratified epithelial cells: induction of transformed phenotype. *Int J Cancer* (2004). 111(5): 662-8.
20. Alam H, Kundu S, Dalal N, Vaidya M. Loss of keratins 8 and 18 leads to alterations in  $\alpha 6\beta 4$ -integrin-mediated signalling and decreased neoplastic progression in an oral-tumor-derived cell line. *J Cell Sci* (2011). 124(12): 2096-106.
21. Tatake RJ, Rajaram N, Damle RN, Balsara B, Bhisey AN, Gangal SG. Establishment and characterization of four new squamous cell carcinoma cell lines derived from oral tumors. *J Cancer Res Clin Oncol* (1990). 116: 179-86.
22. Alam H, Sehgal L, Kundu ST, Dalal SN, Vaidya MM. Novel function of keratins 5 and 14 in proliferation and differentiation of stratified epithelial cells. *Mol Biol Cell* (2011). 22(21):4068-78.
23. Srikanth B, Vaidya MM, Kalraiya RD. O-GlcNAcylation determines the solubility, filament organization, and stability of keratins 8 and 18. *J Biol Chem* (2010). 285(44):34062-71.
24. Iyer SV, Dange PP, Alam H, Sawant SS, Ingle AD, Borges AM, Vaidya MM. Understanding the role of keratins 8 and 18 in neoplastic potential of breast cancer derived cell lines. *PloS one*. (2013). 8(1):e53532.
25. Dange MC, Agarwal AK, Kalraiya RD. Extracellular galectin-3 induces MMP9 expression by activating p38 MAPK pathway via lysosome-associated membrane protein-1 (LAMP1). *Mol Cell Biochem* (2015). 404(1-2):79-86.
26. Dmello C, Sawant S, Alam H, Gangadaran P, Tiwari R, Dongre H, Vaidya MM. Vimentin-mediated regulation of cell motility through modulation of beta4 integrin protein levels in oral tumor derived cells. *Int J Biochem Cell Biol* (2016). 70: 161-72.
27. Huang Q, Yang L, Luo J, Guo L, Wang Z, Yang X, Jin W, Fang Y, Ye J, Shan B, Zhang Y. SWATH enables precise label-free quantification on proteome scale. *Proteomics* (2015). 15: 1215-1223.

28. Moll R, Franke WW, Schiller DL, Geiger B, Krepler R. The catalog of human cytokeratins: patterns of expression in normal epithelia, tumors and cultured cells. *Cell* (1982). 31: 11-24.
29. Mogilner A, Oster G. Cell motility driven by actin polymerization. *Biophys J* (1996). 71: 3030–45.
30. Nobes CD, Hall A. Rho, Rac, and Cdc42 GTPases regulate the assembly of multimolecular focal complexes associated with actin stress fibers, lamellipodia, and filopodia. *Cell* (1995). 07; 81(1): 53-62.
31. T. Takenawa, S. Suetsugu, The WASP-WAVE protein network: connecting the membrane to the cytoskeleton, Nature reviews. *Mol Cell Biol* (2007). 8:37-48.
32. de Vicente JC, Fresno MF, Villalain L, Vega JA, Hernández Vallejo G. Expression and clinical significance of matrix metalloproteinase-2 and matrix metalloproteinase-9 in oral squamous cell carcinoma. *Oral Oncol* (2005). 41(3): 283-93.
33. Yan L, Wen B, Wen L, De Z, Yan Y, Zhi X, Fang Z. Downregulation of NDRG1 promotes invasion of human gastric cancer AGS cells through MMP-2. *Tumor Biol* (2011). 32: 99-105.
34. Sun J, Xhang D, Zheng Y, Richardson D. Targeting the Metastasis Suppressor, NDRG1, Using Novel Iron Chelators: Regulation of Stress Fiber-Mediated Tumor Cell Migration via Modulation of the ROCK1/pMLC2 Signaling Pathway. *Mol Pharmacol* (2013). 83:454–469.
35. Lee JC, Chung LV, Chen YJ, Feng TH, Juang HH. N-myc downstream-regulated gene 1 downregulates cell proliferation, invasiveness, and tumorigenesis in human oral squamous cell carcinoma. *Cancer lett* (2014). 355:242–252
36. Kovacevic Z, Sivagurunathan S, Mangs H, Chikhani S, Zhang D, Richardson D. The metastasis suppressor, N-myc downstream regulated gene 1 (NDRG1), upregulates p21 via p53-independent mechanisms. *Carcinogenesis* (2011). 32(5):732-40.

**Publications in Refereed Journal:**

**a. Published:**

1. Review article: Chaudhari PR and Vaidya MM. Versatile hemidesmosomal linker proteins: structure and function. *Histol Histopathol* (2015). 30(4):425-34.
2. Research article: Chaudhari PR, Charles SE and Vaidya MM. Role of BPAG1e in neoplastic progression of oral squamous cell carcinoma derived cells. *Int J Pharm Bio Sci* (2017). 8(1):(B) 519-27.

**b. Accepted:**

Chaudhari PR, Charles SE, Dsouza ZC and Vaidya MM. Hemidesmosomal linker proteins regulate cell motility, invasion and tumorigenicity in oral squamous cell carcinoma derived cells. *Exp Cell Res* (2017). <http://dx.doi.org/10.1016/j.yexcr.2017.08.034>

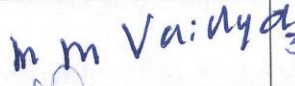
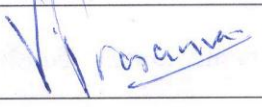
**Other Publications:**

- a. Book/Book Chapter: Nil
- b. Conference/Symposium:
1. Platform presentation at XXXVIII All India Cell Biology Conference on Cellular response to drugs held during 10-12 December, 2014 at Central Drug Research Institute, Lucknow, India. (Received Prof. V. C. Shah memorial award for best platform presentation)
  2. Platform presentation at Gordon Research Seminar on Intermediate Filaments and Poster presentation at Gordon Research Conference on Intermediate Filaments held during 11-17 June, 2016 at Stoweflake Conference Center, Stowe, VT, USA. (Received Nature travel grant to attend the conference)

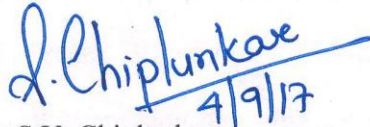
Signature of Student: PR Haudhari

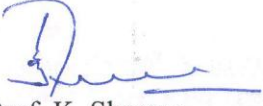
Date: 29/08/2017

**Doctoral Committee:**

| S. No. | Name                 | Designation     | Signature   | Date     |
|--------|----------------------|-----------------|---|----------|
| 1.     | Dr. Sorab N. Dalal   | Chairman        |    | 30/08/17 |
| 2.     | Dr. Milind M. Vaidya | Guide/ Convener |   | 30/08/17 |
| 3.     | Dr. V. Prasanna      | Member          |   | 30/08/17 |
| 4.     | Dr. Sanjay Gupta     | Member          |  | 01/09/17 |

Forwarded Through:

  
Dr. S.V. Chiplunkar  
Director, ACTREC &  
Chairperson, Academic &  
Training Program, ACTREC  
**Dr. S. V. Chiplunkar**  
Director  
Advanced Centre for Treatment, Research &  
Education in Cancer (ACTREC)  
Tata Memorial Centre  
Charghar, Navi Mumbai - 410 210.

  
Prof. K. Sharma  
Director, Academics  
T.M.C.  
**PROF. K. S. SHARMA**  
DIRECTOR (ACADEMICS)  
TATA MEMORIAL CENTRE,  
PAREL, MUMBAI



## List of Figures

| <b>Figure legend</b>  | <b>Page no.</b> |
|---|-----------------|
| Figure 2.1: Schematic representation of hemidesmosomal components   | 34              |
| Figure 2.2: Schematic representation of structural domains of hemidesmosomal linker proteins                            | 39              |
| Figure 4.1: BPAG1e interacts with K8 in AW13516 cells   | 80              |
| Figure 4.2: Loss of hemidesmosomal linker protein(s) does not affect expression of associated proteins                  | 83              |
| Figure 4.3: Loss of BPAG1e leads to reduced cell migration, cell invasion and alterations in actin organization         | 85              |
| Figure 4.4: Loss of Plectin leads to reduced cell migration, cell invasion and alterations in actin organization        | 86              |
| Figure 4.5: Loss of BPAG1e-Plectin leads to reduced cell migration, cell invasion and alterations in actin organization | 87              |
| Figure 4.6: Effect of hemidesmosomal linker protein(s) knockdown on activity of Rho GTPases and actin polymerization    | 88              |
| Figure 4.7: Loss of BPAG1e leads to reduced tumorigenic potential   | 91              |
| Figure 4.8: Loss of Plectin leads to reduced tumorigenic potential  | 92              |
| Figure 4.9: Loss of BPAG1e-Plectin leads to reduced tumorigenic potential   | 93              |
| Figure 4.10: Effect of hemidesmosomal protein(s) knockdown on keratin filament organization                             | 94              |
| Figure 4.11: NDRG1 protein expression in hemidesmosomal linker protein(s) knockdown cells                               | 97              |
| Figure 4.12: NDRG1 downregulation in BPAG1e-Plectin knockdown background rescues cell migration and actin organization  | 99              |
| Figure 4.13: NDRG1 downregulation in BPAG1e-Plectin knockdown background rescues cell invasion and tumorigenicity       | 102             |

|  |     |
|--|-----|
| Figure 4.14: Loss of NDRG1 in AW13516 cells leads to increased cell migration, cell invasion and actin polymerization  | 104 |
| Figure 4.15: Loss of NDRG1 in AW13516 cells leads to increased tumorigenic potential   | 105 |
| Figure 4.16: The tumors isolated from BPAG1e-Plectin and NDRG1-BPAG1e-Plectin cells injected in NOD-SCID mice showed similar molecular alterations to that of <i>in vitro</i> system | 106 |
| Figure 4.17: NDRG1 possibly regulates cell motility through p21  | 108 |
| Figure 4.18: Loss of BPAG1e-Plectin in AW8507 cells leads to decrease in cell migration, invasion and tumorigenicity   | 110 |
| Figure 4.19: NDRG1 downregulation in BPAG1e-Plectin knockdown background rescues the phenotype in AW8507 cells   | 111 |
| Figure 5.1: Schematic representation of the role of Hemidesmosomal linker proteins in OSCC derived cells   | 122 |

## List of Tables

| <b>Table legend</b>  | <b>Page no.</b> |
|--|-----------------|
| Table 2.1: Classification of IFs based on their type and cell-type specificity | 46              |
| Table 3.1: List of reagents with their particulars                             | 53              |
| Table 3.2: List of BPAG1e shRNA sequences along with their target site         | 57              |
| Table 3.3: List of Plectin shRNA sequences along with their target site        | 58              |
| Table 3.4: List of NDRG1 shRNA sequences along with their target site          | 58              |
| Table 3.5: The detailed composition of Stacking and Resolving SDS PAGE gels    | 63              |
| Table 3.6: List of antibodies with their particulars                           | 64              |
| Table 3.7: List of primers used for PCR  | 68              |

## Abbreviations

|        |  |
|--------|--|
| ABD    | Actin binding domain   |
| CAN    | Acetonitrile   |
| APS    | Ammonium persulphate   |
| ARP    | Actin related proteins   |
| BPAG1e | Bullous pemphigoid antigen 1e                                    |
| BPAG2  | Bullous pemphigoid antigen 2                                     |
| BSA    | Bovine Serum Albumin   |
| Cdc42  | Cell division control protein 42                                 |
| DAB    | Diaminobenzidine   |
| DAPI   | 4',6-diamidino-2-phenylindole                                    |
| DEPC   | Diethylpyrocarbonate   |
| DMEM   | Dulbecco's Modified Eagle Media                                  |
| DMSO   | Dimethyl sulfoxide   |
| DSs    | Desmosomes   |
| DTT    | 1, 4-Dithioerythritol  |
| ECL    | Enhanced Chemiluminescence                                       |
| ECM    | Extracellular matrix   |
| EDTA   | Ethylene Diamine Tetra Acetic acid                               |
| EGF    | Epidermal growth factor  |
| EGTA   | Ethylene glycol bis( $\beta$ -aminoethyl ether)-tetraacetic acid |
| EMT    | Epithelial mesenchymal transition                                |
| Ex/Em  | Extension/emission   |
| FA     | Formic acid  |
| FBM    | Fetal buccal mucosa  |
| FBS    | Fetal Bovine Serum   |
| GABEB  | General atrophic benign epidermolysis bullosa                    |
| GAPDH  | Glyceraldehyde 3-phosphate dehydrogenase                         |
| HRPO   | Horse Radish Peroxidase  |
| IFs    | Intermediate filaments   |
| IHC    | Immunohistochemistry   |
| IMDM   | Iscove's Modified Dulbecco's Media                               |
| HDs    | Hemidesmosomes   |
| HNSCC  | Head and Neck Squamous Cell Carcinoma                            |
| IDA    | information-dependent acquisition                                |
| IP     | Immunoprecipitation  |
| K      | Keratin  |

|          |   |
|----------|---|
| K5/14    | Keratin 5 and Keratin 14  |
| K8/18    | Keratin 8 and Keratin 18  |
| kDa      | Kilo Dalton   |
| LB       | Luria Bertani   |
| MMP      | Matrix metalloproteinase  |
| MFs      | Microfilaments  |
| MTs      | Microtubules  |
| MTT      | 3-(4, 5-Dimethylthiazol-2-yl)-2, 5-Diphenyltetrazolium Bromide        |
| NDRG1    | N-myc downstream regulated gene 1                                     |
| NOD-SCID | Nonobese diabetic/severe combined immunodeficiency                    |
| NP-40    | Nonidet P-40  |
| ns       | Non-significant   |
| NSCLC    | non small cell lung carcinoma   |
| OD       | Optical density   |
| OSCC     | Oral squamous cell carcinoma  |
| PAJEB    | Pyloric atresia with junctional epidermolysis bullosa                 |
| PBS      | Phosphate Buffered Saline   |
| PCR      | Polymerase Chain Reaction   |
| PIPES    | 1,4-Piperazinediethanesulfonic acid                                   |
| PRD      | Plakin repeat domain  |
| PVDF     | Poly Vinylenediflouride   |
| QRT-PCR  | Quantitative real time polymerase chain reaction                      |
| RT-PCR   | Reverse transcriptase polymerase chain reaction                       |
| RT       | Room temperature  |
| SCC      | Squamous cell carcinoma   |
| SDS      | Sodium Dodecyl Sulphate   |
| SDS-PAGE | Sodium dodecyl sulfate polyacrylamide gel electrophoresis             |
| SEM      | Standard error mean   |
| shRNA    | Short hairpin RNA   |
| SOB      | Super Optimal Broth   |
| SWATH    | Sequential window acquisition of all theoretical fragment ion spectra |
| TEMED    | N, N, N', N',-Tetramethylethylenediamine                              |
| WASP     | Wiskott–Aldrich syndrome family protein                               |



# *1. Introduction*

The cytoskeletal elements of a cell are connected by anchoring junctions to those of its neighbouring cell or to the extracellular matrix (ECM). Desmosomes (DSs) are cell-cell anchoring junctions, whereas hemidesmosomes (HDs) are cell-extracellular matrix junctions. HDs are located at the basal side of epithelial cells, where they link the ECM to the intermediate filament (IF) network in the cell. Thus, HDs provide stable adhesion of epithelia to the basement membrane and contribute to the resistance to mechanical stress of epithelial tissues (1, 2). There are two types of HDs having different protein composition. The skin and other complex epithelia assemble type I HDs, which consist of the  $\alpha6\beta4$  integrin, plectin, CD151 and the bullous pemphigoid antigens BPAG1e (bullous pemphigoid antigen 1e; BP230) and BPAG2 (bullous pemphigoid antigen 2; BP180).  $\alpha6\beta4$  integrin, BPAG2 and CD151 are transmembrane proteins, while plectin and BPAG1e are located in the cytoplasm. Type II HDs are found in simple epithelia such as intestine and are composed of proteins integrin  $\alpha6\beta4$ , plectin and CD151 (1, 3-5). In case of complex epithelia like skin,  $\alpha6\beta4$  integrin connects the cells to laminin-5 of the basement membrane, whereas plectin and BPAG1e connect the keratin (K) filaments to hemidesmosomal junction through  $\alpha6\beta4$  integrin (1, 2). Mutations in hemidesmosomal proteins lead to severe skin blistering disorders (6). Apart from their anchoring function, HDs are involved in  $\alpha6\beta4$  integrin mediated inside-out and outside-in signaling (1).

BPAG1e and Plectin are members of the plakin family of cytoskeletal linker proteins. The fibronectin domain of  $\beta4$  integrin interacts with N-terminal Plakin domain of BPAG1e and Plectin. Interaction of the BPAG1e and plectin with intermediate filaments is mediated by plakin repeat domain (PRD) within their -COOH terminus (7-9). Loss of either BPAG1e or Plectin expression in mouse keratinocytes results in the formation of blisters (10, 11). These data emphasize the importance of plakins in regulating dermal-epidermal adhesion. BPAG1e

knockout mice also display impaired wound healing *in vivo* (10). This result indirectly suggests that BPAG1e is a potential regulator of keratinocyte migration. Upregulation of BPAG1e expression has been reported in invasive squamous cell carcinomas (12). Further, BPAG1e knockdown in normal human epidermal keratinocytes display aberrant cell migration due to decreased Rac1 activity (13). Contrary to this, human keratinocytes carrying homozygous nonsense mutations in BPAG1e encoding gene show increased spreading and migration (14). Other linker protein, Plectin, promotes the migration and invasion of Head and Neck Squamous Cell Carcinoma (HNSCC) cells through activation of Erk 1/2 (15). It has been also reported that plectin regulates invasiveness in colon carcinoma cells and is targeted to actin rich podosomes (16). Moreover, plectin loss in liver cancer cells promotes cell motility (17, 18). In short, HD linker proteins can be positive or negative regulators of cell motility depending upon tissue type.

Keratins are the largest subgroup of intermediate filament proteins expressed in a tissue specific and differentiation dependent manner (19, 20). They are obligate noncovalent heteropolymers that include at least one type I and one type II keratins which pair together during filament formation (19). Aberrant expression of keratin 8/18 (K8/18) has been consistently shown in squamous cell carcinomas (SCCs) by different groups including ours (21-24). Our laboratory has also demonstrated that K8 overexpression leads to neoplastic transformation and increased invasive as well as metastatic potential in immortalized but nontransformed fetal buccal mucosa (FBM) cell line (25). Subsequent work from our laboratory revealed that knockdown of K8 in oral squamous cell carcinoma (OSCC) derived cell line (AW13516) resulted in alterations in levels of  $\alpha 6\beta 4$  integrin proteins,  $\alpha 6\beta 4$  integrin mediated signaling, reduction in cell motility, downregulation of cell motility associated protein fascin and alterations in actin organization (26). However, the mechanism by which K8/18 modulates  $\beta 4$

integrin signaling and its downstream events is not yet clear. BPAG1e and Plectin are members of the plakin family which anchor the keratin cytoskeleton network to the cell surface via  $\beta 4$  integrin. Although, the importance of plakins in maintaining tissue integrity is well understood, the role of these linker proteins in cell motility and neoplastic progression is not yet well studied.

### **1.1 Aim:**

Knockdown of BPAG1e and Plectin in oral cancer derived cell lines will enable us to understand the role of these proteins in cell motility and delineate one of the possible mechanisms by which K8/18 promote cell motility and tumor progression in OSCC.

### **1.2 Objectives:**

To-

- 1.2.1 Knockdown BP230 gene in an oral SCC derived cell line AW13516 using shRNA technology.
- 4.2.2. Study interactions between keratin 8 and  $\beta 4$  integrin in parental and knockdown cells.
- 1.2.3 Carry out phenotypic assays for cell transformation for parental and knockdown cells and compare them with K8 knockdown cells.
- 1.2.4 Study effects of downregulation of BP230 on polymerization of cytoskeletal elements such as actin, keratins and their regulators.

## *2. Review of Literature*

## 2.1 Hemidesmosomes (HDs):

The basal layer of epithelial cells is connected to Extracellular matrix (ECM) through protein complexes known as hemidesmosomes (HDs). Ultrastructurally, HDs are composed of an electron dense structure whose cytoplasmic plaque anchors keratins to the cell surface (1, 2).

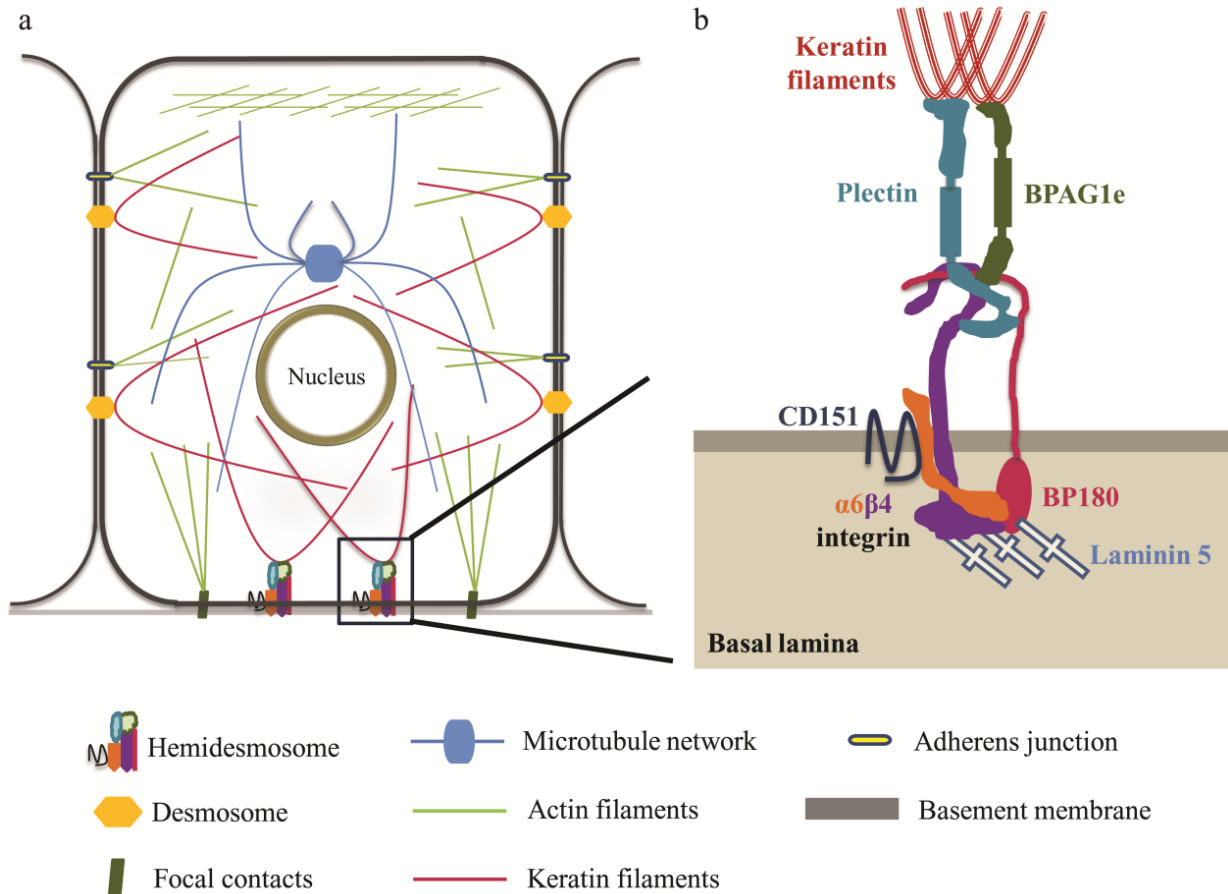


**Figure 2.1: Schematic representation of hemidesmosomal components. (Adapted from (6))**

Depending upon the protein composition, there are two types of HDs, type 1 HDs and type 2 HDs. The type 1 HDs are comprised of the transmembrane proteins like  $\alpha6\beta4$  integrin, BP180 and CD151 which form the outer plaque of HDs and are present in complex epithelia (e.g. skin). The inner plaque of HDs is formed by cytoplasmic linker proteins called BPAG1e and plectin (1, 3, 4, 6, 27-29). These linker proteins connect intermediate filament proteins to the

transmembrane proteins, which in turn interact with extracellular matrix protein laminin 5 (2). Type 2 HDs, which are majorly found in simple epithelia (e.g. intestine) and consist of  $\alpha 6\beta 4$  integrin, plectin and CD151 (1, 3, 4, 6).

## **2.2 $\alpha 6\beta 4$ integrin:**

Integrins are transmembrane glycoproteins present in HDs which comprise of  $\alpha$  and  $\beta$  subunits. Mammalian cells contain 14 different  $\alpha$  and 8 different  $\beta$  subunits which form heterodimers consisting of one  $\alpha$  and one  $\beta$  subunit (30). Integrins act as adhesion transmembrane receptors and interact with ECM of basal lamina. In epithelial cells,  $\beta 4$  integrin couples exclusively with the  $\alpha 6$  subunit to form the  $\alpha 6\beta 4$  heterodimer, which is important component of HDs (31). Loss of either  $\alpha 6$  or  $\beta 4$  integrin in the basal layer leads to perturbation in HD formation and failure of their adhesion to the basement membrane.  $\beta 4$  subunit of the  $\alpha 6\beta 4$  integrin is unique and the cytoplasmic domain of this integrin is distinct both in size (approximately 1000 amino acids long) and structure, from any other integrin subunits and shown to be involved in signal transduction (32-34). Further, the cytoplasmic domain of  $\beta 4$  integrin interacts with various kinases and contains various phosphorylation sites which are responsible for signal transduction (35). In HNSCC, overexpression of  $\alpha 6\beta 4$  integrin has been associated with recurrence and poor prognosis (36). Moreover, increased  $\alpha 6\beta 4$  integrin expression in non-small cell lung cancer (NSCLC) is associated with invasion and decreased overall survival (37). Further,  $\alpha 6\beta 4$  integrin expression is either up or downregulated in various cancers (12, 38, 39). Moreover, the alteration of  $\alpha 6\beta 4$  integrin mediated signaling play an important role in the biology of cancer. A number of prior studies suggest that  $\beta 4$  integrin signaling promotes tumor cell proliferation, migration, invasion and metastasis by different mechanisms e.g. by activating focal adhesion kinase (FAK)

and downstream effectors, amplifying receptor tyrosine kinase (RTK) signaling and modulating ECM components in different tissues (35, 40). It has been shown that the keratinocytes expressing altered keratin filaments displayed reduced activation of Akt and Erk1/2 in response to  $\beta$ 4 integrin ligation by the activating antibody 3E1 (41). Further, previous study from our laboratory reported that K8/18 regulates neoplastic progression by modulating  $\alpha$ 6 $\beta$ 4 integrin mediated signaling in an OSCC derived cells (26). Additionally, increased  $\beta$ 4 integrin surface levels upon vimentin knockdown in OSCC derived cells resulted in strong adhesive contacts which manifested into decreased motility (42).

### **2.3 CD151:**

CD151 is expressed by a variety of epithelial and mesenchymal cells, including hematopoietic cells and myocytes. In the skin, it is expressed in the basal keratinocytes (43). CD151 is a member of the tetraspanin superfamily. These proteins intersect the plasma membrane four times (44, 45). CD151 contains one small and one large extracellular loop with short cytoplasmic carboxy and amino terminal domains. The large extracellular loop is thought to be involved in the binding to integrins (46). CD151 plays a role in a variety of biological processes such as cell adhesion (47, 48), cell migration (46) and cell invasion (49). Furthermore, CD151 plays role in tumor neovascularization (50), actin reorganization (51) and epithelial mesenchymal transition (EMT) (52).

### **2.4 BPAG2 (BP180, COL17A):**

BPAG2 was first identified as an antigen that reacted with autoantibodies of patients suffering with the disease bullous pemphigoid (BP) (53, 54). Mutations in the BPAG2 encoding gene

(COL17A) resulted in reduced epidermal adhesion and skin blistering (55). BPAG2 is expressed in stratified, pseudostratified and transitional epithelia (56). BPAG2 is a homotrimeric transmembrane protein which consists in three collagen alpha-1 chains that are characterized by a globular intracellular domain, a short transmembrane stretch and an extracellular C-terminal domain composed of 15 collagen repeats separated by 16 noncollagenous subdomains (57). BPAG2 has been shown to contain multiple binding sites for plectin, BPAG1e and  $\beta$ 4 integrin in its cytoplasmic domain and  $\alpha$ 6 integrin as well as laminin 5 in the extracellular domain (8, 58, 59). It has been shown that BPAG2 lacking keratinocytes display increased migratory phenotype (60). Moreover, BPAG2 expression correlates with the invasion and metastasis of colorectal cancer (61). Further, BPAG2 is necessary for activation of signaling pathways, motile behavior and lamellipodial stability in keratinocytes (62). Recent studies have demonstrated that the BPAG2 expression is essential for the survival and function of cancer stem cells in colon and lung cancers (63, 64).

## **2.5 Plakin family proteins:**

Plakin family proteins are the cytolinker proteins which connect cytoskeletal elements to junctional complexes such as desmosomes and hemidesmosomes. Desmoplakin, plectin, bullous pemphigoid antigen 1, envoplakin, periplakin, epiplakin and microtubule actin crosslinking factor are known plakin family proteins (65). The N-terminal plakin domain is a defining feature of plakin family proteins (except epiplakin). The plakin domain is comprised of a number of subdomains namely NN, Z, Y, X, W and V which are rich in  $\alpha$ -helical structures. The plakin domain is important for interaction between plakins and specific cell junctions such as HDs (8). The central coiled-coil rod domain, which has heptad repeats, is important for dimerization of

plakins. The C-terminus of plakins varies as per plakin type and is composed of either plakin repeat domains (PRD) or spectrin repeats. The PRD consists of one or many A, B, C subdomains which interact with intermediate filament proteins (7, 66).

## **2.6 Hemidesmosomal linker proteins:**

### **2.6.1 BPAG1e (BP230):**

BP230 protein is encoded by the DST gene. Based on alternative splicing of the gene, there are several isoforms, namely BPAG1n, BPAG1e, BPAG1a and BPAG1b. These alternatively spliced products show tissue specific distribution. BPAG1e (306kDa) is a major isoform expressed in epidermis. BPAG1n (344 kDa), also known as dystonin, is expressed in neurons. BPAG1a (615 kDa) is expressed mostly in pituitary primordia and the dorsal root ganglia (DRG). Muscle specific isoform BPAG1b (824 kDa) is the largest isoform of BP230. BPAG1e consists of a coiled-coil rod domain flanked by a plakin domain and a PRD comprising of B and C subdomains. BPAG1e lacks N-terminal actin binding domain (ABD) and therefore cannot interact with actin filaments. The B and C subdomains of PRD, including the intervening linker region, are required for the interaction with intermediate filament proteins (7, 67).

### **2.6.2 Plectin:**

Plectin can interact with all three forms of cytoskeletal proteins. It is expressed in various tissues except for certain neurons (68, 69). Plectin is encoded by the PLEC1 gene. Due to alternative splicing of the 5' end of PLEC1 gene, there are several isoforms of plectin having molecular weight more than 500 kDa. These isoforms show tissue specific expression pattern. For example, 1, 1a and 1c isoforms of plectin are expressed in epidermis. Amongst these, plectin 1a is predominantly expressed in HDs (70-72). The N-terminus of plectin interacts with actin

filaments by virtue of its actin binding domain (ABD). It has been shown that ABD of plectin preferentially interacts with  $\beta 4$  integrin rather than actin (73). Plectin comprises of 6 PRDs (5 B subdomains and 1 C subdomain). C-terminal Glycine-Serine-Arginine (GSR) domain of Plectin is required for its interaction with microtubules (74).

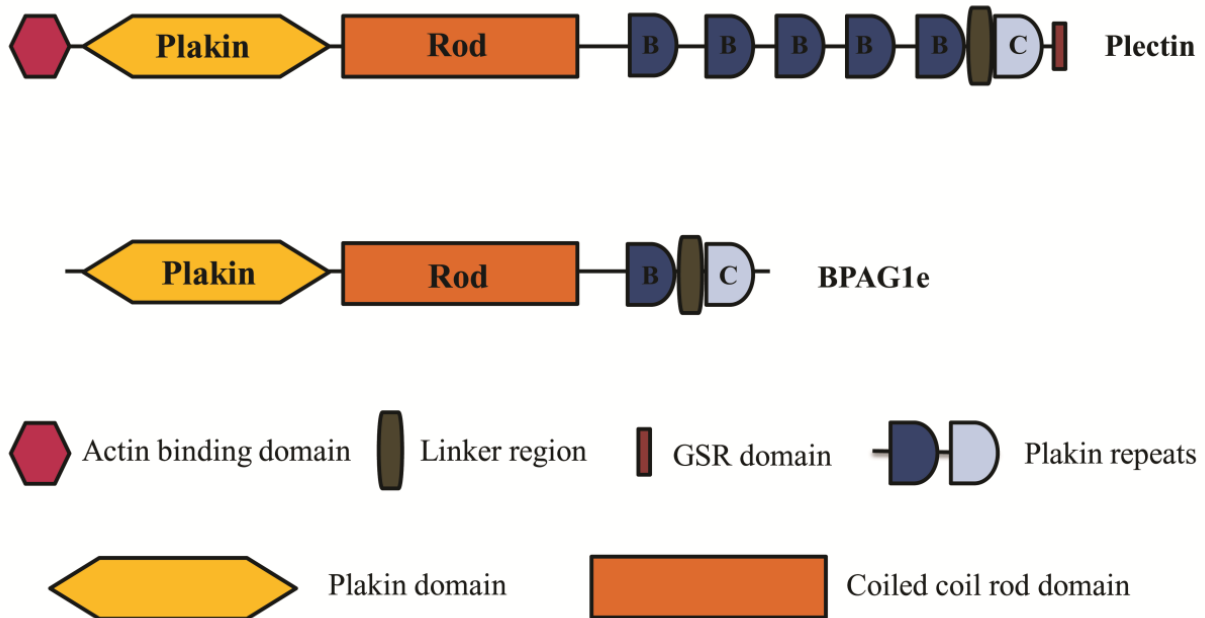


**Figure 2.2: Schematic representation of structural domains of hemidesmosomal linker proteins. (Adapted from (6))**

### 2.7 Interactions mediated by hemidesmosomal linker proteins:

The C-terminal plakin repeat domain of BPAG1e and plectin interacts with intermediate filaments, whereas the N-terminal plakin domain of these linker proteins interacts with the fibronectin domain of  $\beta 4$  integrin (7-9). However, the  $\beta 4$  integrin binding site for plectin and BPAG1e is different (8). A stretch of 85 amino acids located in N terminus of BP180 is essential for its binding to plakin domain (Y subdomain) of BPAG1e and plectin. The binding sites on  $\beta 4$

integrin for BPAG1e and plectin are different from those involved in the binding to BP180 (8, 75). There are reports stating the importance of phosphorylation status of plectin in plectin-cytoskeletal protein interaction. The phosphorylation at specific serine/ threonine residues of plectin results in weakening of plectin-cytoskeletal protein association (76-78).

## **2.8 Events involved in Type I HD assembly:**

$\alpha\beta4$  integrin and its ligand laminin 5 play a crucial role in the hemidesmosomal assembly (79-82). The large cytoplasmic domain of the  $\beta4$  integrin contains two pairs of fibronectin type III (FNIII) repeats separated by a connecting segment (CS), which is essential for the HD formation (83, 84). The first pair of FNIII repeat and the first 35 residues (1321-1355) of the CS of the  $\beta4$  integrin interact with ABD of plectin, which marks the primary interaction between plectin and  $\beta4$  integrin (59, 85, 86). Furthermore, the plakin domain of plectin also interacts with the C-terminal part of CS and region following fourth the FNIII repeat of  $\beta4$  integrin (87). In another study, it has been shown that plectin is involved in localization of chimeric  $\beta4$  integrin lacking extracellular domain into HDs, suggesting that HD formation can take place in absence of  $\alpha\beta4$  integrin-laminin 5 interaction (84). It is not yet clear whether the  $\beta4$  integrin regulates the distribution of plectin to HDs or the plectin is key molecule for localization of  $\beta4$  integrin into HDs. Interestingly, in absence of  $\beta4$  integrin-plectin interaction, BPAG1e and BPAG2 do not get incorporated efficiently into HDs (8, 88). These reports confirmed that interaction of the  $\beta4$  integrin with plectin is essential for HD formation to take place and occurs before BP antigens get recruited into HDs. The colocalization of CD151 with  $\alpha3\beta1$  integrin in pre-hemidesmosomal structures has been demonstrated in  $\beta4$  integrin deficient pyloric atresia with junctional epidermolysis bullosa (PAJEB) cells. On the other hand,  $\beta4$  integrin transfected PAJEB cells

showed enhanced surface expression of CD151 (4). This process occurs only when the  $\alpha 6$  subunit is associated with the  $\beta 4$  subunit. It is possible that CD151 incorporation into HDs occurs after  $\alpha 6\beta 4$  integrin and plectin interaction. BPAG2 can interact with laminin 5 and  $\alpha 6$  integrin via its extracellular domain, while it interacts with  $\beta 4$  integrin, plectin and BPAG1e by virtue of large collagenous cytoplasmic domain (58, 59, 89-92). Reports have demonstrated that efficient localization of BPAG2 into HDs may be dependent on its interaction with both  $\beta 4$  integrin and plectin (59, 91). Further, BPAG1e interacts with the  $\beta 4$  integrin and BPAG2 to get stabilized into HDs (8, 75, 92). There are conflicting reports regarding incorporation of BP antigens into HDs. One of the studies indicates that BPAG2 plays an important role in BPAG1e localization in HD plaque. BPAG2 deficient general atrophic benign epidermolysis bullosa (GABEB) keratinocytes form HDs lacking BPAG1e, indicating that BPAG2 may play a critical role in coordinating the subcellular distribution of BPAG1e (92). Contrary to this, transfection studies have shown that BPAG1e can associate with  $\alpha 6\beta 4$  integrin even in the case of altered BPAG2 localization (75).

## **2.9 Animal models:**

### **2.9.1 BPAG1 null mouse:**

In BPAG1 ablated mice, HDs appeared normal but hemidesmosomal inner plate was absent. Furthermore, IF proteins were not attached to HDs due to which skin blistering was observed in BPAG1 null mice. These mice survived for 4-5 weeks. The localization of other hemidesmosomal proteins was unaffected upon BPAG1 ablation. The mice also developed severe dystonia, myopathy and sensory nerve degeneration (10). This phenotype was observed

due to inactivation of BPAG1a and BPAG1b, which are expressed in neurons and skeletal muscles respectively (67).

### **2.9.2 Plectin null mouse:**

The cell degeneration was observed in plectin knockout mice. In these knockout mice, the dermis was separated from the epidermis and hence severe skin blistering was observed. The plectin null mice survived only for 2-3 days after birth due to severe skin blistering. Ultrastructurally, the DSs and HDs were appeared to be normal. However, levels of  $\beta 4$  integrin and the number of HDs were significantly decreased, indicating that plectin has role in a HD formation. Plectin null mice displayed unaltered keratin filament formation indicating that in the absence of Plectin, BPAG1e may anchor keratins. Moreover, plectin null mice developed myopathy in the skeletal muscle and disintegration of intercalated discs in the heart (11).

Altogether, these *in vivo* studies suggest that hemidesmosomal linker proteins are important for mechanical strengthening of the cell.

## **2.10 Functions of HD linker proteins:**

### **2.10.1 BPAG1e and cell migration:**

BPAG1e null animals displayed impaired wound healing *in vivo*. The keratinocytes of BPAG1e null mice were not flattened, unlike those of normal migrating keratinocytes. These defects in migration may be attributed to delay in initiation of migration of epidermal keratinocytes (10). This study indirectly implicates the role of BPAG1e in keratinocyte migration. One of the reports has shown that BPAG1e ablation in keratinocytes resulted in aberrant motility and loss of front to rear polarity. These defects were rescued by inducing expression of constitutively active Rac1 or active cofilin. Further, immunofluorescence studies have shown that BPAG1e and  $\beta 4$  integrin

colocalize at the leading edge of migrating keratinocytes, indicating that  $\beta 4$  integrin associated BPAG1e may have a role in keratinocyte migration (13). A subsequent report from the same laboratory has demonstrated that BPAG2 plays a role in cell motility and lamellopodial stability by recruiting BPAG1e to  $\alpha 6\beta 4$  integrin at the leading edge of the migrating keratinocytes (62). On the other hand, Michael *et al* have shown reduced adhesion but increased spreading and migration in human keratinocytes carrying homozygous nonsense mutations in BPAG1e encoding gene. Further, altered levels of K14,  $\beta 4$  integrin and  $\beta 1$  integrin were observed in these keratinocytes, although Michael *et al* failed to reproduce similar findings in BPAG1e deficient normal keratinocytes (14). Thus, it is difficult to conclude from these reports whether BPAG1e is a positive or negative regulator of cell motility.

### **2.10.2 BPAG1e and cancer:**

It has been reported that advanced melanoma patients show higher levels of autoantibodies against BPAG1e in serum. Thus, it can prove as potential biomarker for melanomas (93). In another study, upregulation of BPAG1e and  $\alpha 6\beta 4$  integrin expression has been reported in invasive squamous cell carcinomas. Interestingly, pericellular localization of these proteins was observed (12). Contrary to this, Lo *et al* have reported decreased expression of hemidesmosomal components including BPAG1e in nasopharyngeal carcinoma as compared to non-malignant nasopharyngeal epithelia (94). Thus, BPAG1e shows tissue dependent alterations during cancer development.

### **2.10.3 Plectin and cytoskeletal stability:**

The destabilization of cellular integrity was more severe in plectin null mice as compared to BPAG1e null mice. This can be attributed to the fact that Plectin can interact with all three forms of cytoskeletal proteins. Plectin 1, 1a and 1c are expressed in human keratinocytes, out of which

only 1a isoform localizes specifically at the site of HDs. Moreover, only 1a isoform was capable of rescuing hemidesmosomal defects in plectin ablated keratinocytes (71). It is also reported that plectin 1c plays major role in a microtubule (MT) destabilization and hence decreased microtubule dynamics. Further, plectin 1c mediated MT instability led to changes in cell shape, nonpolarized cell migration, smaller sized focal adhesion contacts, higher glucose uptake and mitotic spindle aberrations combined with reduced growth rates of cells. The plectin-MT interaction antagonizes functions of microtubule associated proteins (MAPs), which are involved in MT stability and assembly (95). Moreover, altered actin cytoskeleton was observed in plectin ablated cells as compared to wild type cells (96). These reports suggest that plectin plays role in both microtubule and microfilament destabilization.

#### **2.10.4 Plectin, cancer and cell signaling:**

Several studies indicate that plectin can be used as a potential biomarker in various cancerous conditions (15, 97-99). The transient knockdown of plectin resulted in decreased proliferation, migration and invasion of HNSCC cells. Moreover, plectin knockdown cells displayed reduced levels of phosphorylated Erk. Investigators have argued that a decrease in cell migration and invasion may be attributed to a decrease in activity of Erk. The exact mechanism by which these phenotypic changes took place is unclear. In addition, an inverse relation between plectin expression in HNSCC and survival rate of patients has been shown (15). In another study, loss of plectin in colon carcinoma cells resulted in impairment of cell migration and adhesion. In invasive colon carcinoma cells, plectin 1k expression was observed in actin rich podosome structures. Plectin knockdown inhibited assembly of these actin rich structures. Further, actin rich structures were reformed upon transfection of Plectin 1k N-terminus, indicating that plectin 1k has a role in podosome formation (16). Additionally, increased cell motility was observed

upon transient knockdown of plectin in hepatocellular carcinoma derived cells. The increased motility was attributed to FAK and Rac1 activity (18). In another study, gene expression profiling has revealed upregulation of plectin and vimentin, in highly metastatic bladder cells as compared to low metastatic bladder cells. A dissociation of plectin-vimentin interaction in invasive bladder cancer cells resulted in impairment of invadopodia formation, reduced ECM degradation and metastasis (100). The cell surface localization of plectin has been observed in pancreatic ductal adenocarcinoma (PDAC), which may be the result of trafficking through exosomes. The presence of plectin in exosomes from the serum of PDAC animals indicated that plectin can act as a potential serum marker (101).

### **2.11 Intermediate filaments:**

The cytoskeleton of all mammalian cells is comprised of three distinct filamentous networks: microtubules (MTs), microfilaments (MFs) and intermediate filaments (IFs). 10 nm wide intermediate filaments (IFs) were first described in skeletal muscle (102). IFs function as cytoskeletal scaffolds in the nucleus and cytoplasm of most eukaryotic cells (103, 104). Unlike MTs and MFs, IFs are highly insoluble structures and are resistant to detergent action as well as high and low ionic salt concentration. Further, they have been found to be highly dynamic in spite of their insoluble nature.

### **2.12 IF Structure:**

IF proteins consist of a characteristic tripartite structure, which includes a coiled coil  $\alpha$ -helical central rod domain and the flanking N terminal (head) and C terminal (tail) domains at either end of the rod domain. The central rod domain contains heptad repeats of (abcdefg)<sup>n</sup> of apolar

residues. The rod domain is further subdivided into 1A, 1B, 2A and 2B which are separated by non-helical 8–17 amino acid linker (L1, L12, L2) stretches. The non helical end domains (head and tail domains) are also divided into subdomains based on homologous (H), variable (V) or end (E) sequences. The differences observed in length and primary structure of head and tail domains are responsible for the heterogeneity observed in all IF proteins (103, 105, 106).

### 2.13 IF Classification:

Intermediate filament proteins are further subdivided into 6 subgroups, based on the amino-acid sequence identity and polymerization properties (Table 2.1). They are preferentially expressed in a tissue specific and differentiation dependent manner. Unlike other IFs which are known to form homopolymers, keratins and neurofilaments form heteropolymers. Keratins (acidic and basic) are grouped in type I and II, whereas Vimentin, Desmin, Glial Fibrillary Acidic Proteins (GFAPs) and peripherin are grouped in Type III. Further, Neurofilaments and Nestin are grouped into Type IV, the nuclear lamins as type V and Phakinin, Filensin as orphans. Type I-IV and VI IFs are localized in the cell cytoplasm while the type V forms the cytoskeleton of the nucleus (104, 105, 107).

| Subgrouping | Proteins  | Cell type specificity  |
|-------------|---|--|
| Type I      | Keratins  | Soft complex epithelia (skin, oral mucosa, etc.)   |
| Type II     |   | Soft simple epithelia (liver, gut, kidney, etc.)<br>Hard epithelia (hair, nail, oral papillae) |
| Type III    | Vimentin, Desmin<br>GFAP, Peripherin<br>syncoilin   | Various (fibroblasts, leukocytes, endothelium<br>muscle, astrocytes, glia, peripheral nerves)  |
| Type IV     | NF-L, NF-M, NF-H<br>a-internexin<br>synemin, nestin | CNS & neurons<br>CNS & neurons<br>Muscle, neural stem cells                                    |
| Type V      | Lamins A, B & C                                     | Nucleus  |
| Orphan      | Filensin, Phakinin                                  | Lens   |

**Table 2.1: Classification of IFs based on their type and cell-type specificity (107)**

## **2.14 Keratins:**

Keratins are the largest subgroup of intermediate filament proteins. They are obligate noncovalent heteropolymers that include at least one type I and one type II keratins which pair together during filament formation (19, 105). They are encoded by a large multigene family of more than 60 individual members which are identified from the human genome sequence analysis. 53 of them are found to be functional genes. Expression of 37 different polypeptides of keratins has been reported in different human epithelial tissues (20). Keratins are divided into type I acidic keratins (K9-K28, K31-K40 ) and type II basic keratins (K1-K8, K71-K86) on the basis of their biochemical properties such as molecular weight and isoelectric point (108, 109). They are expressed in all epithelial cells from the single layered epithelia of most internal organs (simple epithelium) to the complex multi layered epithelium (stratified epithelium) of the epidermis. e.g. K8/18 pair is expressed in simple epithelial cells like hepatocytes, whereas K5/14 pair is expressed in stratified squamous epithelia like skin (20). In stratified epithelia, keratins exhibit a complex expression pattern, which is tightly regulated during keratinocyte differentiation. The K5/14 pair is expressed in the basal proliferating layer of these epithelia. As these cells move upward and differentiate, K5/14 levels are gradually reduced and expression of new pair of keratins is induced depending upon the tissue type. Differentiating cells express K1/10 in skin, K4/13 in internal stratified epithelia such as esophagus and K3/12 in corneal cells (110).

### **2.15 Keratin 8/18:**

K8 and K18 are expressed in all simple epithelial cells. They are involved in several regulatory functions which include modulation of protein localization, targeting, trafficking and synthesis (19, 111, 112). Aberrant expression of K8/18 is observed in case of SCCs including OSCC, where their aberrant expression has been correlated with aggressiveness of the tumor and poor prognosis (21-24). Transgenic mice expressing human K8 in the epidermis have a dramatic increase in the progression of papillomas towards malignancy (113). Further, overexpression of K8 and K18 in human melanoma cells led to increased migration and invasion (114). Mouse fibroblasts expressing K8/18 filaments showed higher migratory and invasive ability (115). Previous work in our laboratory has shown that K8 overexpression led to neoplastic transformation and increased invasive and metastatic potential in fetal buccal mucosal (FBM) cells (25). Further, loss of keratins 8/18 led to alterations in  $\alpha\beta4$  integrin mediated signaling and decreased neoplastic progression in an OSCC derived cell line (26). On the other hand, overexpression of K8 in an invasive breast cancer cell line resulted in significant decrease in motility, invasion and tumorigenicity (116). Similarly, Fortier *et al* have shown that K8/18 loss in epithelial cancer cells promotes cell migration (117). Recently, it has been reported that high K8 expression promotes tumor progression and metastasis of gastric cancer (118). Altogether, these reports suggest that role of K8/18 is context dependent.

### **2.16 Fascin:**

Fascin is an actin bundling protein which is highly conserved in both vertebrates and invertebrates. There are three isoforms of fascin observed in mammals, fascin-1 (fascin-1 is referred here as fascin), fascin-2 and fascin-3 (119). Fascin is expressed during embryogenesis in

neural and mesenchymal tissues. In adults, it is largely restricted to specific tissues which include brain, endothelium and testis. Fascin expression is either low or absent in adult epithelia and is often upregulated in several types of epithelial cancers including breast, ovary, skin, pancreas, liver and oral cancer (120-124). It plays an important role in the organization of actin based structures such as filopodia, lamellipodia, invadopodia and microvilli (125, 126). It has been reported that, fascin promotes growth and migration of non small cell lung cancer (NSCLC) cells (127). Additionally, fascin has been shown to promote invasiveness of the colon and esophageal carcinoma derived cells (128, 129). Further, fascin regulates actin polymerization, cell motility, invasion and tumorigenicity in K8 knockdown OSCC cells (26).

### **2.17 NDRG1:**

N-myc downstream regulated gene 1 (NDRG1) is metastatic suppressor protein which is also known as Drg1, RTP, Rit42 or Cap43. NDRG1 is a 43 kDa protein, which is highly conserved among multicellular organisms (130, 131). It is predominantly expressed in cytoplasm of most of the epithelial tissues, whereas nuclear localization of NDRG1 is observed in prostate epithelial cells. Further, NDRG1 is found to be associated with plasma membrane in intestinal and lactating breast epithelia. Moreover, NDRG1 is associated with mitochondrial inner membrane in kidney (130, 132). NDRG1 functions as a metastasis suppressor in numerous cancers including breast, prostate, colon, pancreatic and oral cancer (133-137). Further, Fotovati *et al* have reported that NDRG1 could be used as differentiation marker of breast cancer (138). Moreover, decreased expression of NDRG1 resulted in enhanced cell invasiveness, proliferation and tumorigenesis of OSCC derived cells (137). Furthermore, NDRG1 overexpression in human prostate and colon cancer cells inhibited cell migration by preventing actin filament

polymerization, stress fiber assembly via ROCK1/pMLC2 pathway (139). In prostate and lung cancer cells, NDRG1 significantly suppressed cell migration by modulating p21 levels (140). Moreover, NDRG1 negatively regulated gastric cancer cell invasion through decreased MMP activity (141, 142). Recently, it has been demonstrated that loss of NDRG1 in prostate cancer cells leads to reduced actin mediated cell migration, while it results increased cellular invasion (143). It has been shown that NDRG1 loss promotes epithelial-mesenchymal transition of colorectal cancer via NF- $\kappa$ B signaling (144). NDRG1 also promotes the stemness like properties of NSCLC cells by stabilizing c-Myc. Further, NDRG1 is negatively associated with lung cancer progression and prognosis (145). NDRG1 also regulates apoptosis of colorectal cancer cells via increased ubiquitination of Bcl-2 (146).

Several studies have shown that HD linker proteins are not present in the cells only to anchor specific proteins, but that they have functional role in various cellular processes including cell motility, invasion etc (13-15, 17, 18, 71, 100). Further, the previous data from our laboratory suggests that K8/18 pair promotes cell motility and tumor progression by deregulating  $\beta$ 4 integrin signalling and its downstream events in OSCC (26). Thus, it will be relevant to dissect the role of hemidesmosomal linker proteins (BPAG1e and Plectin) in K8 mediated regulation of cell motility and neoplastic progression.

### *3. Materials and Methods*

### **3.1 Routine maintenance of cell lines:**

The human tongue SCC derived cell lines AW13516 and AW8507 were previously established in Cancer Research Institute, Tata Memorial Centre, Parel, Mumbai, India (147). The cells were cultured in Iscove's Modified Dulbecco's Medium (IMDM) supplemented with 10% fetal bovine serum (FBS) and antibiotics under a 5% CO<sub>2</sub> atmosphere at 37°C. HEK 293FT cells, used for lentivirus production, were cultured in Dulbecco's Modified Eagle Medium (DMEM) supplemented with 10% FBS and antibiotics under a 5% CO<sub>2</sub> atmosphere at 37°C.

### **3.2 Reagents:**

a) Phosphate Buffered Saline (PBS): (150 mM NaCl, 2 mM KCl, 8 mM Na<sub>2</sub>HPO<sub>4</sub>, 1 mM KH<sub>2</sub>PO<sub>4</sub>.) The buffer was autoclaved and used.

b) Trypsin-EDTA: (0.025% Trypsin, 0.2 mM EDTA, 5 mM D-glucose, 5 mM KCl, 0.1 M NaCl and 6 mM NaHCO<sub>3</sub>). The medium was filtered using Millipore assembly – 0.45 µM Membrane filter (Whatman, GE healthcare, Germany). 1 ml of the filtered trypsin was added to the sterility test medium and kept at room temperature (RT) for 6 days under observation, to ensure sterility.

c) Erythrocin B staining solution: 0.4% Erythrocin B in 1X PBS.

d) Freezing medium: 90% Fetal Bovine Serum, 10% Dimethyl sulfoxide (DMSO).

e) IMDM and DMEM: Powdered medium was dissolved in 800 ml of water. For DMEM, 3.7 g of sodium bicarbonate per liter was added and the pH of medium was adjusted to 6.8. For IMDM, 3.024 g of sodium bicarbonate per liter was added. The volume was made up to 1000 ml. The media were filtered using Millipore assembly with 0.45 µM membrane filter.

f) Complete medium: DMEM or IMDM with 10% FBS and 1% antibiotic solution (Anti-Anti 100X, Life technologies, USA)

g) Sterility test medium: 14.9 g of Fluid-Thioglycolate was dissolved in approximately 300 ml of water. The volume was made up to 500 ml in measuring flask and boiled. After aliquoting 6 ml of the medium in glass tubes, a pinch of  $\text{Ca}_2\text{CO}_3$  was added to each tube and autoclaved.

Other reagents with their particulars are described in Table 3.1.

| <b>Reagents</b>                           | <b>Catalogue</b> | <b>Company</b>    | <b>Country</b> |
|---|------------------|-------------------|----------------|
| Acetonitrile (ACN)                        | 34851            | Sigma             | USA            |
| Agarose                                   | GX-40005         | Puregene          | India          |
| Agarose, low melting point                | A9414            | Sigma             | USA            |
| Ammonium persulphate (APS)                | 28575            | SRL               | India          |
| Antibiotic-Antimycotic solution (100X)    | 15240-062        | Life technologies | USA            |
| Bovine Serum Albumin (BSA)                | A7906            | Sigma             | USA            |
| Brilliant blue R                          | B7920            | Sigma             | USA            |
| Calcein AM                                | C1430            | Life technologies | USA            |
| Calpeptin                                 | 03-34-0051       | Calbiochem        | USA            |
| Cesium chloride                           | C4036            | Sigma             | USA            |
| Crystal violet                            | RM 114           | Himedia           | India          |
| Diaminobenzidine (DAB)                    | D5637            | Sigma             | USA            |
| 4',6-diamidino-2-phenylindole (DAPI)      | D9542            | Sigma             | USA            |
| Diethyl pyrocarbonate (DEPC)              | D5758            | Sigma             | USA            |
| Dimethyl sulfoxide (DMSO)                 | D2650            | Sigma             | USA            |
| 1, 4-Dithioerythritol (DTT)               | D8255            | Sigma             | USA            |
| DNA ladder (50 bp)                        | SM1133           | Thermo scientific | USA            |
| DNA ladder (1 kb)                         | SM0311           | Thermo scientific | USA            |
| D.P.X. mountant                           | 61803502500      | Merck             | India          |
| Dulbecco's modified eagle's medium (DMEM) | 12800-017        | Life technologies | USA            |
| Empigen                                   | 45165            | Fluka             | Italy          |
| Epidermal growth factor (EGF)             | PHG0311L         | Invitrogen        | USA            |
| Erythrocin B                              | 200964           | Sigma             | USA            |

|  |                |                   |       |
|--|----------------|-------------------|-------|
| Ethylenediaminetetraacetic acid (EDTA) disodium salt                                     | E5134          | Sigma             | USA   |
| Ethylene glycol bis( $\beta$ -aminoethyl ether)-tetraacetic acid (EGTA) tetrasodium salt | E8145          | Sigma             | USA   |
| Fetal Bovine Serum (FBS)   | 16000-044      | Life technologies | USA   |
| FITC conjugated phalloidin   | P5282          | Sigma             | USA   |
| Fluid Thioglycollate medium  | M009           | Himedia           | India |
| Folin and ciocalteus phenol reagent  | 39520 (062015) | SRL               | India |
| G418   | 5.09290.0003   | Calbiochem        | USA   |
| Gelatin  | G8150          | Sigma             | USA   |
| Glycerol   | 20118          | SDFCL             | India |
| Glycine  | 66327          | SRL               | India |
| HEPES  | H4034          | Sigma             | USA   |
| Hydrogen peroxide  | 18755          | Fisher Scientific | India |
| Hygromycin B   | 10687-010      | Invitrogen        | USA   |
| Iscove's Modified Dulbecco's Medium (IMDM)   | 12200-036      | Life technologies | USA   |
| 2-Mercaptoethanol (BME)  | M3148          | Sigma             | USA   |
| Matrigel   | 354234         | BD Biosciences    | USA   |
| Nonidet P-40   | N6507          | Sigma             | USA   |
| Optical adhesive covers  | 4360954        | Life technologies | USA   |
| 1,4-Piperazinediethanesulfonic acid (PIPES)  | P1851          | Sigma             | USA   |
| Polybrene  | H9268          | Sigma             | USA   |
| Poly-L-lysine  | P8920          | Sigma             | USA   |
| Ponceau S  | P3504          | Sigma             | USA   |
| Prestained protein ladder  | PG700-         | Puregene          | India |
| Protease inhibitor cocktail  | 539131         | Calbiochem        | USA   |
| Protein G-sepharose  | P3296          | Sigma             | USA   |
| Puromycin  | P8833          | Sigma             | USA   |
| PVDF membrane  | RPN303F        | GE Healthcare     | UK    |
| Revert Aid First Strand cDNA synthesis Kit   | K1622          | Thermo Scientific | USA   |

|  |           |                     |       |
|--|-----------|---------------------|-------|
| RhoA / Rac1 / Cdc42 Activation Assay Combo Biochem Kit | BK030     | Cytoskeleton Inc.   | USA   |
| Sodium chloride  | 7647-14-5 | Fisher Scientific   | India |
| Sodium dodecyl sulfate (SDS)                           | L3771     | Sigma               | USA   |
| SYBR Green PCR Master Mix                              | 4367659   | Applied Biosystems  | USA   |
| Tetramethylethylenediamine (TEMED)                     | T9281     | Sigma               | USA   |
| Thiazolyl Blue Tetrazolium Bromide (MTT)               | M2128     | Sigma               | USA   |
| TRI reagent  | T9424     | Sigma               | USA   |
| Trizma base  | T8524     | Sigma               | USA   |
| Trypsin  | T4799     | Sigma               | USA   |
| Tween 20   | 76368     | SDFCL               | India |
| Vectashield mounting medium                            | H-1000    | Vector Laboratories | USA   |
| Vectastain Elite ABC kit                               | PK-6200   | Vector Laboratories | USA   |
| WesternBright™ ECL HRP substrate                       | K-12045   | Advansta            | USA   |

**Table 3.1: List of reagents with their particulars.**

### 3.3 Revival of cells:

The vial containing cells preserved in liquid nitrogen was taken out from liquid nitrogen cylinder and placed into a 37°C water bath for thawing. The thawed cell suspension was mixed gently and transferred into a sterile test tube. 5 ml of complete medium was added drop wise with gentle shaking. The thawed cells with medium were further mixed smoothly using glass pipette. The cell suspension was centrifuged for 10 minutes at 1000 rpm at RT. The supernatant was discarded and the pellet was dislodged by tapping and resuspended in 1ml of complete medium. The suspension was dispensed into tissue culture plate which was then incubated in a humidified CO<sub>2</sub> (5%) incubator at 37°C.

### **3.4 Subculture/Trypsinization and transfer of cells:**

The cells were washed with 1X PBS twice. Trypsin-EDTA was added to the culture plate. The plate was incubated till the cells were partially detached. Complete medium was added to inhibit the trypsin activity into the plate containing detached cells. The resulting cell suspension was mixed by pipette to make a single cell suspension. The suspension was dispensed in tissue culture plate, which was then incubated in humidified CO<sub>2</sub> (5%) incubator at 37°C.

### **3.5 Freezing and cryopreservation of cells:**

Log phase cells were trypsinized and single cell suspension was obtained. After noting the total cell count, the cell suspension was spun at 1000 rpm for 10 minutes at RT. During centrifugation, freezing media (90% FBS and 10% DMSO) was prepared. The supernatant was discarded and the pellet was dislodged by tapping. 1 ml of freezing medium was added into the tube drop wise and mixed gently by pipette. The cell suspension was then transferred to freezing vials which were placed in -80 °C for 24 to 48 hrs. Subsequently, they were kept in liquid nitrogen freeze boxes at -196°C for long term storage.

### **3.6 Plasmids and cloning:**

The pLKO1.puro (plasmid #10878), pLKO1.neo (plasmid #13425) and pLKO1.hygro (plasmid #24150) plasmids were purchased from Addgene, USA. The pLKO1.puro plasmid containing shRNA sequence against BPAG1e was gifted by Dr. Jonathan Jones, Washington State University, USA (Table 3.2). shRNA sequences against Plectin and NDRG1 were designed and cloned in pLKO1.neo and pLKO1.hygro plasmids respectively (Table 3.3 and 3.4). BPAG1e-Plectin double knockdown was generated by transducing lentivirus encoding shRNA against

BPAG1e in Plectin knockdown cells. NDRG1-BPAG1e-Plectin triple knockdown was generated by transducing lentivirus encoding shRNA against NDRG1 in BPAG1e-Plectin double knockdown cells. The empty vector backbone was used to generate the respective vector control clones.

| <b>Oligo name</b>    | <b>Length</b> | <b>Target site</b> | <b>shRNA sequence (5'-3')</b>  |
|----------------------|---------------|--------------------|--|
| Sh1_Fw<br><br>Sh1_Re | 58            | 121-139            | <i>CCGGAGTTATAGTTACCGTAGCACTCGAGTGCT<br/>ACGGTAACCTATAACTTTTTTG<br/>AATTCAAAAAAGTTATAGTTACCGTAGCACTCG<br/>AGTGCTACGGTAACCTATAACT</i>   |
| Sh2_Fw<br><br>Sh2_Re | 58            | 570-588            | <i>CCGGTTCTTCTGTGTACAGCAAACCTCGAG<br/>TTTGCTGTACACAGAAGAATTTTTG<br/>AATTCAAAAATTCTTCTGTGTACAGCAAACCTCG<br/>AGTTTGCTGTACACAGAAGAA</i>   |
| Sh3_Fw<br><br>Sh3_Re | 62            | 4783-4801          | <i>CCGGAATGAAGAATTGGAGAAAACCTCGAGTTTT<br/>CTCAAATTCTTCATT TTTTTG<br/>AATTCAAAAAAATGAAGAATTGGAGAAAA<br/>CTCGAGTTTTCTCAAATTCTTCATT</i>   |
| Sh4_Fw<br><br>Sh4_Re | 62            | 7000-7018          | <i>CCGGAAGCAAGCTCTGTATTACTCTCGAGAGTA<br/>ATACAGAGCTTGGCTT TTTTTG<br/>AATTCAAAAAAAGCAAGCTCTGTATTACT<br/>CTCGAG AGTAATACAGAGCTTGGCTT</i> |

**Table 3.2: List of BPAG1e shRNA sequences along with their target site**

| <b>Oligo name</b> | <b>Length</b> | <b>Target site</b> | <b>Sequence (5'-3')</b>   |
|-------------------|---------------|--------------------|---|
| Sh1_Fw            | 58            | 221-241            | <i>CCGGGGGCCTCTGAGGGCAAGAAAGCTCGAGC</i>   |
| Sh1_Re            |               |                    | <i>TTTCTTGCCCTCAGAGGCCCTTTTTG</i><br><i>AATTCAAAAAGGGCCTCTGAGGGCAAGAAAGC</i><br><i>TCGAGCTTTCTTGCCCTCAGAGGCC</i>          |
| Sh2_Fw            | 58            | 2290-2310          | <i>CCGGAACGCTGCCTACTTTCAGTTCCTCGAGGA</i>  |
| Sh2_Re            |               |                    | <i>ACTGAAAGTAGGCAGCGTTTTTTTG</i><br><i>AATTCAAAAAAACGCTGCCTACTTTCAGTTCCT</i><br><i>CGAGGAACTGAAAGTAGGCAGCGTT</i>          |
| Sh3_Fw            | 62            | 6718-6740          | <i>CCGGGAGACCGACCACCAGAAGAACCTCTCGA</i>   |
| Sh3_Re            |               |                    | <i>GAGGTTCTTCTGGTGGTCGGTCTCTTTTTG</i><br><i>AATTCAAAAAGAGACCGACCACCAGAAGAACC</i><br><i>TCTCGAGAGGTTCTTCTGGTGGTCGGTCTC</i> |
| Sh4_Fw            | 62            | 10831-10853        | <i>CCGGGAAGAGACACAGATCGACATTCCCTCGAG</i>  |
| Sh4_Re            |               |                    | <i>GGAATGTCGATCTGTGTCTCTTCTTTTTG</i><br><i>AATTCAAAAAGAAGAGACACAGATCGACATTCC</i><br><i>CTCGAGGGAATGTCGATCTGTGTCTCTTC</i>  |

**Table 3.3: List of Plectin shRNA sequences along with their target site**

| <b>Oligo name</b> | <b>Length</b> | <b>Target site</b> | <b>Sequence (5'-3')</b>                 |
|-------------------|---------------|--------------------|---|
| Sh1_Fw            | 58            | 175-195            | <i>CCGGCAGGACATCGAGACTTACATCTCGAGAT</i> |
|                   |               |                    | <i>GTAAAGTCTCGATGTCCTGTTTTTG</i>        |

|        |    |         |   |
|--------|----|---------|---|
| Sh1_Re |    |         | AATTCAAAAACAGGACATCGAGACTTTACATCT<br>CGAGATGTAAAGTCTCGATGTCCTG  |
| Sh2_Fw | 58 | 741-761 | CCGGCCTGCACCTGTTTCATCAATGCCTCGAGGC<br>ATTGATGAACAGGTGCAGGTTTTTG |
| Sh2_Re |    |         | AATTCAAAAACCTGCACCTGTTTCATCAATGCCT<br>CGAGGCATTGATGAACAGGTGCAGG |

**Table 3.4: List of NDRG1 shRNA sequences along with their target site**

### 3.7 Preparation of ultra-competent *E. coli* DH5 $\alpha$ cells:

Super Optimal Broth (SOB) (Tryptone 6 g, Yeast extract 1.5 g, NaCl 0.15 g, KCl 5.6 g) was prepared and sterilized. 5 ml of 2M MgCl<sub>2</sub> solution was sterilized separately and added to SOB just before use. A single colony of DH5 $\alpha$  strain of *E. coli*, from an overnight grown LB agar plate was inoculated into SOB for competent cells preparation. The flask was incubated at 18°C at 80-100 rpm till optical density (OD) at 600 nm reaches to 0.4. OD was checked at regular intervals by taking out 1 ml of growing culture in aseptic conditions by using spectrophotometer. The culture was centrifuged at 3000 rpm for 15 minutes at 4°C when OD reaches 0.4 units. The supernatant was discarded and one third volume of ice cold transformation buffer (0.3g PIPES, 0.22g CaCl<sub>2</sub>-2H<sub>2</sub>O, 1.86g KCl, 1.09g MnCl<sub>2</sub>, pH 6.7-6.8) was added slowly onto the pellet. Cell pellet was resuspended in transformation buffer with gentle pipetting for 5-10 minutes and was incubated on ice for additional 10 minutes. Care was taken to avoid any bubbling during re-suspension of cell pellet. After incubation, the cell suspension was centrifuged at 3000 rpm for 15 minutes at 4°C and cell pellet was resuspended in 16 ml of Transformation buffer (1/12.5 volume of initial culture volume i.e. for 200ml) as described in the earlier step. Further, 1.12 ml

of DMSO (final concentration of 7%) was slowly added on the walls of suspension tubes slowly and was mixed by shaking or by gentle pipetting. This solution was then aliquoted in volumes of 100µl in sterilised vials and snap-frozen in liquid nitrogen as quickly as possible. The ultra-competent cell vials were kept at -80<sup>0</sup>C and were taken out on ice just before use.

### **3.8 Transformation:**

The ultra-competent cells were transformed with the plasmid vector of interest. The ligated plasmid mixture was added to thawed competent cells and kept on ice for 30 minutes. Then, the cells were placed at 42°C (water bath) for exactly 90 seconds and subjected to cold shock on ice for 5 minutes. The cells were then mixed with 1 ml of sterile Luria-Bertani (LB) broth and incubated at 37°C for 60 minutes in a shaker incubator. The cells were spun at 5000 rpm for 5 minutes. The pellet was resuspended in 200 µl of LB broth and spread on to LB agar plate and incubated for 16 hours at 37°C.

### **3.9 Plasmid extraction using alkaline lysis method (Mini-Prep):**

Individual colony was picked up and inoculated into 5 ml LB broth containing 100 µg/ml Ampicillin for plasmid extraction and allowed to grow overnight at 37°C. Plasmid isolation from the overnight grown culture was carried out by the alkaline lysis method. 1.5 ml of overnight grown bacterial cultures were centrifuged at 5000 rpm at 4°C for 5 minutes. The medium was removed and the pellets were dried. To the dried bacterial pellets, 100 µl of alkaline lysis solution I (GTE buffer: 50 mM Glucose, 25 mM Tris pH 8.0 and 10 mM EDTA) was added and vortexed till the pellets were completely dissolved. Then, 200 µl of alkaline lysis solution II (0.2 N NaOH and 1% SDS) was added, mixed gently by inverting and kept for 2 minutes at RT. 150

µl of ice-cold alkaline lysis solution III (3 M potassium acetate pH 4.8 in glacial acetic acid) was then added to each tube and kept on ice for 10 minutes. The tubes were centrifuged at 13000 rpm, 4°C for 15 minutes and the supernatants containing the renatured plasmids were transferred to fresh tubes. Equal volume of phenol: chloroform: isoamylalcohol (25:24:1) was added to supernatant for removal of proteins and saccharides, mixed by vortexing and centrifuged as above for 5 minutes. The aqueous phase was transferred to a fresh microcentrifuge tube and double the volume of absolute alcohol was added and mixed well for precipitation of plasmid DNA. The tubes were kept on ice for 15 minutes and centrifuged at the above conditions for 20 minutes. The ethanol was removed and the pellets were washed with 70% chilled ethanol to remove salts. Further, centrifugation was carried out at 13000 rpm for 5 minutes to remove the traces of ethanol. The pellets were completely dried at 37°C for 30 minutes. The dried pellets were reconstituted in 20 µl of autoclaved water.

### **3.10 Virus production:**

HEK293 FT cells were cultured till 50% confluency in DMEM complete medium. Co-transfection of expression and packaging vectors was performed using calcium phosphate precipitation method. The lentiviral transfer vector (6 µg), packaging plasmid psPAX2 (4.5 µg) and envelope plasmid pMD2.G (1.5 µg) were diluted to 250 µl of sterile distilled water. An equal volume of 0.5M CaCl<sub>2</sub> was then added followed by dropwise addition of 500 µl of BES Buffered Saline (BBS). The mixture was incubated at RT for 20 minutes and then added to the culture dishes. The plate was gently swirled and incubated for 16 hours. After incubation, the medium was replaced with fresh complete DMEM. 48 hours post transfection, viral supernatant was collected in sterile 15 ml tube and centrifuged for 10 minutes at 2000 rpm at 4°C to remove

traces of HEK293 FT cells. Supernatant was collected and stored in -80°C or used for transduction.

### **3.11 Lentivirus mediated transduction of OSCC derived cell line:**

The viral supernatant was added to 50% confluent OSCC derived cells along with polybrene 8µg/ml (Polybrene is a polycation that neutralizes charge interactions to increase binding between the pseudoviral envelope and the cellular membrane). After 24 hours, the supernatant was replaced with complete media. Further, stable clones were selected in puromycin (0.5 µg/ml) or G418 (500 µg/ml) or hygromycin (30 µg/ml).

### **3.12 Protein estimation by modified Lowry's method:**

1 ml of 5 to 25 µg/ml of Bovine serum albumin (BSA) was taken in test tubes in duplicates as standard along with blank. 3 µl of whole cell lysates were added in test tubes in duplicates and the volume was made up to 1 ml by distilled water. 1 ml of Copper Tartarate Carbonate (CTC) solution (0.1 % copper sulphate, 0.2 % potassium tartarate, 10 % Sodium carbonate, Solution A (Equal volumes of CTC solution, 10 % SDS, 0.8 N NaOH and distilled water (1: 1: 1: 1 proportion))) was added to each test tube and the tubes were vortexed followed by incubation at RT for 10 minutes. 500 µl of diluted FC reagent (1 part of FC reagent and 5 parts of distilled water) was added to each tube. The tubes were vortexed and incubated at RT for 30 minutes in dark and absorbance was read at 750 nm using a spectrophotometer. The standard curve was plotted. The protein concentration of the samples was determined using standard curve. The protocol was adapted from Peterson *et al*(1977) (148).

### 3.13 Sodium dodecyl sulfate polyacrylamide gel electrophoresis (SDS-PAGE):

SDS-PAGE was performed as described earlier to resolve the proteins based on their molecular size (149, 150). The samples were dissolved in PAGE sample buffer (62.5 mM Tris HCl; pH 6.8, 25% Glycerol, 2% SDS, 0.5% Bromophenol blue) and were separated on 6-15% SDS-PAGE depending on the molecular weight of the proteins. The composition of stacking and resolving gel is described in Table 3.5. Electrophoresis was carried out using electrode buffer (0.02 M Tris base, 0.2% SDS and 0.192M Glycine).

| Components               | Stacking gel (5%) | Resolving gel (6%) | Resolving gel (10%) | Resolving gel (12%) | Resolving gel (15%) |
|--------------------------|-------------------|--------------------|---------------------|---------------------|---------------------|
| H <sub>2</sub> O (ml)    | 2.7               | 5.3                | 4.0                 | 3.3                 | 2.3                 |
| 30% acrylamide mix (ml)  | 0.67              | 2.0                | 3.3                 | 4.0                 | 5.0                 |
| 1.5 M Tris (pH 8.8) (ml) | 0.5               | 2.5                | 2.5                 | 2.5                 | 2.5                 |
| 10% SDS (ml)             | 0.04              | 0.1                | 0.1                 | 0.1                 | 0.1                 |
| 10% APS (ml)             | 0.04              | 0.1                | 0.1                 | 0.1                 | 0.1                 |
| TEMED (ml)               | 0.004             | 0.008              | 0.004               | 0.004               | 0.004               |
| Total volume (ml)        | 4                 | 10                 | 10                  | 10                  | 10                  |

**Table 3.5: The detailed composition of Stacking and Resolving SDS PAGE gels**

### 3.14 Western blotting:

The SDS-PAGE gel with the resolved proteins and activated PVDF membrane were placed in the form of sandwich and wet electro-blotting using transfer buffer (190 mM Glycine, 20% methanol, 0.05% SDS, 25 mM Tris base) was carried out at 100 V for 1 to 4 hours. Transfer of proteins was visualized using Ponceau-S staining (0.2% ponceau stain in 5% acetic acid). The

blot was incubated in blocking solution (5% Bovine Serum Albumin in TBS or 5% skimmed milk in 1X TBS) for 1 hour at RT with shaking. After blocking, the blot was incubated with diluted primary antibody for 1 hour at RT on the rocker. The blot was then washed four times with TBST (0.1% Tween 20, 150 mM NaCl, 10 mM Tris base) followed by incubation with horseradish peroxidase (HRPO) conjugated secondary antibody for 1 hour at RT on the rocker. The secondary antibody was removed and the blot was washed thrice with TBST. Blots were developed using ECL chemiluminescence reagent (WesternBright™ ECL, Advansta, USA) according to the manufacturer's protocol (150).

### 3.15 List of antibodies:

List of antibodies with their particulars are described in Table 3.6.

| <b>Antibody</b> | <b>Clone</b>            | <b>Catalogue No.</b> | <b>Company</b>           | <b>Blocking solution</b> | <b>Antibody dilution</b> |
|-----------------|-------------------------|----------------------|--------------------------|--------------------------|--------------------------|
| β actin         | Mouse monoclonal, AC-74 | A5316                | Sigma, USA               | 5% BSA                   | 1:6000 (WB)              |
| BPAG1e (BP230)  | Mouse monoclonal, 279   | CAC-NU-01-BP1        | Cosmo Bio                | 5% BSA                   | 1:60 (WB)                |
| Plectin         | Mouse monoclonal, 10F6  | sc-33469             | Santa Cruz Biotechnology | 5% BSA                   | 1:1000 (WB)<br>1:30 (IF) |
| BPAG1e (BP230)  | Goat polyclonal, E-14   | sc-13776             | Santa Cruz Biotechnology | 5% BSA                   | IP                       |
| Keratin8        | Mouse                   | C5301                | Sigma                    | 5% BSA                   | 1:5000 (WB)              |

|                        |                                |               |                              |        |  |
|------------------------|--------------------------------|---------------|------------------------------|--------|--|
|                        | monoclonal,<br>M20             |               |                              |        | 1:150 (IF)                             |
| Keratin5               | Mouse<br>monoclonal,<br>XM26   | NCL-CK5       | Novacastra                   | 5% BSA | 1:1000 (WB)                            |
| $\beta$ 4 integrin     | Rabbit<br>polyclonal,<br>H-101 | sc-9090       | Santa Cruz<br>Biotechnology  | 5% BSA | 1:2000 (WB)<br>1:60 (IF)               |
| Fascin                 | Mouse<br>monoclonal,           | MA1-<br>20912 | Thermo<br>Scientific         | 5% BSA | 1:1000 (WB)                            |
| NDRG1                  | Rabbit<br>polyclonal,          | HPA00688<br>1 | Sigma, USA                   | 5% BSA | 1:2000 (WB)<br>1:60 (IF)<br>1:60 (IHC) |
| p21                    | Rabbit<br>polyclonal,<br>C-19  | sc-397        | Santa Cruz<br>Biotechnology  | 5% BSA | 1: 500 (WB)<br>1: 25 (IF)              |
| $\Delta$ Np63 $\alpha$ | Rabbit<br>polyclonal           | 13109         | Cell Signaling<br>Technology | 5% BSA | 1:1000 (WB)                            |
| GAPDH                  | Mouse<br>monoclonal,<br>6C5    | sc-32233      | Santa Cruz<br>Biotechnology  | 5% BSA | 1:3000 (WB)                            |
| $\beta$ tubulin        | Mouse<br>monoclonal,<br>TU-06  | ab7792        | Abcam                        | 5% BSA | 1:2000 (WB)                            |
| Lamin A/C              | Mouse<br>monoclonal            | 4777          | Cell Signaling<br>Technology | 5% BSA | 1:1000 (WB)                            |
| RhoA                   | Mouse<br>monoclonal            | ARH04         | Cytoskeleton,<br>Inc         | 5% BSA | 1:500 (WB)                             |

|   |                   |         |                           |        |             |
|---|-------------------|---------|---------------------------|--------|-------------|
| Rac1  | Mouse monoclonal  | ARC03   | Cytoskeleton, Inc         | 5% BSA | 1:500 (WB)  |
| Cdc42   | Mouse monoclonal  | ACD03   | Cytoskeleton, Inc         | 5% BSA | 1:500 (WB)  |
| ARP2  | Rabbit Polyclonal | 3128    | Cell Signaling Technology | 5% BSA | 1:1000 (WB) |
| ARP3  | Rabbit Polyclonal | 4738    | Cell Signaling Technology | 5% BSA | 1:1000 (WB) |
| Phalloidin-fluorescein isothiocyanate Labeled | -                 | P5282   | Sigma                     | -      | 1:100 (IF)  |
| Anti mouse HRP                                | -                 | A4416   | Sigma                     | -      | 1:5000 (WB) |
| Anti rabbit HRP                               | -                 | sc-2004 | Santa Cruz Biotechnology  | -      | 1:3000 (WB) |
| Anti Goat HRP                                 | -                 | sc-2020 | Santa Cruz Biotechnology  | -      | 1:2000 (WB) |
| Anti mouse Alexa Fluor 488 conjugate          | -                 | A11001  | Invitrogen                | -      | 1:100 (IF)  |
| Anti rabbit Alexa Fluor 568 conjugate         | -                 | A-11011 | Invitrogen                | -      | 1:100 (IF)  |
| Anti goat Alexa Fluor 488 conjugate           | -                 | A-11055 | Invitrogen                | -      | 1:100 (IF)  |

|  |   |       |        |   |            |
|--|---|-------|--------|---|------------|
| Anti mouse<br>DyLight 633<br>conjugate | - | 35512 | Thermo | - | 1:100 (IF) |
|--|---|-------|--------|---|------------|

WB: western blot, IP: immunoprecipitation, IF: Immunofluorescence

**Table 3.6: List of antibodies with their particulars**

### **3.16 RNA extraction:**

The RNA from cell lines was isolated by Tri reagent (Sigma, USA) as per the manufacturer's instructions. Briefly, the cells were grown in a 60 mm petri-dish. The medium was removed and cells were lysed by adding 1 ml of Tri reagent. The lysate was transferred into a 1.5 ml tube and 200  $\mu$ l of chloroform was added and incubated for 10 minutes on ice. An aqueous phase was separated by centrifugation at 12000 rpm and supernatant was transferred to a new tube. RNA was precipitated by adding isopropanol and spun at 12000 rpm for 10 minutes. The pellet was washed by 75% ethanol, air dried and dissolved in 20  $\mu$ l of DEPC treated water. The purity and content of RNA was determined using NanoDrop Spectrophotometer (Thermo Scientific, USA). For tumor tissues, 1 ml Tri reagent was added. Further, the samples were sonicated to extract RNA. The rest of the protocol is as described earlier.

### **3.17 Reverse transcriptase - Polymerase chain reaction (RT-PCR):**

cDNA synthesis was carried out as per the manufacturer's protocol (Thermo Scientific, USA). Briefly, 1  $\mu$ g of total RNA and 0.2  $\mu$ g of random hexamer/oligo(dT) in a volume of 12  $\mu$ l were incubated at 70°C for 5 minutes and chilled on ice. Reaction buffer (1X), RiboLock™ RNase Inhibitor (1 unit/ $\mu$ l) and dNTP mix (1mM) was added and incubated at 25°C for 5 minutes.

RevertAid™ H Minus M-MuLV Reverse Transcriptase (200 units) was added and the reaction mixture was incubated at 25°C for 10 minutes followed by 42°C for 1 hour. The reaction was terminated by heating at 70°C for 10 minutes. The primer sequences used to amplify target genes and GAPDH (internal control) are listed in Table 3.7. PCR products were run on agarose gel electrophoresis to compare RNA levels.

### 3.18 Real-Time Quantitative PCR:

cDNA was prepared as described above and used as the template for qRT-PCR (quantitative reverse transcriptase PCR). Mastermix SYBR Green (Applied Biosystems, UK) was used with 100 nM of forward and reverse primers (Sigma, India). The primer sequences used to amplify target genes and GAPDH (internal control) are listed in Table 3.7. Real time quantitative PCR was performed with the ABI PRISM7700 Sequence Detection System. All expression values were normalized against GAPDH. All amplifications were done in triplicates.

| <b>Primer name</b> | <b>Primer sequence (5'-3')</b> |
|--------------------|--------------------------------|
| GAPDH (F)          | CTTCTTTTGCCTCGCCAGCC           |
| GAPDH (R)          | GAGTTAAAAGCAGCCCTGGTGA         |
| BPAG1e (F)         | TACTGCCCTGGTCACTCTCAT          |
| BPAG1e (R)         | CACTGTTGGCTTCTGACGCT           |
| Plectin (F)        | GGACACACTGCCCTGGAAC            |
| Plectin (R)        | ATCTGCGATGCGAATGACCG           |

|           |                      |
|-----------|----------------------|
| NDRG1 (F) | CTCCTCAAGATGGCGGACTG |
| NDRG1 (R) | CTAGCCGAGGGCATGTATCC |

F: Forward; R: Reverse

**Table 3.7: List of primers used for PCR**

### **3.19 Co-immunoprecipitation (Co-IP):**

The harvested cells were incubated in 1X PBS containing 1% Nonidet P-40 (NP40), 5 mM EDTA, and protease and phosphatase inhibitor mixture at 4°C for 15 minutes, followed by centrifugation at 13,000 rpm for 20 minutes at 4 °C. The supernatant was collected as the NP40 soluble fraction. The resulting insoluble pellet was homogenized in phosphate-buffered saline containing 2% Empigen and incubated for 45 minutes at 4°C, followed by centrifugation at 13,000 rpm for 20 minutes at 4 °C. The supernatant was collected as NP40 insoluble fraction. The soluble and insoluble fractions were pooled together and then incubated with anti-BPAG1e/K8 antibody bound to protein G-Sepharose beads for overnight at 4°C on slow moving rotor (7 rpm). The beads were washed three times with RIPA buffer (20 mM HEPES, 140 mM NaCl, 5 mM EDTA, and 0.4% NP40, pH 7.4). The immune complexes were solubilized in cell lysis buffer, resolved on SDS-PAGE, blotted and probed with respective antibodies. The protocol was adapted from (151).

### **3.20 Immunofluorescence:**

Cells were grown on glass cover slips for 48 hours till they reached a confluency of 70-80%. Adhered cells were washed twice with 1X PBS for 10 minutes each. The cells were fixed either

with chilled 100% methanol in -20°C or 4% paraformaldehyde at RT for 5 and 15 minutes respectively. After fixation, coverslips were washed thrice with 1X PBS for 10 minutes each. The cells were then permeabilized using 0.3% Triton X-100 for 90 seconds in case of methanol fixation and 10 minutes in 0.7% Triton X-100 when cells were fixed with paraformaldehyde. The coverslips were again washed thrice with PBS for 5 minutes each. They were then placed in a small humidified chamber and 5% BSA was layered over the cells for blocking and incubated for 1 hour. BSA was drained and the cells were layered with 50µl of primary antibody diluted in 5% BSA and incubated for 1 hour. The coverslips were washed thrice with 1X PBS for 10 minutes each followed by incubation with 50 µl of anti-mouse (Alexa Fluor 488)/ anti-mouse (Alexa Fluor 568)/ anti-rabbit (Alexa Fluor 488)/ anti-rabbit (Alexa Fluor 568) conjugated secondary antibody for 1 hour and later washed with 1X PBS thrice for 10 minutes each. Coverslips were then mounted using anti-bleaching agent (Vectashield, Vector laboratories, USA) and sealed. Confocal images were obtained using a LSM 780 Carl Zeiss Confocal system (Magnification: 63x, Numerical Aperture: 1.4).

### **3.21 Actin organization:**

The cells were grown on glass cover slips upto 90% confluency in complete medium. After serum starving the cells for 24 hours, wounds were scratched using microtip on monolayer of confluent cells. The cells surrounding the scratch were allowed to migrate into the wounded region for 7-8 hours. Subsequently, cells were fixed using 4% Paraformaldehyde. Further, cells were subjected to Phalloidin staining for 1 hour. The coverslips were then mounted using anti-bleaching agent (Vectashield, Vector laboratories, USA) and sealed. Confocal images were obtained using a LSM 780 Carl Zeiss Confocal system (152).

### **3.22 MTT (3-(4, 5-Dimethylthiazol-2-yl)-2, 5-Diphenyltetrazolium Bromide) cell viability assay:**

1000 cells were seeded per well, in a 96-well microtitre plate. Proliferation was studied every 24 hours up to a period of 4 days. At the desired time points, 100 µl of the medium was replenished from the designated wells and 20 µl MTT solution (5 mg/ml MTT in 1X PBS) was added to each well. Plate was incubated at 37°C in a CO<sub>2</sub> incubator for 4 hours, then 100 µl of acidified SDS (10% SDS in 0.01 N HCl) was added to each well and incubated overnight at 37°C. Next day, the absorbance was measured on an ELISA plate reader at 540 nm against a reference wavelength of 690 nm. Growth curve was plotted from three independent experiments (153).

### **3.23 Colony forming assay:**

Two hundred cells were plated in 60-mm tissue culture plates in triplicates. Cells were grown in complete medium for 10 days, with medium changes every 2–3 days. Cells were first fixed with methanol for 5 minutes at RT and then washed twice with 1X PBS. They were later stained with crystal violet solution (0.5% crystal violet in 20% methanol) for 5 minutes at RT. After washes with distilled water, the plates were allowed to dry.

### **3.24 *In vitro* wound healing assay for migration:**

The cells were grown in 35 mm plates to 95% confluency. The cells were replaced with fresh IMDM with 0.2% serum for 24 hours. After incubation, the medium was discarded and wounds were scratched with the help of a sterile 2 µl pipette tip. The cells were fed with fresh IMDM containing 0.2% serum and observed under an Axiovert 200 M Inverted Carl Zeiss microscope

fitted with a stage maintained at 37°C and 5% CO<sub>2</sub> atmosphere. Cells were observed by time lapse microscopy and the images were taken every 20 minutes for 20 hours using an AxioCam MRm camera with phase 1 objective. Migration was measured using the manual tracking plugin of ImageJ (NIH) software (152).

### **3.25 Transwell migration assay and boyden chamber cell invasion assay:**

The transwell migration assay was performed as described previously with some modifications (116). In brief,  $2 \times 10^5$  cells were seeded in the upper chamber in serum-free medium and the bottom chamber was filled with 0.6 ml of complete IMDM. The cells were incubated for 16 hours at 37°C. At the 15<sup>th</sup> hour, 4 µg/ml Calcein AM (Life technologies, USA) was added to the lower chamber and incubated for 1 hour at 37°C. The cells on the upper surface were carefully removed with a cotton swab at the 16<sup>th</sup> hour. Fluorescence of the invaded cells was read at wavelengths of 488/535nm (Ex/Em) on a bottom-reading fluorescent plate reader (Berthold, Germany). The boyden chamber invasion assay was performed similar to transwell migration assay. Additionally, 8 µm pore sized polycarbonate membrane filters in upper chamber were coated with 40 µl Matrigel (1mg/ml) with 140 µl incomplete IMDM.

### **3.26 Soft agar assay:**

The assay was performed in 35 mm Petri plates. As a first step, 1 ml of the basal layer was made by adding equal volumes of 2X complete IMDM and 2% low melting agarose. 1000 cells in complete medium containing 0.4% low melting agarose were seeded over the basal layer. Plates were fed with complete medium on every alternate day and incubated at 37°C in a 5% CO<sub>2</sub>

atmosphere for 15 days. Opaque and dense colonies were observed and counted microscopically on day 15.

### **3.27 *In vivo* Tumorigenicity assay:**

All protocols for animal studies were reviewed and approved by the “Institutional Animal Ethics Committee (IAEC)” constituted under the guidelines of the “Committee for the Purpose of Control and Supervision of Experiments on Animals (CPCSEA)”, Government of India (Approval ID: 04/2015). The tumorigenic potential of cells was determined by subcutaneous injection in NOD-SCID mice. The cells were suspended in plain medium without serum and  $6 \times 10^6$  cells were injected sub-cutaneously in the dorsal flank of 6–8 weeks old mice. 6 mice were injected per clone and were observed for tumor formation over a period of approximately 2 months. Tumor volume was determined using a digital vernier caliper (Advance, India) and volume was calculated by the modified ellipsoidal formula, [Tumor volume =  $1/2(\text{length} \times \text{width}^2)$ ] (154).

### **3.28 Gelatin zymography:**

To determine the Matrix Metalloproteinase 2 (MMP2) and MMP9 activity in conditioned culture medium, gelatin zymography was carried out as described by Ranjan *et al* (2014) with some modifications (155).  $5 \times 10^5$  cells were seeded in 35 mm tissue culture dish containing complete medium and grown for 24 hours in 5% CO<sub>2</sub> atmosphere at 37°C. The cells were then washed thrice with 1X PBS and grown in serum free medium for 24 hours. After 24 hours, culture medium was recovered and centrifuged at 2000 rpm for 5 minutes at 4°C. Supernatant was dried using Refrigerated CentriVap Concentrator, Labconco at 4°C. After complete drying, pellet was

dissolved in non-reducing Laemmli's sample buffer (62.2 mM Tris-HCl, pH 6.8, 4% SDS, 20% glycerol, 0.01% bromophenol blue) and applied to 10% SDS-PAGE gels polymerized with 1% gelatin. After electrophoresis, the gels were washed three times in a solution containing 2.5% Triton X-100 to eliminate the SDS and to allow reconstitution of the proteins. MMP activity was stimulated by incubating the gels at 37°C for 16 hours in reaction buffer (50 mM Tris-HCl, pH 6.8, 150 mM NaCl, 5 mM CaCl<sub>2</sub>, and 0.05% sodium azide). The activity of the MMPs was visualized by staining the gels in Coomassie Brilliant Blue G-250 solution.

### **3.29 Isolation of Cytoplasmic and nuclear fractions:**

The cells were harvested and resuspended in hypotonic buffer (10mM HEPES [pH 7.9], 1mM MgCl<sub>2</sub>, 100mM KCl). The lysate was mixed by inverting and kept on ice for 30 minutes. 0.6% NP40 was added into lysate and vortexed for 10 seconds. Centrifugation was carried out at 8000 rpm for 5 minutes at 4°C. The supernatant was collected as cytoplasmic fraction. The pellet was resuspended in SDS lysis buffer and boiled for 6 minutes. After centrifugation, the supernatant was collected as nuclear fraction.  $\beta$ -tubulin and Lamin A/C were used as loading control for cytoplasmic and nuclear fractions respectively.

### **3.30 RhoA/Rac1/Cdc42 activation assay:**

RhoA, Rac1 and Cdc42 activation assays were performed using RhoA/Rac1/Cdc42 Activation Assay Combo Biochem Kit (BK030, Cytoskeleton Inc, USA) as per manufacturer's instructions. In brief, the cells were treated with 40 ng/ml epidermal growth factor (EGF; Invitrogen, USA) for 10 minutes to activate Cdc42. Similarly, the cells were treated with 10 ng/ml EGF for 4 minutes and 100  $\mu$ g/ml Calpeptin (Calbiochem, USA) for 10 minutes to activate Rac1 and RhoA

respectively. The cells were lysed using lysis buffer (provided in the kit) on ice. For activation assays, 500 ug protein lysate was incubated with PAK-PBD or Rhotekin RBD beads at 4°C for 1 hour on rocker. After centrifugation, the supernatant was decanted and the pellet was washed thrice with wash buffer (provided in the kit). Further, the pellet was resuspended in lamelli buffer. The lysates prepared from cells, which were not treated with EGF or Calpeptin, were used as a control. The samples were subjected to SDS-PAGE and western blotting. The amount of activated RhoA/Rac1/Cdc42 was determined by western blotting using a RhoA/Rac1/Cdc42 specific antibody (provided in the kit).

### **3.31 Fractionation and Quantification of F-Actin:**

The cells were harvested and resuspended in lysis and F-actin stabilization buffer (50 mM 1,4-piperazinediethanesulfonic acid, 50mM NaCl, 5 mM MgCl<sub>2</sub>, 5 mM ethylene glycol tetra-acetic acid, 5% glycerol, 0.1% Nonidet P-40, 0.1% Triton X-100, 0.1% Tween 20, and 0.1% β-mercaptoethanol). Further, cells were homogenized using 27 gauge needles. The F-actin was separated by ultra-centrifugation at 100000 RCF for 60 minutes at 37°C. The pellet was resuspended in ice cold G-buffer (2 mM Tris-HCl pH 8.0, 0.2 mM CaCl<sub>2</sub>, 0.2 mM ATP, and 0.5 mM dithiothreitol) and incubated for 1 hour on ice to achieve F-actin depolymerization. Further, dissociated F-actin was centrifuged at 14000 RCF for 10 minutes at 4°C. The supernatant was collected and protein content was quantified using modified lowry method. 20 ug lysate was used for loading. The amount of F-actin was examined using monoclonal β-actin antibody. GAPDH was used as the loading control. The protocol was adapted from Sun *et al* (2013) (139).

### **3.32 SWATH (sequential window acquisition of all theoretical fragment ion spectra) analysis:**

SWATH analysis was performed at National Chemical Laboratory (NCL), Pune, India (156).

LC Separation: Peptide digest (3  $\mu$ g) was separated by using Eksigent MicroLC 200 system (Eksigent, Dublin, CA) equipped with Eksigent C18-reverse phase column (100\*0.3mm, 3 $\mu$ m, 120Å). The sample was loaded onto the column with 97% of mobile phase A (100% water, 0.1% Formic acid) and 3% of mobile phase B (100% Acetonitrile, 0.1% Formic acid) at 7  $\mu$ l/min flow rate. Peptides were eluted with a 120 minutes linear gradient of 3% to 50% mobile phase B. The column temperature was set to 40°C and auto sampler at 4°C. The same chromatographic conditions were used for both information-dependent acquisition (IDA) and SWATH acquisition.

Full MS/MS<sup>2</sup> acquisition (IDA for creating library): All samples were analyzed on AB-Sciex 5600 Triple TOF mass-spectrometer in positive and high-sensitivity mode. The dual source parameters were optimized for better results: ion source gases GS1, GS2, curtain gas at 25 psi, temperature 200°C and ion spray voltage floating (ISVF) at 5500V. The accumulation time in full scan was 250 ms for a mass range of 350-1800 m/z. The parent ions are selected based on the following criteria: ions in the MS scan with intensities more than 120 counts per second, charge stage between +2 to +5 and mass tolerance 50 mDa. Ions were fragmented in the collision cell using rolling collision energy (CE) with an additional CE spread of  $\pm$  15 eV.

Samples were acquired in technical triplicate using above mentioned IDA method. IDA mass spectrometric files were searched using ProteinPilot software, Version 4.0.8085 (AB SCIEX, MA, USA) with the Paragon algorithm against human serum albumin protein database (P02768-

UniProt) at 1% FDR. The ProteinPilot output file (.group) was used as a standard peptide spectral library. SWATH MS- In SWATH-MS mode, the instrument was specifically tuned to optimize the quadrupole settings for the selection of precursor ion selection window 25 m/z wide. Using an isolation width of 26 m/z (containing 1 m/z for the window overlap), a set of 34 overlapping windows was constructed covering the precursor mass range of 400-1250 m/z. SWATH MS/MS spectra were collected from 100 to 2000 m/z. Ions were fragmented in the collision cell using rolling collision energy with an additional CE spread of  $\pm 15$  eV. An accumulation time (dwell time) of 96 ms was used for all fragmentation scans in high-sensitivity mode, and for each SWATH-MS cycle a survey scan in high-resolution mode 9 was acquired for 100 ms resulting in a duty cycle of 3.33 seconds. The source parameters were similar to that of IDA acquisition.

SWATH analysis was performed for two technical replicates for each sample. The spectral alignment and targeted data extraction of SWATH-MS data was performed using Peakview software, Version 1.2.03 (AB SCIEX, MA, USA). The peptide data (.MRKVV) files were used for quantification of glycosylated peptides of HSA using Markerview software, Version 1.2.1.1 (AB SCIEX, MA, USA). Normalization was performed using total area sum. The peptides with a p value less than 0.05 were considered for quantification.

### **3.33 Histology and Immunohistochemistry:**

The NOD-SCID mice were sacrificed approximately 8 weeks after subcutaneous injection. The tumor tissues were collected and fixed in 10% neutral buffered formalin and processed for histology. 5 micron sections of formalin fixed and paraffin embedded tissues were used for immunohistochemistry. Immunohistochemical staining was performed according to previously

described method using Vectastain ABC kit, Vector Laboratories, USA (157). The tissue sections were deparaffinized by keeping the slides in xylene twice for 15 minutes each. The slides were then treated with xylene and alcohol (1:1). The sections were dehydrated in 100% ethanol. Further, tissues were treated with 100% methanol for 20 minutes. For endogenous peroxidase inactivation, tissues were treated with 3% hydrogen peroxide in methanol for 30 minutes. The microwave treatment in citrate buffer (pH 6.0) was given to the tissues for antigen retrieval. The sections were then blocked with preimmune horse serum for 45 minutes at RT followed by respective primary antibody incubation overnight at 4°C. This was followed by secondary biotinylated antibody for 60 minutes at RT and then with an avidin-biotin-peroxidase complex for 60 minutes at RT. After each step, sections were washed with Tris buffered saline (pH 7.2). The sections were then subjected to substrate solution containing 0.08% Diaminobenzidine (DAB) and 3% hydrogen peroxide which resulted in brown precipitate formation at the site of enzymatic activity. The counterstaining was performed using haematoxylin.

### **3.34 Densitometry quantification and Statistical analysis:**

Densitometric quantitation of scanned images was performed by ImageJ software (National Institute of Health, USA). Band intensities were normalized to respective loading controls. All the statistical analyses were performed using GraphPad Prism software (version 6.01). Two groups of data were statistically analyzed by *t test*. A *p* value less than 0.05 was considered statistically significant.

## *4. Results*

#### 4.1 BPAG1e interacts with K8 in OSCC derived cells

BPAG1e is expressed in the basal layer of squamous cell epithelia, whereas K8 is normally expressed in simple epithelia (1, 108). In case of OSCC and OSCC derived cell lines, K8/18 pair is aberrantly expressed (21-23, 26). Therefore, to understand whether BPAG1e interacts with K8, immunoprecipitation (IP) assay was performed in OSCC derived AW13516 cells. K8 was detected in IP fraction when antibody for BPAG1e was used for IP (Figure 4.1A, left panel). Similarly, pull down fraction of K8 IP showed presence of BPAG1e (Figure 4.1A, right panel). These results suggest that K8 can interact with BPAG1e in OSCC derived cells.

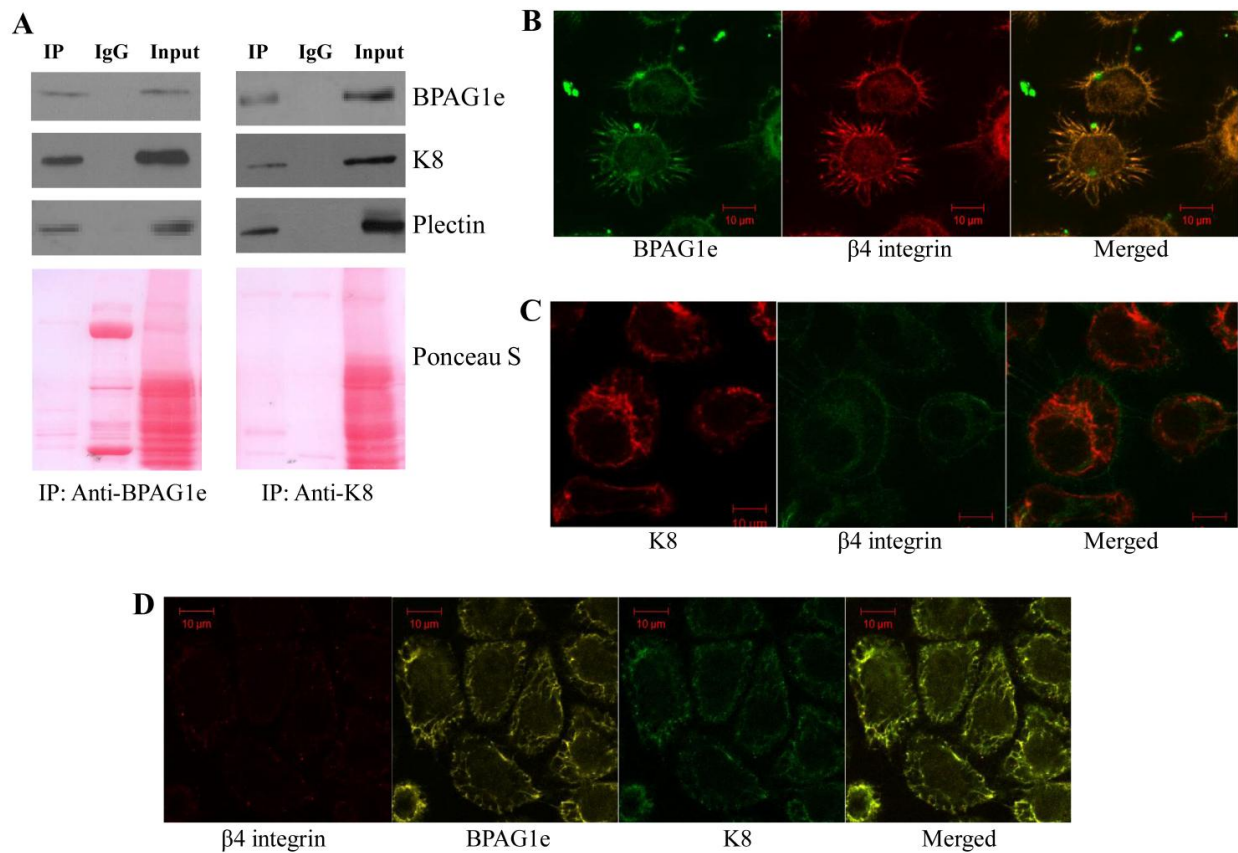


**Figure 4.1: BPAG1e interacts with K8 in AW13516 cells.** (A) Endogenous pull down experiment with anti-BPAG1e and anti-K8 antibody performed using cell lysate from AW13516

*cells. Anti-goat and Anti-mouse IgG antibody was used as secondary antibody control for BPAG1e IP and K8 IP respectively. The immunoprecipitated complex was examined for the presence of BPAG1e, Keratin 8 and Plectin. Input represents 10% of cell lysate used in the IP experiment. This experiment was performed in triplicate. (B) Immunofluorescence analysis showing BPAG1e (stained in green) and  $\beta$ 4 integrin (stained in red) dual staining in AW13516 cells. (C) Immunofluorescence analysis showing K8 (stained in red) and  $\beta$ 4 integrin (stained in green) dual staining in AW13516 cells. (D) Immunofluorescence analysis showing K8 (stained in green), BPAG1e (stained in yellow) and  $\beta$ 4 integrin (stained in red) triple staining in AW13516 cells.*

Further, colocalization experiments using immunofluorescence microscopy were performed for K8, BPAG1e and  $\beta$ 4 integrin to validate results of immunoprecipitation assay. Unfortunately, due to non-specific staining of the BPAG1e antibody in AW13516 cells, the results of K8 + BPAG1e and K8 + BPAG1e +  $\beta$ 4 integrin staining were inconclusive, although, K8 and  $\beta$ 4 integrin dual staining was properly observed in AW13516 cells (Figure 4.1B-D).

To understand a role of HD linker proteins in neoplastic progression of OSCC, these proteins were stably downregulated in OSCC derived cells.

#### **4.2 Knockdown of hemidesmosomal linker protein(s) in AW13516 cells**

Both single and double knockdown of Plectin and/or BPAG1e in AW13516 was carried out using shRNA technology. Downregulation of HD linker protein(s) was confirmed at mRNA and protein level (Figure 4.2). BPAG1e knockdown clones C4 and C12 showed 2.85 and 2.95 fold reduction

in BPAG1e mRNA level (Figure 4.2A), whereas Plectin knockdown clones C1 and C2 demonstrated about 6.7 and 5.9 fold reduction in Plectin expression at mRNA level (Figure 4.2B). Further, BPAG1e-Plectin double knockdown clones C1 and C4 displayed ~2.9 and ~6.5 fold decrease in BPAG1e and Plectin mRNA respectively (Figure 4.2C-D).

BPAG1e knockdown clones C4 and C12 displayed ~79% decrease in BPAG1e protein as compared to vector control clone BVC (Figure 4.2E). Plectin knockdown clones C1 and C2 showed about ~94% reduction in Plectin expression at protein level as compared to vector control clone PVC (Figure 4.2F). Further, decrease in Plectin (~93%) and BPAG1e (~81%) protein levels was observed in double knockdown clones C1 and C4 as compared to respective vector control clone DVC (Figure 4.2G).

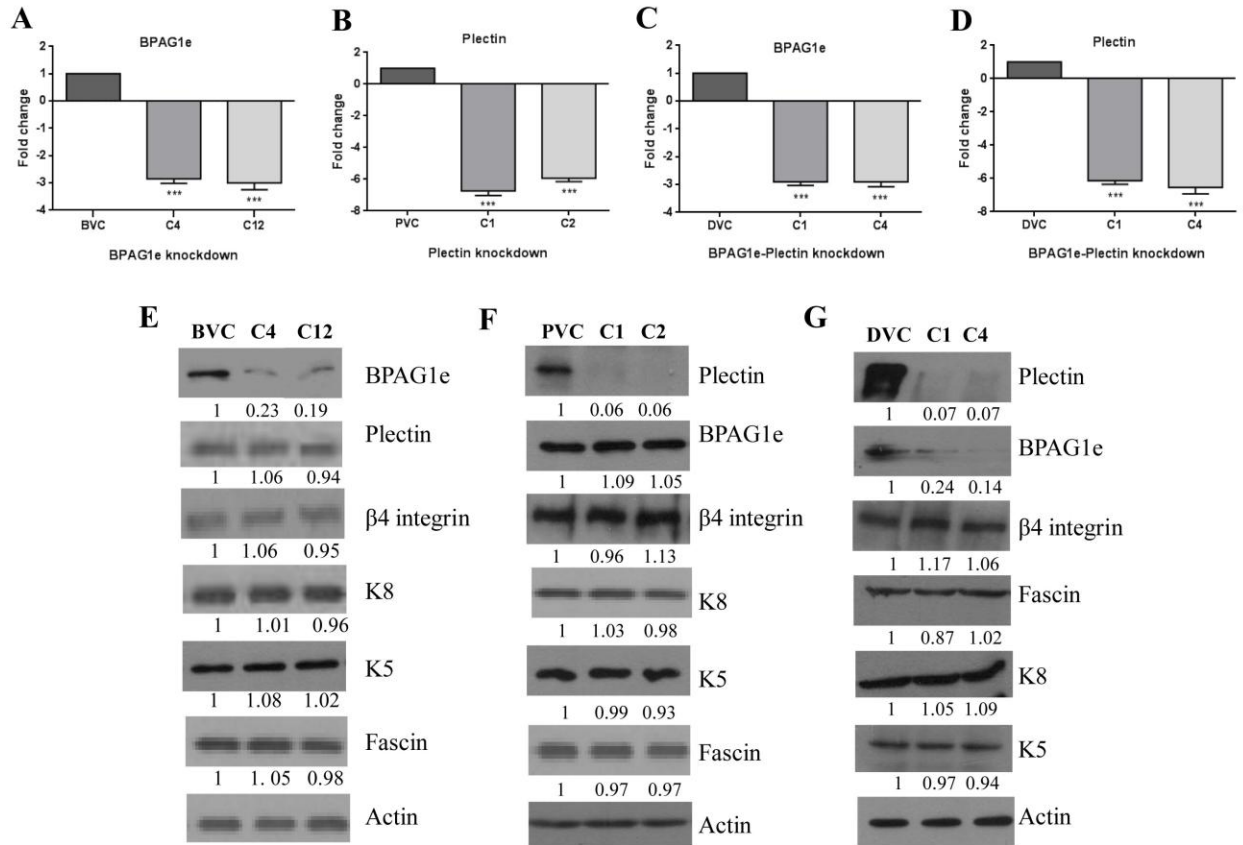


**Figure 4.2: Loss of hemidesmosomal linker protein(s) does not affect expression of associated proteins.** (A) qRT-PCR of BPAG1e and (E) western blot analysis of BPAG1e, Plectin,  $\beta$ 4 integrin, Fascin, K8 and K5 in vector control clone (BVC) and BPAG1e knockdown clones (C4, C12). (B) qRT-PCR of Plectin and (F) western blot analysis of Plectin, BPAG1e,  $\beta$ 4 integrin, Fascin, K8 and K5 in vector control clone (PVC) and Plectin knockdown clones (C1, C2). (C, D) qRT-PCR of BPAG1e, Plectin and (G) western blot analysis of BPAG1e, Plectin,  $\beta$ 4 integrin, Fascin, K8 and K5 in vector control clone (DVC) and BPAG1e-Plectin knockdown clones (C1, C4). Note: the numbers below the blot indicate relative intensity of the bands using densitometric analysis.

In a previous study from our laboratory, it was shown that loss of K8 in AW13516 cells led to reduction in cell migration, cell invasion, *in vitro* and *in vivo* tumorigenicity and alterations in actin organization (26). Therefore, to understand whether knockdown of hemidesmosomal linker proteins leads to similar phenotypic changes as seen in response to K8 knockdown, we performed phenotypic assays using linker protein knockdown cells.

### **4.3 Phenotypic assays for cell transformation**

#### **4.3.1 Loss of Hemidesmosomal linker proteins led to reduced cell migration, cell invasion and alterations in actin organization**

Scratch wound healing assay demonstrated decrease in cell migration in both single and double linker proteins knockdown clones as compared to respective vector control clones. The rate of cell migration was reduced by ~29%, ~33% and ~36% in BPAG1e, Plectin and BPAG1e-Plectin double knockdown AW13516 cells respectively ( $p < 0.001$ ) (Figure 4.3A-B, 4.4A-B and 4.5A-B).

It is well documented that cell migration is regulated by changes in the actin organization (158). Therefore, actin organization was analyzed using phalloidin staining followed by confocal microscopy. The membrane protrusions in vector control cells were found to be uniformly present on cell membrane, whereas in case of loss of hemidesmosomal linker proteins, membrane protrusions were found to be non-uniformly organized (Figure 4.3C, 4.4C and 4.5C). Moreover, the length of membrane protrusions was significantly reduced in BPAG1e (7.04  $\mu\text{m}$ ), Plectin (6.81  $\mu\text{m}$ ), BPAG1e-Plectin (6.49  $\mu\text{m}$ ) knockdown cells as compared to BVC (11.27  $\mu\text{m}$ ), PVC (11.67  $\mu\text{m}$ ), DVC (11.63  $\mu\text{m}$ ) respectively ( $p < 0.001$ ) (Figure 4.3D, 4.4D and 4.5D).

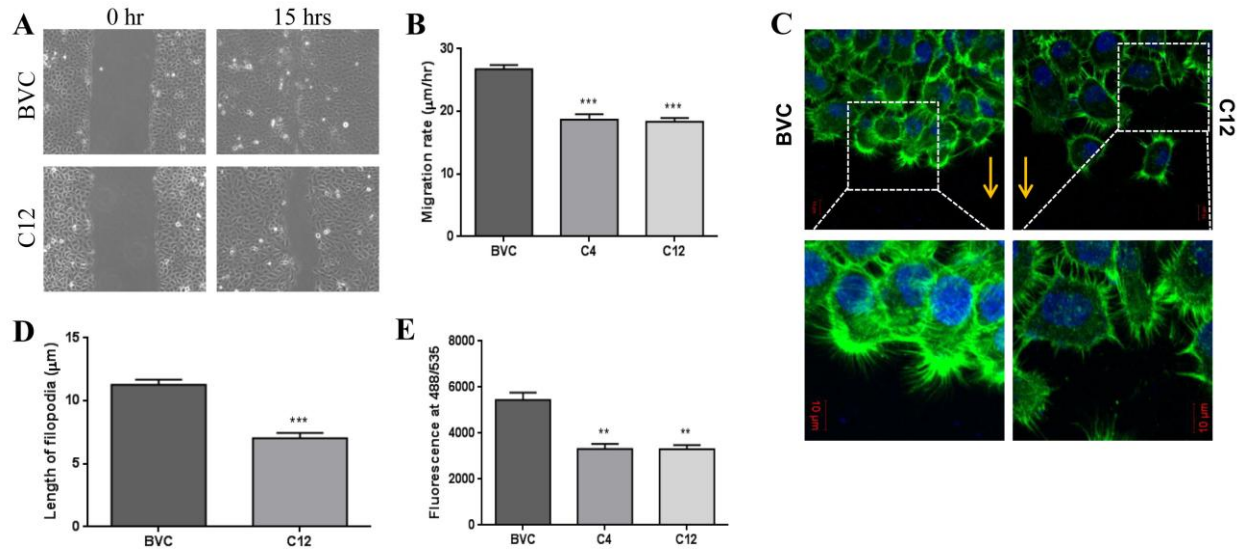


**Figure 4.3: Loss of BPAG1e leads to reduced cell migration, cell invasion and alterations in actin organization.** (A) Representative time lapse microscopy images show wound healing for vector control clone (BVC) and BPAG1e knockdown clone (C12). (B) The graph shows rate of cell migration for vector control clone (BVC) and BPAG1e knockdown clones (C4, C12). (C) Immunofluorescence analysis of actin organization (stained in green) at the wound edge in vector control clone (BVC) and BPAG1e knockdown clone (C12). The nucleus is stained with DAPI. The arrow indicates direction of migration. The inset shows filopodia formed at migratory front. (D) The graph shows length of filopodia in vector control clone (BVC) and BPAG1e knockdown clone (C12). For each clone, 30 cells at the wound front were used for quantification. (E) The graph shows fluorescence of invaded vector control cells (BVC) and BPAG1e knockdown cells (C4, C12) which is read at wavelengths of 488/535nm (Ex/Em).

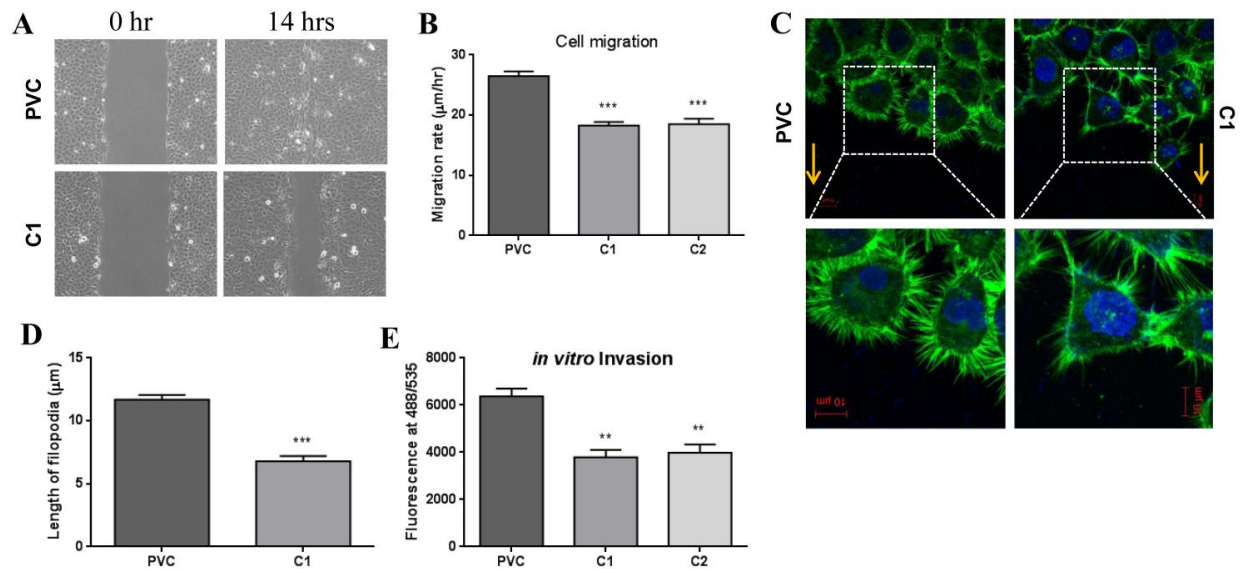


**Figure 4.4: Loss of Plectin leads to reduced cell migration, cell invasion and alterations in actin organization.** (A) Representative time lapse microscopy images show wound healing for vector control clone (PVC) and Plectin knockdown clone (C1). (B) The graph shows rate of cell migration for vector control clone (PVC) and Plectin knockdown clones (C1, C2). (C) Immunofluorescence analysis of actin organization (stained in green) at the wound edge in vector control clone (PVC) and Plectin knockdown clone (C1). The nucleus is stained with DAPI. The arrow indicates direction of migration. The inset shows filopodia formed at migratory front. (D) The graph shows length of filopodia in vector control clone (PVC) and Plectin knockdown clone (C1). For each clone, 30 cells at the wound front were used for quantification. (E) The graph shows fluorescence of invaded vector control cells (PVC) and Plectin knockdown cells (C1, C2) which is read at wavelengths of 488/535nm (Ex/Em).

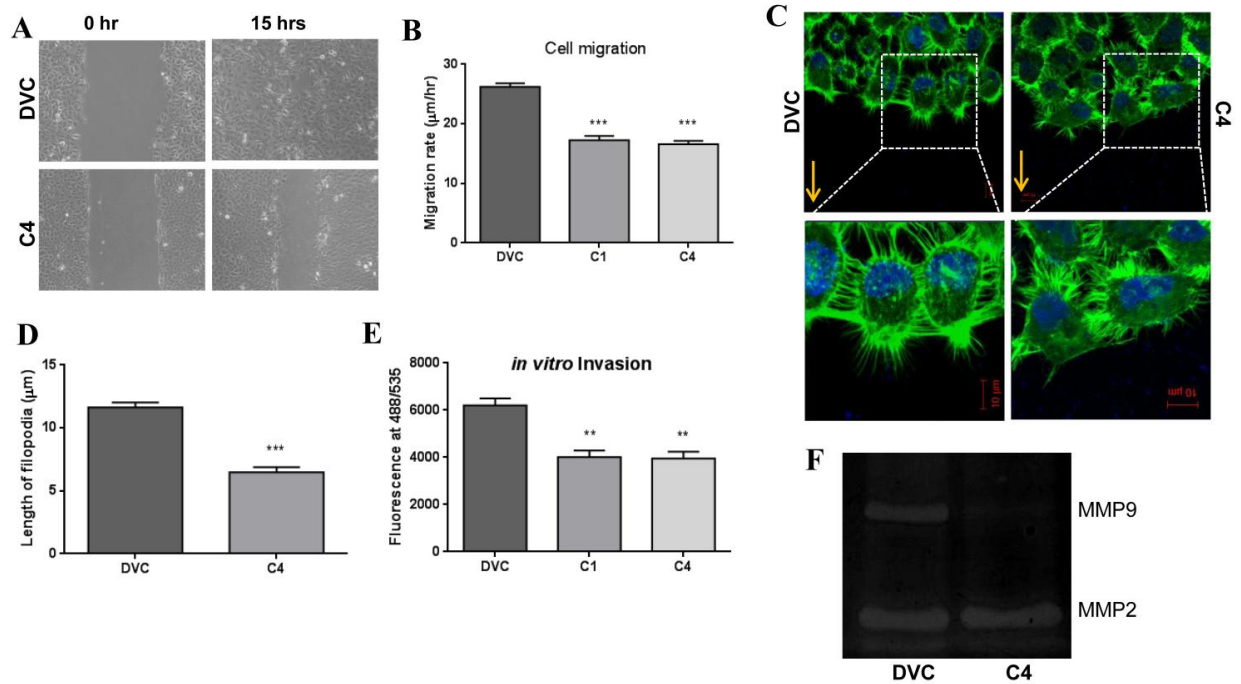


**Figure 4.5: Loss of BPAG1e-Plectin leads to reduced cell migration, cell invasion and alterations in actin organization.** (A) Representative time lapse microscopy images show wound healing for vector control clone (DVC) and BPAG1e-Plectin knockdown clone (C4). (B) The graph shows rate of cell migration for vector control clone (DVC) and BPAG1e-Plectin knockdown clones (C1, C4). (C) Immunofluorescence analysis of actin organization (stained in green) at the wound edge in vector control clone (DVC) and BPAG1e-Plectin knockdown clone (C4). The nucleus is stained with DAPI. The arrow indicates direction of migration. The inset shows filopodia formed at migratory front. (D) The graph shows length of filopodia in vector control clone (DVC) and BPAG1e-Plectin knockdown clone (C4). For each clone, 30 cells at the wound front were used for quantification. (E) The graph shows fluorescence of invaded vector control cells (DVC) and BPAG1e knockdown cells (C1, C4) which is read at wavelengths of 488/535nm (Ex/Em). (F) The gelatin zymography shows MMP2 and MMP9 activity in vector control clone (DVC) and BPAG1e-Plectin knockdown clone (C4).

Rho GTPases family proteins, RhoA, Rac1 and Cdc42, play a crucial role in the actin cytoskeleton organization. RhoA, Rac1 and Cdc42 regulate cellular motility by formation of stress fibres, lamellipodia and filopodia respectively (159). The Cdc42 activity was significantly reduced upon BPAG1e, Plectin and BPAG1e-Plectin knockdown as compared to respective vector control cells (Figure 4.6A-C). On the other hand, no significant difference was observed in Rac1 and RhoA activity of HD linker proteins knockdown cells as compared to DVC (Figure 4.6D-E).

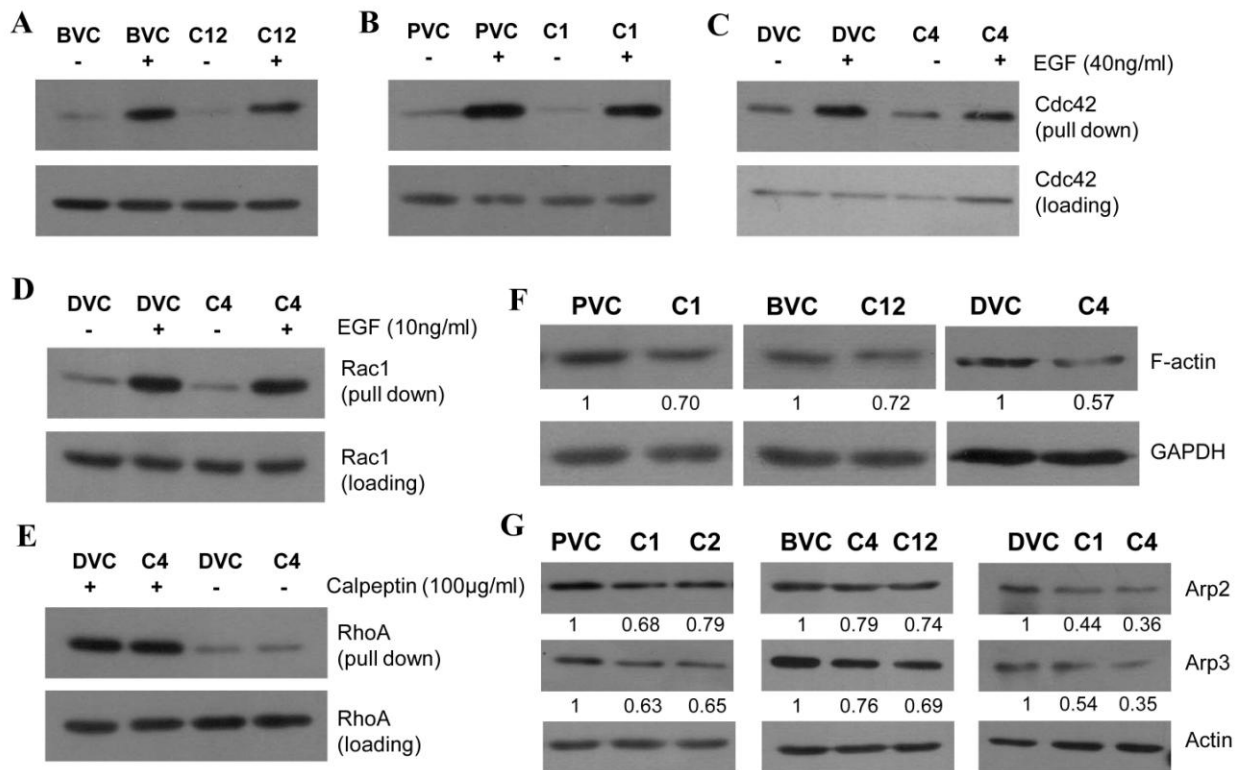


**Figure 4.6: Effect of hemidesmosomal linker protein(s) knockdown on activity of Rho GTPases and actin polymerization.** (A) Western blot analysis of Cdc42 activity in vector control clone (BVC) and BPAG1e clone (C12). (B) Western blot analysis of Cdc42 activity in vector control clone (PVC) and Plectin knockdown clone (C1). (C) Western blot analysis of Cdc42 activity in vector control clone (DVC) and BPAG1e-Plectin knockdown clone (C4). (D) Western

*blot analysis of Rac1 activity in vector control clone (DVC) and BPAG1e-Plectin knockdown clone (C4). (E) Western blot analysis represents RhoA activity in vector control clone (DVC) and BPAG1e-Plectin knockdown clone (C4). (F) Western blot analysis shows F-actin levels in vector control clones (PVC, BVC, DVC), Plectin knockdown clone (C1), BPAG1e knockdown clone (C12) and BPAG1e-Plectin knockdown clone (C4). (G) Western blot analysis of Arp2, Arp3 in vector control clones (PVC, BVC, DVC), Plectin knockdown clones (C1, C2), BPAG1e knockdown clones (C4, C12) and BPAG1e-Plectin knockdown clones (C1, C4). Note: the numbers below the blot indicate relative intensity of the bands using densitometric analysis.*

Further, the appearance of shorter and fewer filopodia upon loss of linker protein(s) prompted us to investigate whether there is any defect in actin polymerization. Indeed, actin polymerization assay revealed reduced levels of F-actin in BPAG1e, Plectin and BPAG1e-Plectin knockdown cells as compared to respective vector control cells (Figure 4.6F). Actin related proteins (Arp) 2/3 complexes are one of the important actin regulators which participate in nucleation and branching of actin filaments. The Arp2/3 complex is activated by the Wiskott–Aldrich syndrome family protein (WASP) family of proteins which are in turn activated by Cdc42 (160). In BPAG1e, Plectin and BPAG1e-Plectin downregulated cells, we observed reduction in Arp2 and Arp3 protein levels (Figure 4.6G). Altogether, these results indicated that reduced Cdc42 activity in linker protein(s) knockdown cells led to decreased expression of Arp2/3 proteins, resulting in shorter and fewer filopodia. This explains the reduced cell migration observed in linker protein(s) knockdown cells.

Further, the HD linker protein(s) knockdown cells were less invasive as compared to respective vector control cells. The invasion was reduced by ~30-35%, ~32-35% and ~37- 40% in BPAG1e,

Plectin and BPAG1e-Plectin knockdown cells respectively ( $p < 0.001$ ) (Figure 4.3E, 4.4E and 4.5E). Cancer cell invasion and metastasis require the crossing of several physical barriers such as the basement membrane. Matrix Metalloproteinases (MMPs) play a major role in breaking these barriers, thus facilitating invasion (161). Further, it has been demonstrated that increased activity of MMPs (MMP2 and MMP9) correlates with invasive potential of OSCC (162). To find out whether activity of MMP2 and/or MMP9 has altered in linker proteins knockdown cells, we carried out gelatin zymography. Our experiment revealed that MMP9 activity was significantly reduced in BPAG1e-Plectin knockdown cells as compared to DVC, whereas MMP2 activity remained unaltered (Figure 4.5F). Thus, decreased MMP9 activity seems to be responsible for reduced cell invasion in the linker proteins downregulated cells.

#### **4.3.2 Downregulation of hemidesmosomal linker proteins led to reduction in the tumorigenic potential of AW13516 cells**

In our previous study, we have demonstrated that loss of K8 in AW13516 cells leads to reduction in tumorigenic potential of OSCC derived cells (26). BPAG1e, Plectin and BPAG1e-Plectin double knockdown clones showed a significant reduction in number of colonies by ~20-30% and colony size by ~60-65% as compared with respective vector control clones ( $p < 0.001$ ) (Figure 4.7A-C, 4.8A-C and 4.9A-C). Further, the MTT and clonogenic assays demonstrated no significant difference in proliferative potential of linker protein(s) knockdown cells as compared to respective vector control cells (Figure 4.7D-E, 4.8D-E and 4.9D-E). Therefore, the decrease in soft agar colony size can be attributed to reduction in transformation potential and not to the proliferative potential of the linker proteins knockdown cells.

Furthermore, the *in vivo* tumorigenicity of HD linker protein(s) downregulated and respective vector control clones was assessed by subcutaneous injection in NOD-SCID mice (n=5). At the end of 8 weeks, the mean tumor volume of the mice bearing BPAG1e, Plectin and BPAG1e-Plectin double knockdown cells was significantly reduced as compared with the average volume of tumors formed by the respective vector control cells ( $p < 0.001$ ) (Figure 4.7F-G, 4.8F-G and 4.9F-G).

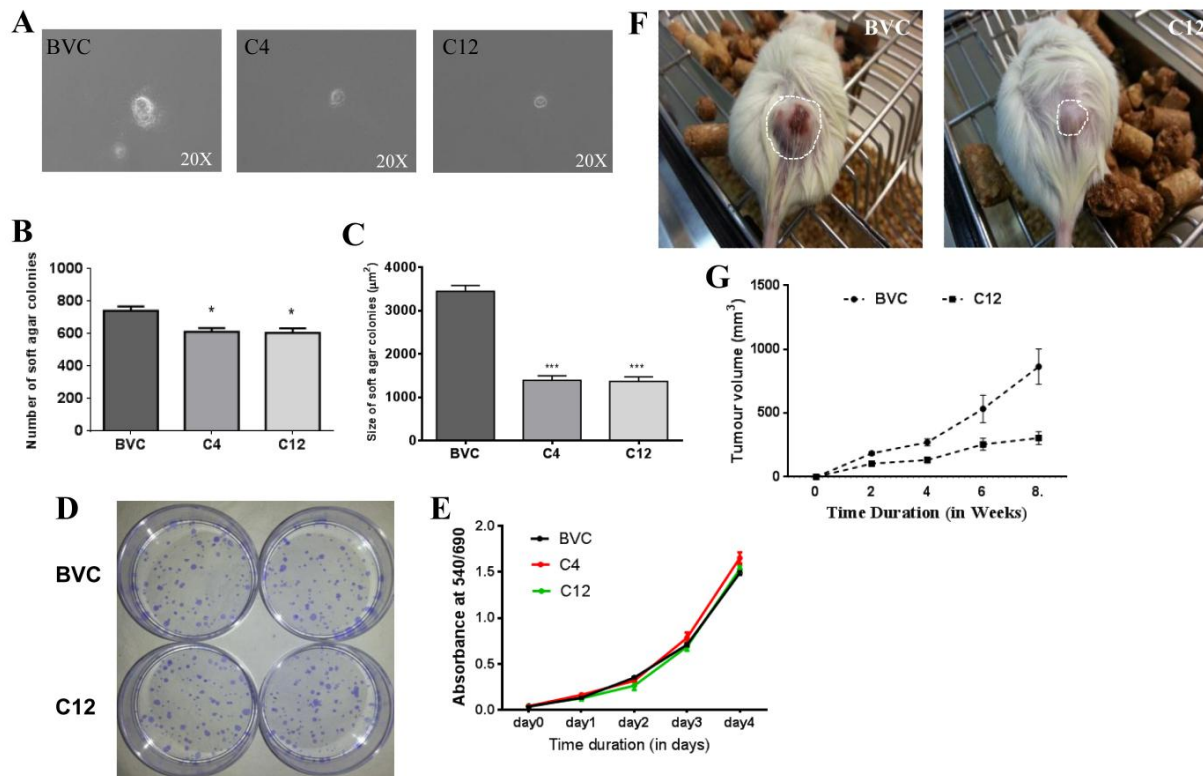


**Figure 4.7: Loss of BPAG1e leads to reduced tumorigenic potential.** (A) The representative images of colonies formed on soft agar and graphical representation of the (B) number of colonies and (C) size of colonies formed on soft agar in vector control clone (BVC) and BPAG1e knockdown clones (C4, C12). (D) Representative images of clonogenic assay for vector control clone (BVC) and BPAG1e knockdown clone (C12). (E) Graphical representation of MTT cell

viability assay for vector control clone (BVC) and BPAG1e knockdown clones (C4, C12). (F) Representative images of NOD-SCID mice bearing tumors formed from vector control cells (BVC) and BPAG1e knockdown cells (C12) after 8 weeks of injection. The tumors are indicated by dotted circles. (G) The graph shows tumor volume plotted against time for vector control clone (BVC) and BPAG1e knockdown clone (C12). It represents mean  $\pm$  SEM for 5 animals injected for each clone.

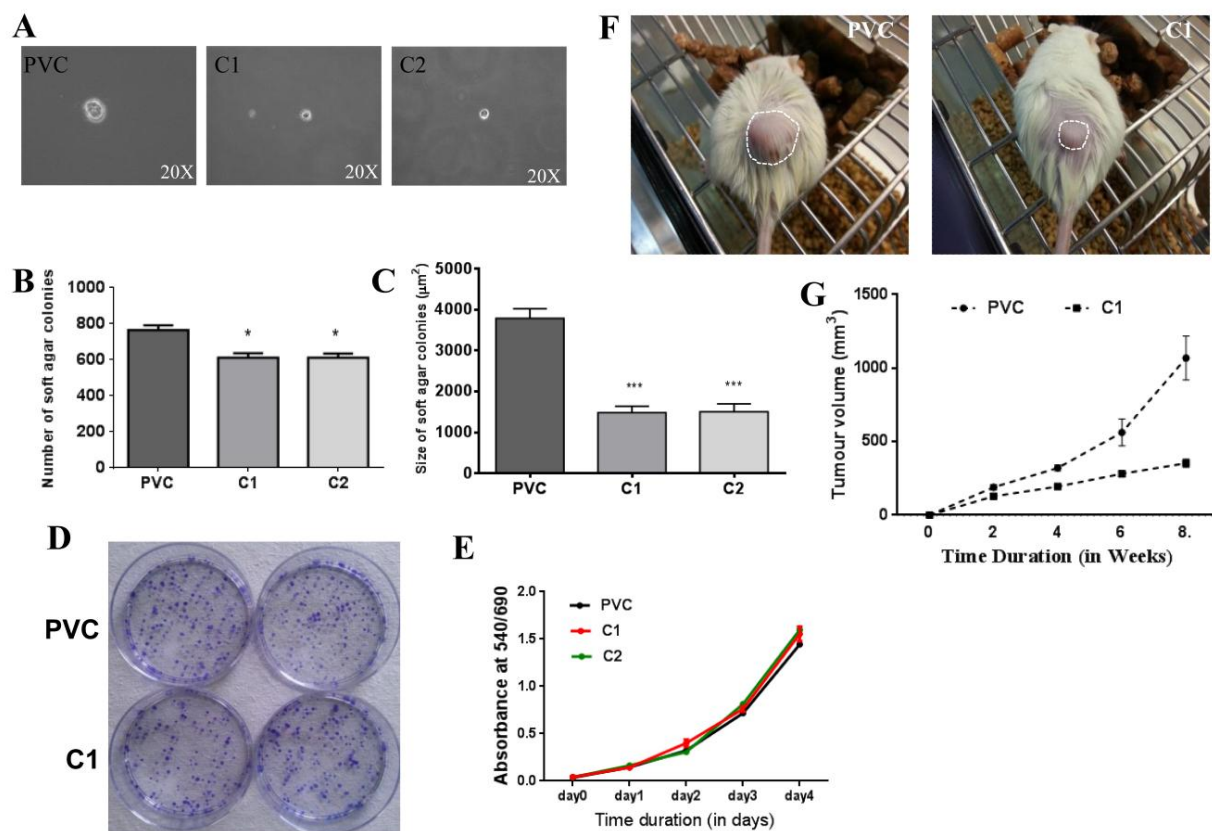


**Figure 4.8: Loss of Plectin leads to reduced tumorigenic potential.** (A) The representative images of colonies formed on soft agar and graphical representation of the (B) number of colonies and (C) size of colonies formed on soft agar in vector control clone (PVC) and Plectin knockdown clones (C1, C2). (D) Representative images of clonogenic assay for vector control

clone (PVC) and Plectin knockdown clone (C1). (E) Graphical representation of MTT cell viability assay for vector control clone (PVC) and Plectin knockdown clones (C1, C2). (F) Representative images of NOD-SCID mice bearing tumors formed from vector control cells (PVC) and Plectin knockdown cells (C1) after 8 weeks of injection. The tumors are indicated by dotted circles. (G) The graph shows tumor volume plotted against time for vector control clone (PVC) and Plectin knockdown clone (C1). It represents mean  $\pm$  SEM for 5 animals injected for each clone.

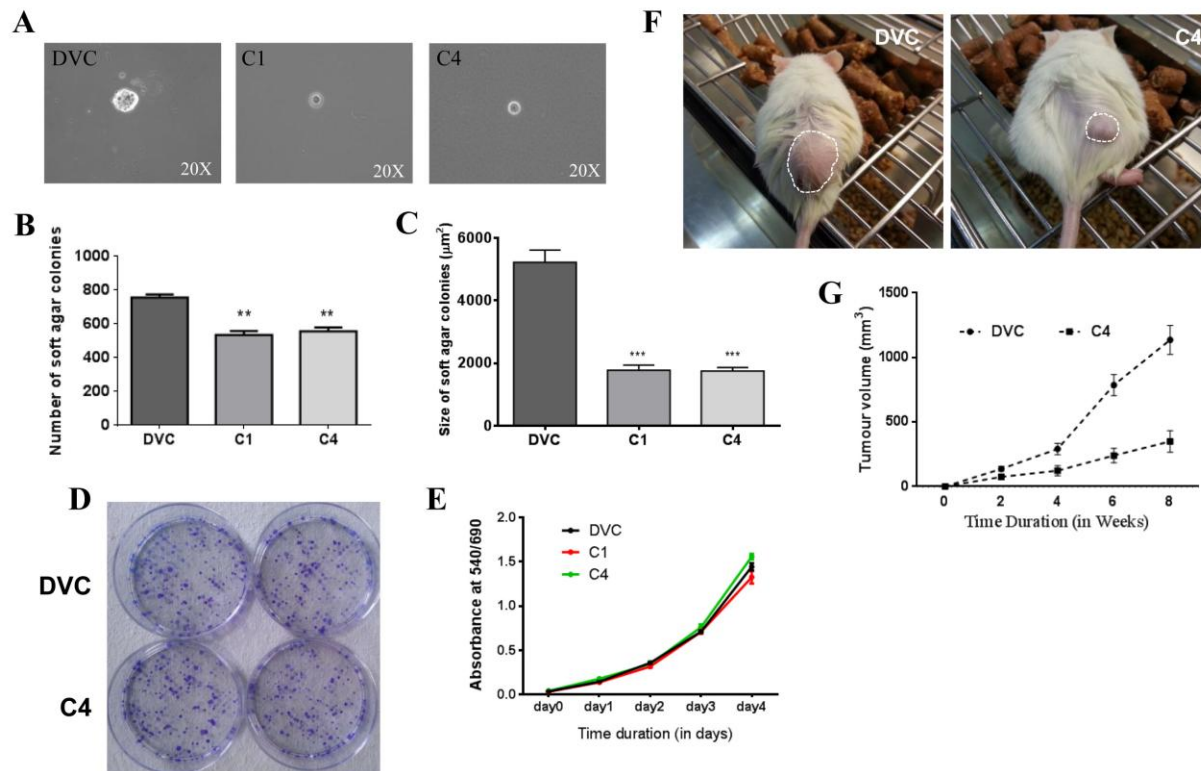


**Figure 4.9: Loss of BPAG1e-Plectin leads to reduced tumorigenic potential.** (A) The representative images of colonies formed on soft agar and graphical representation of the (B) number of colonies and (C) size of colonies formed on soft agar in vector control clone (DVC) and BPAG1e-Plectin knockdown clones (C1, C4). (D) Representative images of clonogenic

assay for vector control clone (DVC) and BPAG1e-Plectin knockdown clones (C4). (E) Graphical representation of MTT cell viability assay for vector control clone (DVC) and BPAG1e-Plectin knockdown clones (C1, C4). (F) Representative images of NOD-SCID mice bearing tumors formed from vector control cells (DVC) and BPAG1e-Plectin knockdown cells (C4) after 8 weeks of injection. The tumors are indicated by dotted circles. (G) The graph shows tumor volume plotted against time for vector control clone (DVC) and BPAG1e-Plectin knockdown clone (C4). It represents mean  $\pm$  SEM for 5 animals injected for each clone.

#### 4.4 Expression of associated proteins upon loss of hemidesmosomal linker proteins

The knockdown of BPAG1e or Plectin did not show any alterations in filament organization of K8 (Figure 4.10A-B). This result indicated that in absence of one linker protein, the other protein is sufficient to anchor keratin proteins. The sparse filament organization for K8 and K5 was observed upon loss of both hemidesmosomal linker proteins, indicating that linker proteins are essential to anchor keratins to the cell surface at hemidesmosomal sites (Figure 4.10C).

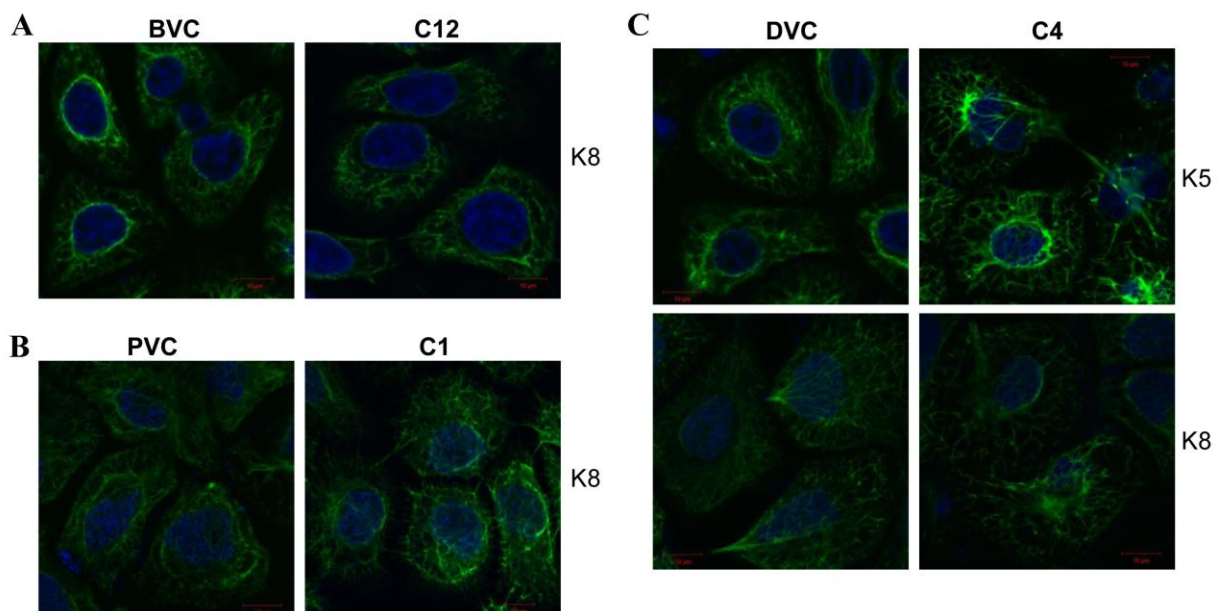


**Figure 4.10: Effect of hemidesmosomal protein(s) knockdown on keratin filament organization.** (A) Immunofluorescence analysis showing K8 filament organization (stained in green) in vector control clone (BVC) and BPAG1e knockdown clone (C12). The nucleus is stained with DAPI. (B) Immunofluorescence analysis showing K8 filament organization (stained in green) in vector control clone (PVC) and Plectin knockdown clone (C1). The nucleus is stained with DAPI. (C) Immunofluorescence analysis showing K5 and K8 filament organization (stained in green) in vector control clone (DVC) and BPAG1e-Plectin knockdown clone (C4). The nucleus is stained with DAPI.

Previous study from our laboratory had shown downregulation of  $\beta$ 4 integrin and actin bundling protein Fascin in response to K8 knockdown in AW13516 cells (26). Surprisingly, no changes were observed in expression of  $\beta$ 4 integrin and Fascin at protein level upon BPAG1e, Plectin and BPAG1e-Plectin double knockdown in AW13516 cells (Figure 4.2E-G). This observation indicated that linker proteins may not have role in K8 mediated effects observed in OSCC cells.

We have observed reduction in cell migration, invasion, tumorigenicity and alterations in actin organization upon knockdown of HD linker proteins in OSCC derived cells. Therefore, to decipher the key molecules having role in phenotypic changes observed upon HD linker proteins downregulation, global protein profiling was performed using SWATH (sequential window acquisition of all theoretical fragment ion spectra) technique.

#### **4.5 SWATH analysis demonstrated differential expression of several proteins in linker proteins knockdown AW13516 cells as compared to vector control cells**

To understand global changes in protein profile of linker proteins knockdown cells as compared to vector control cells, we performed SWATH analysis for BPAG1e-Plectin knockdown clone C4

and vector control clone DVC. We shortlisted proteins with p-value less than 0.05. The cut off value for upregulated and downregulated proteins was 1.3 and 0.76 respectively. After filtering, total 45 proteins were found to be significantly altered. Out of these proteins, 17 were upregulated and 28 were downregulated in BPAG1e-Plectin knockdown clone C4 as compared to respective vector control clone (Annexure I). Some of the differentially expressed proteins were Vimentin, LIMA1, NDRG1, Galectin, 14-3-3 protein epsilon, Ubiquitin-40S ribosomal protein, S100-A6 etc. Out of these proteins, NDRG1 was upregulated by 1.84 fold (Annexure I).

We selected NDRG1 for further analysis as it functions as a metastasis suppressor in number of cancers including oral cancer (134, 137). Furthermore, it plays an important role in cell migration, actin organization, invasion and tumorigenesis (137, 139, 142). NDRG1 overexpression in human prostate and colon cancer cells inhibited cell migration by preventing actin filament polymerization (139). Further, NDRG1 reduced cell invasiveness and tumorigenesis of OSCC derived cells (137). Moreover, NDRG1 regulates gastric cancer cell invasion through decreased MMP9 activity (142).

#### **4.6 NDRG1 upregulation in HD linker protein knockdown cells**

To validate the results obtained from SWATH analysis, we performed western blot for NDRG1 in linker protein knockdown cells. Indeed, NDRG1 protein expression was found to be upregulated in BPAG1e (~1.6 fold), Plectin (~1.75 fold) and BPAG1e-Plectin (~2.1 fold) knockdown clones as compared to respective vector control clone (Figure 4.11A-C).

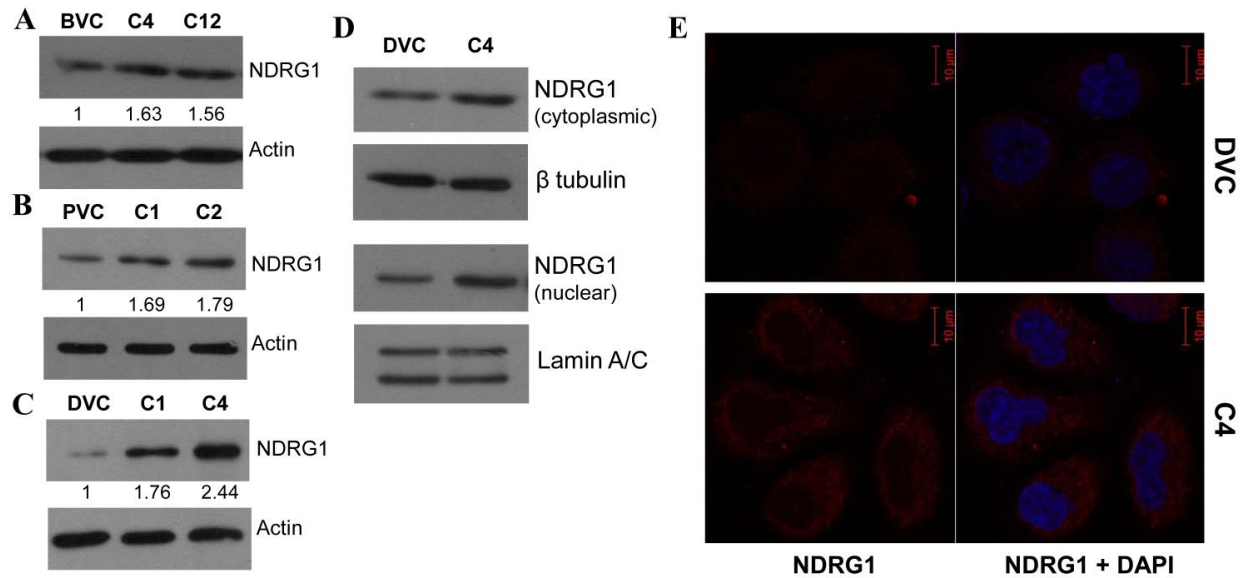


**Figure 4.11: NDRG1 protein expression in hemidesmosomal linker protein(s) knockdown cells.** (A) Western blot analysis of NDRG1 in vector control clone (BVC) and BPAG1e knockdown clones (C4, C12). (B) Western blot analysis of NDRG1 in vector control clone (PVC) and Plectin knockdown clones (C1, C2). (C) Western blot analysis of NDRG1 in vector control clone (DVC) and BPAG1e-Plectin knockdown clones (C1, C4). (D) Western blot analysis shows NDRG1 protein expression in cytoplasmic and nuclear fractions of vector control (DVC) and BPAG1e-Plectin knockdown (C4) cells.  $\beta$ -tubulin was used as a loading control for the cytoplasmic fraction, while Lamin A/C was used as a loading control for the nuclear fraction. (E) Immunofluorescence analysis showing NDRG1 localization (stained in red) in vector control clone (DVC) and BPAG1e-Plectin knockdown clone (C4). The nucleus is stained with DAPI. Note: the numbers below the blot indicate relative intensity of the bands using densitometric analysis.

To investigate whether the increase in NDRG1 upregulation is due to increase in cytoplasmic and/or nuclear levels, subcellular fractionation was carried out to separate the cytoplasmic and nuclear fractions from BPAG1e-Plectin knockdown clone C4 and vector control clone DVC. This experiment demonstrated that the NDRG1 was upregulated in both cytoplasm and nucleus of linker proteins knockdown cells as compared to vector control cells (DVC) (Figure 4.11D). Moreover, immunofluorescence analysis also displayed increased NDRG1 expression in both cytoplasm and nucleus of BPAG1e-Plectin knockdown cells as compared to vector control cells (DVC) (Figure 4.11E).

#### **4.7 Knockdown of NDRG1 in BPAG1e-Plectin downregulated AW13516 (NDRG1-BPAG1e-Plectin triple knockdown) and parental AW13516 cells (NDRG1 single knockdown)**

To verify whether the phenotype associated with cell transformation in HD linker proteins knockdown cells was due to higher NDRG1 levels, it was stably downregulated in BPAG1e-Plectin double knockdown clone C4. NDRG1-BPAG1e-Plectin triple knockdown clones C1 and C7 displayed 2.5 and 2.3 fold decrease at RNA level respectively (Figure 4.12A). Further, NDRG1 protein expression was reduced by ~80% in clone C1 and C7 (Figure 4.12B). Moreover, no changes were observed in expression of  $\beta$ 4 integrin and Fascin at protein level upon NDRG1-BPAG1e-Plectin triple knockdown (Figure 4.12B).

We also carried out single knockdown of NDRG1 in AW13516 cells to investigate the role of NDRG1 alone. NDRG1 knockdown clones (C2, C3) showed ~2.3 fold decrease at mRNA level (Figure 4.14A) and ~82% reduction at protein level as compared to vector control clone NVC (Figure 4.14B).

#### 4.8 NDRG1 downregulation rescues HD linker proteins knockdown phenotype

For phenotypic assays, TVC and TVC2 were used as vector control clones. TVC clone was generated by transfecting pLKO1.hygro empty vector in double vector control DVC, whereas TVC2 clone was generated by transfecting pLKO1.hygro empty vector in BPAG1e-Plectin knockdown clone C4.

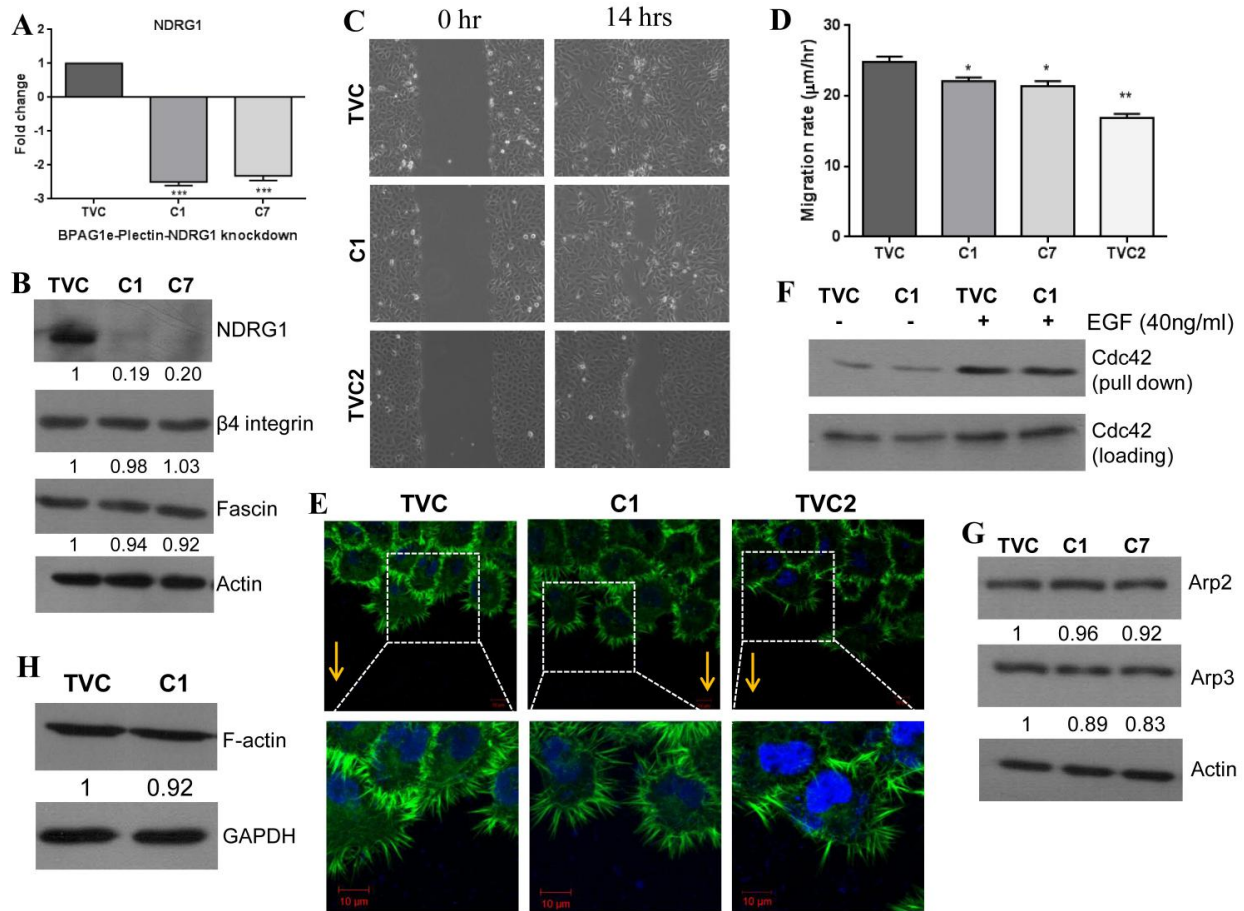


**Figure 4.12: NDRG1 downregulation in BPAG1e-Plectin knockdown background rescues cell migration and actin organization.** (A) qRT-PCR and (B) western blot analysis of NDRG1 in vector control clone (TVC) and NDRG1-BPAG1e-Plectin knockdown clones (C1, C7). (C) Representative time lapse microscopy images show wound healing for vector control clones

*(TVC, TVC2) and NDRG1-BPAG1e-Plectin knockdown clone (C1). (D) Graph shows rate of cell migration for vector control clones (TVC, TVC2) and NDRG1-BPAG1e-Plectin knockdown clones (C1, C7). (E) Immunofluorescence analysis of actin organization (stained in green) at the wound edge in vector control clones (TVC, TVC2) and NDRG1-BPAG1e-Plectin knockdown clone (C1). The nucleus is stained with DAPI. The arrow indicates direction of migration. The inset shows filopodia formed at migratory front. (F) Western blot analysis represents Cdc42 activity in vector control clone (TVC) and NDRG1-BPAG1e-Plectin knockdown clone (C1). (H) Western blot analysis shows F-actin levels in vector control clone (TVC) and NDRG1-BPAG1e-Plectin knockdown clone (C1). (G) Western blot analysis for Arp2, Arp3 in vector control clone (TVC) and NDRG1-BPAG1e-Plectin knockdown clones (C1, C7). Note: the numbers below the blot indicate relative intensity of the bands using densitometric analysis.*

The NDRG1-BPAG1e-Plectin triple knockdown clones (C1, C7) displayed only ~10% decrease in rate of cell migration as compared to vector control clone TVC ( $p=0.006$ ), whereas ~25% increase in rate of cell migration was observed in triple knockdown cells as compared to vector control TVC2 ( $p<0.001$ ) (Figure 4.12C-D). On the other hand, NDRG1 single knockdown clones showed ~20% increase in cell migration as compared to NVC ( $p<0.001$ ) (Fig. 4.14C-D). These results indicated that NDRG1 plays an important role in regulating cell migration of linker proteins deficient OSCC derived cells.

The membrane protrusions in triple knockdown clone C1 were found to be uniformly present which was similar to vector control clone TVC, whereas in case of TVC2, membrane protrusions were found to be non-uniformly organized as similar to BPAG1e-Plectin knockdown clone C4 (Figure 4.12E). Further, Cdc42 activity was partially restored in NDRG1-BPAG1e-Plectin triple

knockdown cells (Figure 4.12F) as compared to BPAG1e-Plectin double knockdown cells (Figure 4.6C). Moreover, Cdc42 activity was substantially increased upon NDRG1 single knockdown as compared to NVC (Figure 4.14F). Furthermore, filamentous actin and Arp2/3 levels were restored in NDRG1-BPAG1e-Plectin triple knockdown cells (Fig. 4.12G-H) as compared to BPAG1e-Plectin double knockdown cells (Figure 4.6F-G). Likewise, filamentous actin and Arp2/3 levels were elevated in NDRG1 single knockdown cells as compared to NVC (Fig. 4.14G-H).

Further, *in vitro* invasion was reduced by only ~10-15% in triple knockdown cells as compared to vector control TVC cells ( $p=0.189$ ) (Figure 4.13A). On the other hand, vector control TVC2 cells showed ~20% decrease in invasion as compared to triple knockdown cells ( $p=0.0174$ ) (Figure 4.13A). In case of only NDRG1 knockdown, the *in vitro* invasion was increased by ~23% as compared to vector control clone (NVC) ( $p=0.022$ ) (Figure 4.14E). MMP2 activity was similar in triple knockdown C1 cells and vector control TVC cells, while, triple knockdown cells displayed increase in MMP9 activity as compared to vector control clone TVC2 (Figure 4.13B). In short, triple knockdown cells showed restoration of MMP9 activity as compared to double knockdown cells. However, MMP2 activity was unaltered in triple knockdown clone C1 as compared to vector control cells (Figure 4.13B).

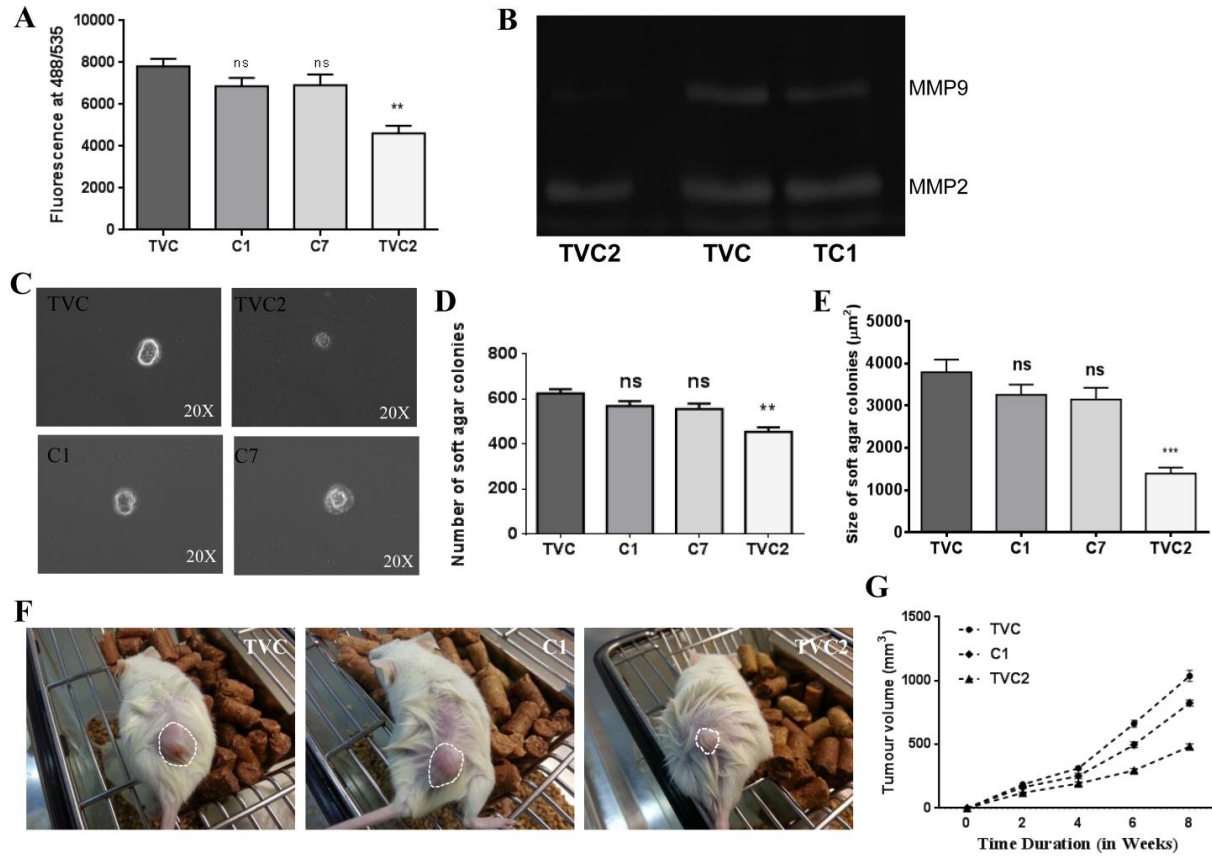


**Figure 4.13: NDRG1 downregulation in BPAG1e-Plectin knockdown background rescues cell invasion and tumorigenicity.** (A) The graph shows fluorescence of invaded vector control cells (TVC, TVC2) and NDRG1-BPAG1e-Plectin knockdown cells (C1, C7) which is read at wavelengths of 488/535nm (Ex/Em) (B) The gelatin zymography shows MMP2 and MMP9 activity in vector control clones (TVC, TVC2) and NDRG1-BPAG1e-Plectin knockdown clone (C1) (C) The representative images of colonies formed on soft agar and graphical representation of (D) the number of colonies and (E) size of colonies formed on soft agar in vector control clones (TVC, TVC2) and NDRG1-BPAG1e-Plectin knockdown clones (C1, C7). (F) Representative images of NOD-SCID mice bearing tumors formed from vector control cells (TVC, TVC2) and NDRG1-BPAG1e-Plectin knockdown cells (C1) after 8 weeks of injection. The

tumors are indicated by dotted circles. (G) The graph shows tumor volume plotted against time for vector control cells (TVC, TVC2) and NDRG1-BPAG1e-Plectin knockdown cells (C1). It represents mean  $\pm$  SEM for 5 animals injected for each clone.

In addition, triple knockdown cells showed ~10% decrease in number of colonies on soft agar as compared to vector control TVC ( $p=0.102$ ), while ~20% increase in number of colonies on soft agar was observed in triple knockdown cells as compared to vector control TVC2 ( $p=0.024$ ) (Figure 4.13C-D). No significant difference in soft agar colony size was observed in NDRG1-BPAG1e-Plectin triple knockdown cells as compared to TVC ( $p=0.43$ ) (Figure 4.13E). Moreover, NDRG1 single knockdown cells displayed ~14% increase in number of colonies on soft agar as compared to NVC ( $p=0.024$ ) (Figure 4.15A-B). Furthermore, ~25% increase in size of colonies formed on soft agar was observed in NDRG1 single knockdown cells as compared to NVC ( $p=0.011$ ) (Figure 4.15C).

Further, *in vivo* experiments suggested that there was no significant difference in mean tumor volume of mice bearing triple knockdown cells and vector control TVC cells, whereas mice bearing triple knockdown cells displayed significantly increased tumor volume as compared to vector control TVC2 ( $p<0.001$ ) (Figure 4.13F-G). On the other hand, only NDRG1 knockdown resulted in an increase in tumorigenicity as compared to NVC ( $p=0.049$ ) (Figure 4.15D-E). Taken together, these results indicated that NDRG1 knockdown displayed partial rescue in HD linker proteins knockdown phenotype.

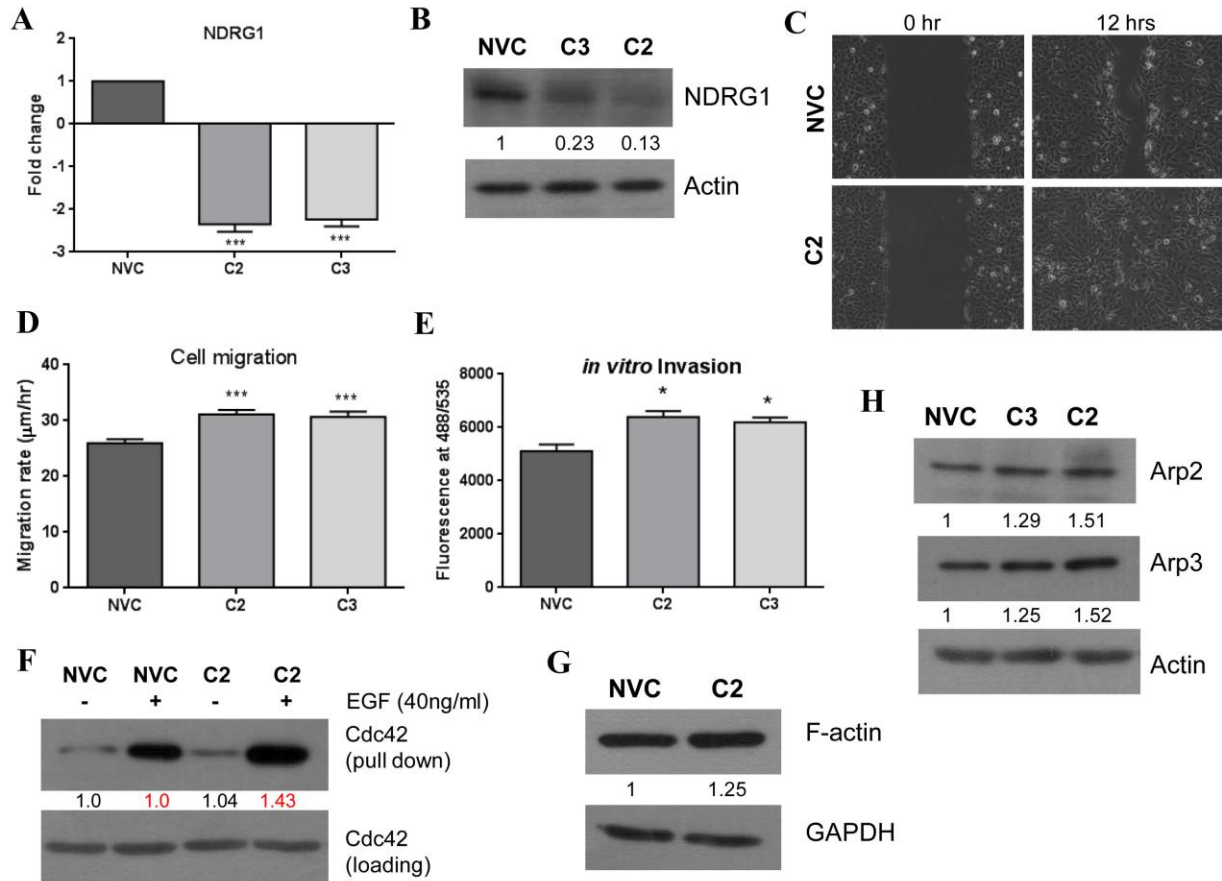


**Figure 4.14: Loss of NDRG1 in AW13516 cells leads to increased cell migration, cell invasion and actin polymerization.** (A) qRT-PCR and (B) western blot analysis of NDRG1 in vector control clone (NVC) and NDRG1 knockdown clones (C2, C3). (C) Representative time lapse microscopy images show wound healing for vector control clone (NVC) and NDRG1 knockdown clone (C2). (D) The graph shows rate of cell migration for vector control clone (NVC) and NDRG1 knockdown clones (C2, C3). (E) The graph shows fluorescence of invaded vector control cells (NVC) and NDRG1 knockdown cells (C2, C3) which is read at wavelengths of 488/535nm (Ex/Em). (F) Western blot analysis represents Cdc42 activity in vector control clone (NVC) and NDRG1 knockdown clone (C2). (G) Western blot analysis shows F-actin levels in vector control clone (NVC) and NDRG1 knockdown clone (C2). (H) Western blot analysis for

*Arp2, Arp3* in vector control clone (NVC) and *NDRG1* knockdown clones (C2, C3). Note: the numbers below the blot indicate relative intensity of the bands using densitometric analysis.

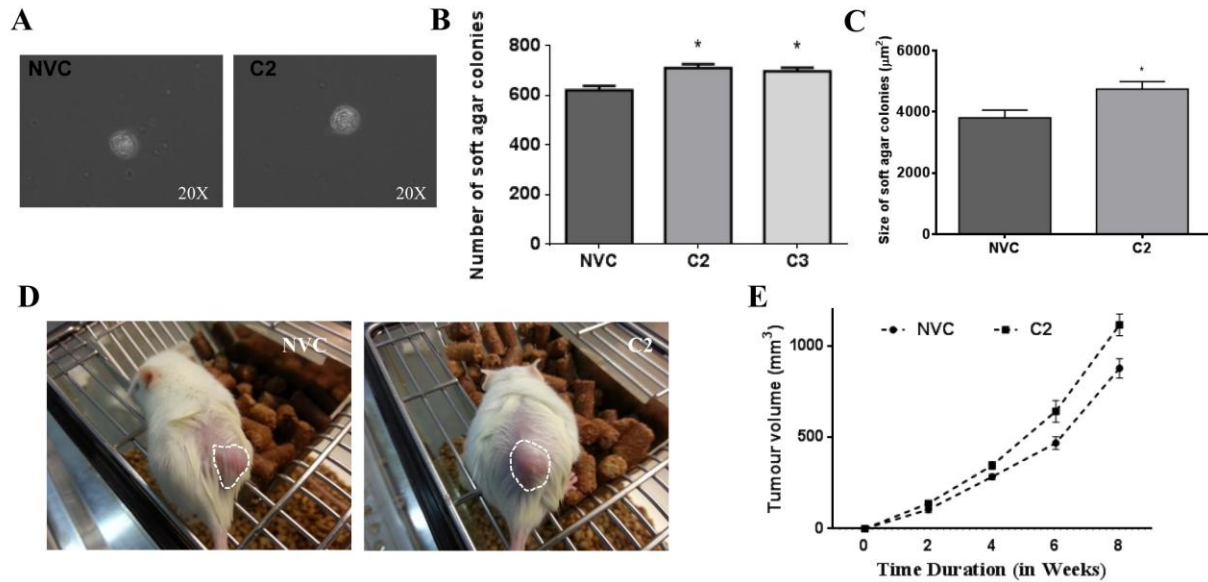


**Figure 4.15: Loss of *NDRG1* in AW13516 cells leads to increased tumorigenic potential.** (A) Representative images of colonies formed on soft agar in vector control clone (NVC) and *NDRG1* knockdown clone (C2). (B) Graphical representation of number of colonies formed on soft agar in vector control clone (NVC) and *NDRG1* knockdown clones (C2, C3). (C) Graphical representation of size of colonies formed on soft agar in vector control clone (NVC) and *NDRG1* knockdown clone (C2). (D) Representative images of NOD-SCID mice bearing tumors formed from vector control cells (NVC) and *NDRG1* knockdown cells (C2) after 8 weeks of injection. The tumors are indicated by dotted circles. (E) The graph shows tumor volume plotted against time for vector control cells (NVC) and *NDRG1* knockdown cells (C2). It represents mean  $\pm$  SEM for 5 animals injected for each clone.

We then carried out immunohistochemistry analysis for tumor tissues obtained from linker proteins knockdown, NDRG1-BPAG1e-Plectin triple knockdown and respective vector control cells injected in NOD-SCID mice. The results for NDRG1 were as similar to that of *in vitro* systems (Figure 4.16A-B). However, antibody to Plectin and BPAG1e did not give specific staining in tissues. Therefore, we performed quantitative real time PCR for tumor tissues obtained from linker proteins knockdown, NDRG1-BPAG1e-Plectin triple knockdown and respective vector control cells injected in NOD-SCID mice. Our results showed that Plectin, BPAG1e and NDRG1 expression in these tumor tissues at RNA level were similar to that of results observed in respective *in vitro* systems (Figure 4.16C-D).

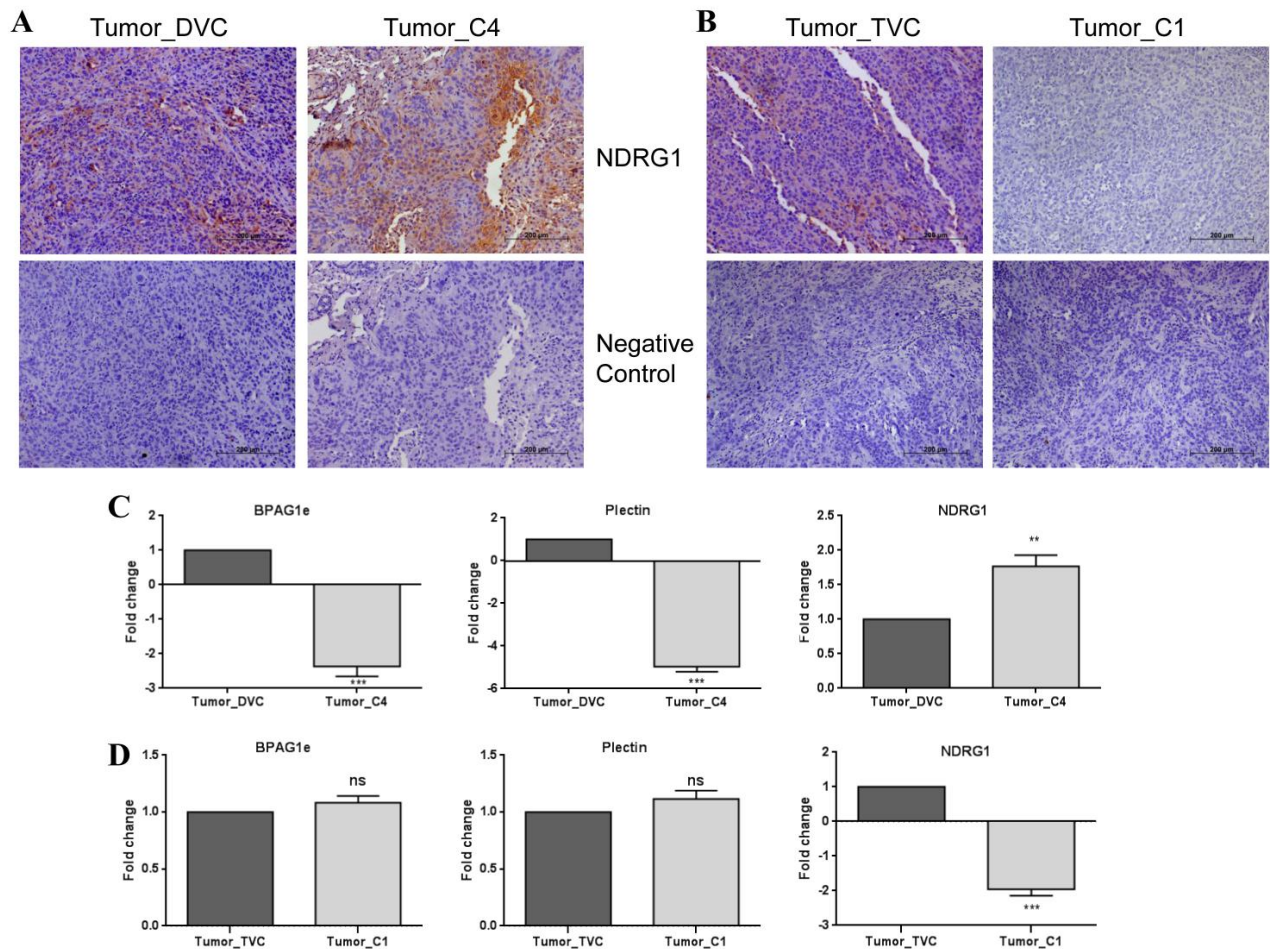


**Figure 4.16: The tumors isolated from BPAG1e-Plectin and NDRG1-BPAG1e-Plectin cells injected in NOD-SCID mice showed similar molecular alterations to that of in vitro system (A) Immunohistochemical staining of NDRG1 in tumors derived from vector control cells (DVC) and BPAG1e-Plectin double knockdown cells (C4) injected in NOD-SCID mice. The primary antibody was not added to negative control. (C) qRT-PCR analysis of BPAG1e, Plectin and NDRG1 in tumors derived from vector control cells (DVC) and BPAG1e-Plectin double knockdown cells (C4) injected in NOD-SCID mice. (B) Immunohistochemical staining of NDRG1 in tumors derived from vector control cells (TVC) and NDRG1-BPAG1e-Plectin triple knockdown cells (C1) injected in NOD-SCID mice. The primary antibody was not added to negative control. (D) qRT-PCR analysis of BPAG1e, Plectin and NDRG1 in tumors derived from vector control cells (TVC) and NDRG1-BPAG1e-Plectin triple knockdown cells (C1) injected in NOD-SCID mice.**

#### **4.9 NDRG1 regulates cell motility through p21**

Previously, it has been reported that NDRG1 expression leads to down regulation of  $\Delta$ Np63 levels, which allows transactivation of the p21 gene by TAp63 leading to upregulated p21 levels. Further, increased p21 can inhibit cell migration and reduce the metastatic potential of cancer cells (140). Upon loss of HD linker proteins in OSCC derived cells, NDRG1 and p21 levels were found to be upregulated, whereas  $\Delta$ Np63 expression was reduced (Figure 4.17A). On the other hand, NDRG1-BPAG1e-Plectin triple knockdown cells showed restoration of p21 and  $\Delta$ Np63 expression (Figure 4.17C). Likewise, NDRG1 single knockdown resulted in decreased p21 and increased  $\Delta$ Np63 protein levels (Figure 4.17B). These results indicate that HD linker proteins may also regulate cell motility through NDRG1-  $\Delta$ Np63-p21 pathway in OSCC derived cells.

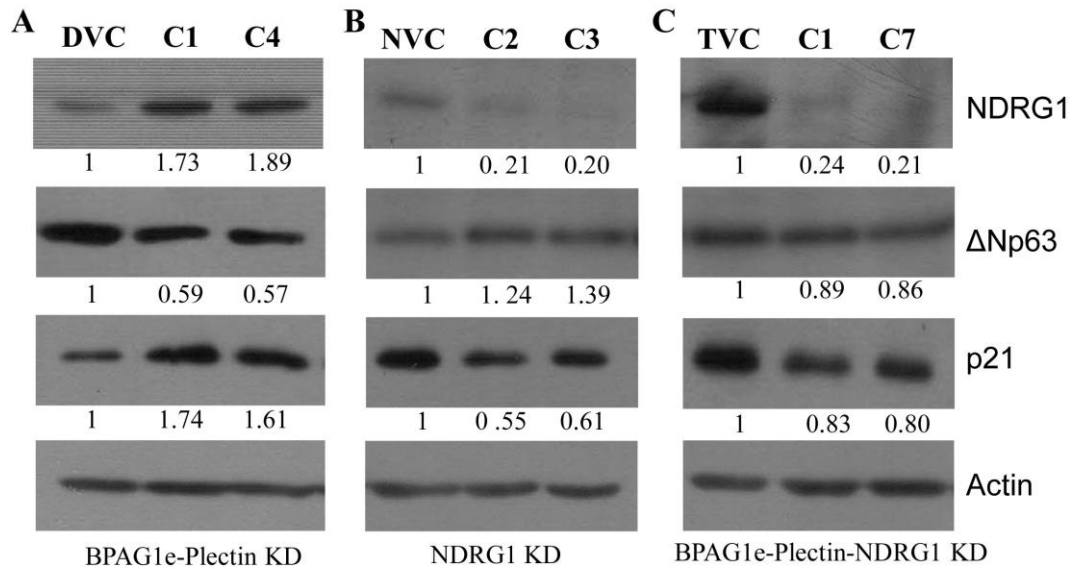


**Figure 4.17: NDRG1 possibly regulates cell motility through p21.** (A) Western blot analysis of NDRG1, ΔNp63 and p21 in vector control cells (DVC) and BPAG1e-Plectin knockdown cells (C1, C4). (C) Western blot analysis of NDRG1, ΔNp63 and p21 in vector control cells (TVC) and NDRG1-BPAG1e-Plectin knockdown cells (C1, C7). (B) Western blot analysis of NDRG1, ΔNp63 and p21 in vector control cells (NVC) and NDRG1 knockdown cells (C2, C3). Note: the numbers below the blot indicate relative intensity of the bands using densitometric analysis.

#### 4.10 The phenotypic and molecular changes observed upon HD linker proteins are not cell line specific

To find out whether the effects observed in AW13516 cells were cell line specific, we carried out similar experiments in another tongue SCC derived cell line AW8507 (derived from poorly differentiated epidermoid carcinoma of the tongue) (147).

Same shRNA sequences were used to knockdown BPAG1e and/or Plectin in AW8507 cells. The linker proteins knockdown AW8507 cells also showed increased NDRG1 levels, whereas  $\beta$ 4 integrin and Fascin levels remained unaltered (Figure 4.18A). Further, to verify whether the phenotype associated with cell transformation in HD linker proteins knockdown AW8507 cells was due to higher NDRG1 levels, NDRG1 was stably downregulated in BPAG1e-Plectin knockdown clone GDC3 (Figure 4.19A) .

The results of phenotypic assays for cell transformation like Boyden chamber transwell assay, *in vitro* invasion assay, soft agar assay and *in vivo* tumorigenicity assay for AW8507 knockdown systems were similar to those found in AW13516 knockdown systems (Figure 4.18B-E). Altogether, loss of hemidesmosomal linker proteins in AW8507 cells led to reduced cell migration, cell invasion and tumorigenicity. Moreover, the partial rescue of phenotype was observed in NDRG1-BPAG1e-Plectin triple knockdown cells (Figure 4.19B-E). These results were similar to results observed in AW13516 knockdown cells indicating that alterations observed upon loss of BPAG1e and Plectin are not cell line specific.

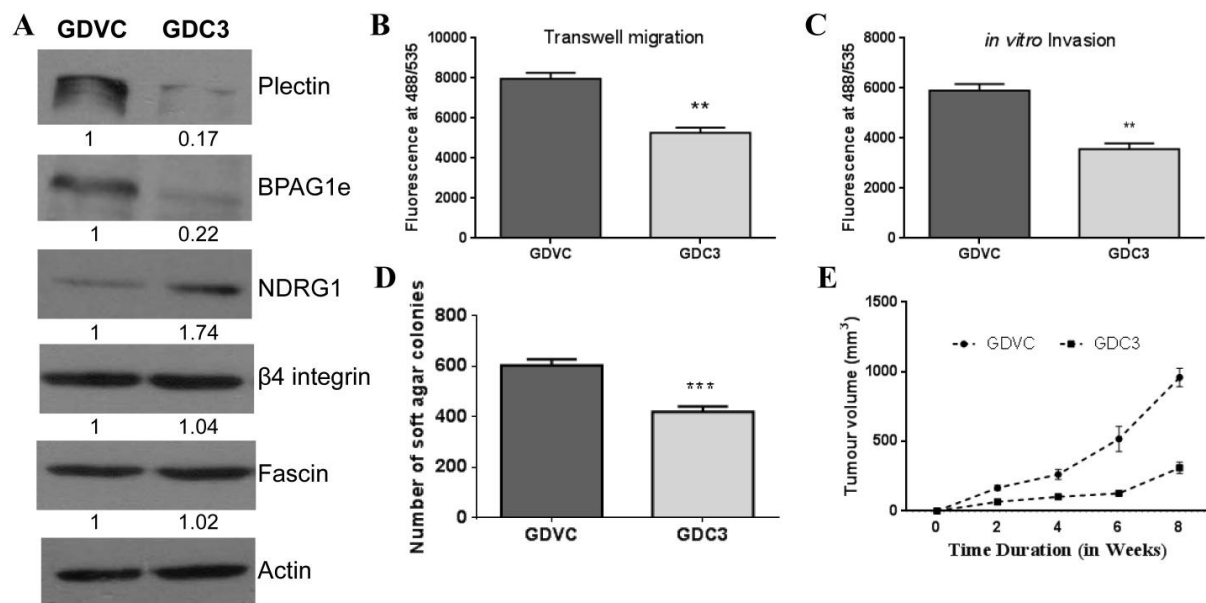


**Figure 4.18: Loss of BPAG1e-Plectin in AW8507 cells leads to decrease in cell migration, invasion and tumorigenicity.** (A) Western blot analysis shows Plectin, BPAG1e, NDRG1,  $\beta$ 4 integrin and Fascin levels in vector control clone (GDVC) and BPAG1e-Plectin knockdown clone (GDC3) (B) The graph shows fluorescence of migrated vector control cells (GDVC) and BPAG1e-Plectin knockdown cells (GDC3) which is read at wavelengths of 488/535nm (Ex/Em) (C) The graph shows fluorescence of invaded vector control cells (GDVC) and BPAG1e-Plectin knockdown cells (GDC3) which is read at wavelengths of 488/535nm (Ex/Em) (D) The graphical representation of the number of colonies formed on soft agar by vector control cells (GDVC) and BPAG1e-Plectin knockdown cells (GDC3) (E) The graph shows tumor volume plotted against time for vector control cells (GDVC) and BPAG1e-Plectin knockdown cells (GDC3). It represents mean  $\pm$  SEM for 5 animals injected for each clone. Note: the numbers below the blot indicate relative intensity of the bands using densitometric analysis.

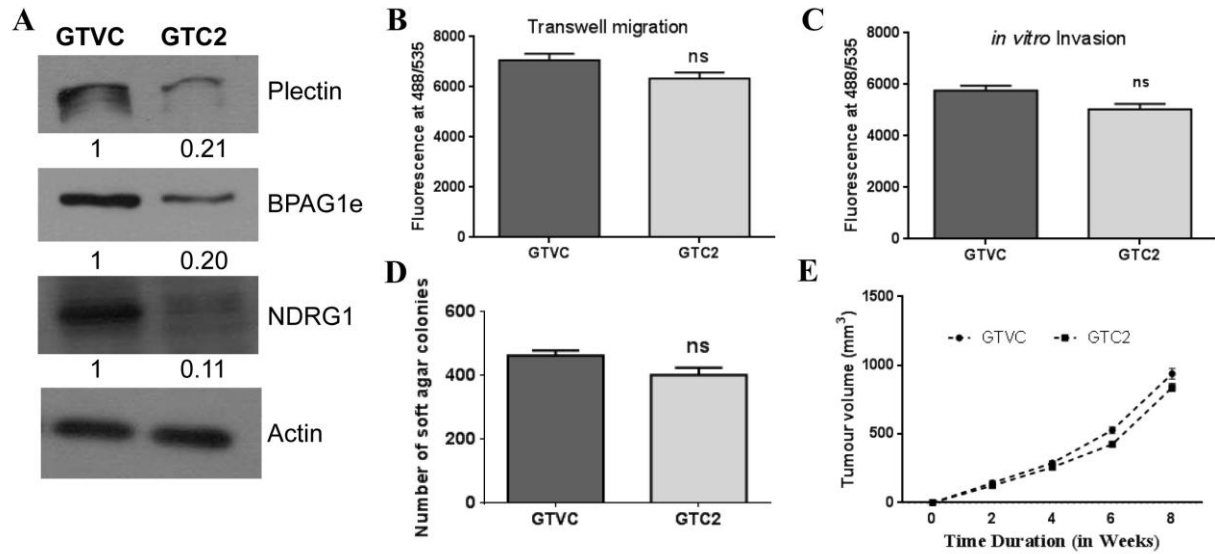


**Figure 4.19: NDRG1 downregulation in BPAG1e-Plectin knockdown background rescues the phenotype in AW8507 cells.** (A) Western blot analysis shows Plectin, BPAG1e, NDRG1 levels in vector control clone (GTVC) and NDRG1-BPAG1e-Plectin knockdown clone (GTC2) (B) The graph shows fluorescence of migrated vector control cells (GTVC) and NDRG1-BPAG1e-Plectin knockdown cells (GTC2) which is read at wavelengths of 488/535nm (Ex/Em) (C) The graph shows fluorescence of invaded vector control cells (GTVC) and NDRG1-BPAG1e-Plectin knockdown cells (GTC2) which is read at wavelengths of 488/535nm (Ex/Em) (D) The graphical representation of the number of colonies formed on soft agar by vector control cells (GTVC) and NDRG1-BPAG1e-Plectin knockdown cells (GTC2) (E) The graph shows tumor volume plotted against time for vector control cells (GTVC) and NDRG1-BPAG1e-Plectin knockdown cells (GTC2). It represents mean  $\pm$  SEM for 5 animals injected for each clone. Note: the numbers below the blot indicate relative intensity of the bands using densitometric analysis.



## *5. Discussion*

In the last two decades, the understanding of the plakin family linker proteins has increased to great extent. Several studies have shown that hemidesmosomal linker proteins (BPAG1e and Plectin) are not present in the cells just to anchor specific proteins, but that they have a functional role in various cellular processes like cell motility, invasion etc (13, 17, 18, 95). However, the literature regarding the role of these proteins in human cancers is scanty. Overall, the existing literature suggests that these proteins may have a context dependent role in cancer. e.g. Plectin promotes cell migration in colon carcinoma cells (16), whereas it can act as a negative regulator of cell migration in liver cancer cells (18). Moreover, very few reports are available regarding the role of these proteins in OSCC. A previous report from our laboratory has shown that K8 knockdown in OSCC derived AW13516 cells resulted in reduced cell motility, cell invasion, tumorigenic potential and altered actin organization (26).

Taking available literature into consideration, in the current study, we have attempted to unravel the role of hemidesmosomal linker proteins in neoplastic progression of OSCC. BPAG1e is normally expressed in basal layer of the squamous epithelia (1). Further, K8/18 pair is normally expressed in simple epithelia, where it interacts with integrins via Plectin, as other linker protein, BPAG1e, is not expressed in simple epithelia (108, 163). Moreover, in case of OSCC and OSCC derived cells, K8/18 pair is aberrantly expressed (21-23, 26). Therefore, it was important to investigate whether K8/18 filaments interact with BPAG1e in OSCC derived AW13516 cells. Immunoprecipitation experiments revealed that BPAG1e interacts with K8 in OSCC derived cells (Figure 4.1A). We tried to validate these results with colocalization experiments using immunofluorescence microscopy for K8, BPAG1e and  $\beta 4$  integrin. Unfortunately, due to non-specific staining of the BPAG1e antibody in AW13516 cells, the

results of K8 + BPAG1e and K8 + BPAG1e +  $\beta$ 4 integrin staining were inconclusive, although K8 and  $\beta$ 4 integrin dual staining was properly observed in AW13516 cells (Figure 4.1B-D).

We then downregulated BPAG1e and/or Plectin in OSCC derived AW13516 cells to understand their role in regulation of cell motility/invasion in oral SCC derived cells. The shRNA mediated knockdown of BPAG1e did not alter expression of the other linker protein, Plectin, demonstrating the specificity of BPAG1e shRNA. Similarly, Plectin knockdown cells did not show alterations in BPAG1e protein levels (Figure 4.2E-F).

It has been previously reported that Plectin null mice showed unaltered keratin filament formation, whereas BPAG1e null mice displayed the severing of connections between keratin filaments and hemidesmosomes (10, 11). However, Hamill *et al* showed that no significant difference in the keratin network was observed in BPAG1e downregulated human epidermal keratinocytes (13). Contrary to this, keratinocytes isolated from individuals carrying homozygous nonsense mutations in DST (BPAG1e encoding gene) showed a significant increase in K14 levels (14). In our BPAG1e and Plectin single knockdown cells, we could not see significant difference in K8 protein level as well as its filament organization (Figure 4.2E-F and 4.10A-B). However, upon loss of both linker proteins together, the sparsely arranged filament network of K8 and K5 was observed (Figure 4.10C). These results indicated the requirement of at least one linker protein to anchor keratin proteins to cell surface.

Next, to understand whether knockdown of HD linker proteins in OSCC derived cells leads to similar phenotypic changes as seen in response to K8 knockdown, we performed phenotypic assays using linker protein(s) knockdown cells. Our results demonstrated significant reduction in cell motility in response to downregulation of the linker proteins singly as well as in combination (Figure 4.3A-B, 4.4A-B and 4.5A-B). These results are consistent with previous

study from our laboratory. In this study our laboratory had shown reduction in cell motility upon K8 knockdown in AW13516 cells. Prior to this study, there was no report available regarding role of BPAG1e in cancer cell motility. Further, the role of Plectin in cancer cell motility is inconsistent. Katada *et al* have shown that Plectin promotes the migration and invasion of HNSCC cells through activation of Erk 1/2 (15). In another study, plectin deficient colon carcinoma cells showed impairment of cell migration and adhesion (16). Contrary to these reports, plectin deficiency in liver cancer cells promoted cell motility (17, 18). These reports together suggest that a role of linker proteins in cell motility is context dependent.

Reduction in cell motility is often associated with alterations in actin organization (158). Indeed, BPAG1e and/or Plectin downregulated AW13516 cells displayed sparsely arranged filopodia (Figure 4.3C, 4.4C and 4.5C). The length of filopodia was also significantly reduced in linker protein(s) knockdown cells as compared to respective vector control cells (Figure 4.3D, 4.4D and 4.5D). Rho GTPases family proteins play a crucial role in the reorganization of the actin cytoskeleton (164). One of the members of Rho GTPases, Cdc42, regulates cellular motility by filopodia formation (159). We observed decrease in Cdc42 activity in linker protein(s) knockdown cells (Figure 4.6A-C). Further, an appearance of shorter and fewer filopodia upon loss of linker protein(s) prompted us to investigate whether there was any defect in actin polymerization. Actin protein exists in the cytoplasm in two different forms, namely the monomeric actin (G-actin) and filamentous actin (F-actin). When G-actin exchanges bound ADP for ATP, it polymerizes into F-actin filaments (165). Indeed, actin polymerization assay revealed decrease in levels of F-actin in linker protein(s) knockdown cells as compared to respective vector control cells (Figure 4.6F). Actin related proteins (Arp) 2/3 complexes are one of the important set of actin regulators which participate in nucleation and branching of actin filaments. The

Arp2/3 complex promotes branching of an existing actin filament and formation of a daughter filament following activation by nucleation-promoting factors (e.g. WASP/WAVE, cortactin etc). The Arp 2/3 complex is activated by the Wiskott–Aldrich syndrome family protein (WASP) family of proteins which are in turn activated by Cdc42 (160). In linker protein(s) knockdown cells, we observed decrease in levels of Arp2 and Arp3 (Figure 4.6G). This result indicated that reduced Cdc42 activity in linker protein(s) knockdown cells led to decrease in expression of Arp2/3 proteins, resulting in shorter and fewer filopodia. The previous study from our laboratory has shown that loss of Fascin in K8 knockdown OSCC cells correlated with reduction in F-actin based structures (26). However, we show here that Cdc42 and Arp2/3, and not Fascin, play a key role in altered filopodia formation observed in linker protein(s) knockdown OSCC cells.

Further, our results demonstrated that cell invasion was reduced in BPAG1e and/or Plectin knockdown AW13516 cells (Figure 4.3E, 4.4E and 4.5E). Cellular invasion is a crucial step in cancer metastasis which requires precise coordination of cell migration and matrix remodeling (166). Furthermore, cancer cell invasion and metastasis require the crossing of several physical barriers such as the basement membrane (161). Matrix Metalloproteinases (MMPs) play an important role in breaking these barriers, thus promoting cellular invasion. It is well documented that increased activity of MMPs, MMP2 and MMP9 in particular, correlates with invasive potential of OSCC samples (162). Therefore, we checked MMP2 and MMP9 activity using gelatin zymography in linker proteins downregulated and vector control cells. Our zymography experiments revealed that MMP9 activity was significantly reduced in linker proteins downregulated cells as compared to vector control cells, whereas MMP2 activity remained unaltered (Figure 4.5F).

In addition, we observed significant reduction in an anchorage independent growth of linker proteins knockdown cells. The significant decrease in the size of soft agar colonies was observed upon loss of linker protein(s) (Figure 4.7A-C, 4.8A-C and 4.9A-C). We did not see any significant difference in cell viability and clonogenic potential of linker protein(s) knockdown cells (Figure 4.7D-E, 4.8D-E and 4.9D-E). These findings indicated that the decrease in soft agar colony size can be solely attributed to reduction in transformation potential, and not to proliferative potential, of the linker protein(s) ablated cells. We also observed decrease in *in vivo* tumorigenic potential (tumor formation in NOD-SCID mice) upon loss of BPAG1e and/or Plectin in OSCC derived cells (Figure 4.7F-G, 4.8F-G and 4.9F-G). These results are consistent with the previous report, where Shin *et al* have shown that loss of plectin results in significant reduction of tumor volume and metastases of pancreatic ductal adenocarcinoma orthotopic mouse models (101). Overall, our results demonstrate that hemidesmosomal linker proteins play an important role in cell transformation.

We observed reduction in cell migration, invasion, tumorigenicity and alterations in actin organization upon downregulation of HD linker proteins in OSCC derived cells. In a previous study from our laboratory, it was shown that there are alterations in levels of  $\alpha 6\beta 4$  integrin proteins,  $\alpha 6\beta 4$  integrin mediated signalling and actin bundling protein Fascin upon knockdown of K8 in AW13516 cells (26). Surprisingly, we did not see changes in  $\beta 4$  integrin and Fascin protein levels in response to BPAG1e and/or Plectin knockdown in AW13516 cells. This observation indicated that linker proteins may not have role in K8 mediated effects observed in OSCC cells.

Next, to decipher the key molecules which may have a role in phenotypic changes observed upon loss of linker proteins in OSCC derived cells, global protein profiling was

performed using SWATH for BPAG1e-Plectin knockdown and vector control cells. Some of the differentially expressed proteins were Vimentin, LIMA1, NDRG1, Galectin, 14-3-3 protein epsilon, Ubiquitin-40S ribosomal protein, S100-A6 etc. Out of which, NDRG1 was upregulated by 1.84 fold in linker proteins knockdown cells. Further, the upregulation of NDRG1 was confirmed at protein level in linker protein(s) knockdown cells. We selected NDRG1 for further studies as it plays a role in actin organization, cell migration, cell invasion and tumorigenesis (137, 139, 142).

To understand whether the phenotype observed upon linker proteins knockdown can be reversed by downregulation of NDRG1, it was stably downregulated in BPAG1e-Plectin double knockdown cells. Our experiments revealed that cell motility, cell invasion, colony formation on soft agar and *in vivo* tumorigenicity were partially rescued upon NDRG1 loss in linker proteins knockdown background as compared to results of linker proteins knockdown systems (Figure 4.12 and 4.13). In case of NDRG1 only knockdown in AW13516, cell migration, invasion and tumorigenicity was increased as compared to vector control cells (Figure 4.14 and 4.15). Previously, it has been reported that NDRG1 overexpression in human prostate and colon cancer cells led to reduced cell migration by preventing actin filament polymerization, stress fiber assembly (139). We show here that, upregulation of NDRG1 upon loss of linker proteins led to defective actin polymerization, which resulted in shorter and fewer filopodia. Further, our results demonstrated that filopodia formation defects observed in linker proteins knockdown cells were restored upon NDRG1-BPAG1e-Plectin triple knockdown. In addition, the defects in Cdc42 activity and F-actin polymerization were rescued in NDRG1-BPAG1e-Plectin triple knockdown cells as compared to respective vector control cells. Also, Arp2/3 levels were restored upon NDRG1 downregulation in linker proteins knockdown background (Figure 4.12). In case of

NDRG1 only knockdown, F-actin and Arp2/3 levels were upregulated as compared to vector control cells. Further, it has been reported in prostate and lung cancer cell lines that NDRG1 expression allows transactivation of the p21 gene by targeting  $\Delta$ Np63 leading to upregulated p21 levels. Furthermore, it has been demonstrated that increased levels of p21 leads to decreased cell migration (140). The cell lines used in that study were either p53 null or mutated. Similarly, the OSCC cell lines used in current study also express mutated p53 (unpublished data). Indeed, p21 levels were found to be upregulated, whereas  $\Delta$ Np63 levels were downregulated in linker proteins knockdown AW13516 cells. Moreover, NDRG1-BPAG1e-Plectin triple knockdown cells showed restoration of p21 and  $\Delta$ Np63 levels as compared to linker proteins knockdown cells. Likewise, NDRG1 only knockdown cells showed decreased levels of p21 and decreased levels of  $\Delta$ Np63 (Figure 4.17). These results indicated that NDRG1 possibly regulates cell motility via p21 in linker proteins knockdown OSCC cells. As stated earlier, NDRG1 regulated decreased Arp2/3 expression leading to defective filopodia formation and thereby reduced cell migration in linker proteins knockdown cells. Thus, the altered cell motility observed upon loss of linker proteins could be the cumulative effect of these two independent mechanisms. Moreover, decreased MMP9 activity in response to BPAG1e-Plectin double knockdown was partially restored upon NDRG1-BPAG1e-Plectin triple knockdown (Figure 4.13B). It has been reported that NDRG1 plays a role in inhibiting gastric cancer metastasis by regulating MMP9 activity (142). Thus, NDRG1 mediated decreased MMP9 activity seems to be responsible for altered *in vitro* invasion in the linker proteins knockdown cells. Taken together, these results indicated that NDRG1 plays a defining role in phenotype associated with cell transformation in linker proteins downregulated OSCC cells.

The next question was how linker proteins regulate NDRG1 in OSCC cells. Myc, AP1, HIF1 $\alpha$ , PTEN etc. are known regulators of NDRG1 (167). The possible link between HD linker proteins and potential NDRG1 regulators is still not known. Thus, in future, it will be interesting to decipher how HD linker proteins regulate NDRG1 expression in OSCC derived cells.

Finally, we carried out similar experiments in another tongue SCC derived cell line AW8507 to investigate whether the effects observed in AW13516 cells were cell line specific. AW8507 cells have been derived from poorly differentiated epidermoid carcinoma of the tongue (147). The same shRNA sequences used earlier in this study were used to downregulate BPAG1e and/or Plectin in AW8507 cells. As observed in AW13516 knockdown systems, NDRG1 expression was also upregulated in linker proteins knockdown AW8507 cells (Figure 4.18A). Next, we downregulated NDRG1 in BPAG1e-Plectin knockdown AW8507 cells to verify whether the phenotype associated with cell transformation in HD linker proteins knockdown AW8507 cells was due to higher NDRG1 levels. Indeed, the results of transwell migration assay, matrigel invasion assay, soft agar assay and *in vivo* tumorigenicity assay for AW8507 double and triple knockdown systems were similar to those found in AW13516 double and triple knockdown systems (Figure 4.18 and 4.19). Thus, these results indicated that alterations observed upon loss of BPAG1e and Plectin are not cell line specific.

Collectively, this study demonstrated that hemidesmosomal linker proteins play a vital role in regulating cell motility, actin organization, cell invasion and tumorigenicity in OSCC derived cells possibly through NDRG1 (Figure 5.1). To our knowledge, this is the first study reporting a role of hemidesmosomal linker proteins (BPAG1e and plectin) in regulating cell migration, cell invasion and cell transformation of OSCC derived cells.

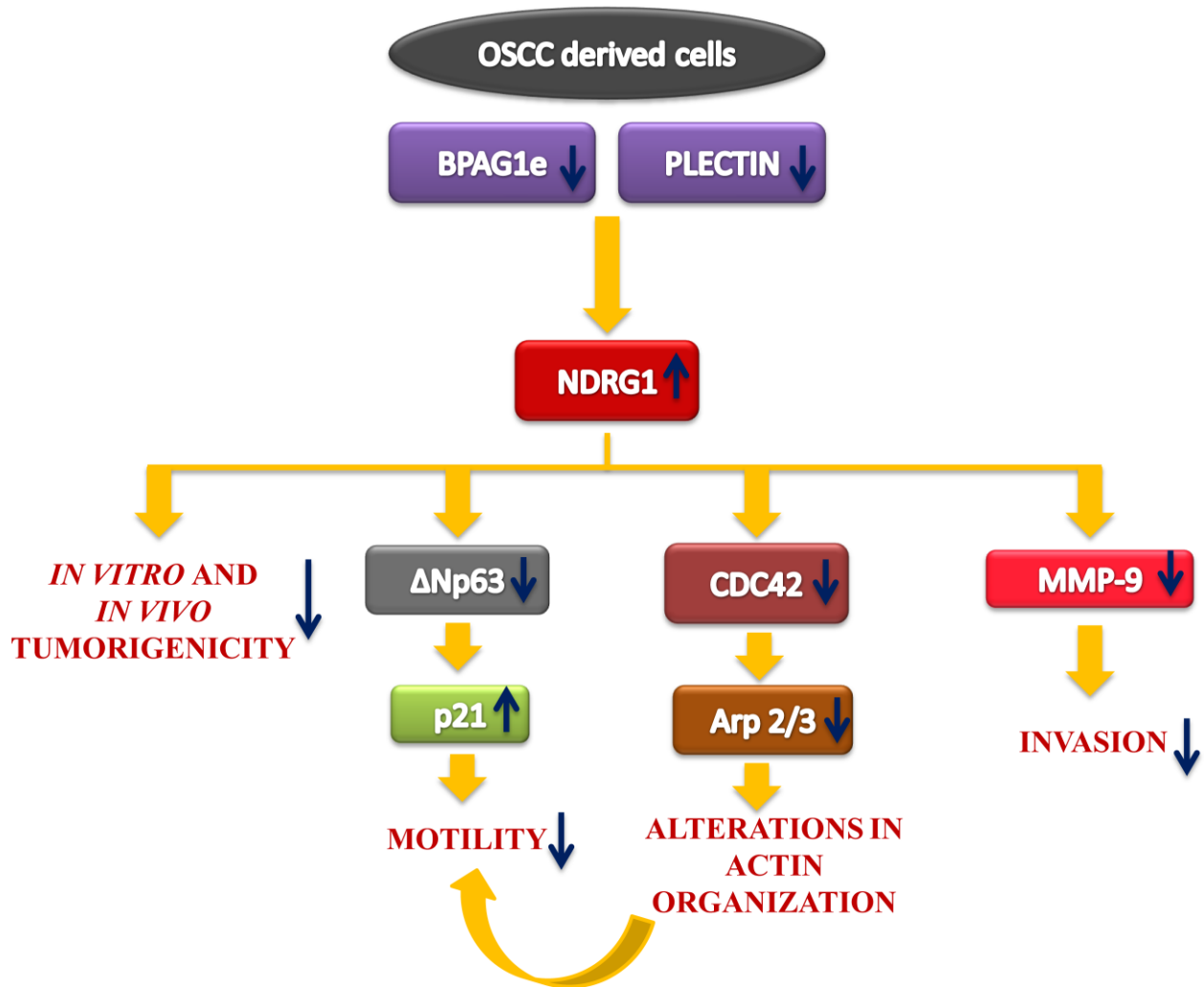


Figure 5.1: Schematic representation of the role of Hemidesmosomal linker proteins in OSCC derived cells

## *6. Summary and Conclusion*

## 6.1 Summary:

- 6.1.1 BPAG1e interacts with K8 in OSCC derived AW13516 cells.
- 6.1.2 BPAG1e and/or Plectin knockdown in tongue SCC cell lines resulted in reduction in cell motility, cell invasion, tumorigenicity and altered actin organization.
- 6.1.3 SWATH analysis for linker proteins knockdown and vector control cells showed alterations in levels of several proteins, out of which, NDRG1 was upregulated in linker proteins knockdown cells.
- 6.1.4 Partial rescue of phenotype for cell transformation was observed upon knockdown of NDRG1 in BPAG1e-Plectin triple knockdown cells as compared to BPAG1e-Plectin double knockdown cells.
- 6.1.5 NDRG1 single knockdown in AW13516 cells showed increase in cell motility, cell invasion and tumorigenic potential.
- 6.1.6 BPAG1e-Plectin knockdown cells displayed non-uniformly organized filopodia, whereas NDRG1-BPAG1e-Plectin knockdown cells showed uniformly arranged filopodia. Consistent with altered actin organization, Cdc42 activity, filamentous actin levels and Arp2/3 levels were reduced in BPAG1e-Plectin double knockdown cells, whereas Cdc42 activity, filamentous actin levels and Arp2/3 expression was rescued in NDRG1-BPAG1e-Plectin triple knockdown cells. This could be one of the possible mechanism by which decreased cell migration was observed upon loss of linker proteins.
- 6.1.7 Upregulation of p21 by targeting  $\Delta$ Np63 in response to NDRG1 upregulation was observed in BPAG1e-Plectin double knockdown cells, whereas NDRG1-BPAG1e-Plectin triple knockdown cells showed restoration of levels of p21 and  $\Delta$ Np63. This could be

another possible mechanism by which reduced cell migration was observed upon loss of linker proteins.

6.1.8 MMP9 activity was substantially decreased in BPAG1e-Plectin double knockdown cells, whereas it was partially restored in NDRG1-BPAG1e-Plectin triple knockdown cells which correlated with results of *in vitro* invasion assay.

6.1.9 The results in another tongue SCC derived cell line (AW8507) revealed that the role of hemidesmosomal linker proteins is not cell line specific.

## **6.2 Conclusion:**

The available literature regarding the role of HD linker proteins in human cancers is inconsistent. In the current study, we have attempted to decipher the role of hemidesmosomal linker proteins in neoplastic progression of OSCC. In conclusion, this study demonstrates that BPAG1e and/or Plectin play a crucial role in regulating cell motility, actin organization, cell invasion and tumorigenicity in OSCC derived cells possibly through NDRG1. Thus, the current project is a step forward in our quest to understand functional significance of aberrant expression of intermediate filaments and their associated proteins (like Plectin and BPAG1e) and further their use as a battery of biomarkers for management of human oral cancer.



## *7. References*

1. Jones JC, Hopkinson SB, Goldfinger LE. Structure and assembly of hemidesmosomes. *BioEssays : news and reviews in molecular, cellular and developmental biology.* 1998;20(6):488-94. doi: 10.1002/(SICI)1521-1878(199806)20:6<488::AID-BIES7>3.0.CO;2-I. PubMed PMID: 9699461.
2. Borradori L, Sonnenberg A. Structure and function of hemidesmosomes: more than simple adhesion complexes. *The Journal of investigative dermatology.* 1999;112(4):411-8. doi: 10.1046/j.1523-1747.1999.00546.x. PubMed PMID: 10201522.
3. Nievers MG, Schaapveld RQ, Sonnenberg A. Biology and function of hemidesmosomes. *Matrix biology : journal of the International Society for Matrix Biology.* 1999;18(1):5-17. PubMed PMID: 10367727.
4. Sterk LM, Geuijen CA, Oomen LC, Calafat J, Janssen H, Sonnenberg A. The tetraspan molecule CD151, a novel constituent of hemidesmosomes, associates with the integrin alpha6beta4 and may regulate the spatial organization of hemidesmosomes. *The Journal of cell biology.* 2000;149(4):969-82. PubMed PMID: 10811835; PubMed Central PMCID: PMC2174566.
5. de Pereda JM, Ortega E, Alonso-Garcia N, Gomez-Hernandez M, Sonnenberg A. Advances and perspectives of the architecture of hemidesmosomes: lessons from structural biology. *Cell adhesion & migration.* 2009;3(4):361-4. PubMed PMID: 19736524; PubMed Central PMCID: PMC2802748.
6. Chaudhari PR, Vaidya MM. Versatile hemidesmosomal linker proteins: structure and function. *Histol Histopathol.* 2015;30(4):425-34. doi: 10.14670/HH-30.425. PubMed PMID: 25421866.

7. Fontao L, Favre B, Riou S, Geerts D, Jaunin F, Saurat JH, et al. Interaction of the bullous pemphigoid antigen 1 (BP230) and desmoplakin with intermediate filaments is mediated by distinct sequences within their COOH terminus. *Mol Biol Cell*. 2003;14(5):1978-92. doi: 10.1091/mbc.E02-08-0548. PubMed PMID: 12802069; PubMed Central PMCID: PMC165091.
8. Koster J, Geerts D, Favre B, Borradori L, Sonnenberg A. Analysis of the interactions between BP180, BP230, plectin and the integrin alpha6beta4 important for hemidesmosome assembly. *Journal of cell science*. 2003;116(Pt 2):387-99. PubMed PMID: 12482924.
9. de Pereda JM, Lillo MP, Sonnenberg A. Structural basis of the interaction between integrin alpha6beta4 and plectin at the hemidesmosomes. *The EMBO journal*. 2009;28(8):1180-90. doi: 10.1038/emboj.2009.48. PubMed PMID: 19242489; PubMed Central PMCID: PMC2683700.
10. Guo L, Degenstein L, Dowling J, Yu QC, Wollmann R, Perman B, et al. Gene targeting of BPAG1: abnormalities in mechanical strength and cell migration in stratified epithelia and neurologic degeneration. *Cell*. 1995;81(2):233-43. PubMed PMID: 7736575.
11. Andra K, Lassmann H, Bittner R, Shorny S, Fassler R, Propst F, et al. Targeted inactivation of plectin reveals essential function in maintaining the integrity of skin, muscle, and heart cytoarchitecture. *Genes & development*. 1997;11(23):3143-56. PubMed PMID: 9389647; PubMed Central PMCID: PMC316746.
12. Herold-Mende C, Kartenbeck J, Tomakidi P, Bosch FX. Metastatic growth of squamous cell carcinomas is correlated with upregulation and redistribution of hemidesmosomal components. *Cell and tissue research*. 2001;306(3):399-408. doi: 10.1007/s004410100462. PubMed PMID: 11735040.

13. Hamill KJ, Hopkinson SB, DeBiase P, Jones JC. BPAG1e maintains keratinocyte polarity through beta4 integrin-mediated modulation of Rac1 and cofilin activities. *Mol Biol Cell*. 2009;20(12):2954-62. doi: 10.1091/mbc.E09-01-0051. PubMed PMID: 19403692; PubMed Central PMCID: PMC2695802.
14. Michael M, Begum R, Fong K, Pourreyaon C, South AP, McGrath JA, et al. BPAG1-e restricts keratinocyte migration through control of adhesion stability. *The Journal of investigative dermatology*. 2014;134(3):773-82. doi: 10.1038/jid.2013.382. PubMed PMID: 24025550.
15. Katada K, Tomonaga T, Satoh M, Matsushita K, Tonoike Y, Kodera Y, et al. Plectin promotes migration and invasion of cancer cells and is a novel prognostic marker for head and neck squamous cell carcinoma. *J Proteomics*. 2012;75(6):1803-15. doi: 10.1016/j.jprot.2011.12.018. PubMed PMID: 22245045.
16. McInroy L, Maatta A. Plectin regulates invasiveness of SW480 colon carcinoma cells and is targeted to podosome-like adhesions in an isoform-specific manner. *Experimental cell research*. 2011;317(17):2468-78. doi: 10.1016/j.yexcr.2011.07.013. PubMed PMID: 21821021.
17. Cheng CC, Chao WT, Liao CC, Tseng YH, Lai YC, Lai YS, et al. Plectin deficiency in liver cancer cells promotes cell migration and sensitivity to sorafenib treatment. *Cell adhesion & migration*. 2017:1-9. doi: 10.1080/19336918.2017.1288789. PubMed PMID: 28276928.
18. Cheng CC, Lai YC, Lai YS, Hsu YH, Chao WT, Sia KC, et al. Transient knockdown-mediated deficiency in plectin alters hepatocellular motility in association with activated FAK and Rac1-GTPase. *Cancer cell international*. 2015;15:29. doi: 10.1186/s12935-015-0177-1. PubMed PMID: 25774093; PubMed Central PMCID: PMC4358909.

19. Coulombe PA, Omary MB. 'Hard' and 'soft' principles defining the structure, function and regulation of keratin intermediate filaments. *Current opinion in cell biology*. 2002;14(1):110-22. PubMed PMID: 11792552.
20. Schweizer J, Bowden PE, Coulombe PA, Langbein L, Lane EB, Magin TM, et al. New consensus nomenclature for mammalian keratins. *The Journal of cell biology*. 2006;174(2):169-74. doi: 10.1083/jcb.200603161. PubMed PMID: 16831889; PubMed Central PMCID: PMC2064177.
21. Vaidya MM, Borges AM, Pradhan SA, Rajpal RM, Bhisey AN. Altered keratin expression in buccal mucosal squamous cell carcinoma. *Journal of oral pathology & medicine* : official publication of the International Association of Oral Pathologists and the American Academy of Oral Pathology. 1989;18(5):282-6. PubMed PMID: 2475617.
22. Schaafsma HE, Van Der Velden LA, Manni JJ, Peters H, Link M, Rutter DJ, et al. Increased expression of cytokeratins 8, 18 and vimentin in the invasion front of mucosal squamous cell carcinoma. *The Journal of pathology*. 1993;170(1):77-86. doi: 10.1002/path.1711700113. PubMed PMID: 7686975.
23. Vaidya MM, Borges AM, Pradhan SA, Bhisey AN. Cytokeratin expression in squamous cell carcinomas of the tongue and alveolar mucosa. *European journal of cancer Part B, Oral oncology*. 1996;32B(5):333-6. PubMed PMID: 8944837.
24. Fillies T, Werkmeister R, Packeisen J, Brandt B, Morin P, Weingart D, et al. Cytokeratin 8/18 expression indicates a poor prognosis in squamous cell carcinomas of the oral cavity. *BMC cancer*. 2006;6:10. doi: 10.1186/1471-2407-6-10. PubMed PMID: 16412231; PubMed Central PMCID: PMC1379654.

25. Raul U, Sawant S, Dange P, Kalraiya R, Ingle A, Vaidya M. Implications of cytokeratin 8/18 filament formation in stratified epithelial cells: induction of transformed phenotype. *International journal of cancer*. 2004;111(5):662-8. doi: 10.1002/ijc.20349. PubMed PMID: 15252834.
26. Alam H, Kundu ST, Dalal SN, Vaidya MM. Loss of keratins 8 and 18 leads to alterations in alpha6beta4-integrin-mediated signalling and decreased neoplastic progression in an oral-tumour-derived cell line. *Journal of cell science*. 2011;124(Pt 12):2096-106. doi: 10.1242/jcs.073585. PubMed PMID: 21610092.
27. Stepp MA, Spurr-Michaud S, Tisdale A, Elwell J, Gipson IK. Alpha 6 beta 4 integrin heterodimer is a component of hemidesmosomes. *Proceedings of the National Academy of Sciences of the United States of America*. 1990;87(22):8970-4. PubMed PMID: 2247472; PubMed Central PMCID: PMC55082.
28. Sawamura D, Li K, Chu ML, Uitto J. Human bullous pemphigoid antigen (BPAG1). Amino acid sequences deduced from cloned cDNAs predict biologically important peptide segments and protein domains. *The Journal of biological chemistry*. 1991;266(27):17784-90. PubMed PMID: 1717441.
29. Hieda Y, Nishizawa Y, Uematsu J, Owaribe K. Identification of a new hemidesmosomal protein, HD1: a major, high molecular mass component of isolated hemidesmosomes. *The Journal of cell biology*. 1992;116(6):1497-506. PubMed PMID: 1541639; PubMed Central PMCID: PMC2289367.
30. Barczyk M, Carracedo S, Gullberg D. Integrins. *Cell and tissue research*. 2010;339(1):269-80. doi: 10.1007/s00441-009-0834-6. PubMed PMID: 19693543; PubMed Central PMCID: PMC2784866.

31. Mercurio AM, Rabinovitz I, Shaw LM. The alpha 6 beta 4 integrin and epithelial cell migration. *Current opinion in cell biology*. 2001;13(5):541-5. PubMed PMID: 11544021.
32. Hogervorst F, Kuikman I, von dem Borne AE, Sonnenberg A. Cloning and sequence analysis of beta-4 cDNA: an integrin subunit that contains a unique 118 kd cytoplasmic domain. *The EMBO journal*. 1990;9(3):765-70. PubMed PMID: 2311578; PubMed Central PMCID: PMC551734.
33. Suzuki S, Naitoh Y. Amino acid sequence of a novel integrin beta 4 subunit and primary expression of the mRNA in epithelial cells. *The EMBO journal*. 1990;9(3):757-63. PubMed PMID: 2311577; PubMed Central PMCID: PMC551732.
34. Margadant C, Frijns E, Wilhelmsen K, Sonnenberg A. Regulation of hemidesmosome disassembly by growth factor receptors. *Current opinion in cell biology*. 2008;20(5):589-96. doi: 10.1016/j.ceb.2008.05.001. PubMed PMID: 18583123.
35. Giancotti FG. Targeting integrin beta4 for cancer and anti-angiogenic therapy. *Trends in pharmacological sciences*. 2007;28(10):506-11. doi: 10.1016/j.tips.2007.08.004. PubMed PMID: 17822782.
36. Wolf GT, Carey TE, Schmaltz SP, McClatchey KD, Poore J, Glaser L, et al. Altered antigen expression predicts outcome in squamous cell carcinoma of the head and neck. *Journal of the National Cancer Institute*. 1990;82(19):1566-72. PubMed PMID: 2119437.
37. Stewart RL, West D, Wang C, Weiss HL, Gal T, Durbin EB, et al. Elevated integrin alpha6beta4 expression is associated with venous invasion and decreased overall survival in non-small cell lung cancer. *Human pathology*. 2016;54:174-83. doi: 10.1016/j.humpath.2016.04.003. PubMed PMID: 27107458; PubMed Central PMCID: PMC4938774.

38. Ding YB, Deng B, Huang YS, Xiao WM, Wu J, Zhang YQ, et al. A high level of integrin alpha6 expression in human intrahepatic cholangiocarcinoma cells is associated with a migratory and invasive phenotype. *Digestive diseases and sciences*. 2013;58(6):1627-35. doi: 10.1007/s10620-012-2524-6. PubMed PMID: 23306848.
39. Primo L, Seano G, Roca C, Maione F, Gagliardi PA, Sessa R, et al. Increased expression of alpha6 integrin in endothelial cells unveils a proangiogenic role for basement membrane. *Cancer research*. 2010;70(14):5759-69. doi: 10.1158/0008-5472.CAN-10-0507. PubMed PMID: 20570893.
40. Guo W, Giancotti FG. Integrin signalling during tumour progression. *Nature reviews Molecular cell biology*. 2004;5(10):816-26. doi: 10.1038/nrm1490. PubMed PMID: 15459662.
41. Kippenberger S, Hofmann M, Zoller N, Thaci D, Muller J, Kaufmann R, et al. Ligation of beta4 integrins activates PKB/Akt and ERK1/2 by distinct pathways-relevance of the keratin filament. *Biochimica et biophysica acta*. 2010;1803(8):940-50. doi: 10.1016/j.bbamcr.2010.03.009. PubMed PMID: 20307589.
42. Dmello C, Sawant S, Alam H, Gangadaran P, Tiwari R, Dongre H, et al. Vimentin-mediated regulation of cell motility through modulation of beta4 integrin protein levels in oral tumor derived cells. *The international journal of biochemistry & cell biology*. 2016;70:161-72. doi: 10.1016/j.biocel.2015.11.015. PubMed PMID: 26646105.
43. Sincock PM, Mayrhofer G, Ashman LK. Localization of the transmembrane 4 superfamily (TM4SF) member PETA-3 (CD151) in normal human tissues: comparison with CD9, CD63, and alpha5beta1 integrin. *The journal of histochemistry and cytochemistry : official journal of the Histochemistry Society*. 1997;45(4):515-25. doi: 10.1177/002215549704500404. PubMed PMID: 9111230.

44. Wright MD, Tomlinson MG. The ins and outs of the transmembrane 4 superfamily. *Immunology today*. 1994;15(12):588-94. doi: 10.1016/0167-5699(94)90222-4. PubMed PMID: 7531445.
45. Maecker HT, Todd SC, Levy S. The tetraspanin superfamily: molecular facilitators. *FASEB journal : official publication of the Federation of American Societies for Experimental Biology*. 1997;11(6):428-42. PubMed PMID: 9194523.
46. Yauch RL, Berditchevski F, Harler MB, Reichner J, Hemler ME. Highly stoichiometric, stable, and specific association of integrin alpha3beta1 with CD151 provides a major link to phosphatidylinositol 4-kinase, and may regulate cell migration. *Mol Biol Cell*. 1998;9(10):2751-65. PubMed PMID: 9763442; PubMed Central PMCID: PMC25552.
47. Hasegawa H, Nomura T, Kishimoto K, Yanagisawa K, Fujita S. SFA-1/PETA-3 (CD151), a member of the transmembrane 4 superfamily, associates preferentially with alpha 5 beta 1 integrin and regulates adhesion of human T cell leukemia virus type 1-infected T cells to fibronectin. *Journal of immunology*. 1998;161(6):3087-95. PubMed PMID: 9743375.
48. Fitter S, Sincock PM, Jolliffe CN, Ashman LK. Transmembrane 4 superfamily protein CD151 (PETA-3) associates with beta 1 and alpha IIb beta 3 integrins in haemopoietic cell lines and modulates cell-cell adhesion. *The Biochemical journal*. 1999;338 ( Pt 1):61-70. PubMed PMID: 9931299; PubMed Central PMCID: PMC1220025.
49. Sugiura T, Berditchevski F. Function of alpha3beta1-tetraspanin protein complexes in tumor cell invasion. Evidence for the role of the complexes in production of matrix metalloproteinase 2 (MMP-2). *The Journal of cell biology*. 1999;146(6):1375-89. PubMed PMID: 10491398; PubMed Central PMCID: PMC2156113.

50. Takeda Y, Kazarov AR, Butterfield CE, Hopkins BD, Benjamin LE, Kaipainen A, et al. Deletion of tetraspanin Cd151 results in decreased pathologic angiogenesis in vivo and in vitro. *Blood*. 2007;109(4):1524-32. doi: 10.1182/blood-2006-08-041970. PubMed PMID: 17023588; PubMed Central PMCID: PMC1794066.
51. Shigeta M, Sanzen N, Ozawa M, Gu J, Hasegawa H, Sekiguchi K. CD151 regulates epithelial cell-cell adhesion through PKC- and Cdc42-dependent actin cytoskeletal reorganization. *The Journal of cell biology*. 2003;163(1):165-76. doi: 10.1083/jcb.200301075. PubMed PMID: 14557253; PubMed Central PMCID: PMC2173453.
52. Ke AW, Shi GM, Zhou J, Huang XY, Shi YH, Ding ZB, et al. CD151 amplifies signaling by integrin alpha6beta1 to PI3K and induces the epithelial-mesenchymal transition in HCC cells. *Gastroenterology*. 2011;140(5):1629-41 e15. doi: 10.1053/j.gastro.2011.02.008. PubMed PMID: 21320503.
53. Diaz LA, Ratrie H, 3rd, Saunders WS, Futamura S, Squiquera HL, Anhalt GJ, et al. Isolation of a human epidermal cDNA corresponding to the 180-kD autoantigen recognized by bullous pemphigoid and herpes gestationis sera. Immunolocalization of this protein to the hemidesmosome. *The Journal of clinical investigation*. 1990;86(4):1088-94. doi: 10.1172/JCI114812. PubMed PMID: 1698819; PubMed Central PMCID: PMC296836.
54. Li K, Tamai K, Tan EM, Uitto J. Cloning of type XVII collagen. Complementary and genomic DNA sequences of mouse 180-kilodalton bullous pemphigoid antigen (BPAG2) predict an interrupted collagenous domain, a transmembrane segment, and unusual features in the 5'-end of the gene and the 3'-untranslated region of the mRNA. *The Journal of biological chemistry*. 1993;268(12):8825-34. PubMed PMID: 8473327.

55. Chung HJ, Uitto J. Type VII collagen: the anchoring fibril protein at fault in dystrophic epidermolysis bullosa. *Dermatologic clinics*. 2010;28(1):93-105. doi: 10.1016/j.det.2009.10.011. PubMed PMID: 19945621; PubMed Central PMCID: PMC2791403.
56. Fairley JA, Heintz PW, Neuburg M, Diaz LA, Giudice GJ. Expression pattern of the bullous pemphigoid-180 antigen in normal and neoplastic epithelia. *The British journal of dermatology*. 1995;133(3):385-91. PubMed PMID: 8546992.
57. Hirako Y, Usukura J, Nishizawa Y, Owaribe K. Demonstration of the molecular shape of BP180, a 180-kDa bullous pemphigoid antigen and its potential for trimer formation. *The Journal of biological chemistry*. 1996;271(23):13739-45. PubMed PMID: 8662839.
58. Hopkinson SB, Findlay K, deHart GW, Jones JC. Interaction of BP180 (type XVII collagen) and alpha6 integrin is necessary for stabilization of hemidesmosome structure. *The Journal of investigative dermatology*. 1998;111(6):1015-22. doi: 10.1046/j.1523-1747.1998.00452.x. PubMed PMID: 9856810.
59. Schaapveld RQ, Borradori L, Geerts D, van Leusden MR, Kuikman I, Nievers MG, et al. Hemidesmosome formation is initiated by the beta4 integrin subunit, requires complex formation of beta4 and HD1/plectin, and involves a direct interaction between beta4 and the bullous pemphigoid antigen 180. *The Journal of cell biology*. 1998;142(1):271-84. PubMed PMID: 9660880; PubMed Central PMCID: PMC2133016.
60. Tasanen K, Tunggal L, Chometon G, Bruckner-Tuderman L, Aumailley M. Keratinocytes from patients lacking collagen XVII display a migratory phenotype. *The American journal of pathology*. 2004;164(6):2027-38. doi: 10.1016/S0002-9440(10)63762-5. PubMed PMID: 15161638; PubMed Central PMCID: PMC1615787.

61. Moilanen JM, Kokkonen N, Loffek S, Vayrynen JP, Syvaniemi E, Hurskainen T, et al. Collagen XVII expression correlates with the invasion and metastasis of colorectal cancer. *Human pathology*. 2015;46(3):434-42. doi: 10.1016/j.humpath.2014.11.020. PubMed PMID: 25623077.
62. Hamill KJ, Hopkinson SB, Jonkman MF, Jones JC. Type XVII collagen regulates lamellipod stability, cell motility, and signaling to Rac1 by targeting bullous pemphigoid antigen 1e to alpha6beta4 integrin. *The Journal of biological chemistry*. 2011;286(30):26768-80. doi: 10.1074/jbc.M110.203646. PubMed PMID: 21642434; PubMed Central PMCID: PMC3143638.
63. Liu CC, Lin JH, Hsu TW, Hsu JW, Chang JW, Su K, et al. Collagen XVII/laminin-5 activates epithelial-to-mesenchymal transition and is associated with poor prognosis in lung cancer. *Oncotarget*. 2016. doi: 10.18632/oncotarget.11208. PubMed PMID: 27531893.
64. Liu CC, Lin SP, Hsu HS, Yang SH, Lin CH, Yang MH, et al. Suspension survival mediated by PP2A-STAT3-Col XVII determines tumour initiation and metastasis in cancer stem cells. *Nature communications*. 2016;7:11798. doi: 10.1038/ncomms11798. PubMed PMID: 27306323; PubMed Central PMCID: PMC4912642.
65. Leung CL, Green KJ, Liem RK. Plakins: a family of versatile cytolinker proteins. *Trends in cell biology*. 2002;12(1):37-45. PubMed PMID: 11854008.
66. Green KJ, Virata ML, Elgart GW, Stanley JR, Parry DA. Comparative structural analysis of desmoplakin, bullous pemphigoid antigen and plectin: members of a new gene family involved in organization of intermediate filaments. *International journal of biological macromolecules*. 1992;14(3):145-53. PubMed PMID: 1390446.
67. Leung CL, Zheng M, Prater SM, Liem RK. The BPAG1 locus: Alternative splicing produces multiple isoforms with distinct cytoskeletal linker domains, including predominant

- isoforms in neurons and muscles. *The Journal of cell biology*. 2001;154(4):691-7. doi: 10.1083/jcb.200012098. PubMed PMID: 11514586; PubMed Central PMCID: PMC2196450.
68. Errante LD, Wiche G, Shaw G. Distribution of plectin, an intermediate filament-associated protein, in the adult rat central nervous system. *Journal of neuroscience research*. 1994;37(4):515-28. doi: 10.1002/jnr.490370411. PubMed PMID: 8021973.
69. Elliott CE, Becker B, Oehler S, Castanon MJ, Hauptmann R, Wiche G. Plectin transcript diversity: identification and tissue distribution of variants with distinct first coding exons and rodless isoforms. *Genomics*. 1997;42(1):115-25. doi: 10.1006/geno.1997.4724. PubMed PMID: 9177781.
70. Fuchs P, Zorer M, Rezniczek GA, Spazierer D, Oehler S, Castanon MJ, et al. Unusual 5' transcript complexity of plectin isoforms: novel tissue-specific exons modulate actin binding activity. *Human molecular genetics*. 1999;8(13):2461-72. PubMed PMID: 10556294.
71. Andra K, Kornacker I, Jorgl A, Zorer M, Spazierer D, Fuchs P, et al. Plectin-isoform-specific rescue of hemidesmosomal defects in plectin (-/-) keratinocytes. *J Invest Dermatol*. 2003;120(2):189-97. doi: 10.1046/j.1523-1747.2003.12027.x. PubMed PMID: 12542521.
72. Walko G, Vukasinovic N, Gross K, Fischer I, Sibitz S, Fuchs P, et al. Targeted proteolysis of plectin isoform 1a accounts for hemidesmosome dysfunction in mice mimicking the dominant skin blistering disease EBS-Ogna. *PLoS genetics*. 2011;7(12):e1002396. doi: 10.1371/journal.pgen.1002396. PubMed PMID: 22144912; PubMed Central PMCID: PMC3228830.
73. Geerts D, Fontao L, Nievers MG, Schaapveld RQ, Purkis PE, Wheeler GN, et al. Binding of integrin alpha6beta4 to plectin prevents plectin association with F-actin but does not interfere

with intermediate filament binding. *The Journal of cell biology*. 1999;147(2):417-34. PubMed PMID: 10525545; PubMed Central PMCID: PMC2174221.

74. Sun D, Leung CL, Liem RK. Characterization of the microtubule binding domain of microtubule actin crosslinking factor (MACF): identification of a novel group of microtubule associated proteins. *Journal of cell science*. 2001;114(Pt 1):161-72. PubMed PMID: 11112700.

75. Hopkinson SB, Jones JC. The N terminus of the transmembrane protein BP180 interacts with the N-terminal domain of BP230, thereby mediating keratin cytoskeleton anchorage to the cell surface at the site of the hemidesmosome. *Mol Biol Cell*. 2000;11(1):277-86. PubMed PMID: 10637308; PubMed Central PMCID: PMC14774.

76. Skalli O, Chou YH, Goldman RD. Cell cycle-dependent changes in the organization of an intermediate filament-associated protein: correlation with phosphorylation by p34cdc2. *Proceedings of the National Academy of Sciences of the United States of America*. 1992;89(24):11959-63. PubMed PMID: 1281546; PubMed Central PMCID: PMC50677.

77. Foisner R, Malecz N, Dressel N, Stadler C, Wiche G. M-phase-specific phosphorylation and structural rearrangement of the cytoplasmic cross-linking protein plectin involve p34cdc2 kinase. *Mol Biol Cell*. 1996;7(2):273-88. PubMed PMID: 8688558; PubMed Central PMCID: PMC275879.

78. Bouameur JE, Schneider Y, Begre N, Hobbs RP, Lingasamy P, Fontao L, et al. Phosphorylation of serine 4,642 in the C-terminus of plectin by MNK2 and PKA modulates its interaction with intermediate filaments. *Journal of cell science*. 2013;126(Pt 18):4195-207. doi: 10.1242/jcs.127779. PubMed PMID: 23843618; PubMed Central PMCID: PMC3772390.

79. Aberdam D, Galliano MF, Vailly J, Pulkkinen L, Bonifas J, Christiano AM, et al. Herlitz's junctional epidermolysis bullosa is linked to mutations in the gene (LAMC2) for the

gamma 2 subunit of nicein/kalinin (LAMININ-5). *Nature genetics*. 1994;6(3):299-304. doi: 10.1038/ng0394-299. PubMed PMID: 8012394.

80. Dowling J, Yu QC, Fuchs E. Beta4 integrin is required for hemidesmosome formation, cell adhesion and cell survival. *The Journal of cell biology*. 1996;134(2):559-72. PubMed PMID: 8707838; PubMed Central PMCID: PMC2120864.

81. Georges-Labouesse E, Messaddeq N, Yehia G, Cadalbert L, Dierich A, Le Meur M. Absence of integrin alpha 6 leads to epidermolysis bullosa and neonatal death in mice. *Nature genetics*. 1996;13(3):370-3. doi: 10.1038/ng0796-370. PubMed PMID: 8673141.

82. van der Neut R, Krimpenfort P, Calafat J, Niessen CM, Sonnenberg A. Epithelial detachment due to absence of hemidesmosomes in integrin beta 4 null mice. *Nature genetics*. 1996;13(3):366-9. doi: 10.1038/ng0796-366. PubMed PMID: 8673140.

83. Murgia C, Blaikie P, Kim N, Dans M, Petrie HT, Giancotti FG. Cell cycle and adhesion defects in mice carrying a targeted deletion of the integrin beta4 cytoplasmic domain. *The EMBO journal*. 1998;17(14):3940-51. doi: 10.1093/emboj/17.14.3940. PubMed PMID: 9670011; PubMed Central PMCID: PMC1170729.

84. Nievers MG, Schaapveld RQ, Oomen LC, Fontao L, Geerts D, Sonnenberg A. Ligand-independent role of the beta 4 integrin subunit in the formation of hemidesmosomes. *Journal of cell science*. 1998;111 ( Pt 12):1659-72. PubMed PMID: 9601096.

85. Niessen CM, Hulsman EH, Oomen LC, Kuikman I, Sonnenberg A. A minimal region on the integrin beta4 subunit that is critical to its localization in hemidesmosomes regulates the distribution of HD1/plectin in COS-7 cells. *Journal of cell science*. 1997;110 ( Pt 15):1705-16. PubMed PMID: 9264458.

86. Niessen CM, Hulsman EH, Rots ES, Sanchez-Aparicio P, Sonnenberg A. Integrin alpha 6 beta 4 forms a complex with the cytoskeletal protein HD1 and induces its redistribution in transfected COS-7 cells. *Mol Biol Cell*. 1997;8(4):555-66. PubMed PMID: 9247637; PubMed Central PMCID: PMC276108.
87. Rezniczek GA, de Pereda JM, Reipert S, Wiche G. Linking integrin alpha6beta4-based cell adhesion to the intermediate filament cytoskeleton: direct interaction between the beta4 subunit and plectin at multiple molecular sites. *The Journal of cell biology*. 1998;141(1):209-25. PubMed PMID: 9531560; PubMed Central PMCID: PMC2132717.
88. Koster J, van Wilpe S, Kuikman I, Litjens SH, Sonnenberg A. Role of binding of plectin to the integrin beta4 subunit in the assembly of hemidesmosomes. *Mol Biol Cell*. 2004;15(3):1211-23. doi: 10.1091/mbc.E03-09-0697. PubMed PMID: 14668477; PubMed Central PMCID: PMC363110.
89. Giudice GJ, Emery DJ, Diaz LA. Cloning and primary structural analysis of the bullous pemphigoid autoantigen BP180. *The Journal of investigative dermatology*. 1992;99(3):243-50. PubMed PMID: 1324962.
90. Hopkinson SB, Baker SE, Jones JC. Molecular genetic studies of a human epidermal autoantigen (the 180-kD bullous pemphigoid antigen/BP180): identification of functionally important sequences within the BP180 molecule and evidence for an interaction between BP180 and alpha 6 integrin. *The Journal of cell biology*. 1995;130(1):117-25. PubMed PMID: 7790367; PubMed Central PMCID: PMC2120509.
91. Aho S, Uitto J. Direct interaction between the intracellular domains of bullous pemphigoid antigen 2 (BP180) and beta 4 integrin, hemidesmosomal components of basal

keratinocytes. *Biochemical and biophysical research communications*. 1998;243(3):694-9. doi: 10.1006/bbrc.1998.8162. PubMed PMID: 9500991.

92. Borradori L, Chavanas S, Schaapveld RQ, Gagnoux-Palacios L, Calafat J, Meneguzzi G, et al. Role of the bullous pemphigoid antigen 180 (BP180) in the assembly of hemidesmosomes and cell adhesion--reexpression of BP180 in generalized atrophic benign epidermolysis bullosa keratinocytes. *Experimental cell research*. 1998;239(2):463-76. doi: 10.1006/excr.1997.3923. PubMed PMID: 9521865.

93. Shimbo T, Tanemura A, Yamazaki T, Tamai K, Katayama I, Kaneda Y. Serum anti-BPAG1 auto-antibody is a novel marker for human melanoma. *PloS one*. 2010;5(5):e10566. doi: 10.1371/journal.pone.0010566. PubMed PMID: 20479946; PubMed Central PMCID: PMC2866734.

94. Lo AK, Yuen PW, Liu Y, Wang XH, Cheung AL, Wong YC, et al. Downregulation of hemidesmosomal proteins in nasopharyngeal carcinoma cells. *Cancer letters*. 2001;163(1):117-23. PubMed PMID: 11163115.

95. Valencia RG, Walko G, Janda L, Novacek J, Mihailovska E, Reipert S, et al. Intermediate filament-associated cytolinker plectin 1c destabilizes microtubules in keratinocytes. *Mol Biol Cell*. 2013;24(6):768-84. doi: 10.1091/mbc.E12-06-0488. PubMed PMID: 23363598; PubMed Central PMCID: PMC3596248.

96. Andra K, Nikolic B, Stocher M, Drenckhahn D, Wiche G. Not just scaffolding: plectin regulates actin dynamics in cultured cells. *Genes & development*. 1998;12(21):3442-51. PubMed PMID: 9808630; PubMed Central PMCID: PMC317224.

97. Bausch D, Mino-Kenudson M, Fernandez-Del Castillo C, Warshaw AL, Kelly KA, Thayer SP. Plectin-1 is a biomarker of malignant pancreatic intraductal papillary mucinous

- neoplasms. *Journal of gastrointestinal surgery : official journal of the Society for Surgery of the Alimentary Tract*. 2009;13(11):1948-54; discussion 54. doi: 10.1007/s11605-009-1001-9. PubMed PMID: 19760374; PubMed Central PMCID: PMC3806105.
98. Lee HJ, Na K, Kwon MS, Kim H, Kim KS, Paik YK. Quantitative analysis of phosphopeptides in search of the disease biomarker from the hepatocellular carcinoma specimen. *Proteomics*. 2009;9(12):3395-408. doi: 10.1002/pmic.200800943. PubMed PMID: 19562805.
99. Bausch D, Thomas S, Mino-Kenudson M, Fernandez-del CC, Bauer TW, Williams M, et al. Plectin-1 as a novel biomarker for pancreatic cancer. *Clinical cancer research : an official journal of the American Association for Cancer Research*. 2011;17(2):302-9. doi: 10.1158/1078-0432.CCR-10-0999. PubMed PMID: 21098698; PubMed Central PMCID: PMC3044444.
100. Sutoh Yoneyama M, Hatakeyama S, Habuchi T, Inoue T, Nakamura T, Funyu T, et al. Vimentin intermediate filament and plectin provide a scaffold for invadopodia, facilitating cancer cell invasion and extravasation for metastasis. *Eur J Cell Biol*. 2014;93(4):157-69. doi: 10.1016/j.ejcb.2014.03.002. PubMed PMID: 24810881.
101. Shin SJ, Smith JA, Rezniczek GA, Pan S, Chen R, Brentnall TA, et al. Unexpected gain of function for the scaffolding protein plectin due to mislocalization in pancreatic cancer. *Proceedings of the National Academy of Sciences of the United States of America*. 2013;110(48):19414-9. doi: 10.1073/pnas.1309720110. PubMed PMID: 24218614; PubMed Central PMCID: PMC3845200.
102. Ishikawa H, Bischoff R, Holtzer H. Mitosis and intermediate-sized filaments in developing skeletal muscle. *The Journal of cell biology*. 1968;38(3):538-55. PubMed PMID: 5664223; PubMed Central PMCID: PMC2108373.

103. Herrmann H, Aebi U. Intermediate filaments: molecular structure, assembly mechanism, and integration into functionally distinct intracellular Scaffolds. *Annual review of biochemistry*. 2004;73:749-89. doi: 10.1146/annurev.biochem.73.011303.073823. PubMed PMID: 15189158.
104. Omary MB, Coulombe PA, McLean WH. Intermediate filament proteins and their associated diseases. *The New England journal of medicine*. 2004;351(20):2087-100. doi: 10.1056/NEJMra040319. PubMed PMID: 15537907.
105. Fuchs E, Weber K. Intermediate filaments: structure, dynamics, function, and disease. *Annual review of biochemistry*. 1994;63:345-82. doi: 10.1146/annurev.bi.63.070194.002021. PubMed PMID: 7979242.
106. Godsel LM, Hobbs RP, Green KJ. Intermediate filament assembly: dynamics to disease. *Trends in cell biology*. 2008;18(1):28-37. doi: 10.1016/j.tcb.2007.11.004. PubMed PMID: 18083519.
107. Chung BM, Rotty JD, Coulombe PA. Networking galore: intermediate filaments and cell migration. *Current opinion in cell biology*. 2013;25(5):600-12. doi: 10.1016/j.ceb.2013.06.008. PubMed PMID: 23886476; PubMed Central PMCID: PMC3780586.
108. Moll R, Franke WW, Schiller DL, Geiger B, Krepler R. The catalog of human cytokeratins: patterns of expression in normal epithelia, tumors and cultured cells. *Cell*. 1982;31(1):11-24. PubMed PMID: 6186379.
109. Moll R, Divo M, Langbein L. The human keratins: biology and pathology. *Histochemistry and cell biology*. 2008;129(6):705-33. doi: 10.1007/s00418-008-0435-6. PubMed PMID: 18461349; PubMed Central PMCID: PMC2386534.
110. Fuchs E, Green H. Changes in keratin gene expression during terminal differentiation of the keratinocyte. *Cell*. 1980;19(4):1033-42. PubMed PMID: 6155214.

111. Owens DW, Lane EB. The quest for the function of simple epithelial keratins. *BioEssays : news and reviews in molecular, cellular and developmental biology*. 2003;25(8):748-58. doi: 10.1002/bies.10316. PubMed PMID: 12879445.
112. Omary MB. "IF-pathies": a broad spectrum of intermediate filament-associated diseases. *The Journal of clinical investigation*. 2009;119(7):1756-62. doi: 10.1172/JCI39894. PubMed PMID: 19587450; PubMed Central PMCID: PMC2701889.
113. Casanova ML, Bravo A, Martinez-Palacio J, Fernandez-Acenero MJ, Villanueva C, Larcher F, et al. Epidermal abnormalities and increased malignancy of skin tumors in human epidermal keratin 8-expressing transgenic mice. *FASEB journal : official publication of the Federation of American Societies for Experimental Biology*. 2004;18(13):1556-8. doi: 10.1096/fj.04-1683fje. PubMed PMID: 15319370.
114. Hendrix MJ, Seftor EA, Chu YW, Seftor RE, Nagle RB, McDaniel KM, et al. Coexpression of vimentin and keratins by human melanoma tumor cells: correlation with invasive and metastatic potential. *Journal of the National Cancer Institute*. 1992;84(3):165-74. PubMed PMID: 1371813.
115. Chu YW, Runyan RB, Oshima RG, Hendrix MJ. Expression of complete keratin filaments in mouse L cells augments cell migration and invasion. *Proceedings of the National Academy of Sciences of the United States of America*. 1993;90(9):4261-5. PubMed PMID: 7683431; PubMed Central PMCID: PMC46486.
116. Iyer SV, Dange PP, Alam H, Sawant SS, Ingle AD, Borges AM, et al. Understanding the role of keratins 8 and 18 in neoplastic potential of breast cancer derived cell lines. *PloS one*. 2013;8(1):e53532. doi: 10.1371/journal.pone.0053532. PubMed PMID: 23341946; PubMed Central PMCID: PMC3546083.

117. Fortier AM, Asselin E, Cadrin M. Keratin 8 and 18 loss in epithelial cancer cells increases collective cell migration and cisplatin sensitivity through claudin1 up-regulation. *The Journal of biological chemistry*. 2013;288(16):11555-71. doi: 10.1074/jbc.M112.428920. PubMed PMID: 23449973; PubMed Central PMCID: PMC3630871.
118. Fang J, Wang H, Liu Y, Ding F, Ni Y, Shao S. High KRT8 expression promotes tumor progression and metastasis of gastric cancer. *Cancer science*. 2017;108(2):178-86. doi: 10.1111/cas.13120. PubMed PMID: 27865045; PubMed Central PMCID: PMC5329158.
119. Adams JC. Roles of fascin in cell adhesion and motility. *Current opinion in cell biology*. 2004;16(5):590-6. doi: 10.1016/j.ceb.2004.07.009. PubMed PMID: 15363811.
120. Grothey A, Hashizume R, Sahin AA, McCrea PD. Fascin, an actin-bundling protein associated with cell motility, is upregulated in hormone receptor negative breast cancer. *British journal of cancer*. 2000;83(7):870-3. doi: 10.1054/bjoc.2000.1395. PubMed PMID: 10970687; PubMed Central PMCID: PMC2374674.
121. Hu W, McCrea PD, Deavers M, Kavanagh JJ, Kudelka AP, Verschraegen CF. Increased expression of fascin, motility associated protein, in cell cultures derived from ovarian cancer and in borderline and carcinomatous ovarian tumors. *Clinical & experimental metastasis*. 2000;18(1):83-8. PubMed PMID: 11206843.
122. Goncharuk VN, Ross JS, Carlson JA. Actin-binding protein fascin expression in skin neoplasia. *Journal of cutaneous pathology*. 2002;29(7):430-8. PubMed PMID: 12139639.
123. Iguchi T, Aishima S, Umeda K, Sanefuji K, Fujita N, Sugimachi K, et al. Fascin expression in progression and prognosis of hepatocellular carcinoma. *Journal of surgical oncology*. 2009;100(7):575-9. doi: 10.1002/jso.21377. PubMed PMID: 19697358.

124. Alam H, Bhate AV, Gangadaran P, Sawant SS, Salot S, Sehgal L, et al. Fascin overexpression promotes neoplastic progression in oral squamous cell carcinoma. *BMC cancer*. 2012;12:32. doi: 10.1186/1471-2407-12-32. PubMed PMID: 22264292; PubMed Central PMCID: PMC3329405.
125. Kureishy N, Sapountzi V, Prag S, Anilkumar N, Adams JC. Fascins, and their roles in cell structure and function. *BioEssays : news and reviews in molecular, cellular and developmental biology*. 2002;24(4):350-61. doi: 10.1002/bies.10070. PubMed PMID: 11948621.
126. Machesky LM, Li A. Fascin: Invasive filopodia promoting metastasis. *Communicative & integrative biology*. 2010;3(3):263-70. PubMed PMID: 20714410; PubMed Central PMCID: PMC2918773.
127. Liang Z, Wang Y, Shen Z, Teng X, Li X, Li C, et al. Fascin 1 promoted the growth and migration of non-small cell lung cancer cells by activating YAP/TEAD signaling. *Tumour biology : the journal of the International Society for Oncodevelopmental Biology and Medicine*. 2016;37(8):10909-15. doi: 10.1007/s13277-016-4934-0. PubMed PMID: 26886283.
128. Hashimoto Y, Ito T, Inoue H, Okumura T, Tanaka E, Tsunoda S, et al. Prognostic significance of fascin overexpression in human esophageal squamous cell carcinoma. *Clinical cancer research : an official journal of the American Association for Cancer Research*. 2005;11(7):2597-605. doi: 10.1158/1078-0432.CCR-04-1378. PubMed PMID: 15814639.
129. Jawhari AU, Buda A, Jenkins M, Shehzad K, Sarraf C, Noda M, et al. Fascin, an actin-bundling protein, modulates colonic epithelial cell invasiveness and differentiation in vitro. *The American journal of pathology*. 2003;162(1):69-80. doi: 10.1016/S0002-9440(10)63799-6. PubMed PMID: 12507891; PubMed Central PMCID: PMC1851132.

130. Kovacevic Z, Richardson DR. The metastasis suppressor, NdrG-1: a new ally in the fight against cancer. *Carcinogenesis*. 2006;27(12):2355-66. doi: 10.1093/carcin/bgl146. PubMed PMID: 16920733.
131. Kovacevic Z, Fu D, Richardson DR. The iron-regulated metastasis suppressor, NdrG-1: identification of novel molecular targets. *Biochimica et biophysica acta*. 2008;1783(10):1981-92. doi: 10.1016/j.bbamcr.2008.05.016. PubMed PMID: 18582504.
132. Lachat P, Shaw P, Gebhard S, van Belzen N, Chaubert P, Bosman FT. Expression of NDRG1, a differentiation-related gene, in human tissues. *Histochemistry and cell biology*. 2002;118(5):399-408. doi: 10.1007/s00418-002-0460-9. PubMed PMID: 12432451.
133. Bandyopadhyay S, Pai SK, Hirota S, Hosobe S, Takano Y, Saito K, et al. Role of the putative tumor metastasis suppressor gene Drg-1 in breast cancer progression. *Oncogene*. 2004;23(33):5675-81. doi: 10.1038/sj.onc.1207734. PubMed PMID: 15184886.
134. Bandyopadhyay S, Pai SK, Hirota S, Hosobe S, Tsukada T, Miura K, et al. PTEN up-regulates the tumor metastasis suppressor gene Drg-1 in prostate and breast cancer. *Cancer research*. 2004;64(21):7655-60. doi: 10.1158/0008-5472.CAN-04-1623. PubMed PMID: 15520163.
135. Guan RJ, Ford HL, Fu Y, Li Y, Shaw LM, Pardee AB. Drg-1 as a differentiation-related, putative metastatic suppressor gene in human colon cancer. *Cancer research*. 2000;60(3):749-55. PubMed PMID: 10676663.
136. Maruyama Y, Ono M, Kawahara A, Yokoyama T, Basaki Y, Kage M, et al. Tumor growth suppression in pancreatic cancer by a putative metastasis suppressor gene Cap43/NDRG1/Drg-1 through modulation of angiogenesis. *Cancer research*. 2006;66(12):6233-42. doi: 10.1158/0008-5472.CAN-06-0183. PubMed PMID: 16778198.

137. Lee JC, Chung LC, Chen YJ, Feng TH, Juang HH. N-myc downstream-regulated gene 1 downregulates cell proliferation, invasiveness, and tumorigenesis in human oral squamous cell carcinoma. *Cancer letters*. 2014;355(2):242-52. doi: 10.1016/j.canlet.2014.08.035. PubMed PMID: 25218595.
138. Fotovati A, Abu-Ali S, Kage M, Shirouzu K, Yamana H, Kuwano M. N-myc downstream-regulated gene 1 (NDRG1) a differentiation marker of human breast cancer. *Pathology oncology research : POR*. 2011;17(3):525-33. doi: 10.1007/s12253-010-9342-y. PubMed PMID: 21221878.
139. Sun J, Zhang D, Zheng Y, Zhao Q, Zheng M, Kovacevic Z, et al. Targeting the metastasis suppressor, NDRG1, using novel iron chelators: regulation of stress fiber-mediated tumor cell migration via modulation of the ROCK1/pMLC2 signaling pathway. *Molecular pharmacology*. 2013;83(2):454-69. doi: 10.1124/mol.112.083097. PubMed PMID: 23188716.
140. Kovacevic Z, Sivagurunathan S, Mangs H, Chikhani S, Zhang D, Richardson DR. The metastasis suppressor, N-myc downstream regulated gene 1 (NDRG1), upregulates p21 via p53-independent mechanisms. *Carcinogenesis*. 2011;32(5):732-40. doi: 10.1093/carcin/bgr046. PubMed PMID: 21398495.
141. Liu YL, Bai WT, Luo W, Zhang DX, Yan Y, Xu ZK, et al. Downregulation of NDRG1 promotes invasion of human gastric cancer AGS cells through MMP-2. *Tumour biology : the journal of the International Society for Oncodevelopmental Biology and Medicine*. 2011;32(1):99-105. doi: 10.1007/s13277-010-0103-z. PubMed PMID: 21052891.
142. Chang X, Xu X, Xue X, Ma J, Li Z, Deng P, et al. NDRG1 Controls Gastric Cancer Migration and Invasion through Regulating MMP-9. *Pathology oncology research : POR*. 2016;22(4):789-96. doi: 10.1007/s12253-016-0071-8. PubMed PMID: 27154576.

143. Sharma A, Mendonca J, Ying J, Kim HS, Verdone JE, Zarif JC, et al. The prostate metastasis suppressor gene NDRG1 differentially regulates cell motility and invasion. *Molecular oncology*. 2017;11(6):655-69. doi: 10.1002/1878-0261.12059. PubMed PMID: 28371345.
144. Ma J, Gao Q, Zeng S, Shen H. Knockdown of NDRG1 promote epithelial-mesenchymal transition of colorectal cancer via NF-kappaB signaling. *Journal of surgical oncology*. 2016;114(4):520-7. doi: 10.1002/jso.24348. PubMed PMID: 27338835.
145. Wang Y, Zhou Y, Tao F, Chai S, Xu X, Yang Y, et al. N-myc downstream regulated gene 1(NDRG1) promotes the stem-like properties of lung cancer cells through stabilized c-Myc. *Cancer letters*. 2017;401:53-62. doi: 10.1016/j.canlet.2017.04.031. PubMed PMID: 28456659.
146. Yang X, Zhu F, Yu C, Lu J, Zhang L, Lv Y, et al. N-myc downstream-regulated gene 1 promotes oxaliplatin-triggered apoptosis in colorectal cancer cells via enhancing the ubiquitination of Bcl-2. *Oncotarget*. 2017. doi: 10.18632/oncotarget.17711. PubMed PMID: 28537875.
147. Tatake RJ, Rajaram N, Damle RN, Balsara B, Bhisey AN, Gangal SG. Establishment and characterization of four new squamous cell carcinoma cell lines derived from oral tumors. *Journal of cancer research and clinical oncology*. 1990;116(2):179-86. PubMed PMID: 1691185.
148. Peterson GL. A simplification of the protein assay method of Lowry et al. which is more generally applicable. *Analytical biochemistry*. 1977;83(2):346-56. PubMed PMID: 603028.
149. Laemmli UK. Cleavage of structural proteins during the assembly of the head of bacteriophage T4. *Nature*. 1970;227(5259):680-5. PubMed PMID: 5432063.
150. Towbin H, Staehelin T, Gordon J. Electrophoretic transfer of proteins from polyacrylamide gels to nitrocellulose sheets: procedure and some applications. *Proceedings of*

the National Academy of Sciences of the United States of America. 1979;76(9):4350-4. PubMed PMID: 388439; PubMed Central PMCID: PMC411572.

151. Srikanth B, Vaidya MM, Kalraiya RD. O-GlcNAcylation determines the solubility, filament organization, and stability of keratins 8 and 18. *The Journal of biological chemistry*. 2010;285(44):34062-71. doi: 10.1074/jbc.M109.098996. PubMed PMID: 20729549; PubMed Central PMCID: PMC2962505.

152. Chaudhari PR, Charles SE, Vaidya MM. Role of BPAG1e in neoplastic progression of oral squamous cell carcinoma derived cells. *Int J Pharm Bio Sci*. 2017;8(1):519-27.

153. Mosmann T. Rapid colorimetric assay for cellular growth and survival: application to proliferation and cytotoxicity assays. *Journal of immunological methods*. 1983;65(1-2):55-63. PubMed PMID: 6606682.

154. Jensen MM, Jorgensen JT, Binderup T, Kjaer A. Tumor volume in subcutaneous mouse xenografts measured by microCT is more accurate and reproducible than determined by 18F-FDG-microPET or external caliper. *BMC medical imaging*. 2008;8:16. doi: 10.1186/1471-2342-8-16. PubMed PMID: 18925932; PubMed Central PMCID: PMC2575188.

155. Ranjan A, Bane SM, Kalraiya RD. Glycosylation of the laminin receptor (alpha3beta1) regulates its association with tetraspanin CD151: Impact on cell spreading, motility, degradation and invasion of basement membrane by tumor cells. *Experimental cell research*. 2014;322(2):249-64. doi: 10.1016/j.yexcr.2014.02.004. PubMed PMID: 24530578.

156. Korwar AM, Vannuruswamy G, Jagadeeshaprasad MG, Jayaramaiah RH, Bhat S, Regin BS, et al. Development of Diagnostic Fragment Ion Library for Glycated Peptides of Human Serum Albumin: Targeted Quantification in Prediabetic, Diabetic, and Microalbuminuria Plasma by Parallel Reaction Monitoring, SWATH, and MSE. *Molecular & cellular proteomics : MCP*.

2015;14(8):2150-9. doi: 10.1074/mcp.M115.050518. PubMed PMID: 26023067; PubMed Central PMCID: PMC4528244.

157. Ranganathan K, Kavitha R, Sawant SS, Vaidya MM. Cytokeratin expression in oral submucous fibrosis--an immunohistochemical study. *Journal of oral pathology & medicine* : official publication of the International Association of Oral Pathologists and the American Academy of Oral Pathology. 2006;35(1):25-32. doi: 10.1111/j.1600-0714.2005.00366.x. PubMed PMID: 16393250.

158. Mogilner A, Oster G. Cell motility driven by actin polymerization. *Biophysical journal*. 1996;71(6):3030-45. doi: 10.1016/S0006-3495(96)79496-1. PubMed PMID: 8968574; PubMed Central PMCID: PMC1233792.

159. Nobes CD, Hall A. Rho, rac, and cdc42 GTPases regulate the assembly of multimolecular focal complexes associated with actin stress fibers, lamellipodia, and filopodia. *Cell*. 1995;81(1):53-62. PubMed PMID: 7536630.

160. Takenawa T, Suetsugu S. The WASP-WAVE protein network: connecting the membrane to the cytoskeleton. *Nature reviews Molecular cell biology*. 2007;8(1):37-48. doi: 10.1038/nrm2069. PubMed PMID: 17183359.

161. Liotta LA, Tryggvason K, Garbisa S, Hart I, Foltz CM, Shafie S. Metastatic potential correlates with enzymatic degradation of basement membrane collagen. *Nature*. 1980;284(5751):67-8. PubMed PMID: 6243750.

162. de Vicente JC, Fresno MF, Villalain L, Vega JA, Hernandez Vallejo G. Expression and clinical significance of matrix metalloproteinase-2 and matrix metalloproteinase-9 in oral squamous cell carcinoma. *Oral oncology*. 2005;41(3):283-93. doi: 10.1016/j.oraloncology.2004.08.013. PubMed PMID: 15743691.

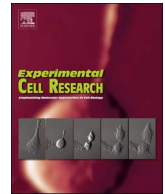
163. Uematsu J, Nishizawa Y, Sonnenberg A, Owaribe K. Demonstration of type II hemidesmosomes in a mammary gland epithelial cell line, BMGE-H. *Journal of biochemistry*. 1994;115(3):469-76. PubMed PMID: 8056759.
164. Tapon N, Hall A. Rho, Rac and Cdc42 GTPases regulate the organization of the actin cytoskeleton. *Current opinion in cell biology*. 1997;9(1):86-92. PubMed PMID: 9013670.
165. Dominguez R, Holmes KC. Actin structure and function. *Annual review of biophysics*. 2011;40:169-86. doi: 10.1146/annurev-biophys-042910-155359. PubMed PMID: 21314430; PubMed Central PMCID: PMC3130349.
166. Friedl P, Wolf K. Tumour-cell invasion and migration: diversity and escape mechanisms. *Nature reviews Cancer*. 2003;3(5):362-74. doi: 10.1038/nrc1075. PubMed PMID: 12724734.
167. Ellen TP, Ke Q, Zhang P, Costa M. NDRG1, a growth and cancer related gene: regulation of gene expression and function in normal and disease states. *Carcinogenesis*. 2008;29(1):2-8. doi: 10.1093/carcin/bgm200. PubMed PMID: 17916902.

## Annexure 1

| Peak Name              | Group (protein)  | p-value | Fold Change        |               |
|------------------------|--|---------|--------------------|---------------|
| sp Q9NTJ3 SMC4_HUMAN   | Structural maintenance of chromosomes protein 4<br>OS=Homo sapiens GN=SMC4 PE=1 SV=2     | 0.05565 | <b>6.170905268</b> | UPREGULATED   |
| sp Q14257 RCN2_HUMAN   | Reticulocalbin-2 OS=Homo sapiens GN=RCN2 PE=1 SV=1                                       | 0.0223  | <b>3.307041249</b> |               |
| sp P55265 DSRAD_HUMAN  | Double-stranded RNA-specific adenosine deaminase<br>OS=Homo sapiens GN=ADAR PE=1 SV=4    | 0.01139 | <b>2.770648721</b> |               |
| sp P08670 VIME_HUMAN   | Vimentin OS=Homo sapiens GN=VIM PE=1 SV=4  | 0.00035 | <b>2.613678335</b> |               |
| sp P11766 ADHX_HUMAN   | Alcohol dehydrogenase class-3 OS=Homo sapiens<br>GN=ADH5 PE=1 SV=4                       | 0.05638 | <b>2.25203012</b>  |               |
| sp Q9UHB6 LIM A1_HUMAN | LIM domain and actin-binding protein 1 OS=Homo sapiens<br>GN=LIMA1 PE=1 SV=1             | 0.00276 | <b>2.228723621</b> |               |
| sp Q92597 NDRG1_HUMAN  | Protein NDRG1 OS=Homo sapiens GN=NDRG1<br>PE=1 SV=1                                      | 0.00582 | <b>1.841330543</b> |               |
| sp P05787 K2C8_HUMAN   | Keratin, type II cytoskeletal 8 OS=Homo sapiens<br>GN=KRT8 PE=1 SV=7                     | 0.00209 | <b>1.789723558</b> |               |
| sp P22626 ROA2_HUMAN   | Heterogeneous nuclear ribonucleoproteins A2/B1<br>OS=Homo sapiens GN=HNRNPA2B1 PE=1 SV=2 | 0.01378 | <b>1.745255056</b> |               |
| sp P09382 LEG1_HUMAN   | Galectin-1 OS=Homo sapiens GN=LGALS1 PE=1<br>SV=2  | 0.00457 | <b>1.640273242</b> |               |
| sp P16144 ITB4_HUMAN   | Integrin beta-4 OS=Homo sapiens GN=ITGB4 PE=1<br>SV=5                                    | 0.02166 | <b>1.525829182</b> |               |
| sp P62942 FKBP1A_HUMAN | Peptidyl-prolyl cis-trans isomerase FKBP1A<br>OS=Homo sapiens GN=FKBP1A PE=1 SV=2        | 0.00121 | <b>1.504845202</b> |               |
| sp Q15637-5 SF01_HUMAN | Isoform 5 of Splicing factor 1 OS=Homo sapiens<br>GN=SF1                                 | 0.01546 | <b>1.449125651</b> |               |
| sp P00338 LDHA_HUMAN   | L-lactate dehydrogenase A chain OS=Homo sapiens<br>GN=LDHA PE=1 SV=2                     | 0.00457 | <b>1.420341429</b> |               |
| sp Q15717 ELAV1_HUMAN  | ELAV-like protein 1 OS=Homo sapiens<br>GN=ELAVL1 PE=1 SV=2                               | 0.0045  | <b>1.372417714</b> |               |
| sp P22234 PUR6_HUMAN   | Multifunctional protein ADE2 OS=Homo sapiens<br>GN=PAICS PE=1 SV=3                       | 0.03914 | <b>1.344477503</b> |               |
| sp P28074 PSB5_HUMAN   | Proteasome subunit beta type-5 OS=Homo sapiens<br>GN=PSMB5 PE=1 SV=3                     | 0.01721 | <b>1.323659029</b> |               |
| sp P38117 ETFB_HUMAN   | Electron transfer flavoprotein subunit beta OS=Homo sapiens<br>GN=ETFB PE=1 SV=3         | 0.02579 | <b>0.74862264</b>  | DOWNREGULATED |
| sp P33316 DUT_HUMAN    | Deoxyuridine 5'-triphosphate nucleotidohydrolase<br>OS=Homo sapiens GN=DUT PE=1 SV=4     | 0.00739 | <b>0.748314322</b> |               |
| sp P62979 RS27A_HUMAN  | Ubiquitin-40S ribosomal protein S27a OS=Homo sapiens<br>GN=RPS27A PE=1 SV=2              | 0.01624 | <b>0.740823223</b> |               |
| sp P62258 1433E_HUMAN  | 14-3-3 protein epsilon OS=Homo sapiens<br>GN=YWHAE PE=1 SV=1                             | 0.00831 | <b>0.730636493</b> |               |
| sp P26641 EF1G_HUMAN   | Elongation factor 1-gamma OS=Homo sapiens<br>GN=EEF1G PE=1 SV=3                          | 0.0346  | <b>0.726886582</b> |               |
| sp O94788 AL1A2_HUMAN  | Retinal dehydrogenase 2 OS=Homo sapiens<br>GN=ALDH1A2 PE=1 SV=3                          | 0.05173 | <b>0.702585449</b> |               |
| sp Q99879 H2B1M_HUMAN  | Histone H2B type 1-M OS=Homo sapiens<br>GN=HIST1H2BM PE=1 SV=3                           | 0.00579 | <b>0.689966445</b> |               |
| sp P31947 1433S_HUMAN  | 14-3-3 protein sigma OS=Homo sapiens GN=SFN  | 0.03438 | <b>0.677922541</b> |               |

|                       |   |         |                    |  |
|-----------------------|---|---------|--------------------|--|
| HUMAN                 | PE=1 SV=1   |         |                    | <b>P<br/>R<br/>O<br/>T<br/>E<br/>I<br/>N<br/>S</b> |
| sp P12956 XRCC6_HUMAN | X-ray repair cross-complementing protein 6<br>OS=Homo sapiens GN=XRCC6 PE=1 SV=2            | 0.05228 | <b>0.659947387</b> |  |
| sp Q8NC51 PAIRB_HUMAN | Plasminogen activator inhibitor 1 RNA-binding protein OS=Homo sapiens GN=SERBP1 PE=1 SV=2   | 0.01442 | <b>0.647919271</b> |  |
| sp P49915 GUAA_HUMAN  | GMP synthase [glutamine-hydrolyzing] OS=Homo sapiens GN=GMPS PE=1 SV=1                      | 0.04231 | <b>0.645900873</b> |  |
| sp P07900 HS90A_HUMAN | Heat shock protein HSP 90-alpha OS=Homo sapiens GN=HSP90AA1 PE=1 SV=5                       | 0.00705 | <b>0.641768247</b> |  |
| sp P34897 GLYM_HUMAN  | Serine hydroxymethyltransferase, mitochondrial OS=Homo sapiens GN=SHMT2 PE=1 SV=3           | 0.00252 | <b>0.63674622</b>  |  |
| sp P62854 RS26_HUMAN  | 40S ribosomal protein S26 OS=Homo sapiens GN=RPS26 PE=1 SV=3                                | 0.0138  | <b>0.621695312</b> |  |
| sp P06703 S10A6_HUMAN | Protein S100-A6 OS=Homo sapiens GN=S100A6 PE=1 SV=1   | 0.00363 | <b>0.609075387</b> |  |
| sp Q9P2E9 RRBP1_HUMAN | Ribosome-binding protein 1 OS=Homo sapiens GN=RRBP1 PE=1 SV=4                               | 0.0263  | <b>0.559279843</b> |  |
| sp P49327 FAS_HUMAN   | Fatty acid synthase OS=Homo sapiens GN=FASN PE=1 SV=3                                       | 0.00432 | <b>0.536297719</b> |  |
| sp Q13509 TBB3_HUMAN  | Tubulin beta-3 chain OS=Homo sapiens GN=TUBB3 PE=1 SV=2                                     | 0.00527 | <b>0.522026556</b> |  |
| sp P08195 4F2_HUMAN   | 4F2 cell-surface antigen heavy chain OS=Homo sapiens GN=SLC3A2 PE=1 SV=3                    | 0.00431 | <b>0.517087719</b> |  |
| sp P13797 PLST_HUMAN  | Plastin-3 OS=Homo sapiens GN=PLS3 PE=1 SV=4   | 0.0471  | <b>0.516612252</b> |  |
| sp Q01650 LAT1_HUMAN  | Large neutral amino acids transporter small subunit 1 OS=Homo sapiens GN=SLC7A5 PE=1 SV=2   | 0.01131 | <b>0.492640547</b> |  |
| sp P06454 PTMA_HUMAN  | Prothymosin alpha OS=Homo sapiens GN=PTMA PE=1 SV=2   | 0.0508  | <b>0.442629118</b> |  |
| sp P62820 RAB1A_HUMAN | Ras-related protein Rab-1A OS=Homo sapiens GN=RAB1A PE=1 SV=3                               | 0.03868 | <b>0.418468779</b> |  |
| sp P15559 NQO1_HUMAN  | NAD(P)H dehydrogenase [quinone] 1 OS=Homo sapiens GN=NQO1 PE=1 SV=1                         | 0.00031 | <b>0.397239962</b> |  |
| sp Q96C86 DCPS_HUMAN  | m7GpppX diphosphatase OS=Homo sapiens GN=DCPS PE=1 SV=2                                     | 0.03626 | <b>0.371471343</b> |  |
| sp Q9H1E3 NUCKS_HUMAN | Nuclear ubiquitous casein and cyclin-dependent kinase substrate 1 OS=Homo sapiens PE=1 SV=1 | 0.00999 | <b>0.343781783</b> |  |
| sp P05362 ICAM1_HUMAN | Intercellular adhesion molecule 1 OS=Homo sapiens GN=ICAM1 PE=1 SV=2                        | 0.00594 | <b>0.337035605</b> |  |
| sp P67936 TPM4_HUMAN  | Tropomyosin alpha-4 chain OS=Homo sapiens GN=TPM4 PE=1 SV=3                                 | 0.02601 | <b>0.33496533</b>  |  |

### SWATH analysis data



# Hemidesmosomal linker proteins regulate cell motility, invasion and tumorigenicity in oral squamous cell carcinoma derived cells



Pratik Rajeev Chaudhari<sup>a,b</sup>, Sylvania Emlit Charles<sup>a</sup>, Zinia Charlotte D'Souza<sup>a</sup>,  
Milind Murlidhar Vaidya<sup>a,b,\*</sup>

<sup>a</sup> Advanced Centre for Treatment, Research and Education in Cancer (ACTREC), Tata Memorial Centre (TMC), Kharghar, Navi Mumbai 410210, India

<sup>b</sup> Homi Bhabha National Institute, Training School Complex, Anushakti Nagar, Mumbai 400085, India

## ARTICLE INFO

### Keywords:

BPAG1e  
Plectin  
NDRG1  
Cell motility  
Cell invasion  
Oral squamous cell carcinoma

## ABSTRACT

BPAG1e and Plectin are hemidesmosomal linker proteins which anchor intermediate filament proteins to the cell surface through  $\beta 4$  integrin. Recent reports indicate that these proteins play a role in various cellular processes apart from their known anchoring function. However, the available literature is inconsistent. Further, the previous study from our laboratory suggested that Keratin8/18 pair promotes cell motility and tumor progression by deregulating  $\beta 4$  integrin signaling in oral squamous cell carcinoma (OSCC) derived cells. Based on these findings, we hypothesized that linker proteins may have a role in neoplastic progression of OSCC. Downregulation of hemidesmosomal linker proteins in OSCC derived cells resulted in reduced cell migration accompanied by alterations in actin organization. Further, decreased MMP9 activity led to reduced cell invasion in linker proteins knockdown cells. Moreover, loss of these proteins resulted in reduced tumorigenic potential. SWATH analysis demonstrated upregulation of N-Myc downstream regulated gene 1 (NDRG1) in linker proteins downregulated cells as compared to vector control cells. Further, the defects in phenotype upon linker proteins ablation were rescued upon loss of NDRG1 in linker proteins knockdown background. These data together indicate that hemidesmosomal linker proteins regulate cell motility, invasion and tumorigenicity possibly through NDRG1 in OSCC derived cells.

## 1. Introduction

Hemidesmosomes (HDs) are located at the basal side of epithelial cells where they link the extracellular matrix (ECM) to the intermediate filament (IF) network in the cell. The complex epithelia like skin assemble type I HDs, which consist of the  $\alpha 6\beta 4$  integrin, plectin, CD151, bullous pemphigoid antigens BPAG1e (BP230) and BPAG2 (BP180).  $\alpha 6\beta 4$  integrin connects the cells to laminin-5 of the basement membrane, whereas plectin and BPAG1e connect the keratin filaments to hemidesmosomal junction through  $\alpha 6\beta 4$  integrin [1,2].

BPAG1e and Plectin belong to the plakin family of cytoskeletal linker proteins. Ablation of HD linker proteins in mouse keratinocytes results in the formation of blisters [3,4]. This illustrates the importance of plakins in regulating dermal-epidermal adhesion. Further, these proteins have a functional role in various cellular processes apart from their known anchoring function [5–8]. BPAG1e null animals display impaired wound healing *in vivo*, indicating that BPAG1e possibly acts as a potential regulator of keratinocyte migration [4]. Upregulation of

BPAG1e expression has been reported in squamous cell carcinomas [9]. Furthermore, BPAG1e regulates keratinocyte migration by acting as a scaffold for  $\beta 4$  integrin mediated signaling to Rac1 [5]. Recently, we have shown that BPAG1e positively regulates cell motility of OSCC derived cells [10]. Contrary to this, human keratinocytes carrying homozygous nonsense mutations in BPAG1e encoding gene displayed reduced adhesion but increased spreading and migration [8]. The other linker protein, Plectin, promotes the migration and invasion of head and neck squamous cell carcinoma (HNSCC) cells through activation of Erk 1/2 [11]. It has been also reported that plectin regulates invasiveness in colon carcinoma cells and is targeted to podosomes [6]. On the other hand, loss of plectin in liver cancer cells promotes cell motility [12,13]. These reports together suggest that the role of HD linker proteins in cell motility is context dependent. Overall, the available information regarding molecular mechanisms underlying BPAG1e and Plectin associated phenotype in cancer is inconsistent.

Keratins (K) are the largest subgroup of intermediate filament proteins expressed in a tissue specific and differentiation dependent

**Abbreviations:** HD, hemidesmosome; OSCC, oral squamous cell carcinoma; NDRG1, N-myc downstream regulated gene 1; SWATH, sequential window acquisition of all theoretical fragment ion spectra; Ex/Em, extension/emission; ns, non significant

\* Corresponding author at: Advanced Centre for Treatment, Research and Education in Cancer (ACTREC), Tata Memorial Centre (TMC), Kharghar, Navi Mumbai 410210, India.

E-mail address: [mvaitya@actrec.gov.in](mailto:mvaitya@actrec.gov.in) (M.M. Vaidya).

<http://dx.doi.org/10.1016/j.yexcr.2017.08.034>

Received 1 June 2017; Received in revised form 29 July 2017; Accepted 24 August 2017

Available online 01 September 2017

0014-4827/ © 2017 Elsevier Inc. All rights reserved.

manner [14]. Aberrant expression of keratin8/18 (K8/18) pair has been consistently shown in OSCC [15–17]. Subsequent work from our laboratory revealed that knockdown of K8 in OSCC derived cell line (AW13516) resulted in alterations in  $\alpha 6\beta 4$  integrin levels and its mediated signaling, actin reorganization, reduction in cell motility, invasion, tumorigenicity and cell motility associated protein fascin [18].

As HD linker proteins anchor keratins to the cell surface via  $\beta 4$  integrin, we hypothesized that these linker proteins may have a role in regulating cell motility and neoplastic progression of OSCC. In the present communication, we show that the HD linker proteins play a role in regulating cell motility, invasion, tumorigenicity and actin organization in OSCC derived cells possibly through NDRG1.

## 2. Materials and methods

### 2.1. Antibodies, qRT-PCR primers and shRNA sequences

List of antibodies, qRT-PCR primers and shRNA sequences have been given in the [Supplementary File 1 \(table 1–3\)](#).

### 2.2. Cell lines and plasmids

The human tongue SCC derived cell lines AW13516 and AW8507 were previously established at Cancer Research Institute (CRI), Mumbai, India [19]. These cell lines were cultured in Iscove's Modified Dulbecco's Medium (IMDM) supplemented with 10% fetal bovine serum (FBS) and antibiotics under 5% CO<sub>2</sub> atmosphere at 37 °C. HEK 293FT cells, used for lentivirus production, were cultured in Dulbecco's Modified Eagle's Medium (DMEM) supplemented with 10% FBS and antibiotics under 5% CO<sub>2</sub> atmosphere at 37 °C.

The pLKO1.puro (plasmid #10878), pLKO1.neo (plasmid #13425) and pLKO1.hydro (plasmid #24150) plasmids were purchased from Addgene, USA. The pLKO1.puro plasmid containing shRNA sequence against BPAG1e was a kind gift from Dr. Jonathan Jones, Washington State University, USA. shRNA sequences against Plectin and NDRG1 were designed and cloned in pLKO1.neo and pLKO1.hydro plasmids respectively. BPAG1e-Plectin double knockdown was generated by transducing lentivirus encoding shRNA against BPAG1e in Plectin knockdown cells. The empty vector backbone was used to generate the respective vector control clones.

### 2.3. Lentivirus production and lentiviral mediated transduction

HEK 293FT cells were cultured till 50% confluency in DMEM complete medium. Co-transfection of lentiviral transfer and packaging vectors was performed by calcium phosphate precipitation method. The lentiviral transfer vector (6  $\mu$ g), packaging plasmid psPAX2 (4.5  $\mu$ g) and envelope plasmid pMD2.G (1.5  $\mu$ g) were diluted to 250  $\mu$ l of sterile distilled water. An equal volume of 0.5 M CaCl<sub>2</sub> was then added followed by dropwise addition of 500  $\mu$ l of BES Buffered Saline (BBS). The mixture was incubated at room temperature (RT) for 20 min and then added to the culture dishes. After 16 h of incubation, the medium was replaced with fresh complete DMEM. After 48–60 h of transfection, viral supernatant was collected and centrifuged for 10 min at 2000 rpm at 4 °C to remove traces of HEK 293FT cells. The supernatant was collected and stored at –80 °C or used for transduction. For transduction, the viral supernatant along with polybrene (8  $\mu$ g/ml) was added to 50% confluent OSCC derived cells. After 24 h, the supernatant was replaced with complete media. Further, the stable clones were selected in puromycin (0.5  $\mu$ g/ml) or G418 (500  $\mu$ g/ml) or hygromycin (30  $\mu$ g/ml).

### 2.4. Quantitative real time-polymerase chain reaction (qRT-PCR)

RNA was isolated with the TRI reagent (Sigma, USA) and cDNA was prepared using Revert Aid First Strand cDNA synthesis Kit (Thermo

Scientific, USA) according to the manufacturer's protocol. SYBR green based qRT-PCR was performed on the ABI 7900HT Fast Real Time PCR System (Applied Biosystems, Foster, CA, USA) as described previously [20]. qRT-PCR analysis was carried out to determine the BPAG1e, Plectin and NDRG1 levels in HD linker proteins knockdown and vector control cells. 10 ng of cDNA was used to perform qRT-PCR analysis using gene specific primers for BPAG1e, Plectin and NDRG1 ([Supplementary File 1, table 3](#)). The relative gene expression was quantified by comparative Ct method using Glyceraldehyde 3-phosphate dehydrogenase (GAPDH) as the loading control.

### 2.5. Western blotting

Western blotting was performed as described earlier [21]. Whole cell lysates were prepared in SDS lysis buffer (2% SDS, 50 mM Tris-HCl; pH 6.8, 0.1%  $\beta$ -mercaptoethanol and 10% glycerol). A protease inhibitor cocktail (Calbiochem, San Diego, USA) was added to lysis buffer. An equal amount of protein was loaded and resolved on SDS-PAGE gels followed by Western blotting. The signals were detected using WesternBright™ ECL western blotting detection kit (Advanta, USA) according to the manufacturer's protocol.

### 2.6. Immunofluorescence

For immunofluorescence, cells were grown on coverslips for 48 h and treated with 0.03% Triton X-100 in chilled methanol for 90 s. Permeabilized cells were then fixed in chilled methanol for 5 min at –20 °C. Further, the procedure followed is as described previously [21]. All confocal images were acquired using Zeiss LSM 780 microscope (Magnification: 63x, Numerical Aperture: 1.4).

### 2.7. Actin organization

The wounds were scratched in confluent cells with the help of a sterile 2  $\mu$ l pipette tip. The cells surrounding the scratch were allowed to migrate into the wounded region for 8 h. Subsequently, the cells were fixed using 4% Paraformaldehyde. Further, the cells were subjected to Phalloidin (Sigma, USA) staining for 1 h and actin organization was visualized at wound front under Zeiss LSM 780 microscope [10].

### 2.8. Phenotypic assays for cell transformation

#### 2.8.1. In vitro wound healing assay for migration

Wound healing assay was performed as described previously [10]. Briefly, the cells were grown up to 95% confluency. Cells were replaced with fresh IMDM with 0.2% FBS for 24 h. After incubation, the medium was discarded and wounds were scratched with the help of a sterile 2  $\mu$ l pipette tip. The cells were fed with fresh IMDM containing 0.2% FBS and observed under an Axiovert 200 M Inverted Carl Zeiss microscope fitted with a stage maintained at 37 °C and 5% CO<sub>2</sub> atmosphere. Cells were observed by time lapse microscopy and the images were taken every 20 min for 20 h using an AxioCam MRm camera with phase 1 objective. The rate of migration was measured using the manual tracking plugin of ImageJ (NIH) software.

#### 2.8.2. Transwell migration assay and boyden chamber cell invasion assay

The transwell migration assay was performed as described previously with some modifications [20]. In brief, 2  $\times$  10<sup>5</sup> cells were seeded in the upper chamber in serum-free medium and the bottom chamber was filled with 0.6 ml of complete IMDM. The cells were incubated for 16 h at 37 °C. At the 15th hour, 4  $\mu$ g/ml Calcein AM (Life technologies, USA) was added to the lower chamber and incubated for 1 h at 37 °C. The cells on the upper surface were carefully removed with a cotton swab at the 16th hour. Fluorescence of the invaded cells was read at wavelengths of 488/535 nm (Ex/Em) on a bottom-reading

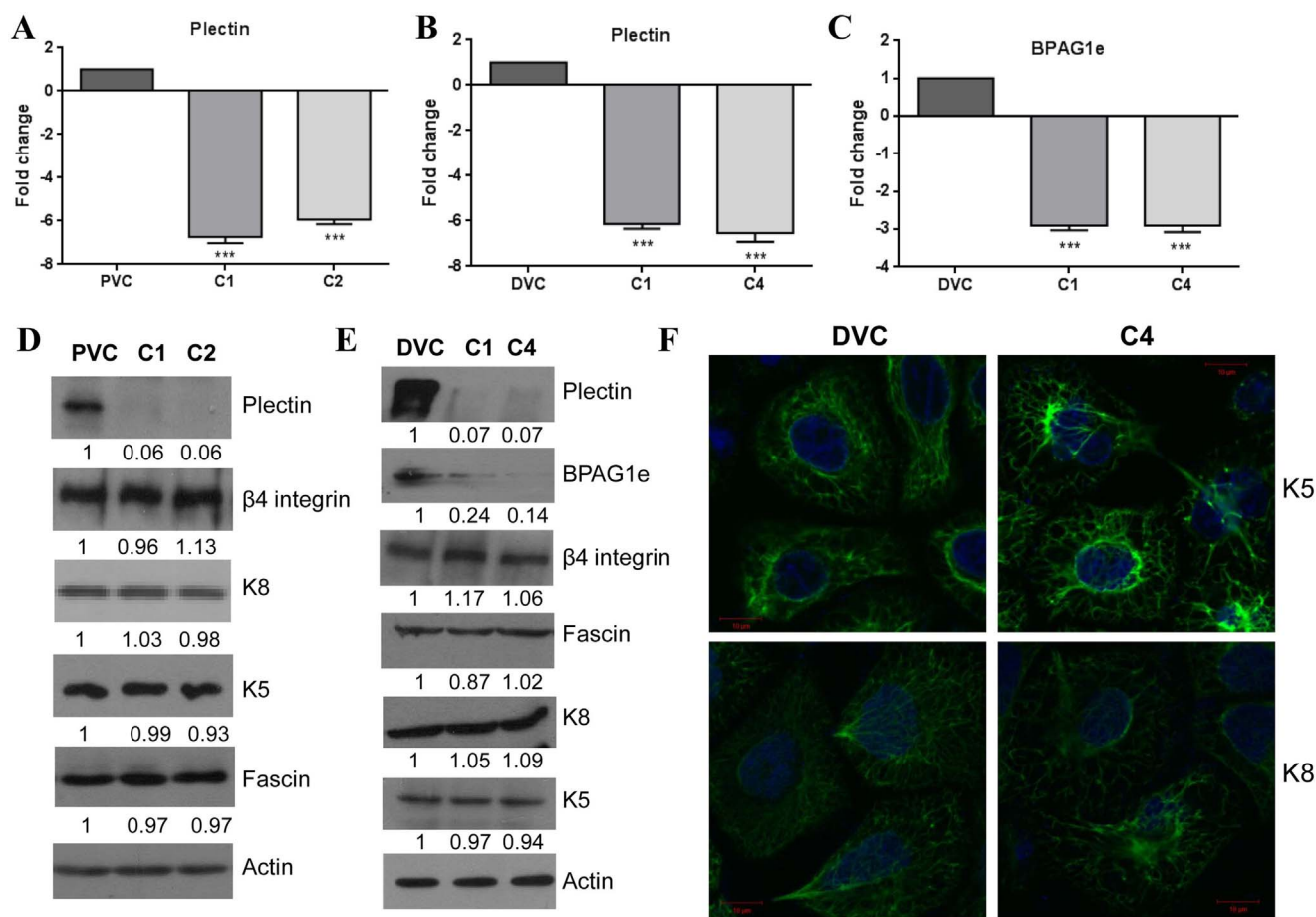


**Fig. 1.** Loss of hemidesmosomal linker proteins does not affect expression of associated proteins. (A) qRT-PCR of Plectin and (D) western blot analysis of Plectin,  $\beta 4$  integrin, Fascin, K8 and K5 in vector control clone (PVC) and Plectin knockdown clones (C1, C2). (B, C) qRT-PCR of BPAG1e, Plectin and (E) western blot analysis of BPAG1e, Plectin,  $\beta 4$  integrin, Fascin, K8 and K5 in vector control clone (DVC) and BPAG1e-Plectin knockdown clones (C1, C4) (F) Immunofluorescence analysis showing K5 and K8 filament organization (stained in green) in vector control clone (DVC) and BPAG1e-Plectin knockdown clone (C4). The nucleus is stained with DAPI. Note: the numbers below the blot indicate relative intensity of the bands using densitometric analysis.

fluorescent plate reader (Berthold, Germany). The boyden chamber invasion assay was performed similar to transwell migration assay [10]. Additionally, 8  $\mu$ m pore sized polycarbonate membrane filters in upper chamber were coated with 40  $\mu$ l Matrigel (1 mg/ml) with 140  $\mu$ l incomplete IMDM.

### 2.8.3. Soft agar colony forming assay

The soft agar colony forming assay was performed as described by Chaudhari et al. [10]. As a first step, 1 ml of the basal layer was made by adding equal volumes of 2X complete IMDM and 2% low melting agarose. 1000 cells in complete medium containing 0.4% low melting agarose were seeded over the basal layer. Plates were fed with complete IMDM on every alternate day and incubated at 37  $^{\circ}$ C in a 5% CO<sub>2</sub> atmosphere for 15 days. Opaque and dense colonies were observed and counted microscopically on day 15.

### 2.8.4. In vivo Tumorigenicity assay

All protocols for animal studies were reviewed and approved by the “Institutional Animal Ethics Committee (IAEC)” constituted under the guidelines of the “Committee for the Purpose of Control and Supervision of Experiments on Animals (CPCSEA)”, Government of India (Approval ID: 04/2015). The tumorigenic potential of cells was determined by subcutaneous injections in NOD-SCID mice as described previously [22]. The cells were suspended in plain IMDM medium without serum and 6  $\times$  10<sup>6</sup> cells were injected subcutaneously in the dorsal flank of 6–8 weeks old mice. 5 mice were injected per clone and were observed for tumor formation over a period of approximately 2

months. Tumor volume was determined using a digital vernier caliper (Advance, India) and volume was calculated by the modified ellipsoidal formula, [Tumor volume = 1/2(length  $\times$  width<sup>2</sup>)].

### 2.8.5. MTT (3-(4, 5-Dimethylthiazol-2-yl) – 2, 5-Diphenyltetrazolium Bromide) cell viability assay

MTT Cell viability assay was performed as explained earlier [10]. 1000 cells were seeded per well in a 96-well microtitre plate. Proliferation was studied every 24 h up to a period of 4 days. At the desired time points, 20  $\mu$ l MTT (5 mg/ml) was added to each well. Plate was incubated at 37  $^{\circ}$ C in a CO<sub>2</sub> incubator for 4 h. Then, 100  $\mu$ l of acidified SDS (10% SDS in 0.01 N HCl) was added to each well and incubated overnight at 37  $^{\circ}$ C in a CO<sub>2</sub> incubator. Next day, the absorbance was measured on an ELISA plate reader at 540 nm against a reference wavelength of 690 nm. Growth curve was plotted from three independent experiments.

### 2.8.6. Colony forming (Clonogenic) assay

The clonogenic assay was carried out as described earlier [23]. Briefly, 200 cells were plated in 60 mm tissue culture plates in triplicates. The cells were grown in complete medium for 10 days, with medium changes every 2–3 days. The cells were first fixed with methanol for 5 min at room temperature (RT) and then washed twice with 1X PBS. They were later stained with crystal violet solution (0.5% crystal violet in 20% methanol) for 5 min at RT. After washes with distilled water, the plates were allowed to dry.

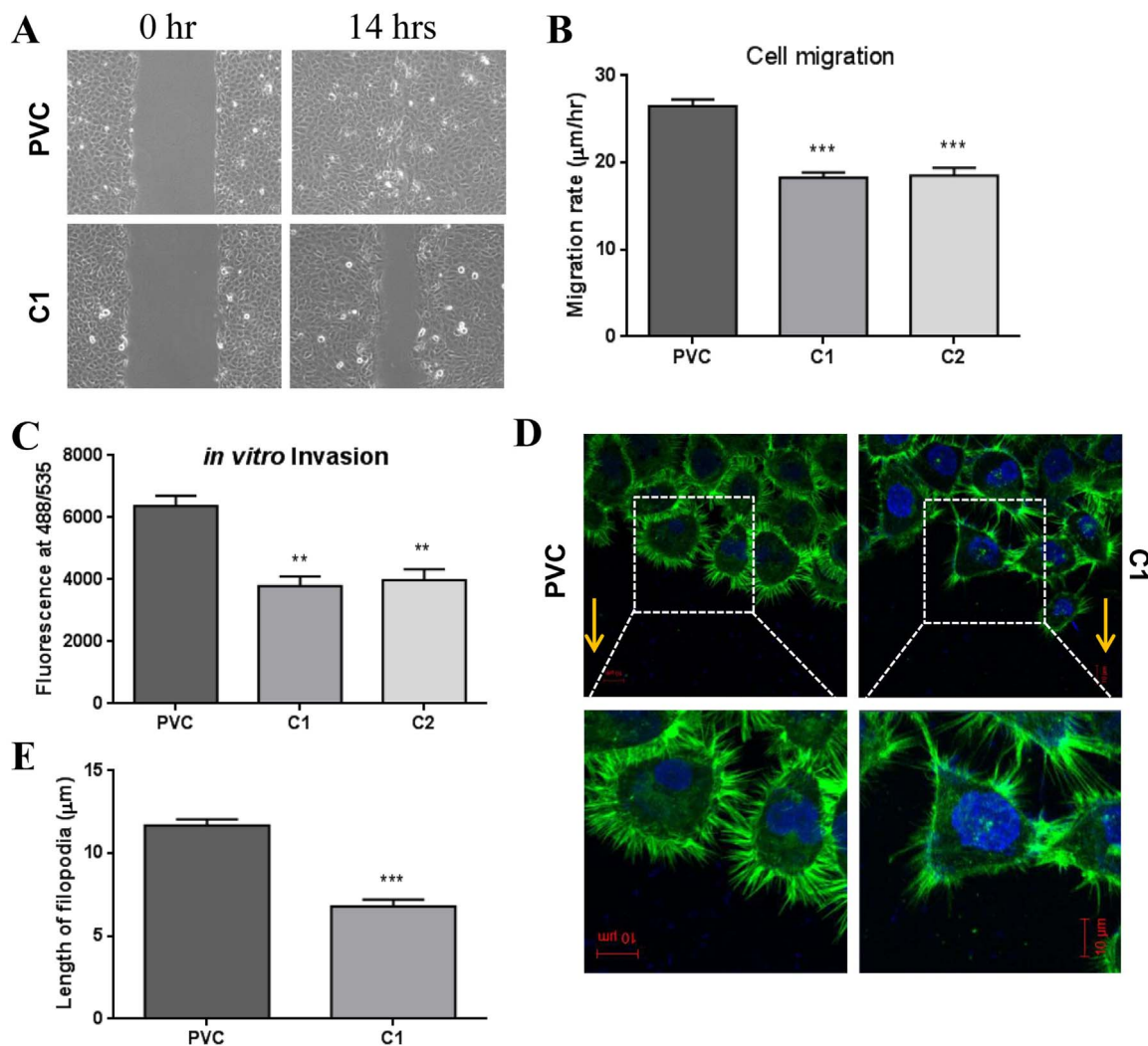


**Fig. 2. Loss of Plectin leads to reduced cell migration, cell invasion and alterations in actin organization.** (A) Representative time lapse microscopy images show wound healing for vector control clone (PVC) and Plectin knockdown clone (C1). (B) The graph shows rate of cell migration for vector control clone (PVC) and Plectin knockdown clones (C1, C2). (C) The graph shows fluorescence of invaded vector control cells (PVC) and Plectin knockdown cells (C1, C2) which is read at wavelengths of 488/535 nm (Ex/Em). (D) Immunofluorescence analysis of actin organization (stained in green) at the wound edge in vector control clone (PVC) and Plectin knockdown clone (C1). The nucleus is stained with DAPI. The arrow indicates direction of migration. The inset shows filopodia formed at migratory front. (E) The graph shows length of filopodia in vector control clone (PVC) and Plectin knockdown clone (C1). For each clone, 30 cells at the wound front were used for quantification. Note: the numbers below the blot indicate relative intensity of the bands using densitometric analysis.

### 2.8.7. Gelatin zymography

To determine the Matrix Metalloproteinase 2 (MMP2) and MMP9 activity in conditioned culture medium, gelatin zymography was carried out as described by Ranjan et al. (2015) with some modifications [24].  $5 \times 10^5$  cells were seeded in 35 mm tissue culture plates containing complete IMDM and grown for 24 h in 5% CO<sub>2</sub> atmosphere at 37 °C. The cells were then washed thrice with 1X PBS and grown in serum free medium for 24 h. After 24 h, culture medium was recovered and centrifuged at 2000 rpm for 5 min at 4 °C. Simultaneously, SDS lysis buffer was added to culture plate containing cells to extract proteins. Then, equal volume of lysates were loaded on SDS PAGE and transferred on PVDF membrane. Subsequently, the blot was probed with antibody against  $\beta$ -actin, which was used as a loading control. The supernatant was dried using refrigerated CentriVap Concentrator, Labconco at 4 °C. After complete drying, pellet was dissolved in non-reducing Laemmli sample buffer (62.5 mM Tris-HCl, pH 6.8, 4% SDS, 20% glycerol, 0.01% bromophenol blue) and applied to 10% SDS-PAGE gels polymerized with 1% gelatin. After electrophoresis, the gels were rinsed three times in a solution containing 2.5% Triton X-100 to eliminate the SDS and to allow reconstitution of the proteins. MMP activity was stimulated by incubating the gels at 37 °C waterbath for at least

16 h in reaction buffer (50 mM Tris-HCl, pH 6.8, 150 mM NaCl, 5 mM CaCl<sub>2</sub> and 0.05% sodium azide). The activity of the MMPs was visualized by staining the gels in Coomassie Brilliant Blue G-250 solution followed by destaining with destaining solution (45% methanol, 45% water and 10% glacial acetic acid).

### 2.9. RhoA/Rac1/Cdc42 activation assay

RhoA, Rac1 and Cdc42 activation assays were performed using RhoA/Rac1/Cdc42 Activation Assay Combo Biochem Kit (BK030, Cytoskeleton Inc, USA) as per manufacturer's instructions. In brief, the cells were treated with 40 ng/ml epidermal growth factor (EGF; Invitrogen, USA) for 10 min to activate Cdc42. Similarly, the cells were treated with 10 ng/ml EGF for 4 min and 100 µg/ml Calpeptin (Calbiochem, USA) for 10 min to activate Rac1 and RhoA respectively. The cells were lysed using lysis buffer (provided in the kit) on ice. For activation assays, 500 µg protein lysate was incubated with PAK-PBD or Rhotekin RBD beads at 4 °C for 1 h on rocker. After centrifugation, the supernatant was decanted and the pellet was washed thrice with wash buffer (provided in the kit). Further, the pellet was resuspended in lamelli buffer. The lysates prepared from cells, which were not treated

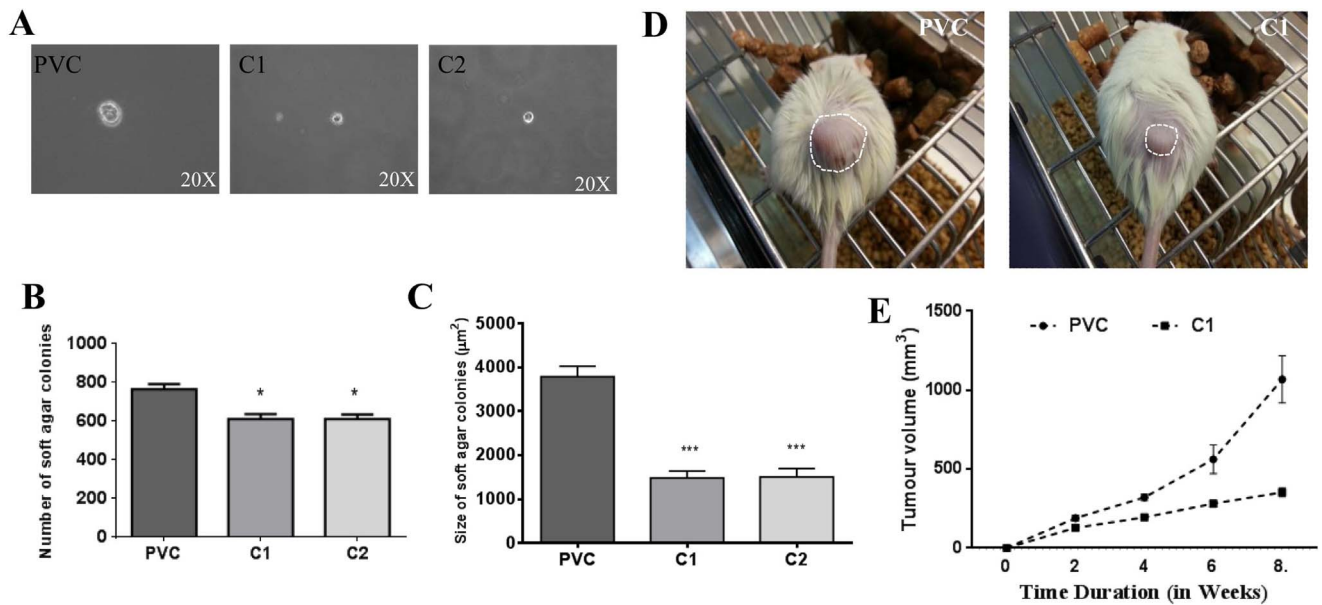


**Fig. 3. Loss of Plectin leads to reduced invasive and tumorigenic potential.** (A) The representative images of colonies formed on soft agar and graphical representation of the (B) number of colonies and (C) size of colonies formed on soft agar in vector control clone (PVC) and Plectin knockdown clones (C1, C2). (D) Representative images of NOD-SCID mice bearing tumors formed from vector control cells (PVC) and Plectin knockdown cells (C1) after 8 weeks of injection. The tumors are indicated by dotted circles. (E) The graph shows tumor volume plotted against time for vector control clone (PVC) and Plectin knockdown clone (C1). It represents mean ± SEM for 5 animals injected for each clone.

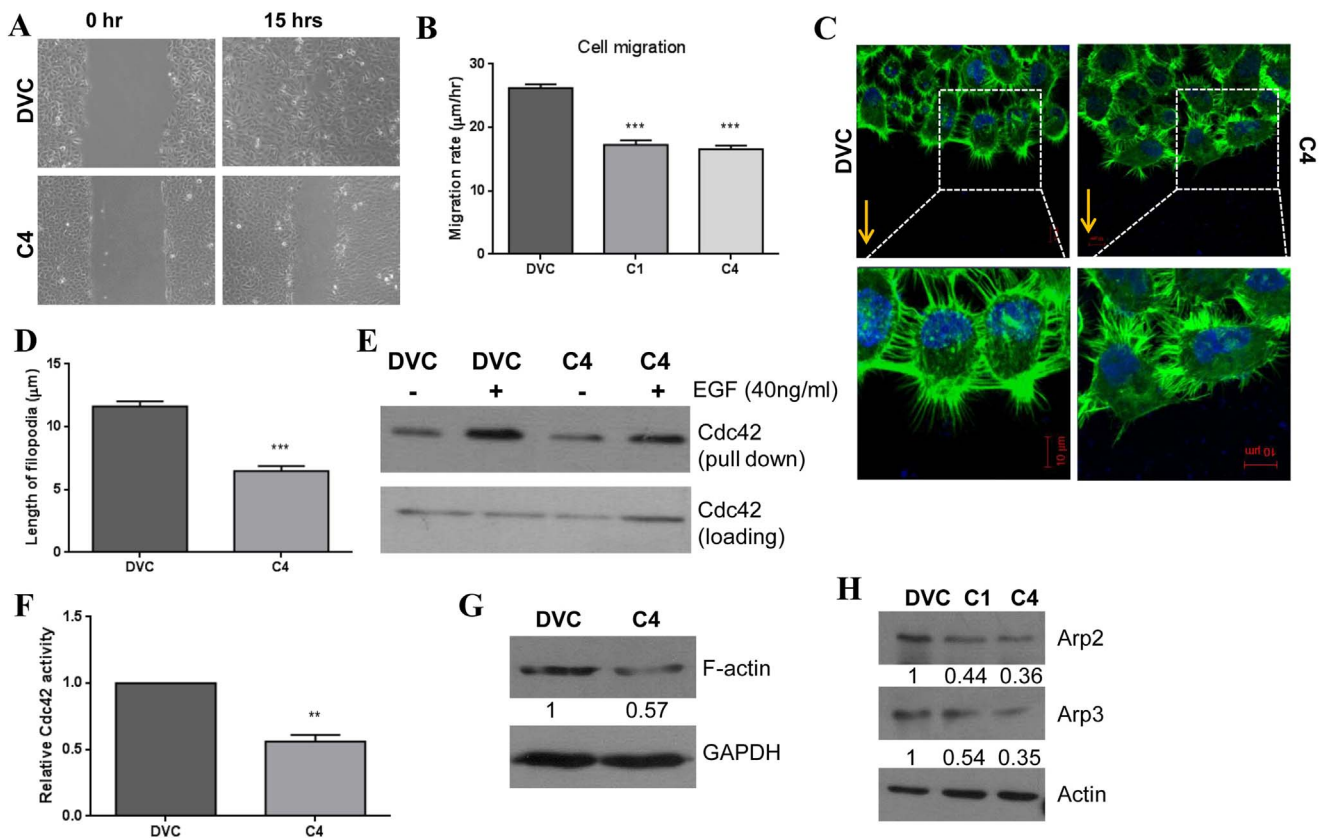


**Fig. 4. Loss of BPAG1e-Plectin leads to reduced cell migration and alterations in actin organization.** (A) Representative time lapse microscopy images show wound healing for vector control clone (DVC) and BPAG1e-Plectin knockdown clone (C4). (B) The graph shows rate of cell migration for vector control clone (DVC) and BPAG1e-Plectin knockdown clones (C1, C4). (C) Immunofluorescence analysis of actin organization (stained in green) at the wound edge in vector control clone (DVC) and BPAG1e-Plectin knockdown clone (C4). The nucleus is stained with DAPI. The arrow indicates direction of migration. The inset shows filopodia formed at migratory front. (D) The graph shows length of filopodia in vector control clone (DVC) and BPAG1e-Plectin knockdown clone (C4). For each clone, 40 cells at the wound front were used for quantification. (E) Western blot analysis and (F) graph represents Cdc42 activity in vector control clone (DVC) and BPAG1e-Plectin knockdown clone (C4). (G) Western blot analysis shows F-actin levels in vector control clone (DVC) and BPAG1e-Plectin knockdown clone (C4). (H) Western blotting of Arp2, Arp3 in vector control clone (DVC) and BPAG1e-Plectin knockdown clones (C1, C4). Note: the numbers below the blot indicate relative intensity of the bands using densitometric analysis.

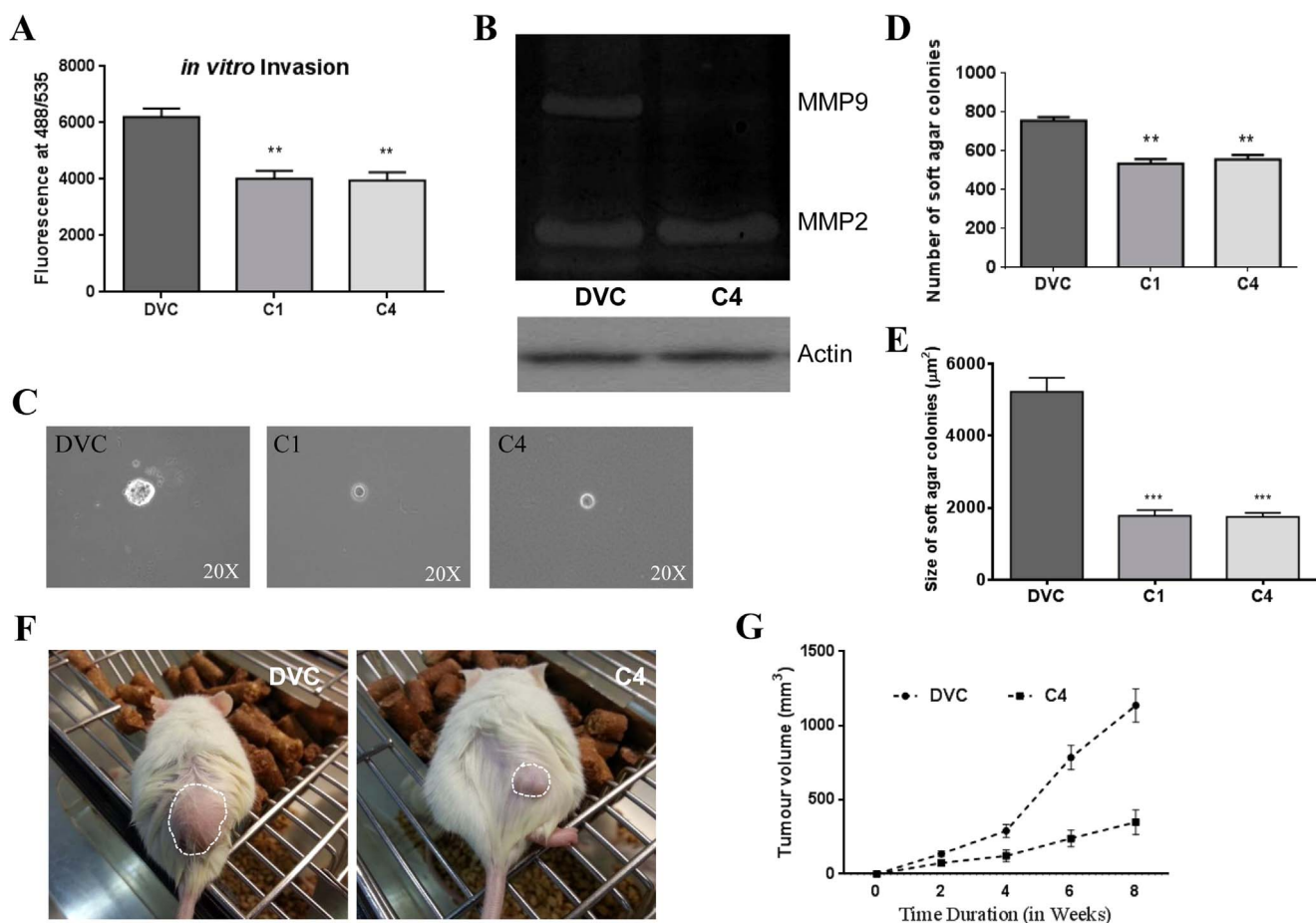


**Fig. 5.** Loss of BPAG1e-Plectin leads to reduced invasive and tumorigenic potential. (A) The graph shows fluorescence of invaded vector control cells (DVC) and BPAG1e-Plectin knockdown cells (C1, C4) which is read at wavelengths of 488/535 nm (Ex/Em). (B) The gelatin zymography shows MMP2 and MMP9 activity in vector control clone (DVC) and BPAG1e-Plectin knockdown clone (C4).  $\beta$  actin is used as a loading control. (C) The representative images of colonies formed on soft agar and graphical representation of the (D) number of colonies and (E) size of colonies formed on soft agar in vector control clone (DVC) and BPAG1e-Plectin knockdown clones (C1, C4). (F) Representative images of NOD-SCID mice bearing tumors formed from vector control cells (DVC) and BPAG1e-Plectin knockdown cells (C4) after 8 weeks of injection. The tumors are indicated by dotted circles. (G) The graph shows tumor volume plotted against time for vector control clone (DVC) and BPAG1e-Plectin knockdown clone (C4). It represents mean  $\pm$  SEM for 5 animals injected for each clone.

with EGF or Calpeptin, were used as a control. The samples were subjected to SDS-PAGE and western blotting. The amount of activated RhoA/Rac1/Cdc42 was determined by western blotting using a Rho/Rac/Cdc42 specific antibody (provided in the kit).

## 2.10. Fractionation and quantification of F-Actin

Fractionation and quantification of F-Actin was performed as described earlier [25]. Briefly, the cells were harvested and homogenized using 27-gauge syringes in 500  $\mu$ l of lysis and F-actin stabilization buffer (50 mM 1,4-piperazinediethanesulfonic acid, 50 mM NaCl, 5 mM MgCl<sub>2</sub>, 5 mM EGTA, 5% glycerol, 0.1% NP-40, 0.1% Triton X-100, 0.1% Tween 20 and 0.1% BME) at 37 °C. Further, the F-actin was separated by ultracentrifugation at 100,000 g for 1 h at 37 °C. The pellet was then resuspended in 500  $\mu$ l ice-cold G-buffer (2 mM Tris-HCl; pH 8.0, 0.2 mM CaCl<sub>2</sub>, 0.2 mM ATP and 0.5 mM DTT) and incubated for 1 h on ice. The dissociated F-actin was centrifuged at 14,000 g for 10 min at 4 °C. The F-actin levels were determined by western blotting using a monoclonal anti- $\beta$ -actin antibody. GAPDH was used as a loading control.

## 2.11. SWATH (sequential window acquisition of all theoretical fragment ion spectra) analysis

SWATH analysis was performed at National Chemical Laboratory (NCL), Pune, India [26].

**LC Separation:** Peptide digest (3  $\mu$ g) was separated by using Eksigent MicroLC 200 system (Eksigent, Dublin, CA) equipped with Eksigent C18-reverse phase column (100 $\times$ 0.3 mm, 3  $\mu$ m, 120 Å). The sample was loaded onto the column with 97% of mobile phase A (100% water, 0.1% Formic acid) and 3% of mobile phase B (100% Acetonitrile, 0.1% Formic acid) at 7  $\mu$ l/min flow rate. Peptides were eluted with a 120 min linear gradient of 3–50% mobile phase B. The column temperature was set to 40 °C and auto sampler at 4 °C. The same chromatographic conditions were used for both information-dependent acquisition (IDA) and SWATH acquisition.

**Full MS/MS2 acquisition (IDA for creating library):** All samples were analyzed on AB-Sciex 5600 Triple TOF mass-spectrometer in positive and high-sensitivity mode. The dual source parameters were optimized for better results: ion source gases GS1, GS2, curtain gas at 25 psi, temperature 200 °C and ion spray voltage floating (ISVF) at 5500 V. The accumulation time in full scan was 250 ms for a mass range of 350–1800  $m/z$ . The parent ions are selected based on the following criteria: ions in the MS scan with intensities more than 120 counts per second, charge stage between +2 to +5 and mass tolerance 50 mDa. Ions were fragmented in the collision cell using rolling collision energy (CE) with an additional CE spread of  $\pm$  15 eV.

Samples were acquired in technical triplicate using above mentioned IDA method. IDA mass spectrometric files were searched using ProteinPilot software, Version 4.0.8085 (AB SCIEX, MA, USA) with the Paragon algorithm against human serum albumin protein database (P02768-UniProt) at 1% FDR. The ProteinPilot output file (.group) was

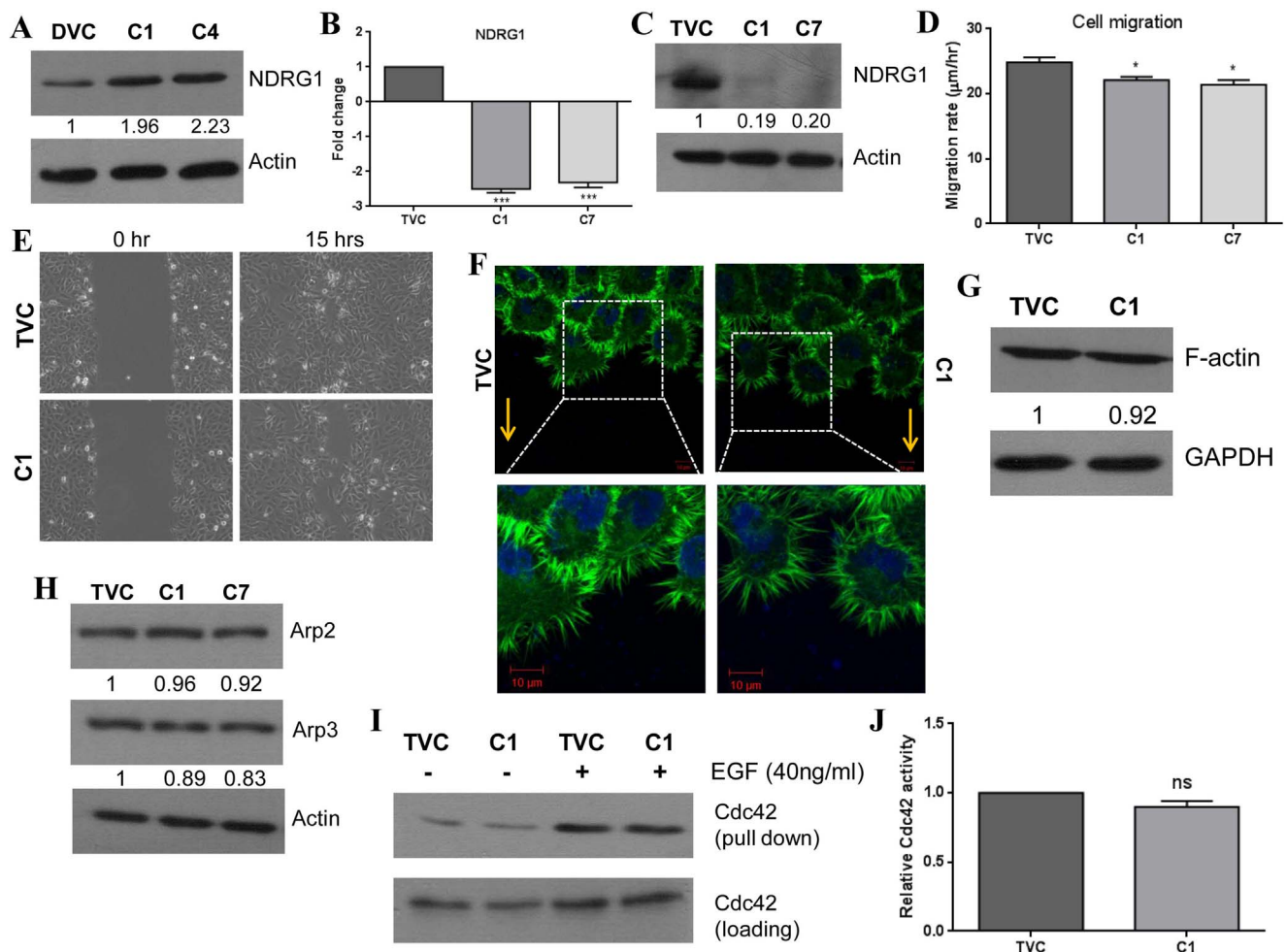


**Fig. 6. NDRG1 downregulation in BPAG1e-Plectin knockdown background rescues cell migration and actin organization** A) Western blot analysis of NDRG1 in DVC, C1 and C4 clones. (B) qRT-PCR and (C) western blot analysis of NDRG1 in vector control clone (TVC) and NDRG1-BPAG1e-Plectin knockdown clones (C1, C7). (E) Representative time lapse microscopy images show wound healing for vector control clone (TVC) and NDRG1-BPAG1e-Plectin knockdown clone (C1). (D) Graph shows rate of cell migration for vector control clone (TVC) and NDRG1-BPAG1e-Plectin knockdown clones (C1, C7). (F) Immunofluorescence analysis of actin organization (stained in green) at the wound edge in vector control clone (TVC) and NDRG1-BPAG1e-Plectin knockdown clone (C1). The nucleus is stained with DAPI. The arrow indicates direction of migration. The inset shows filopodia formed at migratory front. (I) Western blot analysis and (J) graph represents Cdc42 activity in vector control clone (TVC) and NDRG1-BPAG1e-Plectin knockdown clone (C1). (G) Western blot analysis shows F-actin levels in vector control clone (TVC) and NDRG1-BPAG1e-Plectin knockdown clone (C1). (H) Western blot analysis for Arp2, Arp3 in vector control clone (TVC) and NDRG1-BPAG1e-Plectin knockdown clones (C1, C7). Note: the numbers below the blot indicate relative intensity of the bands using densitometric analysis.

used as a standard peptide spectral library. SWATH MS- In SWATH-MS mode, the instrument was specifically tuned to optimize the quadrupole settings for the selection of precursor ion selection window 25  $m/z$  wide. Using an isolation width of 26  $m/z$  (containing 1  $m/z$  for the window overlap), a set of 34 overlapping windows was constructed covering the precursor mass range of 400–1250  $m/z$ . SWATH MS/MS spectra were collected from 100 to 2000  $m/z$ . Ions were fragmented in the collision cell using rolling collision energy with an additional CE spread of  $\pm 15$  eV. An accumulation time (dwell time) of 96 ms was used for all fragmentation scans in high-sensitivity mode, and for each SWATH-MS cycle a survey scan in high-resolution mode 9 was acquired for 100 ms resulting in a duty cycle of 3.33 s. The source parameters were similar to that of IDA acquisition.

SWATH analysis was performed for two technical replicates for each sample. The spectral alignment and targeted data extraction of SWATH-MS data was performed using Peakview software, Version 1.2.03 (AB SCIEX, MA, USA). The peptide data (.MRKVV) files were used for quantification of glycosylated peptides of HSA using Markerview software, Version 1.2.1.1 (AB SCIEX, MA, USA). Normalization was performed using total area sum. The peptides with a p value less than 0.05 were considered for quantification.

## 2.12. Densitometric quantification and statistical analysis

Densitometric quantification of scanned images was performed by ImageJ software (NIH, USA). Band intensities were normalized to respective loading controls. All the statistical analyses were performed using GraphPad Prism software (version 6.01). Two groups of data were statistically analyzed by Student's *t*-test.

## 3. Results and discussion

### 3.1. Loss of hemidesmosomal linker proteins does not affect expression of associated proteins

The single knockdown of Plectin and double knockdown of Plectin-BPAG1e in OSCC derived AW13516 cell line was carried out using shRNA technology. Downregulation of HD linker proteins was confirmed at mRNA and protein level. Plectin knockdown clones C1 and C2 showed  $\sim 6.7$  and  $\sim 5.9$  fold decrease in Plectin mRNA (Fig. 1A), whereas BPAG1e-Plectin double knockdown clones C1 and C4 displayed  $\sim 2.9$  and  $\sim 6.5$  fold decrease in BPAG1e and Plectin mRNA respectively (Fig. 1B and C). Plectin knockdown clones C1 and C2 showed  $\sim 94\%$  reduction at protein level compared to vector control

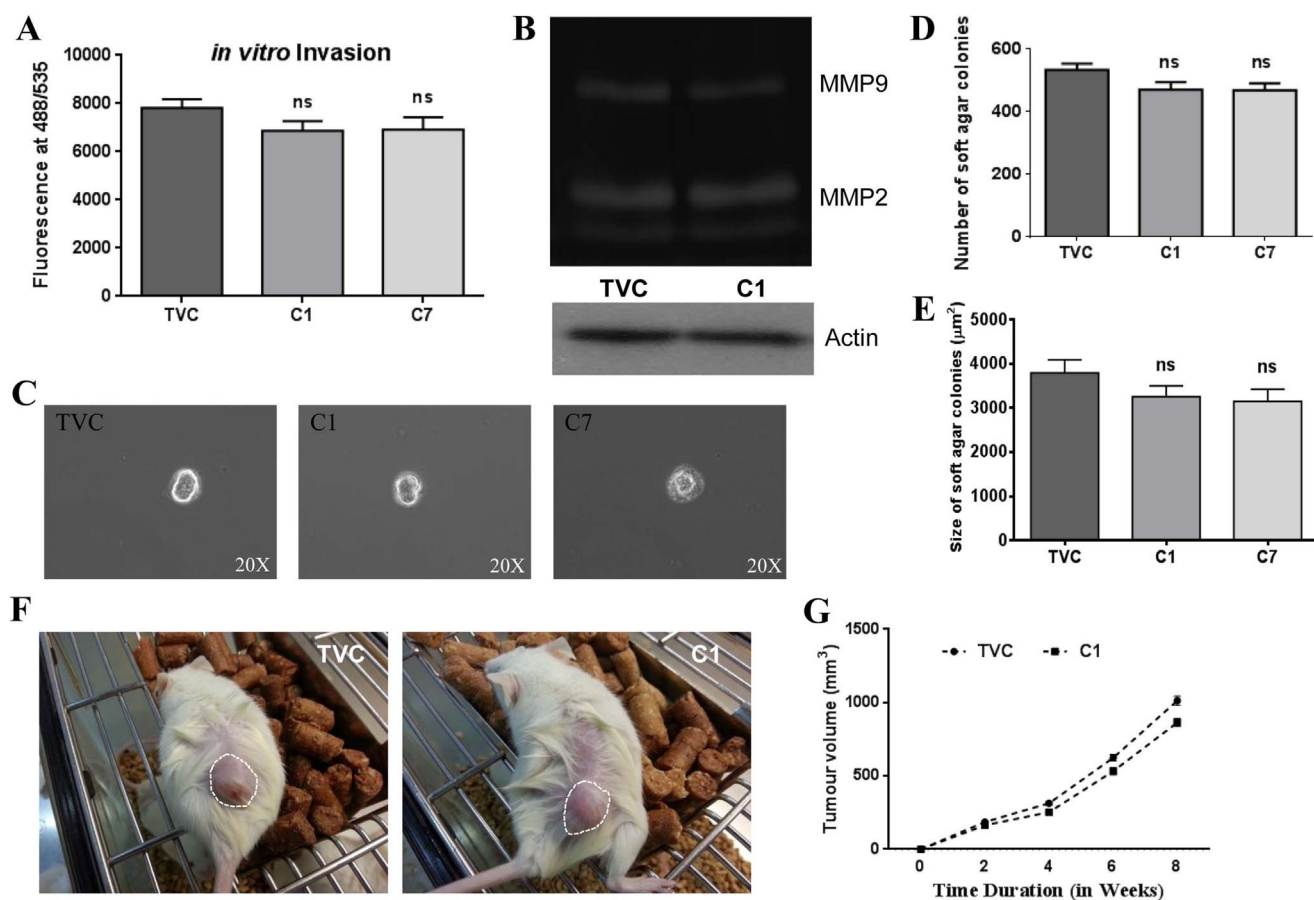


**Fig. 7.** NDRG1 downregulation in BPAG1e-Plectin knockdown background rescues cell invasion and tumorigenicity (A) The graph shows fluorescence of invaded vector control cells (TVC) and NDRG1-BPAG1e-Plectin knockdown cells (C1, C7) which is read at wavelengths of 488/535 nm (Ex/Em) (B) The gelatin zymography shows MMP2 and MMP9 activity in vector control clone (TVC) and NDRG1-BPAG1e-Plectin knockdown clone (C1).  $\beta$  actin is used as a loading control. (C) The representative images of colonies formed on soft agar and graphical representation of (D) the number of colonies and (E) size of colonies formed on soft agar in vector control clone (TVC) and NDRG1-BPAG1e-Plectin knockdown clones (C1, C7). (F) Representative images of NOD-SCID mice bearing tumors formed from vector control cells (TVC) and NDRG1-BPAG1e-Plectin knockdown cells (C1) after 8 weeks of injection. The tumors are indicated by dotted circles. (G) The graph shows tumor volume plotted against time for vector control cells (TVC) and NDRG1-BPAG1e-Plectin knockdown cells (C1). It represents mean  $\pm$  SEM for 5 animals injected for each clone.

clone PVC (Fig. 1D). Further, decrease in Plectin (~93%) and BPAG1e (~81%) protein levels was observed in double knockdown clones C1 and C4 as compared to vector control clone DVC (Fig. 1E).

Plectin and BPAG1e act as linker proteins between  $\beta$ 4 integrin and keratins at HD sites [1]. In our earlier study, we have shown that  $\beta$ 4 integrin and Fascin were downregulated in response to K8 knockdown in OSCC derived cells [18]. In the present study, upon knockdown of HD linker protein(s), no changes were observed in expression of  $\beta$ 4 integrin, K8, K5 and Fascin at protein level (Fig. 1D and E). Further, immunofluorescence analyses demonstrated sparse filament organization for K8 and K5 upon loss of both HD linker proteins in AW13516 cells (Fig. 1F). It has been previously reported that Plectin null mice showed unaltered keratin filament formation, whereas BPAG1e null mice displayed severing of connections between keratin filaments and HDs [3,4]. Recently, we have shown that BPAG1e loss did not alter K8 filament organization in OSCC derived cells [10]. Similarly, Plectin knockdown in AW13516 cells did not show any alterations in K8 filament organization (Supplementary Fig. 1). These results indicated that at least one linker protein, if not both, is required to anchor keratin proteins to the cell surface at HD sites.

In a previous study from our laboratory, it was shown that loss of K8 in AW13516 cells led to reduction in cell migration, cell invasion, tumorigenicity and alterations in actin organization [18]. Therefore, to understand whether knockdown of HD linker proteins leads to similar phenotypic changes as seen in response to K8 knockdown, we performed phenotypic assays using HD linker proteins knockdown cells.

### 3.2. Phenotypic assays for cell transformation

#### 3.2.1. Loss of HD linker proteins leads to reduced cell migration, cell invasion and alterations in actin organization

Scratch wound healing assay demonstrated a decrease in cell migration in HD linker proteins knockdown clones as compared to respective vector control clone (Figs. 2A and 4A). The rate of cell migration was reduced by ~33% and ~36% in Plectin and BPAG1e-Plectin knockdown cells respectively ( $p < 0.001$ ) (Figs. 2B and 4B). These results are consistent with previous studies from our laboratory, where cell motility was reduced upon K8 as well as BPAG1e single knockdown in AW13516 cells [10,18]. Available literature indicates that the role of Plectin in cancer cell motility is context dependent. Cheng et al. have demonstrated that loss of plectin in liver cancer cells promotes cell motility [12,13]. On the other hand, transient knockdown of plectin resulted in decreased proliferation, migration and invasion of HNSCC cells. In these cells, phosphorylated Erk levels were decreased. Authors have argued that a decrease in cell migration and invasion may be attributed to decreased Erk activity [11]. The exact mechanism by which these phenotypic changes occurred is unclear. To our knowledge, ours is the first study demonstrating the role of HD linker proteins (either singly or in combination) in regulating cell migration of OSCC derived cells.

Cell migration is known to be regulated by changes in the actin organization [27]. Therefore, actin organization was analyzed using phalloidin staining followed by confocal microscopy. The filopodia in

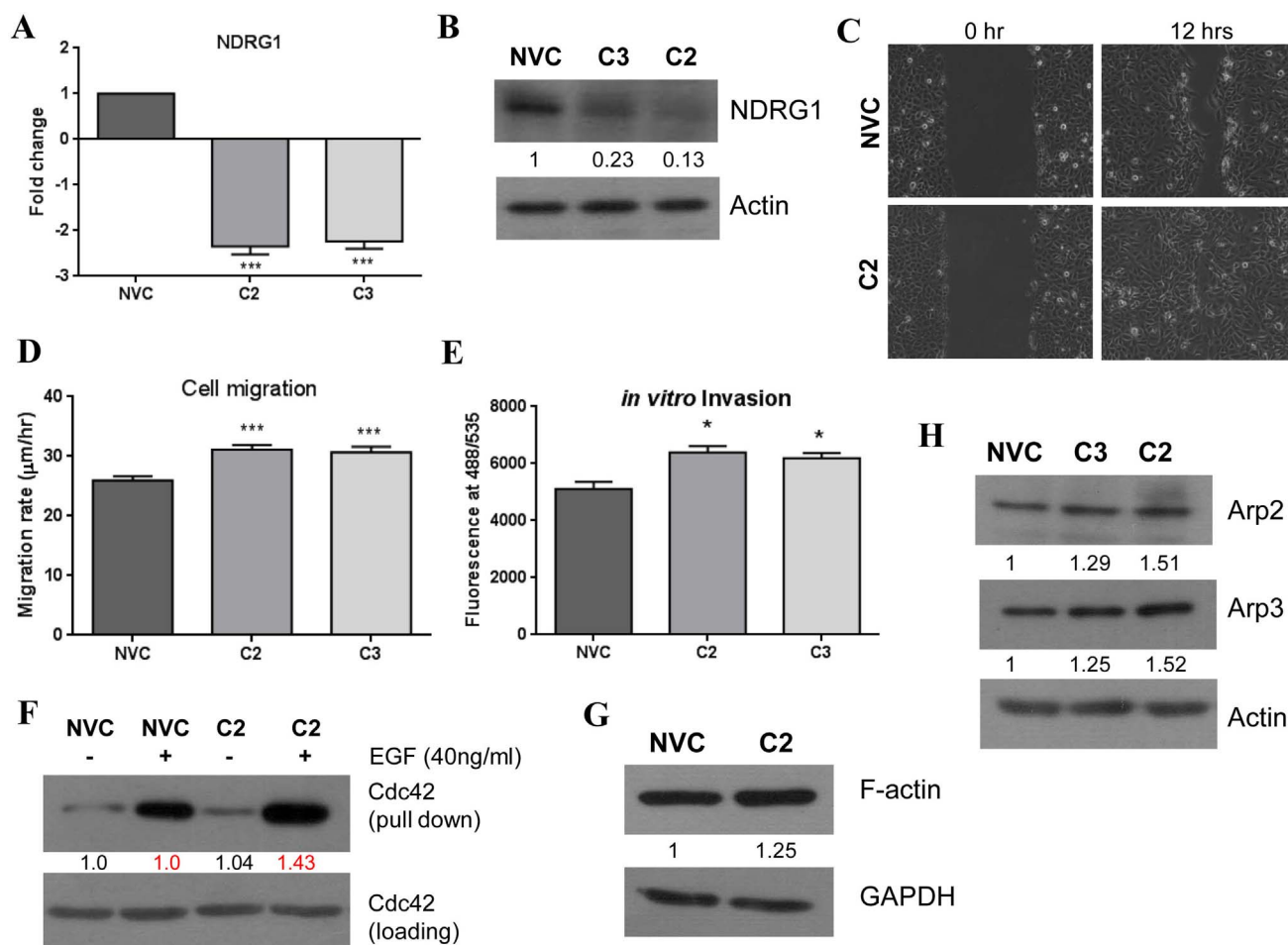


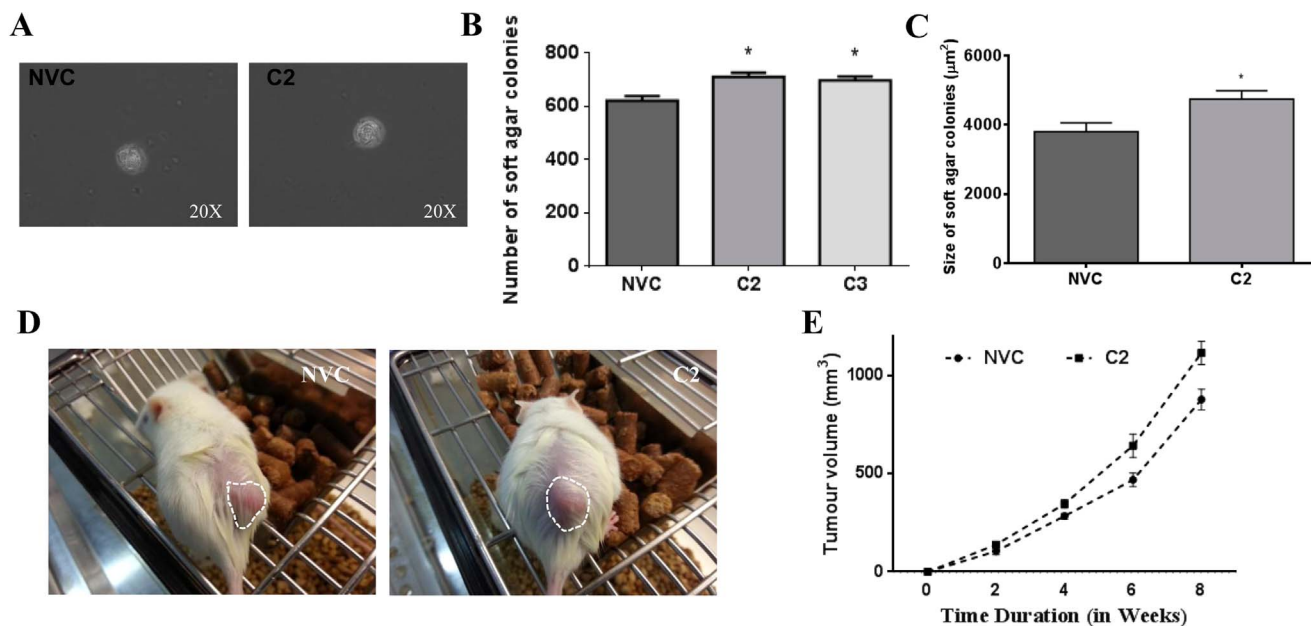
**Fig. 8.** Loss of NDRG1 in AW13516 leads to increased cell migration, cell invasion and actin polymerization. (A) qRT-PCR and (B) western blot analysis of NDRG1 in vector control clone (NVC) and NDRG1 knockdown clones (C2, C3). (C) Representative time lapse microscopy images show wound healing for vector control clone (NVC) and NDRG1 knockdown clone (C2). (D) The graph shows rate of cell migration for vector control clone (NVC) and NDRG1 knockdown clones (C2, C3). (E) The graph shows fluorescence of invaded vector control cells (NVC) and NDRG1 knockdown cells (C2, C3) which is read at wavelengths of 488/535 nm (Ex/Em). (F) Western blot analysis represents Cdc42 activity in vector control clone (NVC) and NDRG1 knockdown clone (C2). (G) Western blot analysis shows F-actin levels in vector control clone (NVC) and NDRG1 knockdown clone (C2). (H) Western blot analysis for Arp2, Arp3 in vector control clone (NVC) and NDRG1 knockdown clones (C2, C3). Note: the numbers below the blot indicate relative intensity of the bands using densitometric analysis.

vector control cells were uniformly present on the cell membrane, whereas in HD linker protein(s) downregulated cells, filopodia were non-uniformly organized (Figs. 2D and 4C). Moreover, the average length of filopodia was significantly reduced in Plectin knockdown cells (6.81 μm) as compared to PVC (11.67 μm) ( $p < 0.001$ ) (Fig. 2E). Similarly, the average length of filopodia was significantly reduced in BPAG1e-Plectin knockdown cells (6.49 μm) as compared to DVC (11.63 μm) ( $p < 0.001$ ) (Fig. 4D). Previously, we have shown that BPAG1e knockdown in OSCC derived cells resulted in changes in actin organization and decrease in length of filopodia [10].

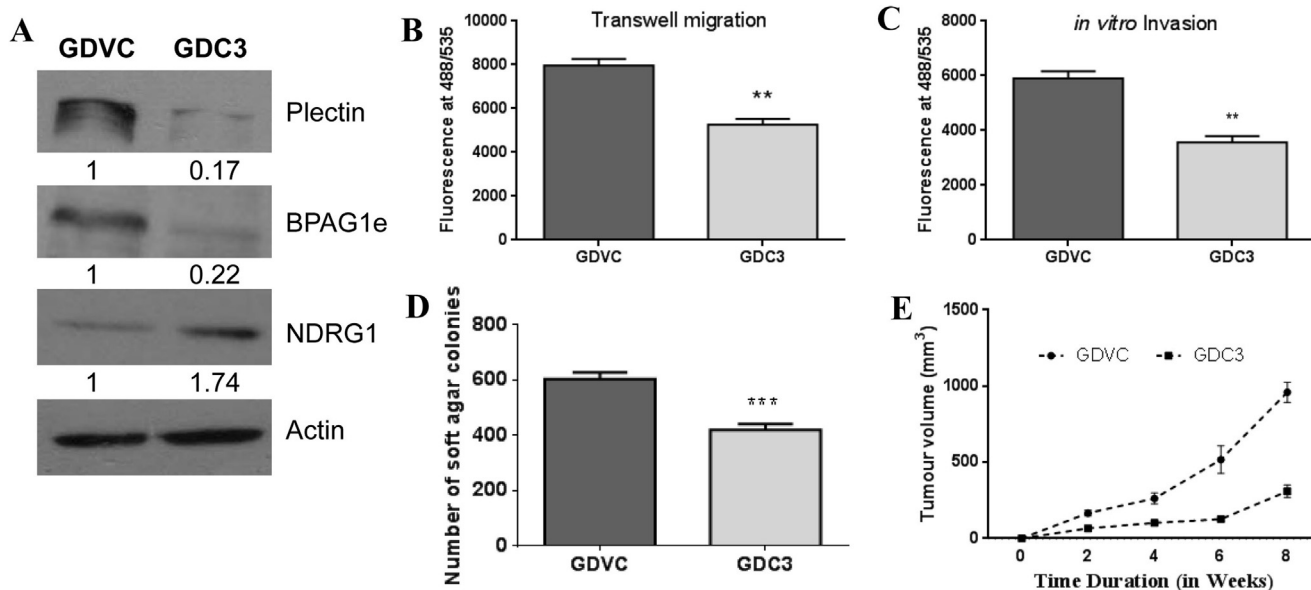
Rho GTPases family proteins like RhoA, Rac1, Cdc42 play a crucial role in the actin cytoskeleton organization. RhoA, Rac1 and Cdc42 regulate cellular motility by formation of stress fibres, lamellipodia and filopodia respectively [28]. The activity of Cdc42 was significantly reduced upon BPAG1e, Plectin and BPAG1e-Plectin knockdown as compared to respective vector control cells (Fig. 4E and F, Supplementary Fig. 2A and B). On the other hand, no significant difference was observed in Rac1 and RhoA activity of Linker proteins knockdown cells as compared to DVC (Supplementary Fig. 2C and D). Further, the appearance of shorter and fewer filopodia upon loss of linker protein(s) prompted us to investigate whether there is any defect in actin polymerization. Indeed, actin polymerization assay revealed reduced levels of F-actin in BPAG1e, Plectin and BPAG1e-Plectin knockdown cells as compared to respective vector control cells (Fig. 4G, Supplementary

Fig. 2E). Actin related proteins (Arp) 2/3 complexes are one of the important actin regulators, which participate in nucleation and branching of actin filaments. The Arp2/3 complex is activated by the Wiskott–Aldrich syndrome family protein (WASP) family of proteins which are in turn activated by Cdc42 [29]. In BPAG1e, Plectin and BPAG1e-Plectin knockdown cells, we observed decrease in levels of Arp2 and Arp3 (Fig. 4H, Supplementary Fig. 2F). Altogether, these results indicated that reduced Cdc42 activity in linker protein(s) knockdown cells led to decreased expression of Arp2/3 proteins, resulting in shorter and fewer filopodia. This explains the reduced cell migration observed in linker protein(s) knockdown cells.

Furthermore, Plectin and BPAG1e-Plectin knockdown cells were less invasive as compared to respective vector control cells (Figs. 2C and 5A). The invasion was reduced by ~34% and ~38% in Plectin and Plectin-BPAG1e knockdown cells respectively ( $p < 0.001$ ) (Figs. 2C and 5A). Cancer cell invasion and metastasis require the crossing of several physical barriers such as the basement membrane. Matrix Metalloproteinases (MMPs) play a major role in breaking these barriers, thus facilitating invasion [30]. Further, it has been demonstrated that increased activity of MMPs (MMP2 and MMP9) correlates with invasive potential of OSCC [31]. To find out whether activity of MMP2 and/or MMP9 has altered in linker proteins knockdown cells, we carried out gelatin zymography. Our experiment revealed that MMP9 activity was significantly reduced in double knockdown cells as compared to DVC,



**Fig. 9.** Loss of NDRG1 in AW13516 leads to increased tumorigenic potential (A) Representative images of colonies formed on soft agar in vector control clone (NVC) and NDRG1 knockdown clone (C2). (B) Graphical representation of number of colonies formed on soft agar in vector control clone (NVC) and NDRG1 knockdown clones (C2, C3). (C) Graphical representation of size of colonies formed on soft agar in vector control clone (NVC) and NDRG1 knockdown clone (C2). (D) Representative images of NOD-SCID mice bearing tumors formed from vector control cells (NVC) and NDRG1 knockdown cells (C2) after 8 weeks of injection. The tumors are indicated by dotted circles. (E) The graph shows tumor volume plotted against time for vector control cells (NVC) and NDRG1 knockdown cells (C2). It represents mean ± SEM for 5 animals injected for each clone.



**Fig. 10.** Loss of BPAG1e-Plectin in AW8507 cells leads to decrease in cell migration, invasion and tumorigenicity (A) Western blot analysis shows Plectin, BPAG1e, NDRG1 levels in vector control clone (GDVC) and BPAG1e-Plectin knockdown clone (GDC3) (B) The graph shows fluorescence of migrated vector control cells (GDVC) and BPAG1e-Plectin knockdown cells (GDC3) which is read at wavelengths of 488/535 nm (Ex/Em) (C) The graph shows fluorescence of invaded vector control cells (GDVC) and BPAG1e-Plectin knockdown cells (GDC3) which is read at wavelengths of 488/535 nm (Ex/Em) (D) The graphical representation of the number of colonies formed on soft agar by vector control cells (GDVC) and BPAG1e-Plectin knockdown cells (GDC3) (E) The graph shows tumor volume plotted against time for vector control cells (GDVC) and BPAG1e-Plectin knockdown cells (GDC3). It represents mean ± SEM for 5 animals injected for each clone. Note: the numbers below the blot indicate relative intensity of the bands using densitometric analysis.

whereas MMP2 activity remained unaltered (Fig. 5B). Thus, decreased MMP9 activity seems to be responsible for reduced cell invasion in the linker proteins knockdown cells.

### 3.2.2. Downregulation of HD linker proteins leads to reduction in the tumorigenic potential of AW13516 cells

Plectin and Plectin-BPAG1e knockdown clones showed a significant reduction in number of colonies on soft agar by ~27% and ~29% respectively (p < 0.001) (Figs. 3A and B, 5C and D). Moreover, the soft

agar colony size was reduced by ~60% and ~63% in Plectin and Plectin-BPAG1e knockdown clones as compared to respective vector control clones (p < 0.001) (Figs. 3C and 5E). Previously, we have demonstrated that BPAG1e loss in OSCC derived cells also results in reduction in number and size of colonies formed on soft agar [10]. The clonogenic assay demonstrated no significant difference in clonogenic potential of Plectin and Plectin-BPAG1e downregulated and respective vector control cells (Supplementary Fig. 3B and D). Similarly, no significant changes were observed in cell viability of Plectin (p = 0.12)

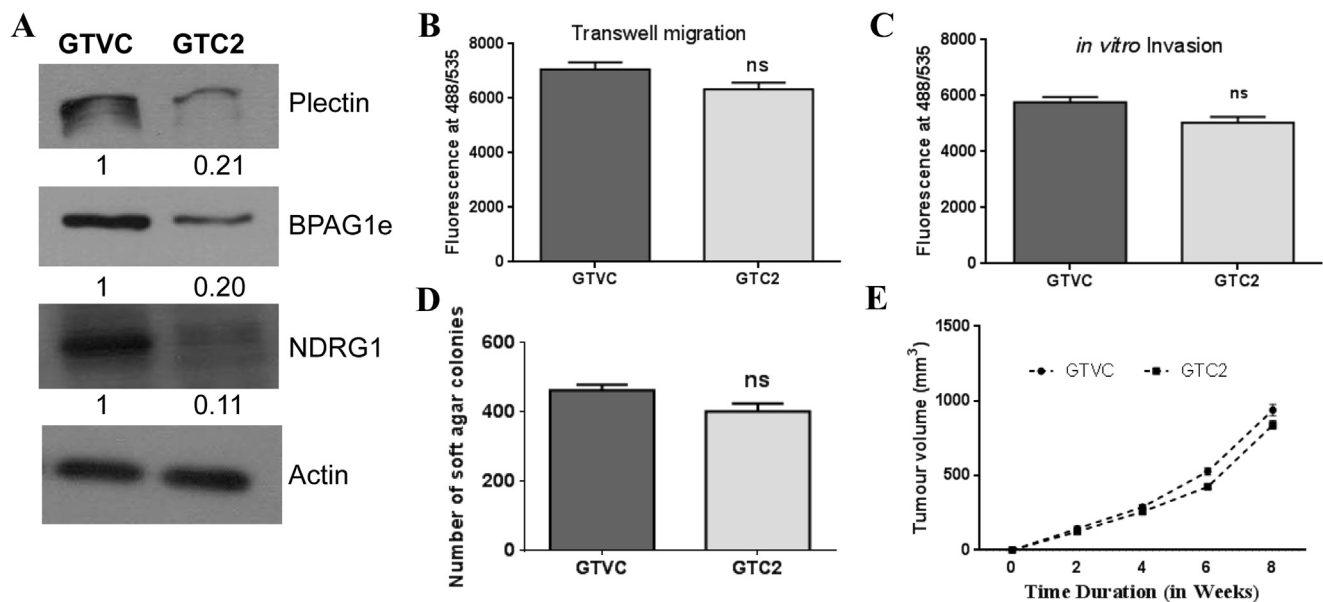


**Fig. 11.** NDRG1 downregulation in BPAG1e-Plectin knockdown background rescues the phenotype in AW8507 cells (A) Western blot analysis shows Plectin, BPAG1e, NDRG1 levels in vector control clone (GTVC) and NDRG1-BPAG1e-Plectin knockdown clone (GTC2) (B) The graph shows fluorescence of migrated vector control cells (GTVC) and NDRG1-BPAG1e-Plectin knockdown cells (GTC2) which is read at wavelengths of 488/535 nm (Ex/Em) (C) The graph shows fluorescence of invaded vector control cells (GTVC) and NDRG1-BPAG1e-Plectin knockdown cells (GTC2) which is read at wavelengths of 488/535 nm (Ex/Em) (D) The graphical representation of the number of colonies formed on soft agar by vector control cells (GTVC) and NDRG1-BPAG1e-Plectin knockdown cells (GTC2) (E) The graph shows tumor volume plotted against time for vector control cells (GTVC) and NDRG1-BPAG1e-Plectin knockdown cells (GTC2). It represents mean  $\pm$  SEM for 5 animals injected for each clone. Note: the numbers below the blot indicate relative intensity of the bands using densitometric analysis.

and Plectin-BPAG1e ( $p = 0.15$ ) downregulated cells as compared to respective vector control cells (Supplementary Fig. 3A and C). These results indicated that the decrease in soft agar colony size can be attributed to reduced transformation potential of the cells.

Furthermore, the *in vivo* tumorigenicity of linker proteins knockdown cells was assessed by subcutaneous injection into NOD-SCID mice ( $n = 5$ ). At the end of 8 weeks, the mean tumor volume of the mice bearing Plectin knockdown cells was significantly reduced as compared with the average volume of tumors formed by PVC ( $p < 0.001$ ) (Fig. 3D and E). Likewise, the mean tumor volume of the mice bearing Plectin-BPAG1e knockdown cells was significantly reduced as compared with the average volume of tumors formed by DVC ( $p < 0.001$ ) (Fig. 5F and G). Previously, we have demonstrated that BPAG1e loss in OSCC derived cells results in reduced tumorigenic potential [10]. Altogether, these results indicated that HD linker proteins play an important role in governing transformation potential.

We observed reduction in cell migration, cell invasion, tumorigenicity and alterations in actin organization upon knockdown of BPAG1e and/or plectin in OSCC derived cells (Figs. 2–5) [10]. However, unaltered levels of  $\beta 4$  integrin and Fascin in linker proteins knockdown cells indicated that linker proteins may not have role in K8 mediated effects observed in OSCC derived cells. Therefore, to decipher the key molecules which may have a role in phenotypic changes observed upon HD linker proteins downregulation, global protein profiling was performed using SWATH.

### 3.3. SWATH analysis demonstrated NDRG1 upregulation in HD linker proteins knockdown cells

SWATH analysis was performed for BPAG1e-Plectin knockdown clone C4 and DVC. Some of the differentially expressed proteins were Vimentin, LIMA1, NDRG1, Galectin, 14-3-3 protein epsilon, Ubiquitin-40S ribosomal protein, S100-A6 etc (Supplementary File 2). Out of these proteins, NDRG1 was upregulated by 1.84 fold (Supplementary File 2). We selected NDRG1 for further analysis as it functions as a metastasis suppressor in number of cancers including oral cancer

[32,33]. Furthermore, it plays an important role in cell migration, actin organization, invasion and tumorigenesis [25,32,34]. NDRG1 overexpression in human prostate and colon cancer cells inhibited cell migration by preventing actin filament polymerization [25]. Further, NDRG1 reduced cell invasiveness and tumorigenesis of OSCC derived cells [32]. Moreover, NDRG1 regulates gastric cancer cell invasion through decreased MMP9 activity [34]. Upregulation of NDRG1 (~2.1 fold) in BPAG1e-Plectin knockdown clones was validated using western blotting (Fig. 6A). NDRG1 protein expression was also found to be upregulated in BPAG1e (~1.6 fold), Plectin (~1.75 fold) single knockdown clones as compared to respective vector control clones (Supplementary Fig. 4A and B).

### 3.4. NDRG1 downregulation in HD linker proteins knockdown cells rescues the phenotype

To verify whether the phenotype associated with cell transformation in HD linker proteins knockdown cells was due to higher NDRG1 levels, it was stably downregulated in Plectin-BPAG1e double knockdown clone C4. NDRG1-BPAG1e-Plectin triple knockdown clones C1 and C7 displayed 2.5 and 2.3 fold decrease in NDRG1 mRNA level respectively (Fig. 6B). Further, NDRG1-BPAG1e-Plectin triple knockdown clones showed ~80% reduction in NDRG1 protein expression as compared to vector control clone TVC (Fig. 6C).

We also carried out single knockdown of NDRG1 in AW13516 cells to investigate the role of NDRG1 alone. NDRG1 knockdown clones (C2, C3) showed ~2.3 fold decrease at mRNA level (Fig. 8A) and ~82% reduction at protein level as compared to vector control clone NVC (Fig. 8B).

The NDRG1-BPAG1e-Plectin triple knockdown clones displayed only ~10% decrease in the rate of cell migration as compared to TVC ( $p = 0.006$ ) (Fig. 6D and E). It is noteworthy that BPAG1e-Plectin double knockdown clones showed ~36% decrease in cell migration ( $p < 0.001$ ) (Fig. 4B). On the other hand, NDRG1 single knockdown clones showed ~20% increase in cell migration as compared to NVC ( $p < 0.001$ ) (Fig. 8C and D). These results indicated that NDRG1 plays an

important role in regulating cell migration of linker proteins deficient OSCC derived cells.

The filopodia in NDRG1-BPAG1e-Plectin triple knockdown cells were uniformly present which was similar to TVC (Fig. 6F). As mentioned earlier, Plectin-BPAG1e double knockdown cells displayed non-uniformly arranged filopodia (Fig. 4C). Further, Cdc42 activity was partially restored in NDRG1-BPAG1e-Plectin triple knockdown cells (Fig. 6I and J) as compared to BPAG1e-Plectin double knockdown cells (Fig. 4E and F). Moreover, Cdc42 activity was substantially increased upon NDRG1 single knockdown as compared to NVC (Fig. 8F). Furthermore, filamentous actin and Arp2/3 levels were restored in NDRG1-BPAG1e-Plectin triple knockdown cells (Fig. 6G and H) as compared to BPAG1e-Plectin double knockdown cells (Fig. 4G and H). Likewise, filamentous actin and Arp2/3 levels were elevated in NDRG1 single knockdown cells as compared to NVC (Fig. 8G and H).

Similarly, *in vitro* invasion was reduced by ~10–15% in triple knockdown cells ( $p = 0.18$ ) as compared to ~38% reduction in BPAG1e-Plectin double knockdown cells ( $p < 0.001$ ) (Figs. 5A and 7A). In case of only NDRG1 knockdown, the *in vitro* invasion was increased by ~23% ( $p = 0.022$ ) (Fig. 8E). Furthermore, NDRG1-BPAG1e-Plectin triple knockdown cells demonstrated partial restoration of MMP9 activity as compared to BPAG1e-Plectin double knockdown cells (Figs. 5B and 7B).

Further, NDRG1-BPAG1e-Plectin triple knockdown cells showed ~10% decrease in number of colonies formed on soft agar ( $p = 0.10$ ) (Fig. 7C and D) as compared to ~29% reduction in colony number in double knockdown cells (Fig. 5C and D). No significant difference in soft agar colony size was observed in NDRG1-BPAG1e-Plectin triple knockdown cells as compared to TVC ( $p = 0.43$ ) (Fig. 7E). Moreover, NDRG1 single knockdown cells displayed ~14% increase in number of colonies on soft agar ( $p = 0.024$ ) (Fig. 9A and B). Furthermore, ~25% increase in size of colonies formed on soft agar was observed in NDRG1 single knockdown cells as compared to NVC ( $p = 0.011$ ) (Fig. 9C).

Additionally, *in vivo* experiments suggested that there was no significant difference in mean tumor volume of mice bearing NDRG1-BPAG1e-Plectin triple knockdown and TVC cells ( $p = 0.068$ ) (Fig. 7F and G), whereas only NDRG1 knockdown resulted in increase in tumorigenicity as compared to NVC ( $p = 0.049$ ) (Fig. 9D and E). Taken together, these results indicated that NDRG1 plays a defining role in phenotype associated with cell transformation in linker proteins ablated OSCC cells.

Next, to find out whether the effects observed in AW13516 cells were cell line specific, we carried out similar experiments in another tongue SCC derived cell line AW8507, which was derived from poorly differentiated epidermoid carcinoma of tongue [19].

### 3.5. The phenotypic changes observed upon HD linker proteins are not cell line specific

The HD linker proteins knockdown AW8507 cells (GDC3) also showed increased NDRG1 protein levels as compared to vector control cells (GDVC). Further, to verify whether the phenotype associated with cell transformation in HD linker proteins knockdown AW8507 cells was due to higher NDRG1 levels, it was stably downregulated in BPAG1e-Plectin knockdown clone GDC3.

The results of phenotypic assays for cell transformation like Boyden chamber transwell assay, *in vitro* invasion assay, soft agar assay and *in vivo* tumorigenicity assay for AW8507 knockdown systems were similar to those found in AW13516 knockdown systems (Figs. 10 and 11). In short, loss of HD linker proteins in AW8507 cells led to reduced cell migration, invasion and tumorigenicity (Fig. 10A-E). Moreover, the partial rescue of phenotype was observed in NDRG1-Plectin-BPAG1e triple knockdown clone GTC2 (Fig. 11A-E). These results were also similar to results observed in AW13516 knockdown systems. Thus, these results indicated that alterations observed upon loss of BPAG1e and Plectin are not cell line specific.

## 4. Conclusions

The available literature regarding the role of HD linker proteins in human cancers is scanty and inconsistent. In the current study, we have attempted to unravel the role of hemidesmosomal linker proteins in neoplastic progression of OSCC. This study demonstrated that hemidesmosomal linker proteins play a vital role in cell motility, cell invasion, actin organization and tumorigenicity in OSCC derived cells possibly through NDRG1. The link between hemidesmosomal linker proteins and NDRG1 is still not known. Therefore, in future, it will be interesting to decipher how hemidesmosomal linker proteins regulate NDRG1 expression in OSCC derived cells.

Thus, the current study is a step forward in our quest to understand functional significance of aberrant expression of intermediate filaments and their associated proteins (like BPAG1e, Plectin) and further their use as a battery of biomarkers for management of human oral cancer. Furthermore, these molecules may prove useful as therapeutic targets for human oral cancer.

## Conflict of interest

None.

## Acknowledgements

We thank Dr. Jonathan Jones (Washington State University, USA) for his generous gift of BPAG1e shRNA encoding pLKO1.puro plasmid. We thank following people from ACTREC-TMC, Navi Mumbai, India for their kind help: Dr. Crismita D'mello, Dr. Richa Tiwari, Dr. Saumya Srivastava and Dr. Bihari Lal Soni for their valuable experimental suggestions; Mr. Shridhar Nadkar for assistance in animal experiments; Mrs. Vaishali Kailaje for assistance in analysis of microscopic images. We thank Dr. Mahesh Kulkarni, Dr. B. Santhakumari and Mr. Yugendra Patil (National Chemical Laboratory, Pune, India) for SWATH analysis. This work was supported by institutional CRI42 funds. PC was supported by fellowship from ACTREC-TMC, Navi Mumbai, India.

## Appendix A. Supporting information

Supplementary data associated with this article can be found in the online version at <http://dx.doi.org/10.1016/j.yexcr.2017.08.034>.

## References

- [1] J.C. Jones, S.B. Hopkinson, L.E. Goldfinger, Structure and assembly of hemidesmosomes, *Bioessays: News Rev. Mol., Cell. Dev. Biol.* 20 (1998) 488–494.
- [2] P.R. Chaudhari, M.M. Vaidya, Versatile hemidesmosomal linker proteins: structure and function, *Histol. Histopathol.* 30 (2015) 425–434.
- [3] K. Andra, H. Lassmann, R. Bitner, S. Shorny, R. Fassler, F. Propst, G. Wiche, Targeted inactivation of plectin reveals essential function in maintaining the integrity of skin, muscle, and heart cytoarchitecture, *Genes Dev.* 11 (1997) 3143–3156.
- [4] L. Guo, L. Degenstein, J. Dowling, Q.C. Yu, R. Wollmann, B. Perman, E. Fuchs, Gene targeting of BPAG1: abnormalities in mechanical strength and cell migration in stratified epithelia and neurologic degeneration, *Cell* 81 (1995) 233–243.
- [5] K.J. Hamill, S.B. Hopkinson, P. DeBiase, J.C. Jones, BPAG1e maintains keratinocyte polarity through beta4 integrin-mediated modulation of Rac1 and cofilin activities, *Mol. Biol. Cell* 20 (2009) 2954–2962.
- [6] L. McInroy, A. Maatta, Plectin regulates invasiveness of SW480 colon carcinoma cells and is targeted to podosome-like adhesions in an isoform-specific manner, *Exp. Cell Res.* 317 (2011) 2468–2478.
- [7] R.G. Valencia, G. Walko, L. Janda, J. Novacek, E. Mihailovska, S. Reipert, K. Andra-Marobela, G. Wiche, Intermediate filament-associated cytolinker plectin 1c destabilizes microtubules in keratinocytes, *Mol. Biol. Cell* 24 (2013) 768–784.
- [8] M. Michael, R. Begum, K. Fong, C. Pourreynon, A.P. South, J.A. McGrath, M. Parsons, BPAG1-e restricts keratinocyte migration through control of adhesion stability, *J. Invest. Dermatol.* 134 (2014) 773–782.
- [9] C. Herold-Mende, J. Kartenbeck, P. Tomakidi, F.X. Bosch, Metastatic growth of squamous cell carcinomas is correlated with upregulation and redistribution of hemidesmosomal components, *Cell Tissue Res.* 306 (2001) 399–408.
- [10] P.R. Chaudhari, S.E. Charles, M.M. Vaidya, Role of BPAG1e in neoplastic progression of oral squamous cell carcinoma derived cells, *Int. J. Pharm. Biol. Sci.* 8 (2017)

- 519–527.
- [11] K. Katada, T. Tomonaga, M. Satoh, K. Matsushita, Y. Tonoike, Y. Kodera, T. Hanazawa, F. Nomura, Y. Okamoto, Plectin promotes migration and invasion of cancer cells and is a novel prognostic marker for head and neck squamous cell carcinoma, *J. Proteom.* 75 (2012) 1803–1815.
- [12] C.C. Cheng, W.T. Chao, C.C. Liao, Y.H. Tseng, Y.C. Lai, Y.S. Lai, Y.H. Hsu, Y.H. Liu, Plectin deficiency in liver cancer cells promotes cell migration and sensitivity to sorafenib treatment, *Cell Adhes. Migr.* (2017) 1–9.
- [13] C.C. Cheng, Y.C. Lai, Y.S. Lai, Y.H. Hsu, W.T. Chao, K.C. Sia, Y.H. Tseng, Y.H. Liu, Transient knockdown-mediated deficiency in plectin alters hepatocellular motility in association with activated FAK and Rac1-GTPase, *Cancer Cell Int.* 15 (2015) 29.
- [14] P.A. Coulombe, M.B. Omary, 'Hard' and 'soft' principles defining the structure, function and regulation of keratin intermediate filaments, *Curr. Opin. Cell Biol.* 14 (2002) 110–122.
- [15] T. Fillies, R. Werkmeister, J. Packeisen, B. Brandt, P. Morin, D. Weingart, U. Joos, H. Buerger, Cytokeratin 8/18 expression indicates a poor prognosis in squamous cell carcinomas of the oral cavity, *BMC Cancer* 6 (2006) 10.
- [16] M.M. Vaidya, A.M. Borges, S.A. Pradhan, A.N. Bhisey, Cytokeratin expression in squamous cell carcinomas of the tongue and alveolar mucosa, *Eur. J. Cancer Part B Oral. Oncol.* 32B (1996) 333–336.
- [17] H.E. Schaafsma, L.A. Van Der Velden, J.J. Manni, H. Peters, M. Link, D.J. Rutter, F.C. Ramaekers, Increased expression of cytokeratins 8, 18 and vimentin in the invasion front of mucosal squamous cell carcinoma, *J. Pathol.* 170 (1993) 77–86.
- [18] H. Alam, S.T. Kundu, S.N. Dalal, M.M. Vaidya, Loss of keratins 8 and 18 leads to alterations in alpha6beta4-integrin-mediated signalling and decreased neoplastic progression in an oral-tumour-derived cell line, *J. Cell Sci.* 124 (2011) 2096–2106.
- [19] R.J. Tataka, N. Rajaram, R.N. Damle, B. Balsara, A.N. Bhisey, S.G. Gangal, Establishment and characterization of four new squamous cell carcinoma cell lines derived from oral tumors, *J. Cancer Res. Clin. Oncol.* 116 (1990) 179–186.
- [20] S.V. Iyer, P.P. Dange, H. Alam, S.S. Sawant, A.D. Ingle, A.M. Borges, N.V. Shirsat, S.N. Dalal, M.M. Vaidya, Understanding the role of keratins 8 and 18 in neoplastic potential of breast cancer derived cell lines, *PLoS One* 8 (2013) e53532.
- [21] U. Raul, S. Sawant, P. Dange, R. Kalraiya, A. Ingle, M. Vaidya, Implications of cytokeratin 8/18 filament formation in stratified epithelial cells: induction of transformed phenotype, *Int. J. Cancer* 111 (2004) 662–668.
- [22] C. Dmello, S. Sawant, H. Alam, P. Gangadaran, S. Mogre, R. Tiwari, Z. D'Souza, M. Narkar, R. Thorat, K. Patil, D. Chaukar, S. Kane, M. Vaidya, Vimentin regulates differentiation switch via modulation of keratin 14 levels and their expression together correlates with poor prognosis in oral cancer patients, *PLoS One* 12 (2017) e0172559.
- [23] H. Alam, L. Sehgal, S.T. Kundu, S.N. Dalal, M.M. Vaidya, Novel function of keratins 5 and 14 in proliferation and differentiation of stratified epithelial cells, *Mol. Biol. Cell* 22 (2011) 4068–4078.
- [24] A. Ranjan, S.M. Bane, R.D. Kalraiya, Glycosylation of the laminin receptor (alpha3beta1) regulates its association with tetraspanin CD151: Impact on cell spreading, motility, degradation and invasion of basement membrane by tumor cells, *Exp. Cell Res.* 322 (2014) 249–264.
- [25] J. Sun, D. Zhang, Y. Zheng, Q. Zhao, M. Zheng, Z. Kovacevic, D.R. Richardson, Targeting the metastasis suppressor, NDRG1, using novel iron chelators: regulation of stress fiber-mediated tumor cell migration via modulation of the ROCK1/pMLC2 signaling pathway, *Mol. Pharmacol.* 83 (2013) 454–469.
- [26] A.M. Korwar, G. Vannuruswamy, M.G. Jagadeeshaprasad, R.H. Jayaramaiah, S. Bhat, B.S. Regin, S. Ramaswamy, A.P. Giri, V. Mohan, M. Balasubramanyam, M.J. Kulkarni, Development of diagnostic fragment ion library for glycosylated peptides of human serum albumin: targeted quantification in prediabetic, diabetic, and microalbuminuria plasma by parallel reaction monitoring, SWATH, and MSE, *Mol. Cell. Proteom.* 14 (2015) 2150–2159.
- [27] A. Mogilner, G. Oster, Cell motility driven by actin polymerization, *Biophys. J.* 71 (1996) 3030–3045.
- [28] C.D. Nobes, A. Hall, Rho, rac, and cdc42 GTPases regulate the assembly of multi-molecular focal complexes associated with actin stress fibers, lamellipodia, and filopodia, *Cell* 81 (1995) 53–62.
- [29] T. Takenawa, S. Suetsugu, The WASP-WAVE protein network: connecting the membrane to the cytoskeleton, *Nat. Rev. Mol. Cell Biol.* 8 (2007) 37–48.
- [30] L.A. Liotta, K. Tryggvason, S. Garbisa, I. Hart, C.M. Foltz, S. Shafie, Metastatic potential correlates with enzymatic degradation of basement membrane collagen, *Nature* 284 (1980) 67–68.
- [31] J.C. de Vicente, M.F. Fresno, L. Villalain, J.A. Vega, G. Hernandez Vallejo, Expression and clinical significance of matrix metalloproteinase-2 and matrix metalloproteinase-9 in oral squamous cell carcinoma, *Oral. Oncol.* 41 (2005) 283–293.
- [32] J.C. Lee, L.C. Chung, Y.J. Chen, T.H. Feng, H.H. Juang, N-myc downstream-regulated gene 1 downregulates cell proliferation, invasiveness, and tumorigenesis in human oral squamous cell carcinoma, *Cancer Lett.* 355 (2014) 242–252.
- [33] S. Bandyopadhyay, S.K. Pai, S. Hirota, S. Hosobe, T. Tsukada, K. Miura, Y. Takano, K. Saito, T. Commes, D. Piquemal, M. Watabe, S. Gross, Y. Wang, J. Huggenvik, K. Watabe, PTEN up-regulates the tumor metastasis suppressor gene Drg-1 in prostate and breast cancer, *Cancer Res.* 64 (2004) 7655–7660.
- [34] X. Chang, X. Xu, X. Xue, J. Ma, Z. Li, P. Deng, J. Chen, S. Zhang, Y. Zhi, D. Dai, NDRG1 Controls gastric cancer migration and invasion through regulating MMP-9, *Pathol. Oncol. Res.: POR* 22 (2016) 789–796.

## Review

# Versatile hemidesmosomal linker proteins: Structure and function

**Pratik R. Chaudhari and Milind M. Vaidya**

Advanced Centre for Treatment, Research and Education in Cancer (ACTREC), Tata Memorial Centre, Kharghar, Navi Mumbai, Maharashtra, India

**Summary.** Hemidesmosomes are anchoring junctions which connect basal epidermal cells to the extracellular matrix. In complex epithelia like skin, hemidesmosomes are composed of transmembrane proteins like  $\alpha 6\beta 4$  integrin, BP180, CD151 and cytoplasmic proteins like BPAG1e and plectin. BPAG1e and plectin are plakin family cytolinker proteins which anchor intermediate filament proteins i.e. keratins to the hemidesmosomal transmembrane proteins. Mutations in BPAG1e and plectin lead to severe skin blistering disorders. Recent reports indicate that these hemidesmosomal linker proteins play a role in various cellular processes like cell motility and cytoskeleton dynamics apart from their known anchoring function. In this review, we will discuss their role in structural and signaling functions.

**Key words:** BPAG1e, Cancer, Cytoskeletal proteins, Hemidesmosome, Plectin

## Introduction

Anchoring junctions connect the cytoskeletal elements of a cell to those of its neighboring cell or to the extracellular matrix. Desmosomes (DSs) are cell-cell anchoring junctions, whereas hemidesmosomes (HDs) are a type of anchoring junctions which connect the basal surface of epithelial cells to the underlying basal

lamina. Ultrastructurally, HDs are composed of an electron dense structure whose cytoplasmic plaque anchors keratins (intermediate filament proteins) to the cell surface (Jones et al., 1998; Borradori and Sonnenberg, 1999). Depending upon the protein composition there are two types of HDs, type 1 HDs and type 2 HDs. Type 1 HDs, present in complex epithelia like skin, are comprised of  $\alpha 6\beta 4$  integrin, BP180 (BPAG2; XVII collagen), tetraspanin CD151 and cytoplasmic linker proteins: plectin and BP230 (BPAG1e: Bullous pemphigoid antigen 1e). Type 2 HDs which are majorly found in simple epithelia consist of  $\alpha 6\beta 4$  integrin, plectin and CD151 (Jones et al., 1998; Nievers et al., 1999; Sterk et al., 2000; de Pereda et al., 2009a). Mutations in hemidesmosomal proteins lead to severe skin blistering disorders. Apart from their anchoring function, HDs play a role in both inside-out and outside-in signal transduction mediated by  $\alpha 6\beta 4$  integrin component (Jones et al., 1998). In the case of type 1 HDs, BPAG1e and plectin anchor keratin proteins to the cell surface via  $\beta 4$  integrin (Jones et al., 1998; Borradori and Sonnenberg, 1999). Ablation of these linker proteins in mice resulted in severe skin blistering (Guo et al., 1995; Andra et al., 1997). A few reports suggest that plectin and BPAG1e play a role in various cellular processes (Andra et al., 1998, 2003; Hamill et al., 2009, 2011; McInroy and Maatta, 2011; Katada et al., 2012; Valencia et al., 2013; Michael et al., 2014; Sutoh Yoneyama et al., 2014). However, not much literature is available related to the functions of these proteins. In this review, we will focus on hemidesmosomal linker proteins namely plectin and BPAG1e which are part of the plakin family of

*Offprint requests to:* Milind M. Vaidya, Advanced Centre for Treatment, Research and Education in Cancer (ACTREC), Tata Memorial Centre Kharghar, 410210, Navi Mumbai, Maharashtra, India. e-mail: [mvoidya@actrec.gov.in](mailto:mvoidya@actrec.gov.in)

cytolinker proteins. Further, we will discuss structural and functional details along with cellular interactions of these proteins. Additionally, we will briefly describe the existing literature regarding involvement of hemidesmosomal linker proteins in blistering diseases of skin and other diseases like cancer.

**Structure of HDs**

HDs are located at the basal side of epithelial cells where they connect the extracellular matrix to the intermediate filament proteins. In complex epithelia like skin, type 1 HDs are present which are comprised of the transmembrane proteins like  $\alpha6\beta4$  integrin, BP180 and CD151 which form the outer plaque of HD. The inner plaque of HDs is formed by cytoplasmic linker proteins called BPAG1e and plectin (Stepp et al., 1990; Sawamura et al., 1991; Hieda et al., 1992; Jones et al.,

1998; Nievers et al., 1999; Sterk et al., 2000; de Pereda et al., 2009a). These linker proteins connect intermediate filament proteins to the transmembrane proteins, which in turn interact with extracellular matrix protein laminin 5 (Fig. 1).

**Plakin family proteins**

Plakins are cytolinker proteins that connect cytoskeletal elements to junctional complexes such as desmosomes and hemidesmosomes. To date seven plakin family members have been identified: desmoplakin, plectin, bullous pemphigoid antigen 1, envoplakin, periplakin, epiplakin and microtubule actin crosslinking factor (reviewed in Leung et al., 2002). The N-terminal plakin domain is a defining feature of plakin family proteins (except epiplakin). The plakin domain is composed of a number of subdomains designated as NN,

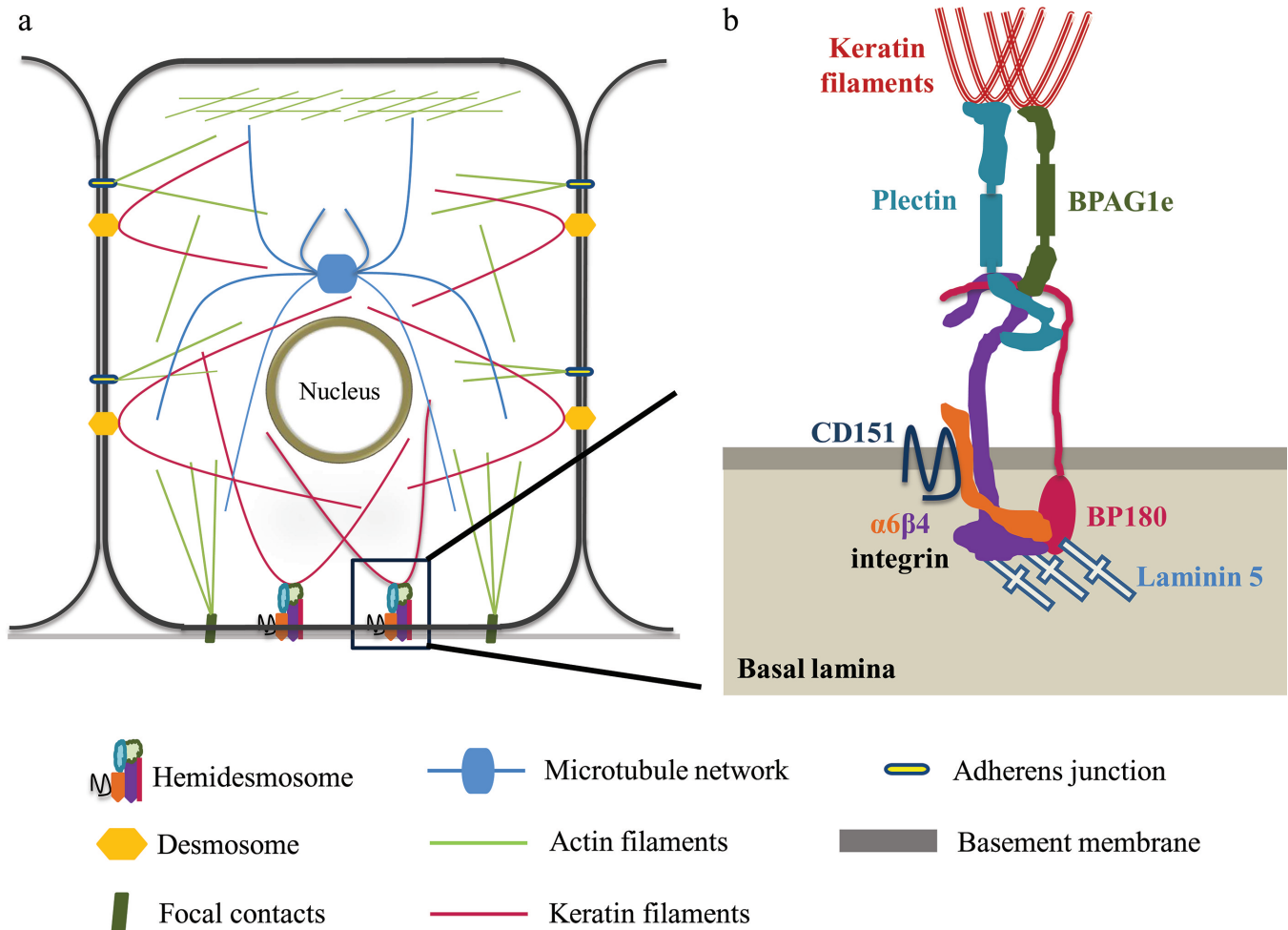


**Fig. 1.** Structure of Hemidesmosome. **a.** Junctional complexes and cytoskeletal elements present in basal epidermal cells; **b.** schematic representation of hemidesmosomal components.  $\alpha6\beta4$  integrin, BP180 and CD151 form the outer plaque while BPAG1e and plectin form inner plaque of hemidesmosomes. Hemidesmosomes link the extracellular matrix protein laminin 5 to the intermediate filament network.

## Hemidesmosomal linker proteins

Z, Y, X, W and V which are rich in  $\alpha$ -helical structures. The plakin domain is thought to be important in targeting plakins to specific cell junctions (Koster et al., 2003). The central coiled-coil rod domain, which has heptad repeats, is important for dimerization of plakins. The C-terminus of plakins varies as per plakin type and is composed of either plakin repeat domains (PRD) or spectrin repeats. The PRD consists of one or many A, B, C subdomains which can associate with intermediate filament proteins (Green et al., 1992; Fontao et al., 2003) (Fig. 2).

### Hemidesmosomal linker proteins

#### BPAG1e

BP230 protein, which is encoded by the *DST* gene, has several isoforms, namely BPAG1n, BPAG1e, BPAG1a, BPAG1b based on alternative splicing of the gene. These alternatively spliced products show tissue specific distribution. BPAG1e (306kDa) is a major isoform expressed in epidermis. BPAG1n (344 kDa), also known as dystonin, is present in neurons. BPAG1a (615 kDa) is produced mostly in pituitary primordia and the dorsal root ganglia (DRG). Muscle specific isoform BPAG1b is the largest isoform of BP230 which is about 824 kDa. BPAG1e consists of a coiled-coil rod domain flanked by a plakin domain and a PRD comprising of B and C subdomains. BPAG1e, unlike BPAG1n, lacks N-terminal actin binding domain (ABD) and therefore cannot interact with actin filaments. The B and C subdomains of PRD, including the intervening linker region, are required for the interaction with intermediate filament proteins (Leung et al., 2001; Fontao et al., 2003) (Fig. 2).

#### Plectin

Plectin is a versatile plakin family member which can associate with all three forms of cytoskeletal proteins. It is expressed in various tissues except for certain neurons (Errante et al., 1994; Elliott et al., 1997). Plectin is encoded by the *PLEC1* gene. Due to alternative splicing of the 5' end of *PLEC1* gene, there are several isoforms of plectin having molecular weight more than 500 kDa. These isoforms show tissue specific expression pattern. For example, 1, 1a and 1c isoforms of plectin are expressed in epidermis. Amongst these plectin 1a is predominant in HDs (Fuchs et al., 1999; Andra et al., 2003; Walko et al., 2011). The N-terminus of plectin has actin binding domain (ABD) by virtue of which it interacts with actin filaments. It has been shown that ABD of plectin preferentially interacts with  $\beta 4$  integrin rather than actin (Geerts et al., 1999). Plectin comprises of 6 PRDs (5 B subdomains and 1 C subdomain). C-terminal Glycine-Serine-Arginine (GSR) domain is required for interacting with microtubules (Sun et al., 2001) (Fig. 2).

#### Interactions mediated by hemidesmosomal linker proteins

The C-terminal plakin repeat domain of BPAG1e and plectin interacts with intermediate filaments whereas the N-terminal plakin domain of these linker proteins interacts with the fibronectin domain of  $\beta 4$  integrin (Fontao et al., 2003; Koster et al., 2003; de Pereda et al., 2009b). However, the  $\beta 4$  integrin binding site for plectin and BPAG1e is different (Koster et al., 2003). A stretch of 85 amino acids located in N terminus of BP180 is crucial for its binding to plakin domain (Y subdomain)

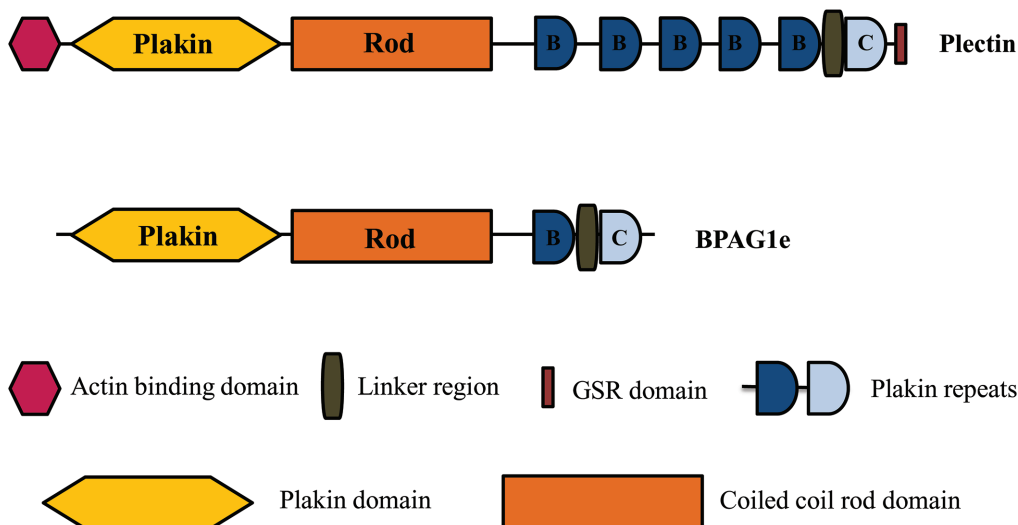


**Fig. 2.** Structural domains of hemidesmosomal linker proteins. Coiled coil rod domain is required for dimerization of linker proteins; N-terminal plakin domain is important for the interaction with transmembrane proteins like  $\beta 4$  integrin, BP180; C-terminal plakin repeat domain and linker domain interacts with intermediate filaments; Actin binding domain of plectin associates with actin filaments; GSR domain of plectin is interacts with microtubules.

of BPAG1e and plectin. The binding sites on BP180 for BPAG1e and plectin are different from those involved in the binding to  $\beta 4$  integrin (Hopkinson and Jones, 2000; Koster et al., 2003). There are reports stating the importance of phosphorylation status of plectin in plectin-cytoskeletal protein association. Site specific phosphorylation of serine/ threonine residues of plectin by kinases results in weakening of plectin-cytoskeletal protein association (Skalli et al., 1992; Foisner et al., 1996; Bouameur et al., 2013).

#### *Events involved in HD assembly*

Several studies have reported that  $\alpha 6\beta 4$  integrin and its ligand laminin 5 play important a role in the assembly of hemidesmosomes (Aberdam et al., 1994; Brown et al., 1996; Dowling et al., 1996; Georges-Labouesse et al., 1996; van der Neut et al., 1996). The large cytoplasmic domain of the  $\beta 4$  integrin (over 1000 residues) harbors two pairs of fibronectin type III (FNIII) repeats separated by a connecting segment (CS) and it is essential for the formation of HDs (Murgia et al., 1998; Nievers et al., 1998). The first pair of FNIII repeat and the first 35 residues (1321-1355) of the CS of the  $\beta 4$  integrin interact with ABD of plectin, which marks the primary interaction between plectin and  $\beta 4$  integrin (Niessen et al., 1997a,b; Schaapveld et al., 1998; Nievers et al., 2000). Furthermore, the plakin domain of plectin also interacts with the C-terminal part of connecting segment and region following fourth the FNIII repeat of  $\beta 4$  integrin (Rezniczek et al., 1998). In another study, Nievers et al have shown that plectin is involved in localization of chimeric  $\beta 4$  integrin lacking extracellular domain into HDs, suggesting that HD formation can take place in absence of  $\alpha 6\beta 4$  integrin-laminin 5 interaction (Nievers et al., 1998). Whether the  $\beta 4$  integrin regulates the distribution of plectin to HDs or the plectin is key molecule for localization of  $\beta 4$  integrin into HDs is not yet clear. Nevertheless, it is well appreciated from *in vitro* studies that the association of the  $\beta 4$  integrin with plectin is crucial for the formation of HDs (Geerts et al., 1999; Koster et al., 2001; Nakano et al., 2001). Interestingly, neither of the BP antigens, BP180 and BPAG1e, gets recruited efficiently into HDs when  $\beta 4$  integrin-plectin interaction did not occur (Koster et al., 2003, 2004). These reports confirmed that interaction of the  $\beta 4$  integrin with plectin is of prime importance for HD formation to take place and occurs before recruitment of BP180 and BPAG1e.

Sterk et al have reported colocalization of CD151 with  $\alpha 3\beta 1$  integrin in pre-hemidesmosomal structures in  $\beta 4$  integrin deficient PAJEB cells. On the other hand,  $\beta 4$  integrin transfected PAJEB cells showed enhanced surface expression of CD151 along with recruitment of CD151 into HDs (Sterk et al., 2000). This process only occurs when the  $\alpha 6$  subunit is associated with the  $\beta 4$  subunit. It is possible that incorporation of CD151 into HDs occurs after  $\alpha 6\beta 4$  integrin and plectin interaction takes place.

BP180, a type II transmembrane protein, can interact with laminin 5 and  $\alpha 6$  integrin by virtue of its extracellular domain while it interacts with  $\beta 4$  integrin, plectin and BPAG1e by means of large collagenous cytoplasmic domain (Giudice et al., 1992; Hopkinson et al., 1995, 1998; Borradori et al., 1997; Aho and Uitto, 1998; Borradori et al., 1998; Schaapveld et al., 1998). Reports have demonstrated that efficient localization of BP180 into hemidesmosomes may be dependent on its interaction with both  $\beta 4$  integrin and plectin, suggesting that co-operative binding of  $\beta 4$  integrin and plectin to BP180 is needed to stabilize HDs (Aho and Uitto, 1998; Schaapveld et al., 1998).

The last step in hemidesmosome assembly is the recruitment of BPAG1e. A stretch of 85 amino acid residues in the cytoplasmic domain of BP180 is crucial for its binding with BPAG1e. The plakin domain (Z-Y domain) contains sequences important for the localization of BPAG1e into HDs most likely via binding to BP180. Further, BPAG1e interacts with the  $\beta 4$  integrin to get stabilized into HDs (Koster et al., 2003). There are conflicting reports regarding incorporation of two BP antigens into HDs. One of the studies indicates that BP180 plays important a role in associating BPAG1e in HD plaque. BP180 lacking GABEB keratinocytes form HDs devoid of BPAG1e, indicating that BP180 may play a critical role in coordinating the subcellular distribution of BPAG1e (Borradori et al., 1998). Conversely, transfection studies have shown that BPAG1e can associate with  $\alpha 6\beta 4$  integrin even in the case of altered BP180 polarization (Hopkinson and Jones, 2000). Likewise, few other studies have demonstrated that most GABEB patients show BPAG1e distribution at the site of HD inner plaque (Jonkman et al., 1995; McGrath et al., 1995; Chavanas et al., 1997).

### **Mutational disorders of hemidesmosomal linker proteins**

#### *Hereditary skin diseases*

HDs provide stable adhesion of epithelia to the basement membrane. Mutations in PLEC1 and DST gene result in a skin blistering disease called epidermolysis bullosa simplex (EBS). Epidermolysis bullosa (EB) is a heterogeneous group of hereditary blistering disorders of skin and mucous membranes. The inheritance of these conditions can be either autosomal dominant or autosomal recessive. EB is divided into three categories: 1. simplex, non-scarring forms of EB (EBS), 2. junctional forms of EB (JEB), 3. dystrophic, severely scarring forms of EB (DEB) (Pearson, 1962). Diseases resulting from mutations in PLEC1 and DST are detailed in Table 1.

Groves et al identified a homozygous truncating mutation in the DST gene encoding the rod domain of BPAG1e which resulted in autosomal recessive epidermolysis bullosa simplex-2 (EBSB2) (Groves et al.,

## Hemidesmosomal linker proteins

2010). Another homozygous mutation which affects BPAG1a and BPAG1b but not BPAG1e results in hereditary sensory autonomic neuropathy type 6 (HSAN6) (Edvardson et al., 2012). Several EBS subtypes are reported to be due to mutations in the PLEC1 gene. Amongst these, EBS with muscular dystrophy (EBS-MD) is an autosomal recessive disorder characterized by early childhood onset of progressive muscular dystrophy and blistering skin changes (Niemi et al., 1988; Fine et al., 1991). EBS-Olga is an autosomal dominant disease that is characterized by skin blistering predominantly on the hands and feet. It is caused by a single amino acid substitution in the rod domain of plectin which makes it sensitive to epidermal specific proteases (Koss-Harnes et al., 2002; Walko et al., 2011).

### Acquired skin diseases

Bullous pemphigoid (BP) is an acquired skin disease of the dermal-epidermal anchoring junction which is prevalent in elderly individuals. BP is characterized by tense blisters and is usually associated with severe itching (Zillikens, 1999). Jordon et al. demonstrated that BP patients produce circulating autoantibodies directed against antigens located in the cutaneous basement membrane zone. In BP patients, circulating immunoglobulin G antibodies to BPAG1 and BPAG2 are found (Jordon et al., 1967). Using immunoprecipitation and immunoblotting techniques, Stanley et al identified BPAG1e as a major antigenic target of BP autoantibodies (Stanley et al., 1981, 1984; Mueller et al., 1989). Further, 180 kDa protein now termed as BP180 was identified in high percentages of BP sera (Labib et al., 1986) which was further characterized by Nishizawa et al. (1993). Antibodies raised against human BPAG1 and BPAG2 cause skin blistering when injected in neonatal mice (Liu et al., 1993). In summary, BP is caused by autoantibodies and inflammation abnormally accumulating in the basement membrane of the skin. These antibodies bind to hemidesmosomal BP antigens

attracting inflammatory cells. There are reports available demonstrating plectin autoantibodies found in a few cases of blistering diseases (Fujiwara et al., 1996; Ohnishi et al., 2000).

Paraneoplastic pemphigus (PNP) is another autoimmune disorder characterized by severe mucosal erosions and various cutaneous lesions associated with lymphoproliferative neoplasms (Anhalt et al., 1990; Zhu and Zhang, 2007). PNP patients exhibit various autoantibodies to the plakin family proteins, namely envoplakin, periplakin, desmoplakin I-II, BPAG1 and plectin (Anhalt et al., 1990; Kim et al., 1997; Borradori et al., 1998; Mahoney et al., 1998; Nguyen et al., 2001).

### Animal models

#### BPAG1e null mouse

Guo et al. targeted the removal of the BPAG1 encoding gene *DST* in mice to explore its protein function. They reported that HDs appeared normal but hemidesmosomal inner plate was absent. Furthermore, IF proteins were not attached to HDs due to which these BPAG1 null mice showed skin blistering. The BPAG1 null mice survived for 4-5 weeks. The localization of other hemidesmosomal proteins seemed unaffected by BPAG1 ablation. The mice also developed severe dystonia, myopathy and sensory nerve degeneration (Guo et al., 1995). This phenotype was observed due to inactivation of BPAG1a and BPAG1b, which act as linker proteins in neurons and skeletal muscles, respectively (Leung et al., 2001).

#### Plectin null mouse

Andra et al studied ablation of plectin in mice. Plectin knockout in mice resulted in cell degeneration. The skin was most severely affected in plectin knockout mice in which the dermis was separated from the epidermis and hence severe blistering was observed. The plectin null mice died 2-3 days after birth due to severe skin blistering. The DSs and HDs were found to be normal ultrastructurally. However, the number of HDs was found to be significantly reduced.  $\beta 4$  integrin levels were also reduced in plectin null mice. The reduction in number of HDs and  $\beta 4$  integrin expression upon ablation of plectin indicated that plectin has role in a HD formation. Plectin null mice, unlike BPAG1e null mice, showed unaltered keratin filament formation indicating that absence of one linker protein is dispensable for other to anchor keratin proteins. Moreover, plectin null mice developed myopathy in skeletal muscle and disintegration of intercalated discs in the heart (Andra et al., 1997).

Altogether, these *in vivo* studies suggest that hemidesmosomal linker proteins are important for mechanical strengthening of the cell.

**Table 1.** Hereditary skin diseases of hemidesmosomal linker proteins.

| Gene/<br>Protein  | OMIM   | Phenotype   | Phenotype<br>MIM | Mode of<br>inheritance |
|-------------------|--------|---|------------------|------------------------|
| PLEC1/<br>Plectin | 113810 | Epidermolysis bullosa simplex with pyloric atresia    | 612138           | autosomal recessive    |
|                   |        | Epidermolysis bullosa simplex, Ogna type              | 131950           | autosomal dominant     |
|                   |        | Epidermolysis bullosa simplex with muscular dystrophy | 226670           | autosomal recessive    |
|                   |        | Muscular dystrophy, limb-girdle, type 2Q              | 613723           | autosomal recessive    |
| DST/<br>BPAG1     | 601282 | Neuropathy, hereditary sensory and autonomic, type VI | 614653           | autosomal recessive    |
|                   |        | Epidermolysis bullosa simplex, autosomal recessive 2  | 615425           | autosomal recessive    |

Information adapted from <http://omim.org/>

### Hemidesmosomal linker proteins and signaling

For the last two decades, there has been growing evidence which demonstrates that hemidesmosomal linker proteins play a role in cellular processes other than maintenance of tissue integrity.

#### BPAG1e

Apart from its known anchoring function, BPAG1e has been involved in various cellular processes.

#### BPAG1e and cell motility

In 1995, Guo et al. reported that BPAG1e null animals display impaired wound healing *in vivo*. The keratinocytes of BPAG1e null mice were not flattened, unlike those of normal migrating keratinocytes. The authors concluded that defects in migration may be attributed to retardation of initiation of migration of epidermal keratinocytes (Guo et al., 1995). This study indirectly implicates the role of BPAG1e in keratinocyte migration. One of the recent reports has shown that BPAG1e regulates keratinocyte migration by acting as a scaffold for  $\beta 4$  integrin mediated modulation of Rac1 and cofilin activities. Additionally, BPAG1e ablation in keratinocytes resulted in aberrant motility and loss of front to rear polarity. Further, immunofluorescence studies have shown that BPAG1e and  $\beta 4$  integrin colocalize at the leading edge of migrating keratinocytes indicating that  $\beta 4$  integrin associated BPAG1e may have a role in keratinocyte migration (Hamill et al., 2009). A subsequent report from the same laboratory has demonstrated that BP180 plays a role in cell motility and lamellopodial stability by recruiting BPAG1e to  $\alpha 6\beta 4$  integrin at the leading edge of the migrating keratinocytes (Hamill et al., 2011). On the other hand, Michael et al have shown reduced adhesion but increased spreading and migration in human keratinocytes carrying homozygous nonsense mutations in BPAG1e encoding gene. Altered levels of K14,  $\beta 4$  integrin and  $\beta 1$  integrin were also observed in these keratinocytes. Michael et al failed to reproduce similar findings in BPAG1e ablated normal keratinocytes (Michael et al., 2014). Taken together, it is difficult to conclude from these reports whether BPAG1e is a positive or negative regulator of cell motility and further research is necessary to resolve this issue.

#### BPAG1e and cancer

There are very few reports available related to altered BPAG1e expression in human cancers. A recent study from Shimbo et al demonstrated that autoantibodies against BPAG1e are found in higher amounts in the serum of patients with advanced melanoma. Thus, it can prove as potential biomarker for melanomas (Shimbo et al., 2010). In another study, it has been reported that upregulation of BPAG1e and  $\alpha 6\beta 4$

integrin expression is found in invasive squamous cell carcinomas. Interestingly, these proteins were not localized to HDs and their pericellular localization was seen. Moreover, polarized localization of BPAG1e was lost in highly invasive tumours (Herold-Mende et al., 2001). Contrary, Lo et al have reported downregulated levels of hemidesmosomal components, including BPAG1e in nasopharyngeal carcinoma as compared to non-malignant nasopharyngeal epithelia (Lo et al., 2001). Thus, BPAG1e shows tissue dependent alterations during cancer development.

#### Plectin

Plectin has been implicated in various cellular processes. eg. dynamics of cytoskeletal proteins, cell migration etc.

#### Plectin and cytoskeletal stability

Plectin can interact with all three forms of cytoskeletal proteins. This might be the reason why destabilization of cellular integrity was more severe in plectin null mice compared to BPAG1e null mice. Plectin 1, 1a and 1c are expressed in human keratinocytes, of which only 1a isoform localizes specifically at the site of HDs. Moreover, only 1a isoform was capable of rescuing hemidesmosomal defects in plectin null keratinocytes (Andra et al., 2003). In another study, Valencia et al have recently shown that plectin 1c plays major role in a microtubule (MT) destabilization and hence decreased microtubule dynamics. Further, Enhanced MT stability due to ablation in plectin 1c led to changes in cell shape, nonpolarized cell migration, smaller sized focal adhesion contacts, higher glucose uptake and mitotic spindle aberrations combined with reduced growth rates of cells. The plectin-MT interaction antagonizes functions of microtubule associated proteins (MAPs), which are involved in MT stability and assembly (Valencia et al., 2013). Unlike plectin, other linker proteins like BPAG1 and ACF7 have been reported to have a role in stabilization of microtubules (Yang et al., 1999; Kodama et al., 2003). The role of plectin in regulation of actin cytoskeleton dynamics has also been reported. The actin cytoskeleton was found to be less extensive in plectin ablated cells as compared to wild type cells (Andra et al., 1998). These reports suggest that plectin is the first cytolinker protein having a role in both microtubule and microfilament destabilization. Together these observations suggest that plectin destabilizes microtubule and microfilament networks while other linker proteins like BPAG1 and ACF7 stabilize these networks.

#### Plectin, cancer and cell signaling

There are several studies indicating use of plectin as a potential biomarker in various cancer conditions (Kelly

## Hemidesmosomal linker proteins

et al., 2008; Bausch et al., 2009, 2011; Lee et al., 2009; Pawar et al., 2011; Katada et al., 2012). The siRNA mediated knockdown of plectin resulted in decreased proliferation, migration and invasion of head and neck squamous cell carcinoma (HNSCC) cells. Moreover, in plectin knockdown cells phosphorylated ERK levels were decreased. Authors have argued that a decrease in cell migration and invasion may be attributed to a decrease in activity of ERK kinase. The exact mechanism by which these phenotypic changes took place is unclear. In addition, an inverse relation between expression of plectin in HNSCC and survival rate of patients was shown (Katada et al., 2012). In another study, plectin downregulation in colon carcinoma cells resulted in impairment of cell migration and adhesion. Plectin 1 and 1k were predominantly expressed in invasive colon carcinoma cells. Plectin 1k was targeted to actin rich podosome structures. Plectin knockdown inhibited assembly of these actin rich structures. Upon transfection of Plectin 1k N-terminus, actin rich structures were formed, indicating that plectin 1k has a role in podosome formation (McInroy and Maatta, 2011). In a recent study, gene expression profiling has revealed upregulation of plectin and type III IF protein, termed vimentin, in highly metastatic bladder cells as compared to low metastatic bladder cells. A dissociation of plectin-vimentin interaction in invasive bladder cancer cells resulted in impairment of invadopodia formation, reduced extracellular matrix degradation and metastasis (Sutoh Yoneyama et al., 2014). Under normal physiology, plectin is localized in the cytoplasm, while in pancreatic ductal adenocarcinoma (PDAC) its cell surface localization has been shown, which may be the result of trafficking through exosomes. The presence of plectin in exosomes from the serum of PDAC animals indicated that plectin can act as a potential serum marker (Shin et al., 2013).

### Conclusion and future perspectives

In the last two decades, there has been a large increase in the understanding of the plakin family linker proteins. Several studies have shown that plakin proteins including BPAG1e and plectin are not present in the cells only to anchor specific proteins, but that they have functional a role in various cellular processes. The consequences of BPAG1e or plectin ablation in animals have given opportunities to explore insights related to these linker proteins. The biggest hurdle in studying HD dynamics in real time is the fact that true HDs are not formed in the majority of cultured cells. Further, very little is known about how HDs assemble and disassemble *in vivo*. The challenge remains to elucidate molecular mechanisms involved in HD stability. Recent studies have shown the role of hemidesmosomal linker proteins in various cellular processes other than their known anchoring function. For example, these proteins impact keratinocyte migration which is partly because they connect keratins to  $\alpha 6 \beta 4$  integrin, which in turn

regulate several signaling pathways which are related to cell migration. In this connection, the challenge is to understand how and why these proteins are mislocalized in a cell to govern cellular migration. Moreover, it will be pertinent to find out whether inside-out or outside-in signaling mechanisms are responsible for this phenotype. To understand the role of linker proteins in various cellular processes we need to decipher interacting partners of these proteins which may provide clues regarding mechanism. Additionally, these plakin proteins have been reported as potential biomarkers in various cancer types. It would be interesting to understand their functions in the process of carcinogenesis. These studies would provide a platform for future applications in diagnostics and therapeutics.

### References

- Aberdam D., Galliano M.F., Vailly J., Pulkkinen L., Bonifas J., Christiano A.M., Tryggvason K., Uitto J., Epstein E.H. Jr, Ortonne J.P. and Meneguzzi G. (1994). Herlitz's junctional epidermolysis bullosa is linked to mutations in the gene (*lamc2*) for the gamma 2 subunit of nicein/kalinin (laminin-5). *Nat. Genet.* 6, 299-304.
- Aho S. and Uitto J. (1998). Direct interaction between the intracellular domains of bullous pemphigoid antigen 2 (bp180) and beta 4 integrin, hemidesmosomal components of basal keratinocytes. *Biochem. Biophys. Res. Commun.* 243, 694-699.
- Andra K., Lassmann H., Bittner R., Shorny S., Fassler R., Propst F. and Wiche G. (1997). Targeted inactivation of plectin reveals essential function in maintaining the integrity of skin, muscle, and heart cytoarchitecture. *Genes Dev.* 11, 3143-3156.
- Andra K., Nikolic B., Stocher M., Drenckhahn D. and Wiche G. (1998). Not just scaffolding: Plectin regulates actin dynamics in cultured cells. *Genes Dev.* 12, 3442-3451.
- Andra K., Kornacker I., Jorgl A., Zorer M., Spazierer D., Fuchs P., Fischer I. and Wiche G. (2003). Plectin-isoform-specific rescue of hemidesmosomal defects in plectin (-/-) keratinocytes. *J. Invest. Dermatol.* 120, 189-197.
- Anhalt G.J., Kim S.C., Stanley J.R., Korman N.J., Jabs D.A., Kory M., Izumi H., Rattie H. 3rd, Mutasim D., Ariss-Abdo L. and Labib R.S. (1990). Paraneoplastic pemphigus. An autoimmune mucocutaneous disease associated with neoplasia. *N. Engl. J. Med.* 323, 1729-1735.
- Bausch D., Mino-Kenudson M., Fernandez-Del Castillo C., Warshaw A.L., Kelly K.A. and Thayer S.P. (2009). Plectin-1 is a biomarker of malignant pancreatic intraductal papillary mucinous neoplasms. *J. Gastrointest. Surg.* 13, 1948-1954.
- Bausch D., Thomas S., Mino-Kenudson M., Fernandez-del C.C., Bauer T.W., Williams M., Warshaw A.L., Thayer S.P. and Kelly K.A. (2011). Plectin-1 as a novel biomarker for pancreatic cancer. *Clin. Cancer Res.* 17, 302-309.
- Borradori L. and Sonnenberg A. (1999). Structure and function of hemidesmosomes: More than simple adhesion complexes. *J. Invest. Dermatol.* 112, 411-418.
- Borradori L., Koch P.J., Niessen C.M., Erkeland S., van Leusden M.R. and Sonnenberg A. (1997). The localization of bullous pemphigoid antigen 180 (bp180) in hemidesmosomes is mediated by its cytoplasmic domain and seems to be regulated by the beta4 integrin subunit. *J. Cell Biol.* 136, 1333-1347.
- Borradori L., Chavanas S., Schaapveld R.Q., Gagnoux-Palacios L.,

- Calafat J., Meneguzzi G. and Sonnenberg A. (1998). Role of the bullous pemphigoid antigen 180 (bp180) in the assembly of hemidesmosomes and cell adhesion--reexpression of bp180 in generalized atrophic benign epidermolysis bullosa keratinocytes. *Exp. Cell Res.* 239, 463-476.
- Bouameur J.E., Schneider Y., Begre N., Hobbs R.P., Lingasamy P., Fontao L., Green K.J., Favre B. and Borradori L. (2013). Phosphorylation of serine 4,642 in the c-terminus of plectin by mnk2 and pka modulates its interaction with intermediate filaments. *J. Cell Sci.* 126, 4195-4207.
- Brown T.A., Gil S.G., Sybert V.P., Lestringant G.G., Tadini G., Caputo R. and Carter W.G. (1996). Defective integrin alpha 6 beta 4 expression in the skin of patients with junctional epidermolysis bullosa and pyloric atresia. *J. Invest. Dermatol.* 107, 384-391.
- Chavanas S., Gache Y., Tadini G., Pulkkinen L., Uitto J., Ortonne J.P. and Meneguzzi G. (1997). A homozygous in-frame deletion in the collagenous domain of bullous pemphigoid antigen bp180 (type xvii collagen) causes generalized atrophic benign epidermolysis bullosa. *J. Invest. Dermatol.* 109, 74-78.
- de Pereda J.M., Ortega E., Alonso-Garcia N., Gomez-Hernandez M. and Sonnenberg A. (2009a). Advances and perspectives of the architecture of hemidesmosomes: Lessons from structural biology. *Cell Adh. Migr.* 3, 361-364.
- de Pereda J.M., Lillo M.P. and Sonnenberg A. (2009b). Structural basis of the interaction between integrin alpha6beta4 and plectin at the hemidesmosomes. *EMBO J.* 28, 1180-1190.
- Dowling J., Yu Q.C. and Fuchs E. (1996). Beta4 integrin is required for hemidesmosome formation, cell adhesion and cell survival. *J. Cell Biol.* 134, 559-572.
- Edvardson S., Cinnamon Y., J alas C., Shaag A., Maayan C., Axelrod F.B. and Elpeleg O. (2012). Hereditary sensory autonomic neuropathy caused by a mutation in dystonin. *Ann. Neurol.* 71, 569-572.
- Elliott C.E., Becker B., Oehler S., Castanon M.J., Hauptmann R. and Wiche G. (1997). Plectin transcript diversity: Identification and tissue distribution of variants with distinct first coding exons and rodless isoforms. *Genomics* 42, 115-125.
- Errante L.D., Wiche G. and Shaw G. (1994). Distribution of plectin, an intermediate filament-associated protein, in the adult rat central nervous system. *J. Neurosci. Res.* 37, 515-528.
- Fine J.D., Bauer E.A., Briggaman R.A., Carter D.M., Eady R.A., Esterly N.B., Holbrook K.A., Hurwitz S., Johnson L., Lin A., Pearson R. and Sybert V.P. (1991). Revised clinical and laboratory criteria for subtypes of inherited epidermolysis bullosa. A consensus report by the subcommittee on diagnosis and classification of the national epidermolysis bullosa registry. *J. Am. Acad. Dermatol.* 24, 119-135.
- Foisner R., Malecz N., Dressel N., Stadler C. and Wiche G. (1996). M-phase-specific phosphorylation and structural rearrangement of the cytoplasmic cross-linking protein plectin involve p34cdc2 kinase. *Mol. Biol. Cell* 7, 273-288.
- Fontao L., Favre B., Riou S., Geerts D., Jaunin F., Saurat J.H., Green K.J., Sonnenberg A. and Borradori L. (2003). Interaction of the bullous pemphigoid antigen 1 (bp230) and desmoplakin with intermediate filaments is mediated by distinct sequences within their cooh terminus. *Mol. Biol. Cell* 14, 1978-1992.
- Fuchs P., Zorer M., Rezniczek G.A., Spazierer D., Oehler S., Castanon M.J., Hauptmann R. and Wiche G. (1999). Unusual 5' transcript complexity of plectin isoforms: Novel tissue-specific exons modulate actin binding activity. *Hum. Mol. Genet.* 8, 2461-2472.
- Fujiwara S., Kohno K., Iwamatsu A., Naito I. and Shinkai H. (1996). Identification of a 450-kda human epidermal autoantigen as a new member of the plectin family. *J. Invest. Dermatol.* 106, 1125-1130.
- Geerts D., Fontao L., Nievers M.G., Schaapveld R.Q., Purkis P.E., Wheeler G.N., Lane E.B., Leigh I.M. and Sonnenberg A. (1999). Binding of integrin alpha6beta4 to plectin prevents plectin association with F-actin but does not interfere with intermediate filament binding. *J. Cell Biol.* 147, 417-434.
- Georges-Labouesse E., Messaddeq N., Yehia G., Cadalbert L., Dierich A. and Le Meur M. (1996). Absence of integrin alpha 6 leads to epidermolysis bullosa and neonatal death in mice. *Nat. Genet.* 13, 370-373.
- Giudice G.J., Emery D.J. and Diaz L.A. (1992). Cloning and primary structural analysis of the bullous pemphigoid autoantigen bp180. *J. Invest. Dermatol.* 99, 243-250.
- Green K.J., Virata M.L., Elgart G.W., Stanley J.R. and Parry D.A. (1992). Comparative structural analysis of desmoplakin, bullous pemphigoid antigen and plectin: Members of a new gene family involved in organization of intermediate filaments. *Int. J. Biol. Macromol.* 14, 145-153.
- Groves R.W., Liu L., Dopping-Hepenstal P.J., Markus H.S., Lovell P.A., Ozoemena L., Lai-Cheong J.E., Gawler J., Owaribe K., Hashimoto T., Mellerio J.E., Mee J.B. and McGrath J.A. (2010). A homozygous nonsense mutation within the dystonin gene coding for the coiled-coil domain of the epithelial isoform of bpag1 underlies a new subtype of autosomal recessive epidermolysis bullosa simplex. *J. Invest. Dermatol.* 130, 1551-1557.
- Guo L., Degenstein L., Dowling J., Yu Q.C., Wollmann R., Perman B. and Fuchs E. (1995). Gene targeting of bpag1: Abnormalities in mechanical strength and cell migration in stratified epithelia and neurologic degeneration. *Cell* 81, 233-243.
- Hamill K.J., Hopkinson S.B., DeBiase P. and Jones J.C. (2009). Bpag1e maintains keratinocyte polarity through beta4 integrin-mediated modulation of rac1 and cofilin activities. *Mol. Biol. Cell* 20, 2954-2962.
- Hamill K.J., Hopkinson S.B., Jonkman M.F. and Jones J.C. (2011). Type xvii collagen regulates lamellipod stability, cell motility, and signaling to rac1 by targeting bullous pemphigoid antigen 1e to alpha6beta4 integrin. *J. Biol. Chem.* 286, 26768-26780.
- Herold-Mende C., Kartenbeck J., Tomakidi P. and Bosch F.X. (2001). Metastatic growth of squamous cell carcinomas is correlated with upregulation and redistribution of hemidesmosomal components. *Cell Tissue Res.* 306, 399-408.
- Hieda Y., Nishizawa Y., Uematsu J. and Owaribe K. (1992). Identification of a new hemidesmosomal protein, hd1: A major, high molecular mass component of isolated hemidesmosomes. *J. Cell Biol.* 116, 1497-1506.
- Hopkinson S.B. and Jones J.C. (2000). The n terminus of the transmembrane protein bp180 interacts with the n-terminal domain of bp230, thereby mediating keratin cytoskeleton anchorage to the cell surface at the site of the hemidesmosome. *Mol. Biol. Cell* 11, 277-286.
- Hopkinson S.B., Baker S.E. and Jones J.C. (1995). Molecular genetic studies of a human epidermal autoantigen (the 180-kd bullous pemphigoid antigen/bp180): Identification of functionally important sequences within the bp180 molecule and evidence for an interaction between bp180 and alpha 6 integrin. *J. Cell Biol.* 130, 117-125.
- Hopkinson S.B., Findlay K., deHart G.W. and Jones J.C. (1998).

## Hemidesmosomal linker proteins

- Interaction of bp180 (type xvii collagen) and alpha6 integrin is necessary for stabilization of hemidesmosome structure. *J. Invest. Dermatol.* 111, 1015-1022.
- Jones J.C., Hopkinson S.B. and Goldfinger L.E. (1998). Structure and assembly of hemidesmosomes. *Bioessays* 20, 488-494.
- Jonkman M.F., de Jong M.C., Heeres K., Pas H.H., van der Meer J.B., Owaribe K., Martinez de Velasco A.M., Niessen C.M. and Sonnenberg A. (1995). 180-kd bullous pemphigoid antigen (bp180) is deficient in generalized atrophic benign epidermolysis bullosa. *J. Clin. Invest.* 95, 1345-1352.
- Jordon R.E., Beutner E.H., Witebsky E., Blumental G., Hale W.L. and Lever W.F. (1967). Basement zone antibodies in bullous pemphigoid. *JAMA* 200, 751-756.
- Katada K., Tomonaga T., Satoh M., Matsushita K., Tonoike Y., Kodera Y., Hanazawa T., Nomura F. and Okamoto Y. (2012). Plectin promotes migration and invasion of cancer cells and is a novel prognostic marker for head and neck squamous cell carcinoma. *J. Proteomics* 75, 1803-1815.
- Kelly K.A., Bardeesy N., Anbazhagan R., Gurumurthy S., Berger J., Alencar H., Depinho R.A., Mahmood U. and Weissleder R. (2008). Targeted nanoparticles for imaging incipient pancreatic ductal adenocarcinoma. *PLoS Med.* 5, e85.
- Kim S.C., Kwon Y.D., Lee I.J., Chang S.N. and Lee T.G. (1997). Cdna cloning of the 210-kda paraneoplastic pemphigus antigen reveals that envoplakin is a component of the antigen complex. *J. Invest. Dermatol.* 109, 365-369.
- Kodama A., Karakesisoglou I., Wong E., Vaezi A. and Fuchs E. (2003). Acl7: An essential integrator of microtubule dynamics. *Cell* 115, 343-354.
- Koss-Harnes D., Hoyheim B., Anton-Lamprecht I., Gjesti A., Jorgensen R.S., Jahnsen F.L., Olaisen B., Wiche G. and Gedde-Dahl T. Jr (2002). A site-specific plectin mutation causes dominant epidermolysis bullosa simplex ogna: Two identical de novo mutations. *J. Invest. Dermatol.* 118, 87-93.
- Koster J., Kuikman I., Kreft M. and Sonnenberg A. (2001). Two different mutations in the cytoplasmic domain of the integrin beta 4 subunit in nonlethal forms of epidermolysis bullosa prevent interaction of beta 4 with plectin. *J. Invest. Dermatol.* 117, 1405-1411.
- Koster J., Geerts D., Favre B., Borradori L. and Sonnenberg A. (2003). Analysis of the interactions between bp180, bp230, plectin and the integrin alpha6beta4 important for hemidesmosome assembly. *J. Cell Sci.* 116, 387-399.
- Koster J., van Wilpe S., Kuikman I., Lijmens S.H. and Sonnenberg A. (2004). Role of binding of plectin to the integrin beta4 subunit in the assembly of hemidesmosomes. *Mol. Biol. Cell* 15, 1211-1223.
- Labib R.S., Anhalt G.J., Patel H.P., Mutasim D.F. and Diaz L.A. (1986). Molecular heterogeneity of the bullous pemphigoid antigens as detected by immunoblotting. *J. Immunol.* 136, 1231-1235.
- Lee H.J., Na K., Kwon M.S., Kim H., Kim K.S. and Paik Y.K. (2009). Quantitative analysis of phosphopeptides in search of the disease biomarker from the hepatocellular carcinoma specimen. *Proteomics* 9, 3395-3408.
- Leung C.L., Zheng M., Prater S.M. and Liem R.K. (2001). The bpag1 locus: Alternative splicing produces multiple isoforms with distinct cytoskeletal linker domains, including predominant isoforms in neurons and muscles. *J. Cell Biol.* 154, 691-697.
- Leung C.L., Green K.J. and Liem R.K. (2002). Plakins: A family of versatile cytolinker proteins. *Trends Cell Biol.* 12, 37-45.
- Liu Z., Diaz L.A., Troy J.L., Taylor A.F., Emery D.J., Fairley J.A. and Giudice G.J. (1993). A passive transfer model of the organ-specific autoimmune disease, bullous pemphigoid, using antibodies generated against the hemidesmosomal antigen, bp180. *J. Clin. Invest.* 92, 2480-2488.
- Lo A.K., Yuen P.W., Liu Y., Wang X.H., Cheung A.L., Wong Y.C. and Tsao S.W. (2001). Downregulation of hemidesmosomal proteins in nasopharyngeal carcinoma cells. *Cancer Lett.* 163, 117-123.
- Mahoney M.G., Aho S., Uitto J. and Stanley J.R. (1998). The members of the plakin family of proteins recognized by paraneoplastic pemphigus antibodies include periplakin. *J. Invest. Dermatol.* 111, 308-313.
- McGrath J.A., Gatalica B., Christiano A.M., Li K., Owaribe K., McMillan J.R., Eady R.A. and Uitto J. (1995). Mutations in the 180-kd bullous pemphigoid antigen (bpag2), a hemidesmosomal transmembrane collagen (col17a1), in generalized atrophic benign epidermolysis bullosa. *Nat. Genet.* 11, 83-86.
- McInroy L. and Maatta A. (2011). Plectin regulates invasiveness of sw480 colon carcinoma cells and is targeted to podosome-like adhesions in an isoform-specific manner. *Exp. Cell Res.* 317, 2468-2478.
- Michael M., Begum R., Fong K., Pourreyron C., South A.P., McGrath J.A. and Parsons M. (2014). Bpag1-e restricts keratinocyte migration through control of adhesion stability. *J. Invest. Dermatol.* 134, 773-782.
- Mueller S., Klaus-Kovtun V. and Stanley J.R. (1989). A 230-kd basic protein is the major bullous pemphigoid antigen. *J. Invest. Dermatol.* 92, 33-38.
- Murgia C., Blaikie P., Kim N., Dans M., Petrie H.T. and Giancotti F.G. (1998). Cell cycle and adhesion defects in mice carrying a targeted deletion of the integrin beta4 cytoplasmic domain. *EMBO J.* 17, 3940-3951.
- Nakano A., Pulkkinen L., Murrell D., Rico J., Lucky A.W., Garzon M., Stevens C.A., Robertson S., Pfendner E. and Uitto J. (2001). Epidermolysis bullosa with congenital pyloric atresia: Novel mutations in the beta 4 integrin gene (itgb4) and genotype/phenotype correlations. *Pediatr. Res.* 49, 618-626.
- Nguyen V.T., Ndoye A., Bassler K.D., Shultz L.D., Shields M.C., Ruben B.S., Webber R.J., Pittelkow M.R., Lynch P.J. and Grando S.A. (2001). Classification, clinical manifestations, and immunopathological mechanisms of the epithelial variant of paraneoplastic autoimmune multiorgan syndrome: A reappraisal of paraneoplastic pemphigus. *Arch. Dermatol.* 137, 193-206.
- Niemi K.M., Sommer H., Kero M., Kanerva L. and Haltia M. (1988). Epidermolysis bullosa simplex associated with muscular dystrophy with recessive inheritance. *Arch. Dermatol.* 124, 551-554.
- Niessen C.M., Hulsman E.H., Oomen L.C., Kuikman I. and Sonnenberg A. (1997a). A minimal region on the integrin beta4 subunit that is critical to its localization in hemidesmosomes regulates the distribution of hd1/plectin in cos-7 cells. *J. Cell Sci.* 110, 1705-1716.
- Niessen C.M., Hulsman E.H., Rots E.S., Sanchez-Aparicio P. and Sonnenberg A. (1997b). Integrin alpha 6 beta 4 forms a complex with the cytoskeletal protein hd1 and induces its redistribution in transfected cos-7 cells. *Mol. Biol. Cell* 8, 555-566.
- Nievers M.G., Schaapveld R.Q., Oomen L.C., Fontao L., Geerts D. and Sonnenberg A. (1998). Ligand-independent role of the beta 4 integrin subunit in the formation of hemidesmosomes. *J. Cell Sci.* 111, 1659-1672.
- Nievers M.G., Schaapveld R.Q. and Sonnenberg A. (1999). Biology and function of hemidesmosomes. *Matrix Biol.* 18, 5-17.

- Nievers M.G., Kuikman I., Geerts D., Leigh I.M. and Sonnenberg A. (2000). Formation of hemidesmosome-like structures in the absence of ligand binding by the  $\alpha 6 \beta 4$  integrin requires binding of hd1/plectin to the cytoplasmic domain of the  $\beta 4$  integrin subunit. *J. Cell Sci.* 113 ( Pt 6), 963-973.
- Nishizawa Y., Uematsu J. and Owaribe K. (1993). Hd4, a 180 kda bullous pemphigoid antigen, is a major transmembrane glycoprotein of the hemidesmosome. *J. Biochem.* 113, 493-501.
- Ohnishi Y., Tajima S., Ishibashi A. and Fujiwara S. (2000). A vesicular bullous pemphigoid with an autoantibody against plectin. *Br. J. Dermatol.* 142, 813-815.
- Pawar H., Kashyap M.K., Sahasrabudhe N.A., Renuse S., Harsha H.C., Kumar P., Sharma J., Kandasamy K., Marimuthu A., Nair B., Rajagopalan S., Maharudraiah J., Premalatha C.S., Kumar K.V., Vijayakumar M., Chaerkady R., Prasad T.S., Kumar R.V. and Pandey A. (2011). Quantitative tissue proteomics of esophageal squamous cell carcinoma for novel biomarker discovery. *Cancer Biol. Ther.* 12, 510-522.
- Pearson R.W. (1962). Studies on the pathogenesis of epidermolysis bullosa. *J. Invest. Dermatol.* 39, 551-575.
- Reznicek G.A., de Pereda J.M., Reipert S. and Wiche G. (1998). Linking integrin  $\alpha 6 \beta 4$ -based cell adhesion to the intermediate filament cytoskeleton: Direct interaction between the  $\beta 4$  subunit and plectin at multiple molecular sites. *J. Cell Biol.* 141, 209-225.
- Sawamura D., Li K., Chu M.L. and Uitto J. (1991). Human bullous pemphigoid antigen (bpag1). Amino acid sequences deduced from cloned cdnas predict biologically important peptide segments and protein domains. *J. Biol. Chem.* 266, 17784-17790.
- Schaapveld R.Q., Borradori L., Geerts D., van Leusden M.R., Kuikman I., Nievers M.G., Niessen C.M., Steenbergen R.D., Sniijders P.J. and Sonnenberg A. (1998). Hemidesmosome formation is initiated by the  $\beta 4$  integrin subunit, requires complex formation of  $\beta 4$  and hd1/plectin, and involves a direct interaction between  $\beta 4$  and the bullous pemphigoid antigen 180. *J. Cell Biol.* 142, 271-284.
- Shimbo T., Tanemura A., Yamazaki T., Tamai K., Katayama I. and Kaneda Y. (2010). Serum anti-bpag1 auto-antibody is a novel marker for human melanoma. *PLoS One* 5, e10566.
- Shin S.J., Smith J.A., Reznicek G.A., Pan S., Chen R., Brentnall T.A., Wiche G. and Kelly K.A. (2013). Unexpected gain of function for the scaffolding protein plectin due to mislocalization in pancreatic cancer. *Proc. Natl. Acad. Sci. USA* 110, 19414-19419.
- Skalli O., Chou Y.H. and Goldman R.D. (1992). Cell cycle-dependent changes in the organization of an intermediate filament-associated protein: Correlation with phosphorylation by p34cdc2. *Proc. Natl. Acad. Sci. USA* 89, 11959-11963.
- Stanley J.R., Hawley-Nelson P., Yuspa S.H., Shevach E.M. and Katz S.I. (1981). Characterization of bullous pemphigoid antigen: A unique basement membrane protein of stratified squamous epithelia. *Cell* 24, 897-903.
- Stanley J.R., Woodley D.T. and Katz S.I. (1984). Identification and partial characterization of pemphigoid antigen extracted from normal human skin. *J. Invest. Dermatol.* 82, 108-111.
- Stepp M.A., Spurr-Michaud S., Tisdale A., Elwell J. and Gipson I.K. (1990).  $\alpha 6 \beta 4$  integrin heterodimer is a component of hemidesmosomes. *Proc. Natl. Acad. Sci. USA* 87, 8970-8974.
- Sterk L.M., Geuijen C.A., Oomen L.C., Calafat J., Janssen H. and Sonnenberg A. (2000). The tetraspan molecule cd151, a novel constituent of hemidesmosomes, associates with the integrin  $\alpha 6 \beta 4$  and may regulate the spatial organization of hemidesmosomes. *J. Cell Biol.* 149, 969-982.
- Sun D., Leung C.L. and Liem R.K. (2001). Characterization of the microtubule binding domain of microtubule actin crosslinking factor (macf): Identification of a novel group of microtubule associated proteins. *J. Cell Sci.* 114, 161-172.
- Sutoh Yoneyama M., Hatakeyama S., Habuchi T., Inoue T., Nakamura T., Funyu T., Wiche G., Ohyama C. and Tsuboi S. (2014). Vimentin intermediate filament and plectin provide a scaffold for invadopodia, facilitating cancer cell invasion and extravasation for metastasis. *Eur. J. Cell Biol.* 93, 157-169.
- Valencia R.G., Walko G., Janda L., Novacek J., Mihailovska E., Reipert S., Andra-Marobela K. and Wiche G. (2013). Intermediate filament-associated cytolinker plectin 1c destabilizes microtubules in keratinocytes. *Mol. Biol. Cell* 24, 768-784.
- van der Neut R., Krimpenfort P., Calafat J., Niessen C.M. and Sonnenberg A. (1996). Epithelial detachment due to absence of hemidesmosomes in integrin  $\beta 4$  null mice. *Nat. Genet.* 13, 366-369.
- Walko G., Vukasinovic N., Gross K., Fischer I., Sibitz S., Fuchs P., Reipert S., Jungwirth U., Berger W., Salzer U., Carugo O., Castanon M.J. and Wiche G. (2011). Targeted proteolysis of plectin isoform 1a accounts for hemidesmosome dysfunction in mice mimicking the dominant skin blistering disease ebs-ogna. *PLoS Genet.* 7, e1002396.
- Yang Y., Bauer C., Strasser G., Wollman R., Julien J.P. and Fuchs E. (1999). Integrators of the cytoskeleton that stabilize microtubules. *Cell* 98, 229-238.
- Zhu X. and Zhang B. (2007). Paraneoplastic pemphigus. *J. Dermatol.* 34, 503-511.
- Zillikens D. (1999). Acquired skin disease of hemidesmosomes. *J. Dermatol. Sci.* 20, 134-154.